

https://dspace.org/

Inhibition of Hepatitis B virus replication using RNAi effectors targeting the viral X-gene

Carmona, Sergio Catril

2018

https://hdl.handle.net/10539/25284

Downloaded from a DSpace repository. https://dspace.org/

Inhibition of Hepatitis B virus replication using RNAi effectors targeting the viral X-gene

Sergio Carmona

A thesis submitted to the Faculty of Health Sciences, University of the Witwatersrand, Johannesburg, in fulfilment of the requirements for the degree of Doctor of Philosophy.

Johannesburg, June 2018

Declaration

I Sergio Carmona declare that this thesis comprises my own work. It is being submitted to the University of the Witwatersrand, Johannesburg, for the degree of Doctor of Philosophy. It has not been submitted for any other degree or examination at any other University.

18 June, 2018

Dedication

"Si no escalas la montaña, jamás podrás disfrutar del paisaje."

Pablo Neruda

A Cecily por tu apoyo desde un principio,

A Sebastián Daniel y Matías Rafael

A mi hermano por haber estado a mi lado siempre

A Cathy…

A mi madre por haber inculcado ser persevérate

List of Publications

The work presented in this thesis has been published in the following peer reviewed manuscripts:

1. Mevel M, Kamaly N, **Carmona S**, Oliver MH, Jorgensen MR, Crowther C, et al. DODAG; a versatile new cationic lipid that mediates efficient delivery of pDNA and siRNA. J Control Release. 2010; 143(2): 222-32.
2. **Carmona S**, Jorgensen MR, Kolli S, Crowther C, Salazar FH, Marion PL, et al. Controlling HBV replication in vivo by intravenous administration of triggered PEGylated siRNA-nanoparticles. Mol Pharm. 2009; 6(3): 706-17.
3. Weinberg MS, Ely A, Barichievy S, Crowther C, Mufamadi S, **Carmona S**, et al. Specific inhibition of HBV replication in vitro and in vivo with expressed long hairpin RNA. Mol Ther. 2007; 15(3): 534-41.
4. **Carmona S**, Ely A, Crowther C, Moolla N, Salazar FH, Marion PL, et al. Effective inhibition of HBV replication in vivo by anti-HBx short hairpin RNAs. Mol Ther. 2006; 13(2): 411-21.
5. Arbuthnot P, **Carmona S**, Ely A. Exploiting the RNA interference pathway to counter hepatitis B virus replication. Liver Int. 2005; 25(1): 9-15.

The declaration of the contribution of the candidate and co-author agreement is provided in the appendix 8.10.

Permission to published was obtained from the publishers where necessary. Articles published in open access journals with Creative Commons Attribution license do not require additional copyright permission

Conferences proceedings

1. Abdullah Ely, **Sergio Carmona**, Carol Crowther, Steven Mufamadi, Marc Weinberg and Patrick Arbuthnot. Inhibiting HBV gene expression in vivo with long hairpin RNA sequences that target the viral X open reading frame. RNAi2006: Advances in RNA Interference Research, Oxford, England, 22-23 March 2006.
2. Abdullah Ely, **Sergio Carmona**, Carol Crowther, Steven Mufamadi, Marc Weinberg and Patrick Arbuthnot. Inhibiting HBV gene expression in vivo with long hairpin RNA sequences that target the viral X open reading frame. SASBMB 2006, Pietermaritzburg, South Africa, 2-5 July 2006.
3. **Sergio Carmona**, Abdullah Ely, Naazneen Moolla, Carol Crowther, Marc Weinberg and Patrick Arbuthnot. Inhibiting HBV replication with short hairpin RNA and siRNAs that target the viral X open reading frame. The 5th anniversary International Symposium for Gene Design and Delivery, Tokyo, Japan, 20-21 May 2005.
4. **Sergio Carmona**, Naazneen Moolla, Abdullah Ely, Carol Crowther, Marc Passman, Marc Weinberg, Patrick Arbuthnot. Effective Inhibition of HBV Replication with Short Hairpin RNAs that Target the Viral X Open Reading Frame. Keystone Symposia, Colorado, USA, 8-14 January 2005.
5. Abdullah Ely, **Sergio Carmona**, Naazneen Moolla, Carol Crowther, Marc Passman, Marc Weinberg, Patrick Arbuthnot. Using Short Hairpin RNAs that Target the Hepatitis B Virus X Open Reading Frame to Inhibit Viral Replication. RNAi Europe, London, England, 18-19 October 2004.
6. Abdullah Ely, Marc Weinberg, Naazneen Moolla, **Sergio Carmona**, Patrick Arbuthnot. Inhibiting HBV Gene Expression in Cultured Cells using Micro-RNA. International Meeting of the Molecular Biology of the Hepatitis B Viruses, Bergamo, Italy, 7-10 September 2003.

Patent:

Publication number	WO2005021751 A1
Publication type	Application
Application number	PCT/IB2004/002816
Publication date	10 Mar 2005
Filing date	31 Aug 2004
Priority date	1 Sep 2003
Also published as	US20080207539

Inventors Patrick Arbuthnot, Marc Weinberg, Sergio Catril Carmona, Ely Abdullah

Abstract:

The invention provides a self-processing RNA expression cassette which includes at least one pair of processing units, an RNAi effector sequence of predetermined length that regulates target gene expression which is flanked by said pair of processing units; and at least one pair of cognate ribozyme cis-cleavage target sites located 5' and 3' of the RNAi effector sequence. The self-processing RNA expression cassette is able to express in vivo and in vitro and the RNAi effector sequence includes at least one target recognition sequence derived from the Hepatitis B Virus (HBV) X gene (HBx).

Abstract

Globally, an estimated 257 million people were living with chronic hepatitis B virus (HBV) infection in 2015. The epidemic is concentrated predominantly in sub-Saharan Africa and Southeast Asia. Long-term complications of chronic HBV infection are cirrhosis and hepatocellular carcinoma. Currently licensed therapies have limited efficacy in eradication of HBV. Therefore, the need for new therapeutic modalities remains.

RNA interference (RNAi) is a highly conserved sequence-specific gene silencing pathway. RNAi is activated by short interfering RNAs (siRNAs) which have therapeutic potential and can be exploited against HBV. RNAi effectors may be synthetically produced or derived from expressed RNA sequences. This approach requires efficient and safe delivery of these effectors.

The aim of this thesis was to determine whether HBV replication could be inhibited by exploiting the RNAi pathway. We targeted HBV *X* open reading frame (ORF), a highly conserved sequence that overlaps all viral transcripts and codes for HBx, a viral protein critical for replication and persistence. We developed and evaluated novel lipid based vectors to deliver siRNAs.

Effective, short hairpin RNAs (shRNA), long hairpin RNAs (lhRNA) and synthetic siRNAs were selected *in vitro*. Viral- and non-viral vectors (NVV) were developed for delivery. These included recombinant adenoviral vectors, lipid-based pegylated-siRNA nanoparticles and cationic lipid vectors. These therapeutic complexes were assessed in a model of transient infection, using hydrodynamic tail vein injection, and one with features of chronic infection, using HBV transgenic mice.

We demonstrated effective HBV inhibition by RNAi effectors. Molecular analysis revealed intracellular processing of the shRNAs was more effective than lhRNAs. Highly effective shRNAs demonstrated processing of the intended strand. HBV inhibition did not elicit innate immune responses. Assembly of cationic lipid-based NVV with anti-HBV synthetic siRNA was successful and resulted in HBV inhibition *in vitro* and *in vivo* models.

This body of work provides substantial evidence that different RNAi modalities can suppress HBV replication culture and animal models of acute and chronic HBV infection. *HBx* ORF was shown to be a highly suitable target. Despite these optimistic findings, several challenges still remain for RNAi-based therapies to reach the clinic. Safe and effective delivery strategy is an important future objective.

Acknowledgements

I am grateful to my supervisor and mentor Professor Patrick Arbuthnot for inculcating in me to the rigor of science, sharing the enthusiasm for molecular biology and the possible applications in medicine. Most of all, I am appreciative for his guidance and patience.

I would like to extend my gratitude to Dr Alexio Capovilla, Prof Abdullah Ely, and Prof. Marco Weinberg for their assistance and invaluable collegiate support during the course of this work. Thank you to Dr Carol Crowther and Mrs Gladys Gagliardi for providing technical support during the study.

I am indebted to Dr. Felix Salazar and Dr. Patricia Marion from Stanford University, Stanford and Hepadnavirus Testing, Inc. Mountain View, CA, USA. The *in vivo* studies on the HBV transgenic mice were possible because of their support.

I am thankful to the vector core facility of the University Hospital of Nantes, supported by the Association Française contre les Myopathies (AFM) for providing the adenovirus vectors and also to Michael Nassal for providing the pCH-9/3091 plasmid.

This study was possible thanks to the financial support from, The South African Innovation Fund, The National Research Foundation and the South African Poliomyelitis Research Foundation.

TABLE OF CONTENTS

DECLARATION ..... **II**

DEDICATION ..... **III**

LIST OF PUBLICATIONS ..... **IV**

CONFERENCES PROCEEDINGS ..... **V**

PATENT: ..... **VI**

ABSTRACT ..... **VII**

ACKNOWLEDGEMENTS ..... **IX**

LIST OF FIGURES ..... **XIV**

LIST OF TABLES ..... **XVII**

LIST OF ABBREVIATIONS ..... **XVIII**

LIST OF SYMBOLS ..... **XX**

CHAPTER 1: INTRODUCTION **1**

1.1 THE HEPATITIS B VIRUS EPIDEMIC 1

1.1 HBV INFECTION 3

1.2 MANAGEMENT OF CHRONIC HBV INFECTION 4

1.3 THE HEPATITIS B VIRUS 7

1.3.1 The virion *7*

1.3.2 The Viral Proteins *8*

1.3.2.1 Core 8

1.3.2.2 Envelope 9

1.3.2.3 Reverse Transcriptase 9

1.3.2.4 HBx 9

1.3.3 The HBV genome *11*

1.3.4 Stages of the HBV replication cycle *12*

1.3.5 HBx and cccDNA *14*

1.4 RNA INTERFERENCE 16

1.4.1 The RNAi pathway *17*

1.4.2 Harnessing the therapeutic potential of siRNA *19*

1.4.2.1 Expressed RNAi effectors 20

1.4.2.2 Synthetic siRNAs 23

1.1.1.1.1 Modifications to synthetic siRNAs 23

1.1.1.1.2 Minimising Off-target effects 24

1.1.1.1.3 Reducing siRNA's stimulation of non-specific immune responses 26

1.5 DELIVERY OF RNAI EFFECTORS: VIRAL VECTORS AND NON-VIRAL VECTORS 27

1.5.1 Viral Vectors *27*

1.5.1.1 Adenovirus vectors 28

1.5.1.2 Adeno-associated virus vectors 28

1.5.2 Non-viral vectors *29*

1.5.2.1 Lipid based siRNA effector vectors 31

1.6 AIMS AND OBJECTIVES 34

CHAPTER 2: EXPLOITING THE RNA INTERFERENCE PATHWAY TO COUNTER HEPATITIS B VIRUS REPLICATION 36

2.1 ABSTRACT: 37

2.2 RNAI-BASED INHIBITION OF HBV GENE EXPRESSION 39

2.3 CHARACTERISTICS OF ANTI-HBV SIRNA SEQUENCES 40

2.4 NON-SPECIFIC EFFECTS OF INTERFERING RNA 42

2.5 CONCLUSIONS 42

2.6 REFERENCES 42

CHAPTER 3: EFFECTIVE INHIBITION OF HBV REPLICATION *IN VIVO* BY *ANTI-HBX* SHORT HAIRPIN RNAS 44

3.1 INTRODUCTION 45

3.2 RESULTS AND DISCUSSION 46

3.3 MATERIALS AND METHODS 53

3.4 REFERENCES 54

CHAPTER 4: SPECIFIC INHIBITION OF HBV REPLICATION *IN VITRO* AND *IN VIVO* WITH EXPRESSED LONG HAIRPIN RNA 56

4.1 INTRODUCTION 57

4.2 RESULTS 58
4.3 DISCUSSION 61
4.4 MATERIALS AND METHODS 62
4.5 REFERENCES 63

CHAPTER 5: CONTROLLING HBV REPLICATION *IN VIVO* BY INTRAVENOUS ADMINISTRATION OF TRIGGERED PEGYLATED SIRNA-NANOPARTICLES 65

5.1 ABSTRACT 66
5.2 INTRODUCTION 66
5.3 EXPERIMENTAL SECTION 68
5.4 RESULTS 72
5.5 DISCUSSION 75

CHAPTER 6: DODAG; A VERSATILE NEW CATIONIC LIPID THAT MEDIATES EFFICIENT DELIVERY OF PDNA AND SIRNA 78

6.1 ABSTRACT 79
6.2 INTRODUCTION 79
6.3 MATERIALS AND METHODS 81
6.4 RESULTS 83
6.5 DISCUSSION 86
6.6 CONCLUSION 88
6.7 REFERENCES 88

CHAPTER 7: DISCUSSION AND CONCLUSION 90

7.1 DESIGN AND EFFICACY OF RNAI EFFECTORS 90
7.2 DELIVERY OF RNAI EFFECTORS 93
7.3 RNAI EFFECTOR OFF-TARGET EFFECTS 97
7.4 CONCLUSION 98

CHAPTER 8: APPENDICES 99

8.1 ETHICS CERTIFICATES 99
8.2 CHAPTER 3 - SUPPLEMENTARY DATA 104
8.2.1 Interferon Response 104

8.3 CHAPTER 4 - SUPPLEMENTARY DATA 106

8.4 CHAPTER 5 - SUPPLEMENTARY DATA 107

8.5 PROCESSING OF SHRNA 6 AND SHRNA 10 111

8.6 POL II AND POL III PROMOTER DRIVEN EXPRESSION OF ANTI HBV SHRNAS 112

8.7 SEQUENCE ALIGNMENT OF U6 SHRNA 5 PASSENGER STRAND 115

8.8 RELATED ADDITIONAL PUBLICATION 119

8.9 SIMILARITY REPORT 130

8.10 DECLARATIONS AND CO-AUTHORS AGREEMENT 135

CHAPTER 9: REFERENCES 141

LIST OF FIGURES

FIGURE 1.1: GLOBAL PREVALENCE OF HEPATITIS B INFECTION. 2

FIGURE 1.2: HEPATITIS B VIRUS GENOME. 8

FIGURE 1.3: HEPATITIS B VIRUS X PROTEIN FUNCTIONAL DOMAINS. 10

FIGURE 1.4: THE HBV REPLICATION CYCLE. 13

FIGURE 1.5 BIOGENESIS OF MIRNA (REPRODUCED WITH PERMISSION). 18

FIGURE 1.6: SCHEMATIC REPRESENTATION OF THE STRUCTURE OF EXPRESSED RNAI EFFECTORS. 21

FIGURE 1.7: CONVENTIONAL AND MODIFIED SYNTHETIC RNAI ACTIVATORS 25

FIGURE 1.8: COMPOSITION OF LIPID BASED NON-VIRAL DELIVERY VECTORS 31

FIGURE 2.1 ORGANIZATION OF THE HEPATITIS B VIRUS (HBV) GENOME 38

FIGURE 3.1 HBV TARGET SITES AND SHRNA-ENCODING VECTORS 46

FIGURE 3.2 SHRNA-MEDIATED INHIBITION OF HBSAG SECRETION AND HBV–EGFP FUSION MARKER PROTEIN EXPRESSION IN TRANSFECTED CELLS. 48

FIGURE 3.3 RNA ANALYSIS 49

FIGURE 3.4 EFFECTS OF SHRNA SEQUENCES ON HBV ANTIGEN PRODUCTION IN THE HYDRODYNAMIC INJECTION MODEL OF HBV REPLICATION 51

FIGURE 3.5 EFFECTS OF RECOMBINANT ADENOVIRUS-MEDIATED SHRNA DELIVERY ON VIRAL REPLICATION MARKERS IN THE HBV TRANSGENIC MOUSE MODEL 52

FIGURE 4.1 LHRNA SEQUENCES AND HBV TARGET SITES 58

FIGURE 4.2 HBSAG SECRETION AND IFN RESPONSE-RELATED GENE EXPRESSION IN TRANSFECTED CELLS IN CULTURE 58

FIGURE 4.3 EFFECTS OF HAIRPIN SEQUENCES ON MARKERS OF HBV REPLICATION IN THE HYDRODYNAMIC INJECTION MODEL OF HBV REPLICATION. 59

FIGURE 4.4 ASSESSMENT OF IN VIVO IFN RESPONSE 59

FIGURE 4.5 ASSESSMENT OF SILENCING EFFICACY OF SHRNA 5, SHRNA 6, AND LHRNA 1 AGAINST MUTANT AND WILD-TYPE HBV TARGETS. 60

FIGURE 4.6 DETECTION OF SIRNA SEQUENCES PRODUCED FROM EXPRESSED LHRNA 1 AND SHRNA 5. 60

FIGURE 4.7 SILENCING EFFICIENCY ACROSS THE SPAN OF THE LHRNA1 TARGET SEQUENCE. 61

FIGURE 5.1 CHEMICAL COMPONENTS AND STABILITY OF SIRNA NANOPARTICLES. 68

FIGURE 5.2 BIODISTRIBUTION AND EXPERIMENTAL TOXICITY ASSESSMENT OF SIRNA NANOPARTICLE FORMULATIONS 74
FIGURE 5.3EFFECT OF SIFECTPLUS NANOPARTICLES ON MARKERS OF HBV REPLICATION IN CELL CULTURE AND MHI MODELS. 75
FIGURE 5.4 MARKERS OF VIRAL REPLICATION AND IMMUNOSTIMULATION IN HBV TRANSGENIC MICE. 76
FIGURE 6.1 SCHEMATIC ILLUSTRATION OF STRUCTURES OF CATIONIC LIPIDS AND NEUTRAL CO-LIPIDS CONSTITUENTS SYNTHESIZED OR USED IN TRANSFECTION STUDIES. 80
FIGURE 6.2 TRANSFECTION DATA FOR THREE CELL LINES AND 20 DIFFERENT LIPOPLEX NANOPARTICLE SYSTEMS WITH LIPOFECTAMINE 2000 TRANSFECTION AS POSITIVE CONTROL (PDNA:LIPID RATIO: 1:2.5, W/W). 85
FIGURE 6.3 PERCENTAGE LDH CYTOTOXICITY DATA FOR LIPOPLEX NANOPARTICLES FORMULATED WITH CATIONIC LIPIDS DODAG 8, CDAN 5, CEAG 6 AND CAPG 7 WITH EITHER DOPE 1 OR MM27 3 AS HELPER CO-LIPIDS. 86
FIGURE 6.4 FLUORESCENCE MICROSCOPY OF HELA CELLS POST TRANSFECTION WITH DODAG 8/DOPE 1 CATIONIC LIPOSOME–PDNA COMPLEXES (LIPOPLEXES, X400 MAGNIFICATION). 86
FIGURE 6.5 FORMULATION AND EXPERIMENTAL ASSESSMENT OF SIRNA-DODAG 8 NANOPARTICLE FORMULATIONS. 87
FIGURE 8.1 ASSESSING ACTIVATION OF THE INTERFERON RESPONSE – 105
FIGURE 8.2: REPRESENTATIVE FIELDS OF TRANSFECTED HEK293 CELLS TRANSFECTED WITH AN HBV GFP REPORTER PLASMID. 106
FIGURE 8.3 UREA, CREATININE AND ELECTROLYTE LEVELS IN BLOOD POST IV ADMINISTRATION 107
FIGURE 8.4 REPRESENTATIVE SMEARS OF MURINE BLOOD POST IV ADMINISTRATION 108
FIGURE 8.5 HISTOLOGICAL EXAMINATION OF NMR-1 MURINE LIVER SECTIONS POST ADMINISTRATION OF CONTROL AND SIRNA 109
FIGURE 8.6 ALIGNMENT OF SIRNAS WITH REPRESENTATIVE HBV GENOTYPE SEQUENCES. 110
FIGURE 8.7 NORTHERN BLOT HYBRIDISATION ANALYSIS OF PROCESSED SHRNA 6 AND 10 MRNA EXPRESSED FROM U6 PROMOTER. 111
FIGURE 8.8 PREDICTED - CMV SHRNA 6 - RNA SECONDARY STRUCTURE 112
FIGURE 8.9 SILENCING EFFECT OF SHRNAS EXPRESSED FROM CMV AND U6 PROMOTERS 113
FIGURE 8.10 POL II AND POL III PROMOTER DRIVEN EXPRESSION OF ANTI HBV SHRNAS. 114
FIGURE 8.11 SCHEMATIC REPRESENTATION OF THE PREDICTED HAIRPIN STRUCTURE OF SHRNA 5 115

FIGURE 8.12 GRAPHIC SUMMARY OF BLAST SEARCH USING THE PASSENGER STRAND OF U6 SHRNA 5 AS THE SEARCH STRING. 116

FIGURE 8.13 SEQUENCES PRODUCING HITS AGAINST THE U6 SHRNA PASSENGER STRAND RANKED BY MAXIMUM SCORE. 116

FIGURE 8.14 REPRESENTATIVE ALIGNMENT OF THE U6 SHRNA 5 PASSENGER STRAND ON CHROMOSOME 1 117

FIGURE 8.15 DETAILED ALIGNMENT OF THE U6 SHRNA 5 PASSENGER STRAND ON TWO HITS ON CHROMOSOME 4 118

LIST OF TABLES

TABLE 1-1: NOVEL ANTI-HBV ANTIVIRAL AGENTS IN EARLY CLINICAL AND PRECLINICAL DEVELOPMENT. 6

TABLE 2-1SCORING OF ANTI-HBV SIRNAS ACCORDING TO EIGHT-COMPONENT ALGORITHM THAT PREDICTS SIRNA EFFECTIVENESS 41

TABLE 3-1 NUCLEOTIDE SEQUENCES OF PCR REVERSE PRIMERS USED TO GENERATE HBV U6 SHRNA CASSETTES 47

TABLE 5-1 DESIGNED ANTI-HBV SIRNAS AND THEIR HBV TARGET SEQUENCES 75

TABLE 6-1 LIPOSOME AND LIPOPLEX NANOPARTICLE SIZES WITH INCLUDED POLYDISPERSITY INDICES. 84

TABLE 6-2 EXPERIMENTAL TOXICITY AND INFLAMMATION MARKERS 87

TABLE 8-1 NUCLEOTIDE SEQUENCES OF OVERLAPPING OLIGONUCLEOTIDES USED TO GENERATE CMV SHRNA-ENCODING SEQUENCES. 112

List of Abbreviations

AAV	Adeno-associated virus
Ad	Adenovirus
Ago 2	Argonaute protein 2
APO	Apolipoprotein
AUG	Start codon
BCP	Basal core promoter
bp	base pair
cccDNA	covalently closed circular DNA
CP	Core promoter
Cul4	Cullin4
DDB1	damaged DNA-binding protein 1
DGCR8	diGeorge critical region 8 protein
DOPE	dioleoylphosphatidylethanolamine
DR1	Direct repeat 1
dsDNA	double-stranded DNA
dsRNA	double-stranded RNA
EnhI	HBV enhancer element I
HBc	HBV core protein
HBcAg	Hepatitis B virus core antigen
HBeAg	HBV e antigen
HBsAg	Hepatitis B virus surface antigen
HBV	Hepatitis B virus
HBx	X protein
HCC	Hepatocellular carcinoma
HD Ad	Helper-dependent adenovirus
HIV	Human immunodeficiency virus
IFN	Interferon
IL	Interleukin
kb	kilobase
kDa	kilo Daltons
L	Large surface protein
LNA	Locked nucleic acid
lnRNA	long hairpin RNA
M	Middle surface protein
MCP-1	Monocyte chemotactic protein-1
miRNA	microRNA
mirR*	passenger strand of the micro RNA
MW	Molecular weight
nm	nanometre
nt	nucleotide
NTCP	sodium taurocholate co-transporting polypeptide
NVV	non-viral vector

OAS-1	Oligoadenylate synthetase-1
ORF	Open reading frame
P	Polymerase
PEG	Polyethylene glycol
pgRNA	Pre-genomic RNA
Pol	RNA polymerase
pre-miR	precursor miRNA
preC	pre-core
pri-miR	primary miRNA
PTGS	Post-transcriptional gene silencing
rcDNA	relaxed circular DNA
RISC	RNA-induced silencing complex
RNAi	RNA interference
RT	Reverse transcriptase
S	Major surface protein
shRNA	short hairpin RNA
siRNA	small interfering RNA
sisiRNA	small internally segmented interfering RNA
Smc	structural maintenance of chromosomes
SNALPs	Stable nucleic acid lipid particles
TALEN	Transcription activator-like effector nuclease
TLR	Toll-like receptors
TNF	Tumour necrosis factor
TP	Terminal protein
TRBP	HIV transactivating response RNA-binding protein
VV	Viral vector
WHO	World health organization
WHV	Woodchuck hepatitis virus
X	X protein

List of symbols

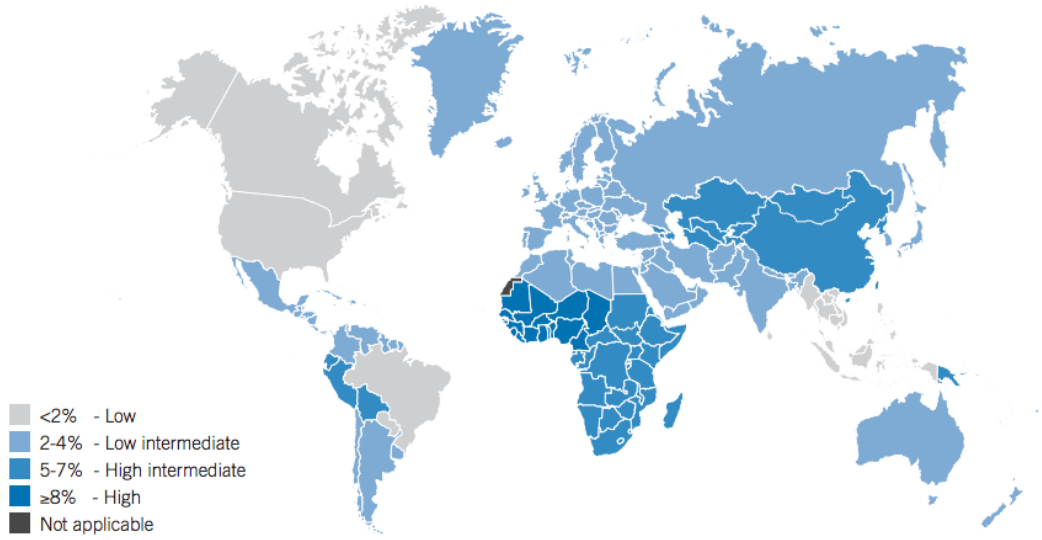
α	alpha
ß	beta
ε	epsilon
γ	gamma

Chapter 1: INTRODUCTION

1.1 The Hepatitis B Virus epidemic

In 2015, an estimated 257 million people were living with chronic hepatitis B virus (HBV) infection and 2.7 million are co-infected with HIV (1). Worldwide, it is estimated that approximately two billion people have evidence of present or past infection with HBV. The prevalence of chronic infection, defined as persistence of HBV surface antigen (HBsAg) for at least six months, varies markedly by age and by geographic distribution (Figure 1.1), with the highest burden of disease observed in sub-Saharan Africa and East Asia (2). The large burden of disease is exacerbated further by the partial efficacy of available licensed antivirals and limited access of these agents in highly endemic areas. Developing new strategies to target chronic HBV infection thus remains critical.

A



B

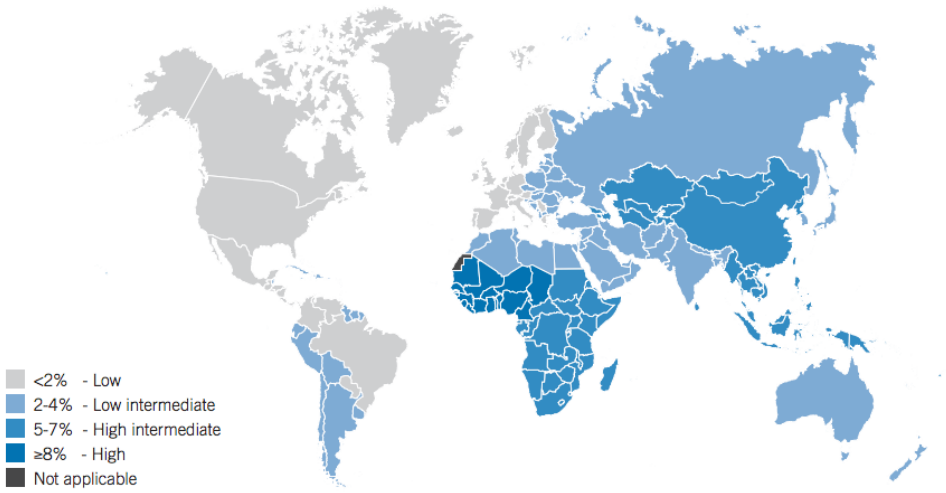


Figure 1.1: Global prevalence of hepatitis B infection.

The worldwide HBsAg seroprevalence of children 5-9 years (**A**) and adults 19-49 years (**B**). Source: WHO 2015 Guidelines for the prevention, care and treatment of persons with chronic Hepatitis B Infection, March 2015, Geneva, Switzerland.

The elimination of HBV infection will require multiple approaches, including universal immunisation and viral suppression to avert new transmissions. However, many decades of intense immunisation programmes would be required to eliminate HBV infection by immunologic prevention on its own. Moreover, elimination of chronic HBV would depend on a highly compliant universal programme of immunisation in infants, adolescents (3) and persons at high risk of infection (4). Despite availability of a plasma-derived hepatitis B vaccine since 1982 (5) and introduction of vaccination by the World Health Organization (WHO) as part of the Expanded Programme for Immunisation in 1992 (6, 7), over 240 million carriers remain worldwide. Remarkably, from 1990 to 2005, the global HBV prevalence has decreased as a result of expanded vaccination (8). However, alternative therapeutic approaches need to be developed as the eradication of HBV would take more than can be achieved by further scale-

up of immunisation programmes alone. The prospect of eliminating HBV is hampered further as the current licensed therapies do not cure chronic HBV infection.

1.1 HBV Infection

HBV is transmitted by exposure of mucosal membranes or non-intact skin to infected blood and body fluids, including saliva, semen and vaginal fluids. HBV infection is usually perinatal from mother-to-child or through parenteral contact (9, 10).

The clinical course of HBV infection may be acute or chronic. It may present sub-clinically, asymptomatically and very rarely as acute fulminant hepatitis (11). The risk of developing chronic infection correlates inversely with age at the time of infection. This risk ranges from 90%, if infection occurs during the neonatal period from HBV e antigen (HBeAg) positive mothers, to less than 5%, if infection occurs during adulthood (12, 13). A less aggressive host response often denotes a modest cell-mediated immune reaction. This often runs a subclinical course which leads to persistent viral carrier state and frequently results in chronic active liver disease. In chronic infection, viral DNA load is generally lower than during acute infection, although it may vary substantially among infected individuals. High viral titres usually correlate with the expression of HBeAg. Interestingly, following acute infection, as defined by the loss of viral antigens and the emergence of anti-HBs immunoglobulin, low levels of HBV DNA may persist for many years (14). HBeAg-negative chronically infected individuals retain the virus through a “non-replicative” mechanism as the rate of viral replication appears negligible. However, mutations in the preC region result in viral infections in the absence of HBeAg (15, 16). Mutations in this region may account for approximately 95% of HBeAg-negative asymptomatic carriers in sub-Saharan Africa (17).

There are several reviews that address the current and future approaches to the management of chronic HBV (18, 19). The field of HBV molecular virology and new drug discovery has developed at an unprecedented pace. To cover the breadth of evidence in all these areas would be challenging and beyond the scope of this thesis. The following is a focused review on the biology of HBV relevant to this thesis, the key role HBV X (HBx) protein plays in viral replication and how the RNA interference (RNAi) pathway could be exploited to control viral replication by targeting HBx.

1.2 Management of chronic HBV infection

Despite the remarkable advances made in elucidating the molecular biology of the virus, currently available therapeutic agents remain limited to two broad classes: immunomodulators (such as interferon (IFN)-α) and nucleoside or nucleotide analogues (such as, lamivudine, entecavir and tenofovir). These have shown to be effective in supressing HBV replication, prevent progression to cirrhosis, reduce HCC risk and death (20). However, IFN therapy is of limited effect with only 4% loss of HBsAg after six months of treatment (21, 22). Long-term management remains challenging with the risk of emergence of drug resistance and drug-associated side effects. The WHO recommends the use of either tenofovir or entecavir as first-line treatment because of their high genetic barrier to resistance (20). Although these are potent viral polymerase inhibitors, they have no effect on viral transcription from persistent covalently closed circular DNA (cccDNA). The stability of cccDNA ensures viral persistence through the life-span of infected hepatocytes. Thus, treatment with nucleotide or nucleoside analogues is required for life. In chronic infection, loss of cccDNA from long-term treatment is likely a reflection of hepatocytes death (23).

Elucidating the molecular biology of HBV replication and the viral dependencies on host cellular pathways has opened avenues for potential novel therapeutics. New direct antivirals in early clinical trial include novel HBV polymerase inhibitors, entry inhibitors directed against sodium taurocholate co-transporting polypeptide (NTCP) receptor and cccDNA cleaving agents. Compounds targeting host sites include Toll-like receptor (TLR)- agonists and IFN inducers (reviewed in (18)). Examples of candidate therapeutic agents, target sites and clinical phase of development are summarised in Table 1-1 .

Table 1-1: Novel anti-HBV antiviral agents in early clinical and preclinical development.

(Modified from references (18, 24))

Drug class	Antiviral agent	Status	Comments	Reference:
Entry inhibitors	Myrcludex B	Phase II	First-in-class entry inhibitor inactivating the HBV receptor sodium taurocholate co-transporting polypeptide	(25)
	Irbesartan (Avapro)	FDA-approved (for hypertension and diabetic nephropathy)	Potent inhibitor of HBV. Disrupts Na(+)-dependent taurocholate co-transporting polypeptide activity.	(26)
Inhibitors of viral mRNA	ALN-HBV	Phase I-II	siRNA against *X* ORF	
	ARB-1467	Phase II	LNP siRNA	(27)
	RO7020322 (RG7834)	Phase I	Oral agent. Small molecule that inhibits HBV mRNA expression. Reduces HBsAg levels and viremia.	(28)
	IONIS-HBVLRx (GSK33389404)	Phase I	Antisense molecule	(29)
Gene editing	EBT106	Preclinical	CRISPR/Cas9 system	(30)
	Anti-HBV sgRNA	Preclinical	CRISPR/Cas9 system.	(31)
	TALEN	Preclinical		(32)
	Zinc finger nuclease	Preclinical		(33)
HBsAg secretion inhibitor	REP2139 & REP2165	Phase II		(34)
cccDNA inhibitor	Disubstituted sulphonamides	Preclinical		(35)
Therapeutic vaccine	GS-4774	Phase I	Recombinant X, S & C epitopes	(36)
	TG-1050	Phase I	Non-replicative adenovirus. C, pol & S epitopes.	(37)
TLR agonists	GS-9620	Phase II	TLR-7 agonist	(38)
Immuno-modulators	SB9200 (Iranigivir)	Phase II	RIG-I and NOD-2 agonist	(39)

1.3 The hepatitis B virus

1.3.1 The virion

HBV is a relatively small, enveloped virus of approximately 42 nm in diameter that belongs to the *Hepadnaviridae* family. This family includes a number of related viruses with mammalian and avian hosts. HBV is a DNA virus that replicates by protein-primed reverse transcription of an RNA intermediate (40).

The nucleocapsid carries a single copy of partially double-stranded, non-covalently closed circular DNA of approximately 3.2 kb in length, referred to as relaxed circular DNA (rcDNA). The rcDNA comprises a full length minus strand DNA and a shorter-than-genome length plus strand. The 5' end of the minus strand is covalently linked to the viral reverse transcriptase or P protein (polymerase), while the 5' end of the plus strand consists of an RNA oligonucleotide (Figure 1.2).

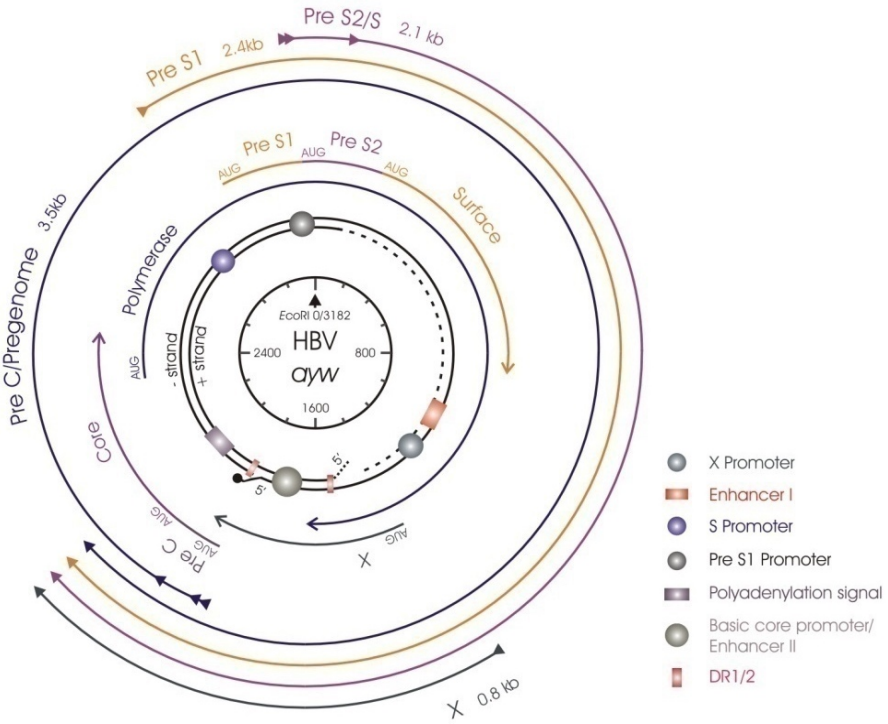


Figure 1.2: Hepatitis B virus genome.

Schematic representation of the partially double stranded 3.2 kb HBV genome. The outer circumferential arrows represent the four major viral transcripts with a single terminal polyadenylation site. Transcriptional regulatory elements and nucleotide co-ordinates are indicated at the centre. Of significance is the HBV *X* open reading frame, which overlaps all the viral transcripts, (adopted from ref. (41)).

1.3.2 The Viral Proteins

1.3.2.1 Core

Translation initiated from the preC AUG codon generates a precursor protein (pre-core) containing a peptide signal that directs it to the endoplasmic reticulum (42), where it undergoes post-translational modification by host proteases to produce a 15 kDa peptide/protein. This protein, known as HBeAg, is secreted into circulation (43), exhibits distinct antigenic properties and is not required for viral assembly or replication. In fact, preC early chain termination

mutants replicate in culture and have been isolated during natural infection (44). Presence of HBeAg in the serum of chronic carriers indicates high viral replication. Translation initiated at the second preC/C AUG codon gives rise to HBV core protein (HBc), a 21 kDa protein that dimerises. The C-terminal domain harbours the nuclear localisation signal for HBc, the protein dimers assemble into an approximately 28 nm viral nucleocapsid.

1.3.2.2 Envelope

There are three surface antigens expressed by initiation of translation at three in-frame codons located in the pre-surface/surface region (45). These define the amino terminal end of the large (L), middle (M) and major (S) surface proteins respectively. The L, M and S proteins are found in the envelope of the virus at a ratio of 1:1:4 (46). The nucleocapsid is covered by a membrane formed by these three envelope proteins in conjunction with host lipids acquired during budding into the endoplasmic reticulum (47, 48). These three surface proteins are glycosylated and form part of the transmembrane structure (46).

1.3.2.3 Reverse Transcriptase

The viral polymerase has a molecular weight of approximately 90 kDa and three functional domains: i) terminal protein (TP) which functions as a primer during the DNA synthesis of the minus-strand, ii) reverse transcriptase (RT) and iii) RNase H domains involved in viral replication and degradation of the Pre-genomic RNA (pgRNA) (47).

1.3.2.4 HBx

HBx is 154 amino acids long and produces a protein of ~17.5 kDa (Figure 1.3). It is under transcriptional control of HBV enhancer element I (EnhI) and by its own internal promoter (49, 50). The structure and function of HBx has been difficult to decipher because of unreliable *in vitro* assays that have been limited to transfection of plasmid DNA expressing HBx (Comprehensively reviewed by others (51, 52)). HBx is phosphorylated (53) and acetylated

when expressed in cell lines (54). Serial deletion studies of the *HBx* ORF demonstrate that the region spanned by amino acids 58 to 140 is essential for its major ascribed functions (55, 56). Removal of the N-terminal domain results in HBx over expression, which indicates presence of a transcriptional suppressor in this region (57, 58). A summary of the HBx functional domains is illustrated in Figure 1.3.

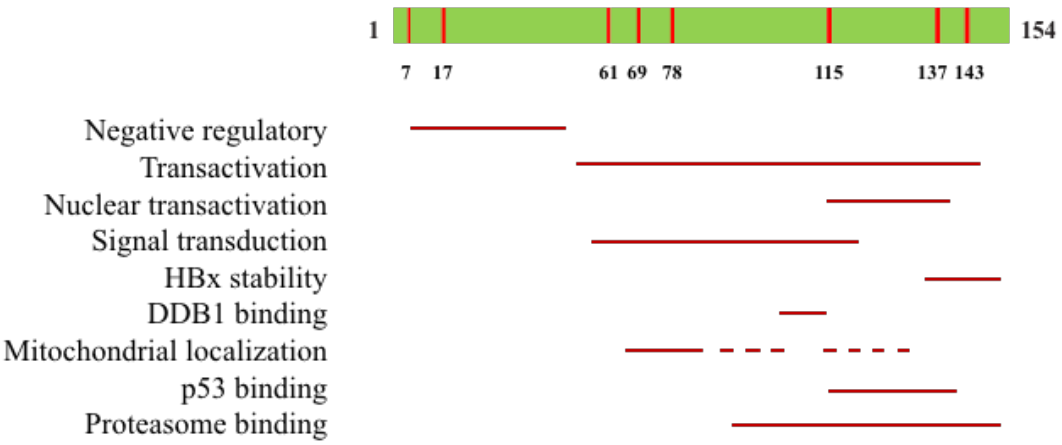


Figure 1.3: Hepatitis B virus X protein functional domains.
The HBx protein consists of 154 amino acids and has multiple functions that are essential for viral replication and cccDNA persistence. (figure has been modified from source (51)).

HBx is localised both in the cytoplasm and the nucleus (59-61), where it associates with a range of host proteins to alter many cellular mechanisms that range from regulation of signal-transduction (62, 63), cell cycle, (64), apoptosis, and DNA repair (65). HBx has also been implicated in HBV-associated carcinogenesis through interactions with p53. Furthermore, HBx alters the cellular pathways of quiescent hepatocytes to provide a more permissive environment for viral replication (51). The global effect of HBx could be viewed as a disruptor of the cellular milieu to enhance viral replication with the concomitant accumulation of cellular derangements with ultimate oncogenic consequences (reviewed in (63)). The cumulative body of evidence confirms HBx as a key therapeutic target.

1.3.3 The HBV genome

The viral genome is exceptionally compact with overlapping open reading frames (ORFs). All the ORFs, *Core* (*C*), *polymerase* (*P*), *envelope* (*S*) and *X* (*HBx*) are arranged in the same direction. Viral replication and transcription regulatory elements are incorporated within these ORF. Phylogenetic analysis has identified nine genotypes and several subgenotypes (66, 67). The virion carries a minus-strand DNA which spans the full genome and a plus-strand that covers approximately two-thirds of the genome and has a variable 3' end (Figure 1.2).

The major transcripts detected by Northern blot analysis are 3.5 kb, 2.4 kb, 2.1 kb and 0.8 kb in length. These are named pre-C/Pregenome, pre-S1, pre S2/S and X mRNAs respectively. The *C* ORF has two in-frame start codons designated preC (pre-core) and C (core) (Figure 1.2). The *P* ORF is devoid of its own promoter and is translated as part of a second cistron of the preC or pgRNA. The viral polymerase is involved in DNA- and RNA-dependent DNA polymerisation during viral replication (68). The large surface protein is translated from the 2.4 kb HBV transcript, while the middle and major surface protein arise from translation of the 2.1 kb mRNA (Figure 1.2).

The fourth ORF is the smallest of the HBV genome and codes for the HBx protein. The *HBx* ORF is present in all viral transcripts, is transcribed independently, under the control of its own promoter and Enh I which generates a small ~0.8 kb mRNA (69). The X promoter is positioned approximately 140 nucleotides (nt) upstream of the transcription initiation site and comprises only 20 nt (70, 71). Although this regulatory element overlaps with the 3' end of Enh I, the minimal X promoter can be separated from Enh I while still retaining its function (49). In

addition, HBx has been shown to transactivate Enh I and the X promoter, suggesting that *HBx* is autoregulated (52).

1.3.4 Stages of the HBV replication cycle

The replication cycle of HBV starts with infectious particles being trapped in the space of Disse (an area spanned by sinusoids and hepatocytes) through reversible attachment to the low affinity heparan sulphate proteoglycans on hepatocytes (72). This proceeds to attachment of N-terminal myristic acid of the preS1 site (72) to the extracellular loops of a hepatocyte-specific receptor, NTCP (73). Although this multiple transmembrane transporter had been described over two decades ago (74), it was not until recently that is was conclusively identified to be the HBV specific receptor. The discovery of the HBV receptor has been pivotal to the field as it has provided much awaited insight into molecular biology of HBV hepatocytes entry. This has resulted in development of *in vitro* and *in vivo* models of HBV life cycle and allowed for more effective testing of potential entry inhibitor antivirals (75-77). The preS1 domain is indispensable for receptor binding (78) and triggers viral entry which occurs by endocytosis or direct fusion of the hepatocyte plasma membrane to the viral envelope (Figure 1.4). The nucleocapsid, which is comprised of rcDNA and core protein, is released into the cytoplasm and then transferred to the nucleus (79).

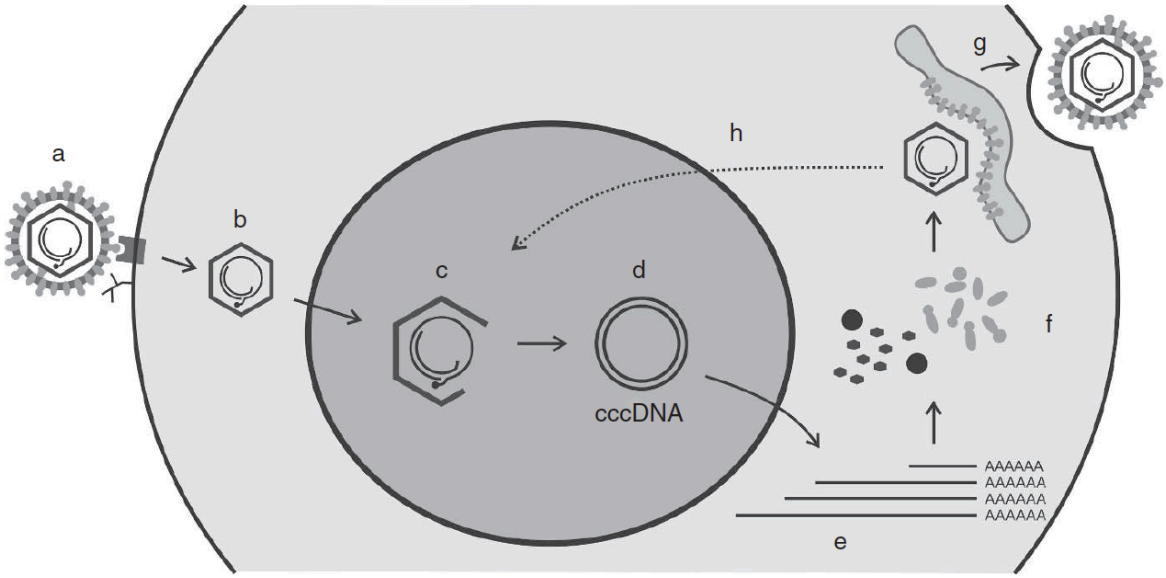


Figure 1.4: The HBV replication cycle.

(a) The small surface protein binds to glycosaminoglycans on the surface of hepatocytes. The virion attaches specifically and with high affinity to the sodium taurocholate co-transporting peptide receptor through interaction with the myristolated N-terminal region of the large surface protein. (b) After entry into the cytoplasm, the viral capsid containing relaxed circular DNA (rcDNA) is released and transported to the nucleus. (c) The rcDNA is released from the capsid and (d) "repaired" to form covalently closed circular DNA (cccDNA). This stable and problematic replication intermediate is the target of strategies employing gene editing to disable HBV replication. (e) The cccDNA serves as template for transcription of viral pregenomic RNA (pgRNA) and protein-coding mRNAs. (f) Translation to form viral proteins leads to assembly of capsid particles containing packaged pgRNA, reverse transcription of this replication intermediate and (g) release via the secretory pathway. Licensed nucleoside and nucleotide analogues inhibit reverse transcription, and candidate therapeutic RNA interference activators disable viral RNAs. (h) Some rcDNA may be recycled from nascent core particles to generate cccDNA within the nucleus.
Source: (adopted from ref. (80))

Once receptor-mediated endocytosis has taken place, the nucleocapsid is released into the cytosol where it is guided to the nucleus by the nuclear localisation signal of the C protein.

In the nucleus, the rcDNA is repaired to form cccDNA, which serves as the template for transcription of all viral RNAs. There are two groups of transcripts: genomic (pgRNA and preC RNA) and subgenomic (surface and X mRNAs) that are generated from four promoters and two enhancers on the cccDNA. They all have a 5' cap structure and are polyadenylated at a common 3' site. The essential transcript for viral replication is the pgRNA, which is generated by read-through transcription from the cccDNA (Figure 1.4). This is greater in length than the viral genome with a terminal repeated sequence of approximately 120 nt that includes a second copy of the DR1, ε signal and a polyadenylated tail (Figure 1.4). The cccDNA is a stable DNA form which serves as a template for the synthesis of multiple copies of progeny HBV genomes. Hepadnaviruses achieve this by maintaining their genome as a nuclear episomal cccDNA.

Viral replication is initiated by an unusual priming process. The N-terminal TP domain contains a tyrosine residue that serves as the primer for initiation of minus strand synthesis (81). This is covalently linked and remains bound to the minus strand and remains present in the virion. The binding of the P protein to ε induces two essential steps: recruitment of core proteins to form the viral capsid and synthesis of a 2-4 nt DNA (82-84). Finally, P protein reverse transcribes pgRNA into a progeny rcDNA genome (85). Reverse transcription of pgRNA to form viral genomic DNA occurs during the process of capsid formation (86). Mature nucleocapsids enter the secretory pathway and are exported as enveloped virions.

1.3.5 HBx and cccDNA

HBx does not bind DNA directly, but instead acts through interactions with host proteins (63, 87, 88). One of these binding partners is the damaged DNA-binding protein 1 (DDB1), which associates with HBx in response to damaged DNA and induces DNA repair (89, 90).

Remarkably, mutations that altered the binding between DDB1 and HBx result in inhibition of HBV replication (89, 91-93). The significance of this interaction arises from DDB1 binding to Cullin4 (Cul4), to form part of an E3 ubiquitin ligase complex (94). HBx, by capturing DDB1-E3 ubiquitin ligase, opens the pathway for the degradation of host proteins implicated in inhibition of viral replication. This sequestration strategy, which promotes viral replication, is also exploited by viruses other that HBV (95). Recently, two independent groups have identified the host regulatory factor that is degraded to be the structural maintenance of chromosomes (Smc) complex Smc5/6, (96, 97). This indicates that HBV replication is restricted by Smc5/6-mediated repression of viral extrachromosomal cccDNA. Thus, HBx orchestrates HBV replication by hijacking of the DDB1-E3 ubiquitin ligase and proteosomal degradation of Smc5/6. These are key observations and elucidate the role of HBx in providing cccDNA stability.

Woodchuck hepatitis virus (WHV) produces cccDNA, while transgenic mice do not (75). Previously, it was observed that HBV replication in transgenic mice harbouring HBx-deleted mutants was identical to wild type HBV (98, 99). This was contrary to findings in woodchucks infected with X-protein deleted WHV, which resulted in undetectable viral infection or viraemia (100, 101). Furthermore, in *trans*-complementation studies with HBx-expressing mice (which do not produce cccDNA), augmentation of HBV replication and persistence of infection was demonstrated (99). Subsequent work conducted *in vitro* and *in vivo* demonstrated that HBx expression significantly enhanced HBV viraemia (102). Hence, murine models are considered models of viral replication, whereas the woodchuck model is one of infection. Now, with the evidence provided by Decorsiere *et al*. and Murphy *et al*, we recognise that this is as a result of HBx lifting the block of Smc5/6 on episomal DNA transcription. Therefore, we can infer that

by targeting the *HBx* ORF we would not only disrupt all the HBV transcripts but would reduce HBx expression and consequently augment the inhibition on HBV replication (96, 97).

1.4 RNA interference

Since the breakthrough observation by Fire and Mello in 1998, of sequence specific gene silencing in *Caenorhabditis elegans* following the introduction of double-stranded RNA (dsRNA) (103), many studies unveiled a well conserved post-transcriptional process of RNAi which was found to be present across many phyla (104-106). Subsequent evidence that RNAi could be harnessed to induce post-transcriptional gene silencing (PTGS) of virtually any target gene, transformed the field of gene therapy (107). The seminal work from Elbashir and colleagues demonstrated that an exogenous synthetic 21 nt dsRNA duplex specifically suppresses the expression of endogenous genes in different mammalian cells (107). Since then, investigators have extensively studied the cellular mechanisms that enable RNAi (108)).

The cellular or endogenous effectors of RNAi are mature microRNAs (miRs). Mature miRs range from 19 to 20 nt and induce PTGS by partial base pairing to target RNA. miRs are members of a large class of non-coding RNA that regulate a wide range of biological processes in organisms ranging from nematodes to humans (109). miRs are essential in cellular functions from embryogenesis, differentiation to apoptosis (110-112) and have been shown to be dysregulated in many diseases (113, 114). RNAi effectors are now recognised not only for their role in PTGS but also in the regulation of gene transcription (115).

1.4.1 The RNAi pathway

The biogenesis of miR commences with transcription by RNA polymerase II (Pol II) of the primary miR (pri-miR). As is the case for mRNA, Pol II-transcribed pri-miRs are protected by a 5'-cap structure and have a poly-adenylation tail (116, 117). pri-miR can be found as single or in multiple (polycistronic) motifs within non-coding mRNA, or in an antisense orientation within transcripts or in transcripts that are within introns or in intergenic regions (112). miRs may also be generated from viral transcripts, where they regulate host function and viral replication during infection (118). Processing of pri-miRs occurs in the nucleus and is executed by the microprocessor complex, comprising the RNase III enzyme Drosha and its dsRNA-binding partner, diGeorge critical region 8 protein (DGCR8) (119-123). Drosha cleaves the pri-miRs two helical RNA turns into the stem at approximately 22 nt from the loop/stem junction (124).

Following cleavage of the pri-miR, a precursor-miR (pre-miR) hairpin of 70-100 nt in length is generated and contains a 5' phosphate group at the base of the stem and a 2 nt 3' hydroxyl overhang. The pre-miR is recognised by Exportin-5 and is transferred across the nuclear membrane in a Ran-GTP-dependant manner (125-127) (Figure 1.5)

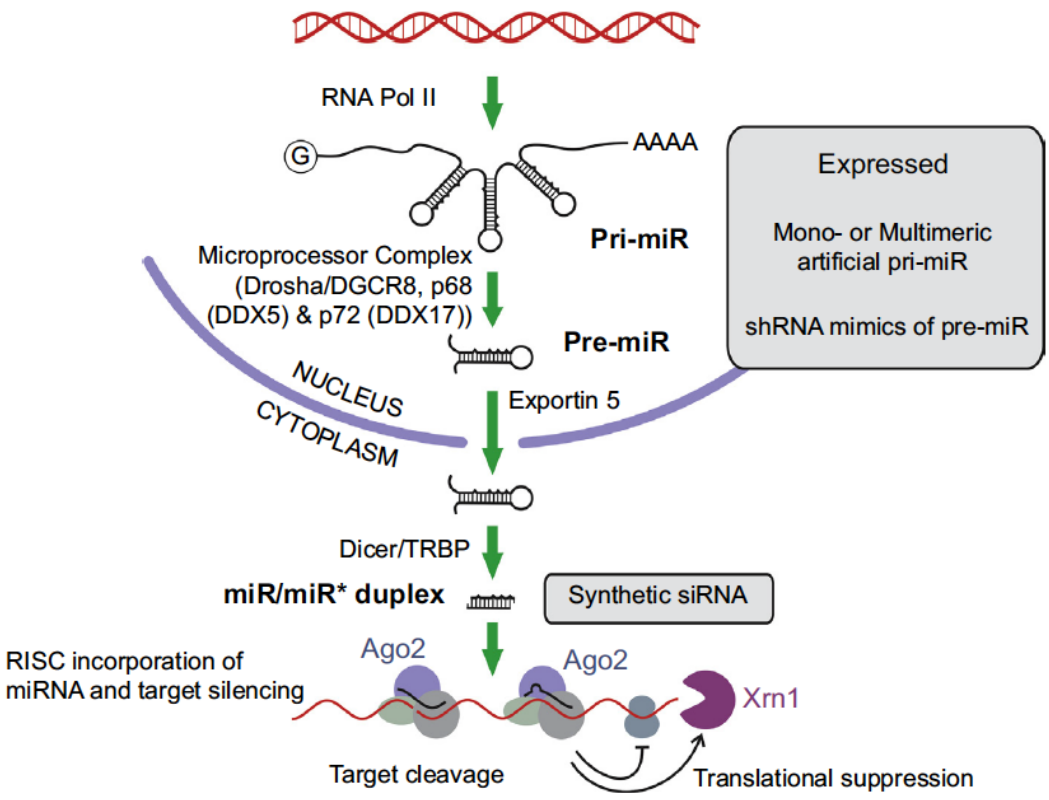


Figure 1.5 Biogenesis of miRNA (reproduced with permission).
Source: (adopted from ref. (128)).

In the cytoplasm, the pre-miR is cleaved by the RNase III enzyme Dicer to produce the miR duplex, in conjunction with the HIV-1 transactivator response element RNA-binding protein (TRBP) (129-135). Processing of pre-miRNA by Dicer/TRBP yields a miR duplex. Cleavage removes the loop of the hairpin to produce a miR of 22 nt and the complementary passenger strand with 2 nt overhangs at each 3' end. The duplex enters a ribonucleoprotein complex, the

RNA-induced silencing complex (RISC), and one strand is released, the passenger strand. The strand that remains behind is the mature miR, *i.e.* the guide strand. RISC utilises the guide strand to find mRNA with a complementary sequence that leads to endonucleolytic cleavage of the target mRNA (136). The miR strand that is retained in RISC serves as the guide strand and directs the complex to its RNA target by Watson-Crick base pairing. Loading into RISC is asymmetric, in that the strand with the highest 5' end thermodynamic instability is preferentially incorporated to become the guide strand (137). This bias is a function of the helicase domain of RISC (138). The other strand is referred to as the passenger strand, miR*. If the complementarity between the miR and its target mRNA is perfect, the target RNA is cleaved by Ago2 of the RISC complex (108, 139-142). When miR and the target sequences are partially complementary, translational suppression is induced and target cleavage does not occur. Target specificity is provided by the "seed" region of the guide strand. This is the region that spans from nucleotides 2-8 on the guide strand and which has to be fully complementary to the target sequence to induce silencing (143).

1.4.2 Harnessing the therapeutic potential of siRNA

Following the discovery of the RNAi pathway, ample evidence soon gathered showing that exogenous mimics of intermediates of the RNAi pathway could be introduced into cells to reprogramme RNAi. These could induce specific and highly-efficacious gene silencing.

The RNAi pathway can be induced by expressed and synthetic RNAi effectors. Expressed effectors have been designed to mimic the miR duplex (as expressed siRNAs), pre-miR (pre-miR mimics and shRNA) and pri-miRNA. These siRNAs are produced by expressing each individual strand from a separate Pol II or III promoter. The strands are separated by a loop that

forms a short hairpin-like structure (shRNA). Synthetic effectors are typically produced as siRNA as these mimic the shortest RNAi intermediate. These synthetic siRNAs resemble the miR duplex. The guide strands designed from exogenous inducers of RNAi are generally fully complementary to the intended target. This improves gene silencing efficiency by Argonaute protein 2 (Ago2) enzymatic "slicing". This is in contrast to translational suppression of the target when there is only partial sequence complementarity, which results in weaker effect than of RNAi.

Fulfilling the maximum potential of reprogramming RNAi for HBV inhibition requires careful consideration of several aspects. These include: i) the required duration of inhibition and the stability of the effector (*i.e.* synthetic or expressed mimics), ii) selection of suitable vector to deliver the exogenous RNAi activator and iii) target or sequence site selection to achieve optimal silencing, while avoiding off-target effects.

1.4.2.1 Expressed RNAi effectors

Synthetic siRNAs may only silence gene expression transiently, posing a significant limitation if long-term gene silencing is required as would be for treatment of chronic HBV infection. In comparison, expressed shRNAs mediate inhibition of the target gene for as long as the shRNAs are transcribed (144, 145).

Generally, shRNAs are transcribed from expression cassettes that include a sense and antisense sequence intervened by a short loop sequence of 4 to 10 bases in length and a transcription termination signal. The RNA transcript forms a pre-miR-like hairpin structure with a 22 bp duplex and single-stranded terminal loop. Longer precursors have also been designed to

emulate the structure of pri-miRNA mimics (Figure 1.6). The dsRNA transcripts are exported from the nucleus, serve as a Dicer substrate in the cytoplasm and enter the RNAi pathway.

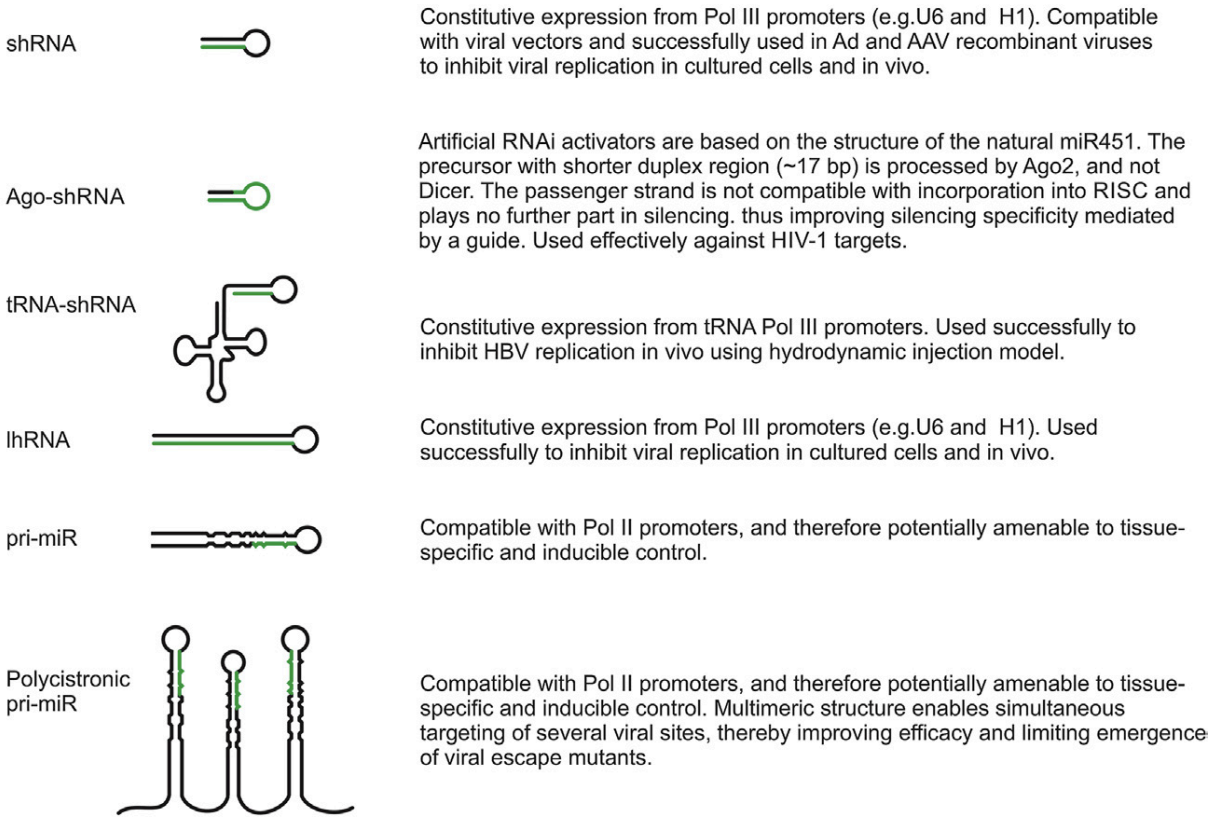


Figure 1.6: Schematic representation of the structure of expressed RNAi effectors.
(source: adopted from ref. (128))

Exogenous or artificial RNAi activators may be expressed under control of Pol II or Poll III promoters, (146). Pol III promoters drive high levels of expression and generate shorter transcripts that resemble pre-miRs. The most commonly used transcription regulatory elements have been derived from U6 (147) and H1 (148) promoters because they are short, easy to clone and produce transcripts with well-defined initiation sites (149). However, ubiquitous expression of Pol III promoters, in many cell types, limits targeted control. Moreover, overexpression of shRNAs can result in liver toxicity, loss of gene expression and death (150). These negative

effects were initially attributed to over loading of exportin-5 (150) and involvement of several members of the Ago family of proteins (151). However, subsequent evidence points to saturation of the miR pathway in the liver by sequestration of miR-122 (152). This saturation effect may be mitigated by harnessing the RNAi pathway closer to its origin, that is generating pri-miRs mimics or by supplementation of exogenous expressed miR-122. In addition, shRNAs that more closely resemble endogenous miRs favour Drosha processing and generate closer to endogenous levels of these effectors. These findings indicate that the redundancy available to exploit RNAi for therapeutic purposes has a quantifiable limit in hepatocytes and exceeding the threshold may be toxic.

The inclusion of engineered control or inducible elements of shRNA expression can prevent unnecessary over expression of shRNAs (153-155) with the use of Pol II promoters. These can be tissue specific and generate pri-miR-like transcripts that mature through the microprocessor complex. Pol II shRNAs are transcribed as longer precursors, with polyA signals that require processing (156). Furthermore, Pol II promoters may generate multiple shRNAs from a single transcript able to target several sites. This polycistronic structure is similar to some naturally occurring pri-miRs (157, 158). Emulating this arrangement, a modular trimeric anti-HBV pri-miR-31 derived shuttles has been constructed to target three regions of HBV. However, the silencing effect induced may have been attenuated by diminished processing of these precursors. Albeit, these effects were specific and had no effect on endogenous miR function (159). There are benefits in generating multiple effectors using this approach, however this may encounter some inefficiencies and limit the expected efficiency.

1.4.2.2 Synthetic siRNAs

The use of synthetic siRNAs is now a well-established tool to demonstrate viral and host gene silencing. Synthetic siRNAs have conventionally been designed to mimic the Dicer product, which consists of a 19 nt duplex with 2-nt 3' overhangs (Figure 1.7). The benefit of using synthetic siRNAs is that they can be produced in large scale and are amenable to various modifications to improve safety and efficacy. These can be readily purified to comply with standards of Good Manufacturing Practices for clinical studies. In addition, delivery to the cytoplasm is sufficient to induced silencing, this averts nuclear transfer, contrary to what is required for expressed siRNAs.

Effective knockdown of gene expression can be achieved by a well-considered synthetic siRNA. Several algorithms have been devised based on "rules of silencing" that include thermodynamic-based modelling among other factors, to improve on target and siRNA sequence design (160-162). However, as a result of the biological complexity the RNAi pathway, evaluation *in vitro* and *in vivo* models are still required for full characterisation.

1.1.1.1.1 Modifications to synthetic siRNAs

As with other dsRNAs, siRNAs are susceptible to degradation by nucleases and have the potential to induce strong immune-stimulatory effects. They may also cause undesired silencing, "off-target" effects, if the unintended strand is incorporated as the "guide". Elucidation of the crystal structure of the Argonaute-DNA-RNA complex has provided a better understanding of the mRNA cleavage by Ago 2 and has prompted evaluation of multiple structural and chemical modifications to exploit the full therapeutic potential of siRNAs (163, 164).

Chemical modifications to siRNAs result in enhanced stability, improve pharmacokinetic profiles, diminished non-specific immune activation and decreased off-target effects without altering their biological efficacy *in vivo* (reviewed in (164)). These modifications can be made to the base in the case of 5-methyluridine (m5U), to the carbohydrate moiety such as the methylene bridge between the 2' and 4' residue in locked nucleic acid (LNA) or other parts of the RNA backbone such as is the case with peptide nucleic acids (A detailed reviewed is provided by Lares *et al*.,(165)). Modifications to uridines or guanosine have attenuated cytokine induction (166). Similarly, LNA-siRNAs have improved serum stability (167). The benefit of the enhanced stability provided by LNAs and thiophosphate replacement, has been demonstrated in early clinical studies. The intravenous or subcutaneous, delivery of a 15 nt antisense nucleic acid directed to miR-122, which is essential for HCV replication, effectively treated HCV infection (168) with reportedly long-term safety and efficacy (169). siRNAs with bases containing phosphorothiolation (P=S) of the non-bridging oxygen at the 3'-end and 2'-carbohydrate modifications (*e.g.* as 2'-OMe or 2'-F) have shown superior gene silencing effects at a reduced dose and frequency of administration (167). siRNAs containing these modifications have also demonstrated improved stability and potency *in vivo* (170, 171) and attenuation of innate immune responses (172).

1.1.1.1.2 Minimising Off-target effects

There is a possibility that off-target effects may occur in several instances for example when: i) the guide sequence binding non-specifically to a transcript and ii) with the incorporation of the passenger strand into RISC which may cause unintended silencing. These off-target effects may be difficult to predict and may be elicited in the presence of partial base-pairing of the guide strand and the target (173-175).

For the guide strand to be loaded into RISC, a phosphate group is required at the 5' end. Off-target effects may be mitigated by the inclusion of 2'-O-methyl modifications at the 5' end of the passenger strand. This may ensure that only the intended guide is incorporated into RISC (Figure 1.7). Further target specificity can be achieved by disrupting the passenger strand into two continuous 10-12 nt strands that remain complementary to the guide. These small internally segmented interfering RNA (sisiRNA) contain LNA nucleotides to increase the melting temperature (Tm) to provide internal stability of the three components of the siRNA while remaining fully functional (176) (Figure 1.7).

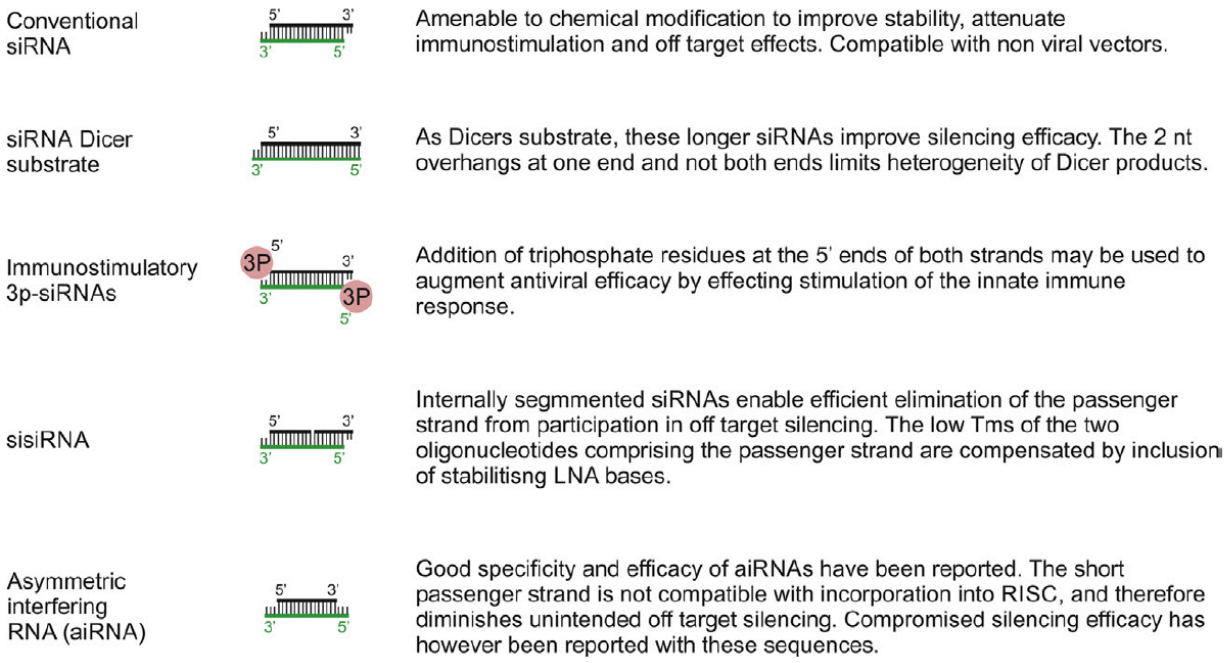


Figure 1.7: Conventional and modified synthetic RNAi activators
(source: (adopted from ref. (128))

1.1.1.1.3 Reducing siRNA's stimulation of non-specific immune responses

Prior to the landmark observation by Elbashir and colleagues (107), the accepted notion was that dsRNA induces innate immune responses leading to suppression of protein synthesis and cellular death. dsRNA molecules are recognised by cell surface TLRs 3(177), while TLR-7 and 8 bind single stranded RNA and stimulate IFN response genes such as IFN-β, IFN-γ, oligoadenylate synthetase-1 (OAS-1), interleukin 6 (IL-6), monocyte chemoattractant protein-1 (MCP-1), and tumour necrosis factor (TNF). Induction of this response may be, at least in the case of TLR7, a sequence-dependent phenomenon (178, 179). Some of these undesired effects can be eliminated by using modified siRNAs containing 2'-F, 2'-O-methyl and 2'-H backbone (180). 2'-Uridine modifications in the siRNA duplex suppresses TLR downstream signalling, despite being recognised with high affinity by TLR7 and TLR 8 (181).

Synthetic siRNAs with chemical modifications have been successfully employed for the knockdown of HBV transcripts. Placement of one to three ribonucleotides at the 5' end of the modified siRNA improved the median inhibitory concentration of the stabilised siRNA by up to five-fold (180). siRNAs containing nucleotides with 2'-O-guanidinopropyl modifications against HBV have been effective, non-toxic and free of IFN responses, both in cell culture and *in vivo* (182). The inclusion of altritol carbohydrate moieties (ANA) in siRNAs have been described (183) and thought to contribute to helix stability and improved silencing. ANA siRNAs delivered as lipoplexes to cultured cells and *in vivo* show nearly 50% HBV inhibition and significantly diminished immune response when compared to unmodified siRNAs (184).

Activation of the innate immune system has a direct effect on viral replication, tumour growth, neovascularisation and wider inflammatory responses which may confound the observed

therapeutic benefits ascribed to the specific RNAi effectors (185). Thus, the use of siRNAs targeting *HBx* requires careful sequence selection, chemical modifications and close monitoring of the innate immune system response.

1.5 Delivery of RNAi effectors: viral vectors and non-viral vectors

There has been substantial progress in the development of RNAi-based therapies to control HBV infection. However, the full potential has been limited by the lack of efficient delivery of the effector nucleic acid sequences. Two types of RNAi delivery systems have been employed, viral vectors (VV) and non-viral vectors (NVV).

Vectors intended for HBV therapy require strong hepatotropism. For optimal efficacy, both VV and NVV should be of approximately 100 nm in size to allow extravasation through the fenestrated sinusoidal epithelium for direct contact with hepatocytes (186). VV have been used to deliver expression cassettes that encode RNAi effectors to target cells, while NVV have been designed and more commonly used to deliver synthetic RNAi effectors.

1.5.1 Viral Vectors

Viruses have evolved to exploit the host cellular mechanism for replication of the viral genome and adapted various strategies to define their tropism. To this end, lentiviruses, adenoviruses (Ad) and adeno-associated viruses (AAV) have been modified into VV to deliver expression cassettes harbouring effector sequences (41, 187-189). Ad and AAV have been commonly used. In clinical trials Ad vectors have been used in up to 21,2% (n=535 trials) and AAV in 7.3 % (n=183 trials) of all reported gene therapy studies registered (http://www.abedia.com/wiley/vectors.php accessed 8 Dec. 2017).

Ads and AVV are particularly attractive to deliver RNAi effectors against HBV because of their efficient liver transduction properties and persistent gene expression in the transduced cells (190). A description of the advantages and disadvantages of these vectors to deliver RNAi therapeutics to target HBV are reviewed elsewhere (128, 191).

1.5.1.1 Adenovirus vectors

Ads bear a linear double-stranded DNA genome of approximately 36 kb in length. This genome comprises "immediate early" and "early" genes, in addition to five "late" genes which code the viral proteins. The virion capsid diameter is of approximately 90 nm which permits traversing the fenestrated vascular endothelium (192, 193). Entry into hepatocytes is receptor mediated and driven by the interaction between the Ad hexon protein and blood clotting factor X (194).

Despite the efforts taken to re-engineer Ad vectors to produce Helper Dependent-Ads (HD-Ad) they appear to have retained some of their undesired effects. Some of these challenges may be overcome by modulating host response to the viral antigens. The immunogenic and cytotoxic effects induced by this and earlier generation Ad vectors has been a strong motivation for the development of HD-Ad vectors. The outcomes of early clinical studies using AAV vectors for gene therapy to the liver suggest that these may be a highly suitable option for shRNA delivery for chronic HBV (195).

1.5.1.2 Adeno-associated virus vectors

AAV belong to the *Parvoviridae* family, are non-enveloped and contain a single-stranded DNA genome of 4.8 kb. AAV are non-pathogenic and have reduced immunogenicity compared to adenoviral vectors. Furthermore, AAV have been recently validated to be safe in several clinical settings. The infusion of an engineered AAV containing the coagulation Factor IX gene,

corrected the coagulation profile in ten haemophilia B men (196). Wild type AAV are dependent on Ad or herpes virus co-infection for replication. AAV vectors have a carrying capacity of up to 4.6 kb, provide sustained gene expression and thus are highly suitable for expression of RNAi effectors (195, 197). These vectors are suitable for anti-HBV shRNA delivery to hepatocytes as they confer long term gene expression (198, 199). Successful viral suppression has been demonstrated using shRNAs delivered with a self-complementary AAV (scAVV) pseudotyped vector 2/8 to an HBV transgenic mouse model. A single delivery of scAAV2/8 vector resulted in effective inhibition of viral proteins, a 2-3 $\log_{10}$ reduction in HBV viraemia and free of IFN induction (187). Encouraging results were observed in subsequent experiments where the knockdown effect could be prolonged with sequential administration of serotypes 7, 8 and 9 (200). Improved efficacy was reported in a multi-strategy approach by Michler *et al.* using a re-engineered AAV8 vector co-expressing HBV targeted shRNAs and a shRNA sense decoy to reduce off-target effects (201). This novel approach resulted in strong HBV inhibition *in vivo*, that was sustained for an 84-day period without detectable toxicity. Although lethal effects have been observed with use of AAV to deliver shRNAs (150), subsequent evidence demonstrated that this was not attributed to the vector (152).

1.5.2 Non-viral vectors

Non-viral vectors are required for the efficient liver delivery of siRNAs to inhibit HBV replication. Although vector-free delivery of modified naked siRNAs has been successfully employed to disrupt HCV replication (168), currently this modality of delivery is more of an exception. Most approaches to target HBV require NVV to deliver siRNAs to the liver. The robust immune-responses elicited by VV, has further stimulated the development of NVV for nucleic acid delivery strategies. Effective NVV have advanced the clinical use of RNAi because they confer several advantages relative to the viral counterparts (202). NVV are

amenable to safe and large-scale production, have relatively favourable immune and cytotoxic profiles and depending on the formulations used, both RNA and DNA effectors can be delivered. However, these vectors have some limitations; NVV require a careful balance between the negatively charged nucleic acid and positively charged lipids (N/P ratio) for stability (203). Liposomes in the presence of membrane proteins can induce unintended fusion and leakage of nucleic acid (204). Lipid nanoparticles may aggregate due to colloidal instability that arises from serum proteins and red blood cells, may result in sequestration by the reticulo-endothelial system, phagocytosis and capillary pulmonary emboli (205). Altered bio-distribution may also occur, which can be mitigated by using modified lipids and different formulation processes (reviewed by Yin et al., (202)). NVV are not necessarily inert to the immune system and various components of the lipid nanoparticles may elicit innate immune responses of varied magnitude (206). NVV components can be recognised by TLRs and cytoplasmic receptors, which are part of the group of Pattern Recognition Receptors (PPRs). Stimulation of PPRs triggers the release of an array of proinflammatory mediators, such as TNF-α, INF-γ, and IL-6 (207). Lipid nanoparticles are at risk of opsonisation to serum proteins and may aggregate and rapidly cleared by phagocytosis, altering the intended biodistribution (208).

Successful development and evaluation of NVV intended for managing chronic HBV requires some specific considerations. For hepatocyte delivery, as noted earlier, this would include a 100 nm size restriction of the particles to ensure unhindered transit through the fenestrated hepatic sinusoidal endothelium. This may be resolved with recent development of microfluidic production methods, where liposomes are formed within a controlled microenvironment. Microfluidic methods have achieved the assembly of liposomes with more predictable size and size distribution (209). In addition, minimising reticulo-endothelial sequestration is essential

for effective silencing by siRNAs in hepatocytes rather than histiocytes. This, can be achieve by polyethylene glycol (PEG) coupling of NVV (210-212). Experimental evidence of such approach is presented and discussed in chapter 5 of this thesis.

1.5.2.1 Lipid based siRNA effector vectors

Lipid-based NVV are currently the most widely used and while there is vast heterogeneity in this group, they are characterised structurally by three main components: a cationic head group that binds nucleic acids, a hydrophobic tail that promotes vesicle formation and a linker that couples the two other components. DOSPA, DOTAP and DC-cholesterol and many other cationic lipids have been used to generate NVVs (213). Neutral lipids, or "helper lipids" such as DOPE have been used to improve transfection and stability. Helper lipids enable hydrophilic polymers like PEG to be incorporated into NVV (Figure 1.8).

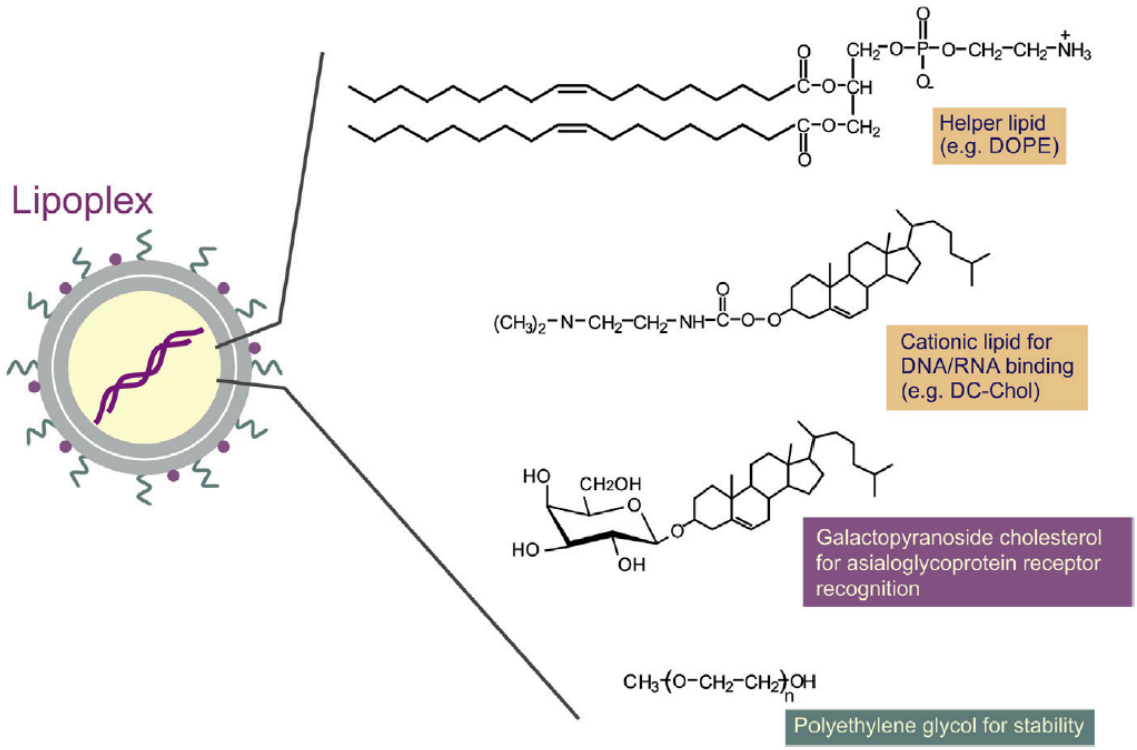


Figure 1.8: Composition of lipid based Non-viral delivery vectors
(source: (adopted from ref. (128)).

Stabilised siRNAs have been encapsulated in specialised lipid bilayers named SNALPs (stable nucleic acid lipid particles) and have been employed for the systemic delivery of siRNAs (180, 214). SNALPs essentially are comprised of a cationic and neutral lipid bilayer enveloped with hydrophilic PEG. Morrissey *et al.* were the first to use this formulation for delivery of modified siRNAs against HBV in a transgenic mice model. They demonstrated impressive inhibition of viral markers in a 6-week period (180). A study of systemic delivery of siRNAs against apolipoprotein (Apo) B using SNALPs also demonstrated an effective therapeutic RNAi response in non-human primates. The inhibitory effect of a single dose of SNALP-mediated siRNA delivery resulted in a significant reduction of the targeted mRNA in the liver (214). SNALPs are currently in use as NVV for the treatment of advanced cancer, solid tumours, Ebola virus infection, hypercholesterolaemia and HBV ((202).

Uptake of the NVV is now understood to follow a similar pathway to that of endogenous chylomicrons (215, 216). Enhanced tissue specific delivery can be achieved with the inclusions of ligands to direct receptor mediated endocytosis (217). In the case of chronic HBV, achieving hepatocyte-specific delivery of siRNA effectors is a crucial aspect in the development of a complete therapeutic approach. Ligands employed for liver specific ligand-receptors mediated endocytosis include among others, i) asialoglycoprotein receptors, ii) low-density lipoprotein, iii) epidermal growth factor receptor, iv) integrin receptors targeted by Arg-Gly-Asp peptide, v) folate, and vi) transferrin (218). The coupling of ligands to the lipid nanoparticles, such as Apo E or a multivalent N-acetylgalactosamine cluster, results in high affinity to the asialoglycoprotein receptor expressed on hepatocytes (219, 220). Hean and colleagues developed lipoplexes containing DOPE and a cholesterol galactoside component to deliver anti-HBV siRNAs to HBV transgenic mice (184). Notably, HBV silencing was achieved in the absence of toxic effects or an innate immune response (184). Like chylomycrons, NVV

containing ionisable cationic lipids are processed *in vivo* by incorporation of engodenous ApoE into theses lipoplexes. This confers hepatotropism by providing affinity to low density lipoprotein receptor in the liver (216).

In recent years, there has been a remarkable progress in the elucidation of the RNAi pathway and the accumulated evidence reaffirms its potential as a tool to target viral infections. Although, at the onset of the work presented in this thesis, there was a paucity of evidence to support the use of siRNAs to target HBV. In contrast, there was ample data on HBx indicating the pivotal role this viral protein played on HBV replication and carcinogenesis, which made this a suitable target. A review of the field is presented in Chapter 2 (221). The work described in the subsequent chapters endeavoured to address some of these gaps.

While others have shown that HBV replication can be inhibited by exploiting the RNAi pathway (222-227), it remained to be determined whether novel sites could be identified within the conserved regions of HBx. In addition, the design of hairpin RNAs with features of endogenous miRs that would influence a desired strand bias required the necessary experimental evidence to support this proposition. Furthermore, because of the limited *in vivo* models available to study HBV replication, the evidence had been largely generated *in vitro*. These studies had limited translational value in assessing potential in a clinical setting. To address this gap, effectiveness was assessed comprehensively in a murine model of transient HBV replication and in an HBV transgenic mouse model. The findings are presented in Chapter 3 (41).

Development of drug resistance to nucleoside analogues, such as lamivudine, following prolonged use in chronic HBV has been reported (228). Similarly, siRNA escape mutants have been observed in HCV (229). This prompted the design of a novel long hairpin that would mimic a precursor miR with the potential to generate multiple shRNAs aimed at various HBV sites. A principle that is not dissimilar to that of multiple drug therapy to prevent drug resistance. The details of the study design and findings are described in Chapter 4 (230).

Lastly, suitable non-viral vectors for liver delivery available for siRNA delivery to the liver were limited. Hence, we developed PEG coupled NVVs to deliver siRNAs to HBV and evaluated them in tissue culture and in two animal models. Effects on HBV markers of replication were compared to lamivudine. The performance of this NVV is presented in Chapter 5 (212). Furthermore, the synthesis of novel lipids were used to assemble lipoplexes containing previously characterised effective siRNAs targeting HBV and were evaluated in a similar manner to that described in chapter 3 and 5. The effect of these lipoplexes on HBV replication are presented in Chapter 6 (231).

1.6 Aims and objectives

RNAi-based therapies are well suited to manage chronic hepatitis B and have the potential to reduce long-term complications such as cirrhosis and HCC. At the commencement of this study, there was limited evidence of RNAi effectors targetting HBV.

The aim of the work presented in this thesis was to determine whether HBV replication could be inhibited by exploiting the RNAi pathway using novel targets and designed effectors. We aim to target the *HBx* ORF because of its highly conserved sequence, the overlap of the target

sites across all the viral transcripts and because of the essential role of HBx in viral replication. We intended to find effective siRNAs by using expression systems to produce effectors to various sites within the ORF and to further validate these using synthetic siRNAs *in vitro* and *in vivo*. Furthermore, NVVs for liver delivery of nucleic acids remain an essential part of an effective strategy against chronic HBV. We therefore pursued the development and evaluation of novel lipid based vectors that would carry the identified effective siRNAs

Chapter 2: Exploiting the RNA interference pathway to counter hepatitis B virus replication

Arbuthnot, P., Carmona, S. & Ely, A

Liver Int. 2005;25(1):9-15.

This article reviewed the burden of the HBV epidemic and the conventional therapeutic modalities available, in addition it provided a brief overview of the HBV genome and made the case for why the virus is so amenable to inhibition using small interfering RNA. The evidence of early HBV inhibition studies exploiting the RNAi pathways were highlighted as well as the likely limitations, such as the different inhibitory potential of specific siRNAs, toxic side effects and the lack of effective hepatotropic delivery vectors.

Contribution by the author:

SC contributed to the review and selection of relevant literature, contributed to the review outline, draft manuscript writing and final review.

Liver International 2005: 25: 9–15
Printed in Denmark. All rights reserved

Copyright © Blackwell Munksgaard 2004

Liver International
DOI: 10.1111/j.1478-3231.2004.0966.x

Review Article

Exploiting the RNA interference pathway to counter hepatitis B virus replication

Arbuthnot P, Carmona S, Ely A. Exploiting the RNA interference pathway to counter HBV replication.
Liver International 2005: 25: 9–15. © Blackwell Munksgaard 2004

Abstract: Chronic infection with hepatitis B virus (HBV) is endemic to sub-Saharan Africa and parts of Asia where persistence of the virus is commonly associated with complicating cirrhosis and hepatocellular carcinoma (HCC). Licensed therapies for HBV are partially effective in selected patients and development of novel treatments remains an important global medical objective. HBV has an unusually compact genome that restricts the ability of the virus to evade potentially therapeutic nucleic acid hybridization. Thus, exploiting the RNA interference (RNAi) pathway, which enables sequence-specific target RNA degradation using small interfering RNA (siRNA), is well suited to developing novel treatment for HBV infection. Several studies, both *in vitro* and *in vivo*, have demonstrated that HBV replication can be inhibited in transfected cells by synthetic siRNA duplexes and also Pol III-derived short hairpin RNA (shRNA) sequences. The effectiveness of anti-HBV sequences varies considerably, and is likely to result from differences in activation of the RNAi pathway by individual siRNA species. Exclusion of potentially toxic off-target effects and also development of efficient methods of hepatotropic nucleic acid delivery are important prerequisites before RNAi can be used successfully for anti-HBV treatment.

Patrick Arbuthnot, Sergio Carmona and Abdullah Ely

Hepatitis B Virus Research Programme, Department of Molecular Medicine and Haematology, University of the Witwatersrand, Private Bag 3, Wits 2050, South Africa

Patrick Arbuthnot, Hepatitis B Virus Research Programme, Department of Molecular Medicine and Haematology, University of the Witwatersrand, Private Bag 3, Wits 2050, South Africa.
Tel.: + 27-11-717-2365
Fax: + 27-11-717-2395
e-mail: arbuthnotpb@pathology.wits.ac.za

Received 16 April 2004,
accepted 14 May 2004

Chronic infection with hepatitis B virus (HBV) is endemic to sub-Saharan Africa, the western Pacific islands, east and south-east Asia. There are approximately 387 million carriers of HBV in the world today, and as many as 40% of these will develop hepatocellular carcinoma (HCC) and/or cirrhosis as complications (1–5). In those populations where chronic HBV infection is endemic, parenteral viral transmission occurs perinatally or in early childhood. Despite the availability of an effective and safe vaccine, the global prevalence of HBV infection has not diminished significantly. Licensed therapies that have been employed to eliminate HBV from chronic carriers of the virus include interferon-α, and the nucleoside analogues, lamivudine and adefovir (6, 7). Interferon-α has an immunomodulatory mechanism of action and the nucleoside analogues interfere with viral DNA replication. These drugs are partially effective only in HBV e antigen (HBeAg)-positive carriers. Moreover, prolonged therapy with lamivudine is associated with an increased incidence of viral resistance (8, 9). The limitations of HBV therapy, together with an improved understanding of HBV molecular biology, have prompted exploration of novel approaches to inhibiting HBV replication.

The genome of HBV, as with other hepadnaviruses, is composed of circular partly double-stranded DNA (Fig. 1) (10, 11). The long (minus) strand is approximately 3200 bases in length, and contains four open reading frames (ORFs) that encode precore/core, polymerase, surface and HBVx (HBx) proteins. A plus strand of variable length maintains the circular structure of the genome by cohesive hybridization that straddles the 5′ and 3′ ends of the minus strand. Each ORF overlaps at least one other, and together they cover the entire genome. The *precore/core* ORF contains two in-phase start codons that encode two overlapping proteins. Translation initiated from the precore AUG codon generates a precursor protein that is modified by proteolysis and secreted as the soluble HBeAg. Presence of HBeAg in the serum of chronic carriers is an indicator of a high HBV replication state. Translation initiated at the second precore/core initiation codon gives rise to core protein that forms the nucleocapsid. The *polymerase* ORF is the largest and encodes the enzyme that is responsible

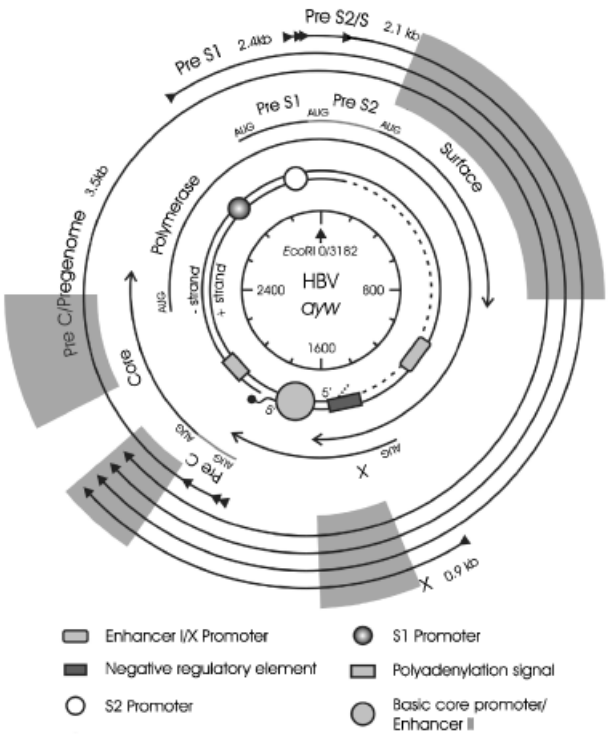


Fig. 1. Organization of the hepatitis B virus (HBV) genome with shaded regions indicating the Surface, HBx, PreC and Core regions that have been used as targets of RNA interference (RNAi)-based inhibition of viral gene expression. The partially double-stranded genome with *cis* elements that regulate HBV transcription are represented schematically and co-ordinates of the genome are given relative to the single *Eco*RI restriction site. Immediately surrounding arrows indicate the viral open reading frames (with initiation codons) that encompass the entire genome. The four outer arrows, which give the 5′–3′ polarity, indicate the HBV transcripts. Multiple arrowheads at the 5′ ends of the Pre C/Pregenome and Pre S2/S transcripts indicate heterogeneous transcription start sites. The identical termination site depicts the common 3′ end of all the HBV transcripts.

for priming and reverse transcription of the pregenomic HBV RNA. Pre S1, pre S2 and S in-phase translational start codons define the amino terminal ends of the large, middle and major surface proteins, respectively, which are required for the formation of the virion envelope. The viral *cis*-elements that are required for HBV gene expression and replication are located within sequences that also encode viral proteins. For example, the *HBx* region overlaps with *polymerase* and *precore* ORFs and includes the basic core promoter/enhancer II. After infecting hepatocytes, the partly double-stranded HBV genome is converted to covalently closed circular DNA, which is the template that is transcribed by cellular RNA polymerase II (12–14). HBV transcripts, which are required as viral replication intermediates as well as for translation of HBV proteins, are initiated from different promoters and a single polyadenylation signal terminates transcription of all of the mRNA species at the same site. Thus, HBV transcripts have different 5′ ends but the 3′ sequence, which includes *HBx*, is common to each of the HBV mRNA species (Fig. 1). Moreover, the multifunctional properties of HBV sequences restrict plasticity and limit the ability of the virus to mutate. This highly compact arrangement of the HBV genome makes it a good target for potentially therapeutic hybridizing nucleic acids. Nucleic acid-based gene-silencing techniques include use of antisense sequence, ribozymes, DNAzymes and siRNA molecules that utilize the RNAi pathway. Interest in RNAi has recently been fuelled by the relative ease with which effective gene knockdown can be achieved by exploiting this pathway. The focus of this review is the application of RNAi to the inhibition of HBV replication and development of new antiviral therapy.

RNAi by siRNA duplexes has been shown to be a highly efficient method of gene 'knockdown' (15–17). The process is initiated by double-stranded RNA (dsRNA) that is homologous to the silenced gene. Naturally, the mechanism involves processing of larger dsRNA by Dicer, which is a RNAse III enzyme. The resulting short RNA duplexes function as guide sequences and are incorporated into the cytoplasmic RNA-induced silencing complex (RISC), which degrades mRNA that forms base pairs with the guide RNA. Exogenous silencing sequences are typically either synthetic RNA duplexes or RNA derived from intracellular promoter-based transcription. Analysis reveals that most efficient gene silencing with synthetic duplexes is attained by sequences that comprise 21 nucleotide (nt) sense and antisense strands (17). Ideally, 21 nt RNA duplexes should be paired in such a manner to have a 2 nt overhang at the 3′ end of each of the oligoribonucleotides to resemble Dicer products of long dsRNA (17). Importantly, dsRNA of 30 base pairs or longer can trigger a sequence-non-specific interferon response in mammalian cells that induces programmed cell death (17). Intracellular generation of interfering RNA molecules is typically achieved by inserting a DNA transcription template downstream of a Pol III promoter (18–21). The U6 or H1PolIII promoters are the most commonly used. Unlike Pol II promoters, these sequences have the advantage of containing all of their control elements, with the exception of the first transcribed nt, upstream of the transcription initiation site. The Pol III termination site is defined by a poly dT sequence (usually dTdTdTdT) in the sense sequence of the transcription template. These properties are ideally suited to the production of defined siRNA

sequences. Pol III expression cassettes for siRNA typically encode hairpin RNA sequences that are Dicer substrates. Individual sense and antisense Pol III cassettes have also been used to generate siRNA duplexes within a cell. Compared with synthetic sequences, uses of DNA cassettes that encode interfering RNA have the benefits of obviating problems of RNAse contamination and low cost of synthesis. However, synthetic RNA has the advantage of relative ease with which cellular delivery can be achieved.

RNAi-based inhibition of HBV gene expression

Several sites of the HBV genome have been targeted in studies to assess efficiency of using RNAi against HBV (22–29). These include *preC/Core*, *surface* and *HBx* (Fig. 1). To date, siRNA sequences have been evaluated *in vitro* and *in vivo* in a murine model of HBV replication. Cell-culture models of HBV replication that have been tested include both transiently transfected cells as well as lines that constitutively produce HBV particles (e.g. HepG 2.2.15 cells). The recently described murine hyperdynamic tail vein injection (MHI) has provided a convenient method for determining effects of siRNA on inhibition of HBV replication *in vivo* (30). The procedure entails rapid injection (over 5–10 s) of a large volume (approximately 10% of mouse body weight) of a solution containing HBV replication competent plasmid. Plasmid DNA is efficiently taken up by the hepatocytes, which leads to expression of HBV genes and transient viral replication.

McCaffrey et al. (24) assessed the anti-HBV efficacy of a panel of six U6 promoter cassettes that encoded hairpin RNA sequences. Methods of assessing the inhibition of HBV replication included the measurement of viral antigen secretion from transfected cells, HBV antigen and nucleic acid production in normal and NOD SCID mice after MHI. The data demonstrated inhibition of markers of HBV gene expression with some variation in the efficiency of the hairpin-encoding cassettes. The most effective sequence, which targeted a region of the *surface* and overlapping *pol* ORF, inhibited hepatitis B surface antigen (HBsAg) secretion by 94% in transfected cultured cells, and 85% *in vivo* in the MHI model. Measurement of HBV RNA in immunocompetent (C57BL/6) as well as NOD SCID mice revealed that this sequence diminished viral RNA significantly in both strains. Similar observations in both murine strains indicate that the RNA expression cassettes have a direct effect on viral RNA and the effect is not dependent on an antigen-dependent immune response. Immunohistochemical staining of liver sections corroborated these data. An interesting finding was that a modest decrease in markers of HBV replication was observed in cells or animals that had been treated with negative control hairpin-encoding cassettes that targeted hepatitis C (virus) sequences. The exact significance of this is not clear, and may be a result of a minor non-specific off target effect of siRNA sequences.

Giladi and colleagues (26) assessed the efficacy of five synthetic siRNA duplexes that targeted different sites within the *surface* ORF of HBV. A duplex that targeted sequences 9–27 nt from the *surface* ORF initiation codon was found to be the most effective. HBsAg and HBeAg secretion from stable and transiently transfected cells as well as in the MHI model was markedly diminished by this synthetic RNA duplex. Besides HBV transcripts, HBsAg and HBV core antigen expression in liver sections were diminished by siRNA. Variation in the concentrations of HBV RNA that was extracted from hepatocytes of different animals was thought to be as a result of regional fluctuations in HBV plasmid and siRNA transfection efficiency. Further characterization revealed that the siRNA duplex had a direct inhibitory effect on viral replication without a requirement for HBV DNA synthesis (26). The siRNA sequences diminished HBsAg production from a Pol-deficient HBV plasmid in MHI model. This is an important property that is distinct from anti-HBV nucleoside analogues, which have inhibitory effects on viral DNA synthesis and require HBV replication to be effective.

In another study (28), inhibition of HBsAg and HBeAg secretion was observed in hyperdynamic injected mice that were treated with synthetic RNA duplexes, which targeted the core and surface genes of HBV. HBV antigen secretion and also the production of HBV RNA (as measured by RT-PCR) were diminished by both siRNA duplexes, and the siRNA that targeted the surface region was a more effective inhibitor of antigen secretion. Using the same murine model, nucleoside analogues (lamivudine and adefovir) also diminished HBV polymerase activity.

Synthetic siRNA duplexes that target the polyadenylation (PA), preC and surface regions were tested in the HepG2.2.15 cell line that constitutively produces HBV particles (29). The PA siRNA sequence was the most effective inhibitor of HBsAg secretion, HBV RNA and HBV DNA production. Immunocytochemistry measurement in HepG2.2.15 cells confirmed a decrease of HBsAg in these cells. An interesting observation

was that sequential transfection increased the efficacy of inhibition of HBsAg secretion from the HepG2.2.15 cell line. A similar analysis, in which HepG2 and Huh7 cells were transfected with an HBV plasmid together with siRNA that targeted the core region, revealed a significant decrease in HBsAg, HBeAg as well as HBV RNA and HBV DNA in transfected cells (27).

Shlomani and Shaul (23) generated plasmid vectors that encoded hairpin precursors of siRNA that target the *core* and *HBx* ORFs. Sequence-specific reductions in the secretion of HBV antigens, RNA and DNA were demonstrated in transfected cells. The vector that targeted *HBx* was found to be more effective than that which targeted the *core* region.

The effect of a synthetic siRNA duplex, which targeted the core region, in inducible HBV-producing cells that produced wild type or the lamivudine-resistant tyrosine–methionine–aspartate–aspartate (YMDD) variant of HBV was assessed by Ying et al. (22). siRNA caused significant inhibition of HBV synthesis in both cell lines. Transfection of wild-type cells at a concentration of 4 μg/ml in the medium decreased in HBV DNA concentration by 98% of the control at 48 h posttransfection. The effect was less marked in the YMDD variant cells where reduction of HBV DNA was to 11% of the control. These data were corroborated by similar observations on the effect of siRNA on core antigen production.

Using an alternative approach (25), cultured HepG2 cells were stably transfected with plasmid vectors that produce anti-HBV small hairpin transcripts from a Pol III promoter. Several different sites were targeted in the HBV genome, and were selected according to differences in the predicted secondary structure of the HBV RNA target sites. Approximately 96% gene knockdown was achieved with the most effective hairpin expressing vectors. Potential synergy between shRNA and the currently available nucleoside analogue lamivudine was also assessed. When shRNA was combined with lamivudine, inhibition of HBV replication was more effective. shRNA with lamivudine reduced HBV genome DNA sixfold more than lamivudine alone and threefold more than the shRNA alone. Importantly, under the conditions that were described, the shRNA was a more effective inhibitor of HBV DNA synthesis than lamivudine.

Comparison of anti-HBV activity of synthetic and Pol III-derived small hairpin RNA shows that, although both types of sequence effectively inhibit HBV gene expression, synthetic siRNA duplexes may have a more rapid effect (26). However, small hairpin constructs generated endogenously from Pol III promoters may have more sustained effects. Complete characterization of the differences between these two classes of interfering RNAs is yet incomplete.

Characteristics of anti-HBV siRNA sequences

Considerable variation has been reported in the efficiency of gene knockdown that is effected by siRNA sequences. To date, empirical comparison of efficacy has been the method of identifying the most promising of anti-HBV therapeutic sequences. It has recently been reported that functionality is determined by siRNA-specific properties and not by the target mRNA (31). As the mechanisms involved in RNA processing during activation of the RNAi pathway are becoming better understood, more rational approaches to the design of siRNA are emerging (31–33). In a recent study, eight criteria were identified as siRNA-specific features that contribute to siRNA efficiency (31). Each criterion individually contributes marginally to improved functionality, but combination into an eight-component-scoring algorithm effectively identifies functional duplexes. The complete list of criteria is given in Table 1 and includes the following. A GC content of 30–52% is thought to be optimal for efficient unwinding of the duplex, while at the same time retaining sufficient stability of the siRNA/target interaction. Stability at the 5′ ends of the siRNA duplex is an important determinant of strand bias. The strand that is incorporated into RISC is that which is less tightly paired (A/U rich) to the complement at its 5′ end. A sequence that is rich in A and U at positions 15–19 (sense strand) is more likely to be functional, and a point is awarded for each A/U pair in the sequence from bases 15–19 of the sense strand. A base preference for A at position 19 is similar to the naturally occurring sequence that is found in microRNA (miRNA) and supports the idea that miRNA and siRNA are processed by similar pathways. Preference for a U at position 10 of the sense strand has an important influence on siRNA functionality, and may be related to the nucleic acid sequence preference at the active site of cellular endonucleases. Most siRNA sequences that earn a score of six are functional with silencing efficiency of more than 50%. At higher scores, the siRNA functionality is further improved.

To assess whether this eight-component algorithm is applicable to the siRNA synthetic duplexes that have been used to inhibit HBV gene expression, sequences were analyzed from four

Table 1. Scoring of anti-HBV siRNAs according to eight-component algorithm that predicts siRNA effectiveness

			Scores for individual criteria								
siRNA sequence (sense strand)	siRNA name (ref)	Suppression of HBsAg (or HBeAg) (%)	GC content 30–52%	A/U pairs 15–19*	Lack of inverted repeats†	A 19*	A 3*	U 10*	NonG/C 19*	Non G 13*	Total
5′cauuguucaccucaccauatt 3′	siHBV (core) (27)	0 (79)‡	1 (38)	3	1	1	0	0	1	1	8
5′aagccuuagagucuccugagc 3′	siRNA (C) (28)	0 (60)§	1 (52)	2	0	1	0	0	1	1	6
5′aauuguucaguggutcguag 3′	siRNA (S) (28)	70 (80)§	1 (38)	3	1	0	0	0	1	0	6
5′caucacaucaggauuccuatt 3′	siRNA-1 (26)	80–92‡,§	1 (38)	3	0	1	0	0	1	1	7
5′ccuccaaucacucaccaactt 3′	siRNA-2 (26)	80‡,§	1 (48)	2	1	0	0	0	0	1	5
5′ccaguacgggaccaugcaatt 3′	siRNA-3 (26)	55–80‡,§	1 (52)	3	0	1	1	0	1	1	8
5′uaccuaugggaguggccutt 3′	siRNA-4 (26)	1–85§	0 (57)	0	0	0	0	0	1	1	2
5′gucuguacagcaucgugagtt 3′	siRNA-5 (26)	55–75‡,§	1 (48)	2	0	0	0	0	0	1	4
5′acccuuauaaagaauuuggag 3′	HBVPA (29)	78‡	1 (33)	3	0	0	0	0	0	1	5
5′gcugugccuuggguggcuutt 3′	HBVPreC (29)	67‡	0 (57)	2	0	0	0	1	1	0	4
5′uaccgcagagucuagacuctt 3′	HBVS (29)	42*	1 (48)	2	0	0	0	0	0	1	4

*Sense strand nucleotide positions. †Tm of inverted repeat sequences $< 20^{\circ}C$ determined using MFold (39). ‡HBV antigens measured using cell culture models of viral replication. §HBV antigens measured using murine hyperdynamic injection model of viral replication. HBV, hepatitis B virus; SiRNA, small interfering RNA; HBsAg, hepatitis B surface antigen; HBeAg, HBV e antigen.

publications that aimed at inhibiting HBV replication with siRNA (26–29). Studies that entailed the use of shRNA were excluded from the analysis. The reason is that processing of anti-HBV hairpins is yet to be characterized, and the exact 5′ and 3′ ends of the sequence that is incorporated into RISC is not known. Thus, coordinates cannot be determined, as for the synthetic 21 mer siRNA duplexes. Of the 11 synthetic anti-HBV siRNAs that have been characterized, five had scores of 6 or more (Table 1). Two (siHBV (core) (27), and siRNA-3 (26)) had the highest score of eight and both were efficient inhibitors of HBsAg and/or HBeAg secretion from cultured cells. siRNA-3 also efficiently inhibited HBsAg secretion from mice treated using the MHI procedure (26). The target sequence of siHBV (core) (27) is not included in the HBsAg-encoding HBV transcripts (Fig. 1) and did not diminish HBsAg secretion from transfected cells (Table 1). siRNA-1, which had a score of seven, was found to be the most efficient inhibitor of markers of HBV replication in the study reported by Giladi et al. (26). siRNA sequences with scores between four and six demonstrated varying degrees of efficiency of knockdown of HBV markers of replication and correlation between degree of knockdown and HBsAg secretion was difficult to establish. Interestingly, the siRNA, which scored lowest, siRNA-4, which had a score of two, also had no inhibitory effect on HBsAg secretion from cells in culture (26). In fact, a modest stimulatory effect by siRNA-4 on HBsAg secretion was observed in HBV-producing cells. It is not clear why a significantly different observation was made in the MHI model (Table 1). The lack of control for variation in hepatocyte nucleic acid delivery using the MHI method (e.g. using a marker gene) may contribute to these apparently discrepant observations.

Overall, differences between the real and predicted efficacy of siRNAs include variations in experimental conditions and non-specific inhibition of HBV replication by siRNA sequences. It is clear that algorithms for the prediction of siRNA efficacy require further refinement before they can be used reliably to identify optimal siRNA targets. Although siRNA sequences that target HBV seem to have functionality that is generally predicted from this eight-component algorithm (31), verifying experimental observation remains an essential component of siRNA characterization. Importantly, in addition to evaluating antiviral effects, determining the functionality of anti-HBV interfering RNA requires rigorous assessment of off-target effects.

Non-specific effects of interfering RNA

Essential to the development of RNAi-based HBV therapy is specificity of the therapeutic sequence for its viral cognate. Off-target effects of siRNA may result from induction of the interferon response (34, 35) as well as cross hybridization between siRNA and non-targeted sequences (36). It is clear that if activation of RNAi is to be used as therapy for HBV, it is important that non-specific effects be characterized fully, and acceptable levels of off-target effects are determined.

The interferon response may be induced by siRNA through activation of double-stranded RNA-activated protein kinase (PKR) (summarized by Moss and Taylor (37)). This kinase phosphorylates the eukaryotic translation initiation factor 2α (eIF2α) to arrest protein synthesis and apoptosis. Activation of 2′–5′ oligoadenylate synthetase is also effected by PKR, and this leads to non-specific degradation of cellular RNA by RNAseL. Activation of PKR by the interferon response thus shuts down essential cellular functions and may lead to apoptosis and cell death. PKR has 2 dsRNA binding domains that are likely to be important for its activation (38). Originally, it was thought that dsRNA that is shorter than 30 bp evades the interferon response in mammalian cells; however, a non-specific response may also be induced by shorter RNA duplexes in high concentration (37). Importantly, none of the studies reporting the use of interfering RNA to counter HBV replication has characterized an effect of the interferon response on knockdown of viral gene expression.

Cross-hybridization of interfering RNA with transcripts that have partial sequence identity to the intended target may also contribute to non-specific effects. Direct silencing of non-targeted sequences with as few as 11 contiguous complementary sequences has been reported (36). A less stringent requirement for exact matching of the full length of the siRNA sequence for its cognate sequence significantly diminishes the specificity of siRNA effects and would significantly undermine the use of siRNA for HBV treatment. A careful analysis of silencing of unintended transcripts needs to be undertaken as a prerequisite for using RNAi-based therapy to treat HBV infection.

Conclusions

Several reports have documented inhibition of HBV gene expression that is effected by synthetic and Pol III-derived RNA molecules that are designed to exploit the RNAi pathway. Since there is a limited sequence plasticity and lack of redundancy of the HBV genome, this virus is unable to evade nucleic acid hybridization and is potentially a good candidate for RNAi-based therapy. Efficacy of several different siRNA sequences has been assessed in cells in culture as well as in murine models of HBV infection and significant inhibition of HBV gene expression has been documented. Both synthetic RNA duplexes and intracellular Pol III promoter-derived hairpin RNA have been shown to have varying efficiency, which may be attributable to siRNA-specific properties.

Although the results augur well, there are issues that need to be resolved before effective RNAi-based therapy for HBV infection will be realized. In particular, off-target effects of anti-HBV RNA sequences need to be characterized and acceptable (if any) levels need to be defined. Delivery of nucleic acid sequences to cells remains an important technical hurdle. Although viral vectors (e.g. recombinant adenoviruses) achieve highly efficient delivery of DNA to hepatocytes *in vivo*, their anti-HBV therapeutic usefulness remains to be established. Non-viral vectors are currently less competent delivery vehicles, but may ultimately prove to be the method of choice for delivering anti-HBV RNA *in vivo*. Synthetic sequences have the advantage of small size and simpler requirement for delivery to the cytoplasm (and not to the nucleus) to be effective. However, expense and lack of stability of RNA may compromise the application of synthetic RNA. Also, toxic effects of RNA-stabilizing nucleic acids are potentially problematic. Although expression cassettes within DNA sequences offer improved stability and sustained production of therapeutic RNA molecules, efficient delivery of DNA to the hepatocyte nucleus *in vivo* is technically difficult. Nevertheless, studies to date reveal that the virus is susceptible to gene knockdown by hairpin RNA as well as synthetic duplexes. Exploiting the use of RNAi to treat HBV infection holds promise for the effective management of this important global medical problem.

Acknowledgements

Work conducted in the authors' laboratory was supported by the South African Innovation Fund, Cancer Association, Medical Research Council, Carnegie Fund and Griffin Trust. This is gratefully acknowledged.

References

1. Szmuness W, Neurath A R, Stevens C E, Strick N, Harley E J. Prevalence of hepatitis B 'e' antigen and its

antibody in various HBsAg carrier populations. Am J Epidemiol 1981; 113(2): 113–21.
2. Beasley R P, Hwang L Y. Hepatocellular carcinoma and hepatitis B virus. Semin Liver Dis 1984; 4(2): 113–21.
3. Beasley R P, Hwang L Y, Lin C C, Leu M L, Stevens C E, Szmuness W, et al. Incidence of hepatitis B virus infections in preschool children in Taiwan. J Infect Dis 1982; 146(2): 198–204.
4. Botha J F, Ritchie M J, Dusheiko G M, Mouton H W, Kew M C. Hepatitis B virus carrier state in black children in Ovamboland: role of perinatal and horizontal infection. Lancet 1984; 1(8388): 1210–2.
5. Arbuthnot P, Kew M. Hepatitis B virus and hepatocellular carcinoma. Int J Exp Pathol 2001; 82(2): 77–100.
6. Van Nunen A B, Janssen H L, Wolters L M, Niesters H G, de Man R A, Schalm S W. Is combination therapy with lamivudine and interferon-alpha superior to monotherapy with either drug? Antiviral Res 2001; 52(2): 139–46.
7. Hanazaki K. Antiviral therapy for chronic hepatitis B: a review. Curr Drug Targets Inflamm Allergy 2004; 3(1): 63–70.
8. Colacino J M, Staschke K A. The identification and development of antiviral agents for the treatment of chronic hepatitis B virus infection. Prog Drug Res 1998; 50: 259–322.
9. Delaney W E T, Locarnini S, Shaw T. Resistance of hepatitis B virus to antiviral drugs: current aspects and directions for future investigation. Antivir Chem Chemother 2001; 12(1): 1–35.
10. Mason W S, Aldrich C, Summers J, Taylor J M. Asymmetric replication of duck hepatitis B virus DNA in liver cells: free minus-strand DNA. Proc Natl Acad Sci USA 1982; 79(13): 3997–4001.
11. Weiser B, Ganem D, Seeger C, Varmus H E. Closed circular viral DNA and asymmetrical heterogeneous forms in livers from animals infected with ground squirrel hepatitis virus. J Virol 1983; 48(1): 1–9.
12. Tiollais P, Pourcel C, Dejean A. The hepatitis B virus. Nature 1985; 317(6037): 489–95.
13. Mason W S, Halpern M S, England J M, Seal G, Egan J, Coates L, et al. Experimental transmission of duck hepatitis B virus. Virology 1983; 131(2): 375–84.
14. Ruiz-Opazo N, Chakraborty P R, Shafritz D A. Evidence for supercoiled hepatitis B virus DNA in chimpanzee liver and serum Dane particles: possible implications in persistent HBV infection. Cell 1982; 29(1): 129–36.
15. Hammond S M, Bernstein E, Beach D, Hannon G J. An RNA-directed nuclease mediates post-transcriptional gene silencing in Drosophila cells. Nature 2000; 404(6775): 293–6.
16. Sharp P A. RNA interference – 2001. Genes Dev 2001; 15(5): 485–90.
17. Elbashir S M, Harborth J, Lendeckel W, Yalcin A, Weber K, Tuschl T. Duplexes of 21-nucleotide RNAs mediate RNA interference in cultured mammalian cells. Nature 2001; 411(6836): 494–8.
18. Brummelkamp T R, Bernards R, Agami R. A system for stable expression of short interfering RNAs in mammalian cells. Science 2002; 296(5567): 550–3 (Epub 2002 Mar 21.).
19. Lee N S, Dohjima T, Bauer G, Li H, Li M J, Ehsani A, et al. Expression of small interfering RNAs targeted against HIV-1 rev transcripts in human cells. Nat Biotechnol 2002; 20(5): 500–5.
20. Miyagishi M, Taira K. U6 promoter driven siRNAs with four uridine 3′ overhangs efficiently suppress targeted gene expression in mammalian cells. Nat Biotechnol 2002; 20(5): 497–500.
21. Paul C P, Good P D, Winer I, Engelke D R. Effective expression of small interfering RNA in human cells. Nat Biotechnol 2002; 20(5): 505–8.
22. Ying C, de Clercq E, Neyts J. Selective inhibition of hepatitis B virus replication by RNA interference. Biochem Biophys Res Commun 2003; 309(2): 482–4.
23. Shlomai A, Shaul Y. Inhibition of hepatitis B virus expression and replication by RNA interference. Hepatology 2003; 37(4): 764–70.
24. McCaffrey A P, Nakai H, Pandey K, Huang Z, Salazar F H, Xu H, et al. Inhibition of hepatitis B virus in mice by RNA interference. Nat Biotechnol 2003; 21(6): 639–44.
25. Chen Y, Du D, Wu J, Chan C P, Tan Y, Kung H F, et al. Inhibition of hepatitis B virus replication by stably expressed shRNA. Biochem Biophys Res Commun 2003; 311(2): 398–404.
26. Giladi H, Ketzinel-Gilad M, Rivkin L, Felig Y, Nussbaum O, Galun E. Small interfering RNA inhibits hepatitis B virus replication in mice. Mol Ther 2003; 8(5): 769–76.
27. Hamasaki K, Nakao K, Matsumoto K, Ichikawa T, Ishikawa H, Eguchi K. Short interfering RNA-directed inhibition of hepatitis B virus replication. FEBS Lett 2003; 543(1–3): 51–4.
28. Klein C, Bock C T, Wedemeyer H, Wustefeld T, Locarnini S, Dienes H P, et al. Inhibition of hepatitis B virus replication in vivo by nucleoside analogues and siRNA. Gastroenterology 2003; 125(1): 9–18.
29. Konishi M, Wu C H, Wu G Y. Inhibition of HBV replication by siRNA in a stable HBV-producing cell line. Hepatology 2003; 38(4): 842–50.
30. Yang P L, Althage A, Chung J, Chisari F V. Hydrodynamic injection of viral DNA: a mouse model of acute hepatitis B virus infection. Proc Natl Acad Sci USA 2002; 99(21): 13825–30.
31. Reynolds A, Leake D, Boese Q, Scaringe S, Marshall W S, Khvorova A. Rational siRNA design for RNA interference. Nat Biotechnol 2004; 22(3): 326–30.
32. Schwarz D S, Hutvagner G, Du T, Xu Z, Aronin N, Zamore P D. Asymmetry in the assembly of the RNAi enzyme complex. Cell 2003; 115(2): 199–208.
33. Khvorova A, Reynolds A, Jayasena S D. Functional siRNAs and miRNAs exhibit strand bias. Cell 2003; 115(2): 209–16.
34. Bridge A J, Pebernard S, Ducraux A, Nicoulaz A L, Iggo R. Induction of an interferon response by RNAi vectors in mammalian cells. Nat Genet 2003; 34(3): 263–4.
35. Sledz C A, Holko M, De Veer M J, Silverman R H, Williams B R. Activation of the interferon system by short-interfering RNAs. Nat Cell Biol 2003; 5(9): 834–9 (Epub 2003 Aug 24.).
36. Jackson A L, Bartz S R, Schelter J, Kobayashi S V, Burchard J, Mao M, et al. Expression profiling reveals off-target gene regulation by RNAi. Nat Biotechnol 2003; 21(6): 635–7.
37. Moss E G, Taylor J M. Small-interfering RNAs in the radar of the interferon system. Nat Cell Biol 2003; 5(9): 771–2.
38. Saunders L R, Barber G N. The dsRNA binding protein family: critical roles, diverse cellular functions. FASEB J 2003; 17(9): 961–83.
39. Zuker M. Mfold web server for nucleic acid folding and hybridization prediction. Nucleic Acids Res 2003; 31(13): 3406–15.

Chapter 3: Effective inhibition of HBV replication *in vivo* by *anti-HBx* short hairpin RNAs

Carmona, S., Ely, A., Crowther, C., Moolla, N., Salazar, F. H., Marion, P. L., Ferry, N., Weinberg, M. S. & Arbuthnot, P

Molecular Therapy. 2006;13(2):411-21.

This manuscript described the efficacy of each of a panel of 10 Pol III U6 promoter generated short hairpin RNAs (shRNAs). The shRNA design contained mismatches in the stem region and a microRNA-23 terminal loop to aid intracellular processing. Two shRNAs (shRNA 5 and 6) demonstrated 80-100% knockdown of HBV replication in transfected hepatocytes and in a murine hydrodynamic injection model in the absence of the inhibitory effect associated with the non-specific interferon response. To assess efficacy of these shRNAs in a transgenic HBV mouse model, recombinant adenovirus vectors were constructed to deliver shRNA 5 and 6. The knockdown effect was significant and confirmed that these shRNAs could be promising therapeutic candidates against HBV.

Contribution by the author:

SC contributed to the study design. SC designed synthetic siRNAs, constructed the shRNA cassettes, handled all tissue culture, hydrodynamic injections, Northern blot hybridization and transgenic mice work and constructed the recombinant adenovirus vectors. With the support of Prof Arbuthnot and co-authors, SC analysed data and contributed to the drafting and final review of the manuscript.

doi:10.1016/j.ymthe.2005.10.013

ARTICLE

Effective Inhibition of HBV Replication *in Vivo* by Anti-*HBx* Short Hairpin RNAs

Sergio Carmona,[1] Abdullah Ely,[1] Carol Crowther,[1] Naazneen Moolla,[1] Felix H. Salazar,[2,3] Patricia L. Marion,[3] Nicolas Ferry,[4] Marc S. Weinberg,[1] and Patrick Arbuthnot[1,*]

[1]*Hepatitis B Virus Research Unit, Department of Molecular Medicine and Haematology, University of the Witwatersrand Medical School, Private Bag 3, Wits 2050, South Africa*
[2]*Stanford University, Stanford, CA 94305, USA*
[3]*Hepadnavirus Testing, Inc., Mountain View, CA, USA*
[4]*INSERM CIC-04, CHU Hotel-Dieu, Nantes, France*

**To whom correspondence and reprint requests should be addressed. Fax: +27 11 717 2395. E-mail: arbuthnotpb@pathology.wits.ac.za.*

Available online 5 December 2005

Exploiting the RNA interference pathway has shown promise for developing novel and effective treatment of hepatitis B virus (HBV) infection. To advance this approach, we analyzed the antiviral efficacy of a panel of 10 Pol III U6 promoter-encoded short hairpin RNAs (shRNAs) that target conserved sequences of the oncogenic *HBx* open reading frame. To facilitate intracellular processing, the shRNAs included mismatches in the 25-bp stem region and a terminal loop of miRNA-23. Two shRNAs (shRNA 5 and shRNA 6) showed knockdown of HBV markers by 80–100% in transfected hepatocytes and also in a murine hydrodynamic injection model of HBV replication. Intracellular processing of hairpin RNA with the intended strand bias correlated with antiviral efficacy. Moreover, markers of HBV replication were inhibited without inducing genes associated with the nonspecific interferon response. To assess the antiviral efficacy of the shRNAs in a context that is similar to natural HBV infection, shRNA-encoding cassettes were tested against the virus in a HBV transgenic murine model. When delivered using recombinant adenovirus vectors, U6 shRNA 5 and U6 shRNA 6 mediated significant HBV knockdown. Collectively, these observations indicate that U6 shRNA 5 and U6 shRNA 6 are promising candidates for therapy of chronic HBV infection.

Key Words: RNAi, short hairpin RNA, HBV, hydrodynamic injection, HBV transgenic mice, recombinant adenovirus, interferon response

INTRODUCTION

Persistent hepatitis B virus (HBV) infection remains an important global public health problem with an estimated 6% of the world's population chronically infected with the virus [1–3]. The clinical course of HBV infection is not constant and may be influenced by properties of individual viral variants [4,5]. For example, chronic infection with HBV subgenotype A1, which is hyperendemic to South Africa, is associated with a particularly high risk of hepatocellular carcinoma [6]. Licensed treatments for HBV infection, which include interferon-α and nucleoside (lamivudine) and nucleotide (adefovir) analogues, produce a long-term response in only a minority of chronic carriers [7,8]. The continued search for an effective therapy to prevent life-threatening complications thus remains a priority. HBV has a compact genome (Fig. 1) that makes it well suited to developing antiviral therapies that are based on nucleic acid hybridization. Overlapping open reading frames (ORFs) cover the entire viral genome [9] and conserved regions may encode more than one protein as well as HBV *cis* elements required for viral replication. *HBx* is an example of a multifunctional HBV sequence. It encodes the HBx protein, which has been implicated in HBV-mediated hepatocarcinogenesis (reviewed in [1]) and is required for HBV replication [10,11]. *HBx* also overlaps with the 3′ end of the polymerase ORF, direct repeats that are required during virus reverse transcription, and regions important for transcription control (basic core promoter and negative regulatory elements). HBV transcripts are usually unspliced and have a common 3′ end that includes *HBx* (Fig. 1). The key role of HBx in viral replication and hepatocarcinogenesis, together with the presence of the conserved *HBx* sequence in all of the HBV transcripts, makes it a good target to develop nucleic acid hybridization-based therapy.

Exploiting the RNA interference (RNAi) pathway has shown exciting promise for the development of novel

Copyright © The American Society of Gene Therapy
1525-0016/$30.00

doi:10.1016/j.ymthe.2005.10.013

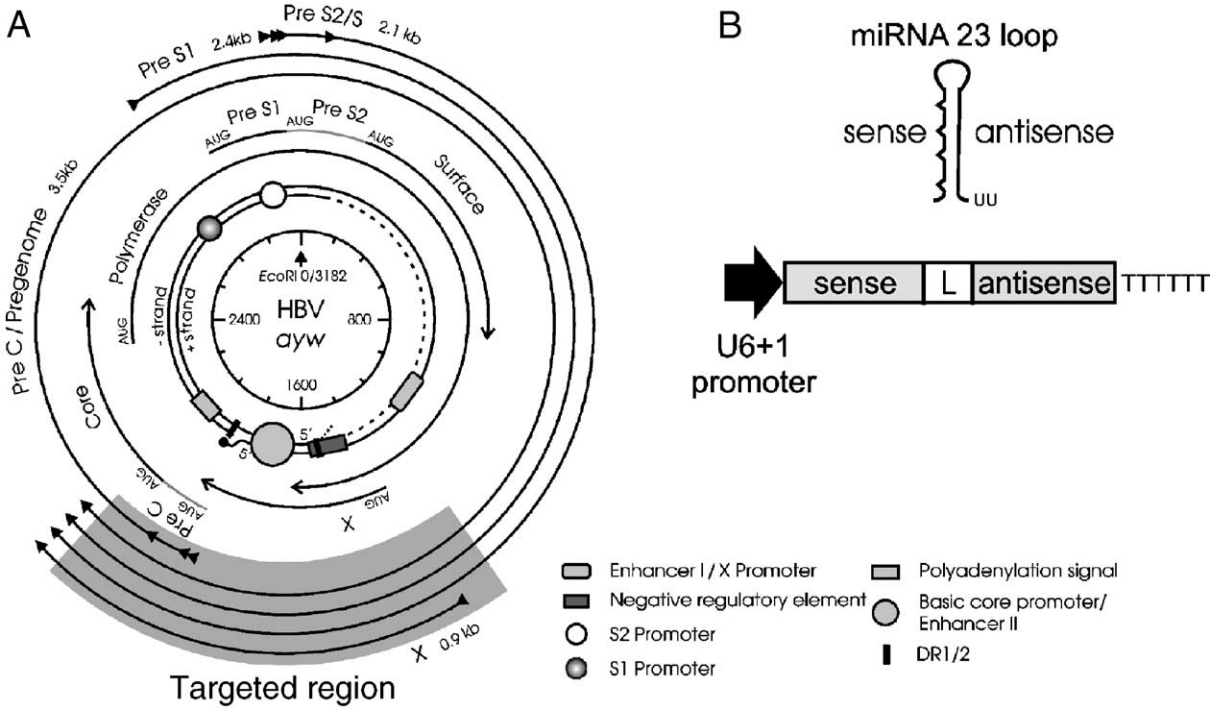


FIG. 1. HBV target sites and shRNA-encoding vectors. (A) Organization of the hepatitis B virus genome showing sites targeted by shRNA sequences. Coordinates of the genome are given relative to the single *Eco*RI restriction site. Partially double-stranded HBV DNA comprises + and − strands with cohesive complementary 5′ ends. The *cis* elements that regulate HBV transcription are represented by the circular and rectangular symbols. Immediately surrounding arrows indicate the viral open reading frames (with initiation codons) that encompass the entire genome. Four outer arrows indicate the HBV transcripts, which have common 3′ ends that include *HBx*. (B) (Top) Schematic illustration of anti-HBV shRNA indicating mismatches in the sense strand, miRNA 23 loop, and sequence of two U residues that are derived from the transcription termination signal. The DNA cassette with U6 promoter, sense, miRNA 23 loop (L), and antisense-encoding sequences is indicated below.

antiviral therapy. Naturally, the mechanism involves processing of larger dsRNA by Dicer to form short interfering RNA (siRNA) duplexes [12–14]. One of the strands of the siRNA is incorporated into the RNA-induced silencing complex (RISC) and acts as a guide to target degradation of complementary cytoplasmic RNA. Exogenous silencing is typically induced by synthetic RNA or transcripts produced from Pol III cassettes [12,15–17]. A number of studies have demonstrated that activation of RNAi has potential for the development of novel treatments of HBV infection [18–27]. As the pathway of RNAi becomes better understood, more rational approaches to the design and characterization of potentially therapeutic RNAi inducers are being sought. Avoidance of the interferon response, efficacy at a low concentration of RNAi-inducing sequences, specificity for the viral cognate, and processing of the duplexes with appropriate strand bias are important considerations. In this study, we report that anti-subgenotype A1 short hairpins RNAs (shRNAs) targeted to *HBx*, which have features of endogenous micro RNA (miRNA) that allow for influencing strand bias, are powerful and specific inhibitors of HBV replication. Inhibition of HBV replication was observed *in vitro* in transfected cells, *in vivo* after gene transfer using hydrodynamic DNA injection, and in HBV transgenic models. Sequences found to be most effective also have homology to other HBV genotypes and potentially have broad therapeutic applications.

RESULTS AND DISCUSSION

HBV Targets and Design of DNA Encoding Antiviral shRNA Sequences

We generated a panel of 10 U6 shRNA cassettes, which target the most conserved sites of the *HBx* sequence from South African genotype A1 isolates of the virus [28]. We designed hairpins to comprise a 25-bp stem with four GU or CA mismatches in the shRNA strand of HBV sense polarity, and the *HBx* antisense sequence was perfectly complementary to the viral target (Fig. 1 and Table 1). The 10-nt loop sequence was common to all of the hairpins and was derived from miRNA-23 [29]. These features were incorporated to facilitate intracellular processing and may also diminish non-specific effects of activating the interferon response [30,31].

Copyright © The American Society of Gene Therapy

TABLE 1: Nucleotide sequences of PCR reverse primers used to generate HBV U6 shRNA cassettes

HBV target[a]	Name	Primer sequence
1168–1192	U6 shRNA 1.1	5′-**TGACG**TGACAGGAAGCGTTAGCAGACACTTGGCATAGGCCCGGTGTTTCGTCCTTTCCACA-3′
	U6 shRNA 1.2	5′-CCCAGATCTACGCGTAAAAAAGGTCTGTGCCAAGTGTTTGCTGACGTGACAGGAAGCGTTA-3′
1432–1456	U6 shRNA 2.1	5′-**GGACG**TGACAGGAAGCGTTCGTGGGATTCAGCGTCGATGGCGGTGTTTCGTCCTTTCCACA-3′
	U6 shRNA 2.2	5′-CCCAGATCTACGCGTAAAAAACCGTCGGCGCTGAATCCCGCGGACGTGACAGGAAGCGTTC-3′
1514–1538	U6 shRNA 3.1	5′-**CTTTA**TGACAGGAAGCAAAGAGAGATGCGCCCCATGGCCGCGGTGTTTCGTCCTTTCCACA-3′
	U6 shRNA 3.2	5′-CCCAGATCTACGCGTAAAAAACGACCACGGGGCGCACCTCTCTTTATGACAGGAAGTAAAG-3′
1518–1542	U6 shRNA 4.1	5′-**ACGCG**TGACAGGAAGCGTGTGAAGAGAGGTGTGCCCTGTGCGGTGTTTCGTCCTTTCCACA-3′
	U6 shRNA 4.2	5′-CCCAGATCTACGCGTAAAAAACACGGGGCGCACCTCTCTTTACGCGTGACAGGAAGCGTGT-3′
1575–1599	U6 shRNA 5.1	5′-**CTCTG**TGACAGGAAGCAGAGGCGAAGCAAAGCGCACACGACGGTGTTTCGTCCTTTCCACA-3′
	U6 shRNA 5.2	5′-CCCAGATCTACGCGTAAAAAACCGTGTGCACTTCGCTTCACCTCTGTGACAGGAAGCAGAG-3′
1580–1604	U6 shRNA 6.1	5′-**CACGT**TGACAGGAAGATGTGTAGAGGTGAAGCGAGGTGTACGGTGTTTCGTCCTTTCCACA-3′
	U6 shRNA 6.2	5′-CCCAGATCTACGCGTAAAAAATGCACTTCGCTTCACCTCTGCACGTTGACAGGAAGATGTG-3′
1640–1664	U6 shRNA 7.1	5′-**GGACT**TGACAGGAAGAGTTCTTTTATGTAGGACTTTGGGCCGGTGTTTCGTCCTTTCCACA-3′
	U6 shRNA 7.2	5′-CCCAGATCTACGCGTAAAAAAGCCCAAGGTCTTACATAAGAGGACTTGACAGGAAGAGTTC-3′
1678–1702	U6 shRNA 8.1	5′-**GAGGC**TGACAGGAAGGCTTCAAGGTTGGTTGTTGACGTTGCGGTGTTTCGTCCTTTCCACA-3′
	U6 shRNA 8.2	5′-CCCAGATCTACGCGTAAAAAACAATGTCAACGACCGACCTTGAGGCTGACAGGAAGGCTTC-3′
1774–1798	U6 shRNA 9.1	5′-**TTGGT**TGACAGGAAGACTAATTTGTGCCTACAGCTTCTTACGGTGTTTCGTCCTTTCCACA-3′
	U6 shRNA 9.2	5′-CCCAGATCTACGCGTAAAAAATAGGAGGCTGTAGGCATAAATTGGTTGACAGGAAGACTAA-3′
1863–1887	U6 shRNA 10.1	5′-**CTTGG**TGACAGGAAGCCAAAGCACAACTCGGAGGCTCGAACGGTGTTTCGTCCTTTCCACA-3′
	U6 shRNA 10.2	5′-CCCAGATCTACGCGTAAAAAATTCAAGCCTCCAAGCTGTGCCTTGGTGACAGGAAGCCAAG-3′

Overlapping sequences are underlined. Mismatches incorporated into the sense strand of the hairpin stems are indicated with a double underline. The region complementary to the U6 promoter is italicized. Sequences encoding *HBx* antisense RNA are bold.

[a] HBV coordinates are relative to the single *Eco*RI site as indicated in Fig. 1.

Effects of shRNA on HBsAg Secretion from Transfected Cells and Assessment of Efficacy *in Situ*

Initially, to assess efficacy against HBV, we cotransfected Huh7 cells with hairpin-encoding sequences and the pCH-9/3091 HBV target plasmid [32]. Variable efficacy of knockdown of viral antigen secretion was achieved by each of the sequences (Fig. 2A). U6 shRNA 5 and U6 shRNA 6 were most effective and plasmids encoding these hairpins decreased HBsAg concentration in the culture supernatant to less than 5% of the mock-treated cells' level. Transfection of the vector encoding U6 shRNA 10 had little if any effect on HBsAg secretion. We corroborated these data using a reporter gene plasmid (pCH-eGFP) to measure knockdown *in situ* (Fig. 2B) [33]. In pCH-eGFP, the preS2/S sequence of pCH-9/3091 was replaced with the enhanced green fluorescent protein (eGFP) ORF, with the targeted *HBx* ORF remaining intact. Cotransfection of pCH-eGFP with shRNA-encoding vectors allows for the convenient measurement of anti-HBV shRNA efficacies using flow cytometry and fluorescence microscopy. Analysis showed that the number of cells expressing eGFP was diminished significantly by U6 shRNA 5 and U6 shRNA 6, while U6 shRNA 10 was least effective (Fig. 2C). The sites targeted by these shRNAs 5 and 6 overlap each other, which suggests that this region of *HBx* is particularly susceptible to RNAi-mediated knockdown. Activators of the RNAi pathway can potentially stimulate nonspecific inflammatory effects by activating the interferon response, which in turn is capable of inducing cell death by apoptosis [34,35]. To exclude this effect, we measured mRNA from three genes that are key components of the interferon response: IFN-β, OAS1, and MxA (Supplemental Fig. 1). Expression of interferon response genes was not increased in Huh7 and HEK293 cells that were transfected with shRNA-expressing plasmids. These observations indicate that the knockdown of HBsAg secretion and eGFP marker expression was specific to activation of RNAi and not a result of causing interferon response-mediated programmed cell death.

Effects of shRNAs on HBV RNA Concentrations

We extracted total cellular RNA from Huh7 cells that had been transiently transfected with shRNA-encoding plasmids together with HBV target DNA. Analysis using Northern blot hybridization confirmed that shRNA 5 efficiently reduced the concentration of HBV RNA (Fig. 3A). When normalized for loading differences using the GAPDH mRNA band intensity, U6 shRNA 5 diminished HBV transcript concentration to approximately 35% of the control value. Concentrations of HBV transcripts in cells cotransfected with the U6 shRNA 10 vector were 90–100% of the controls. Cotransfection of Huh7 cells with U6 shRNA 9 had an intermediate knockdown effect on HBV RNA and diminished concentrations by approximately 40%. These data correlate with the observations on the shRNA effects on HBsAg secretion and *in situ* marker gene expression.

shRNA Processing

To assess processing of expressed shRNA sequences, we carried out primer extension analysis on total RNA that was extracted from the transfected Huh7 liver cell line.

Copyright © The American Society of Gene Therapy

doi:10.1016/j.ymthe.2005.10.013

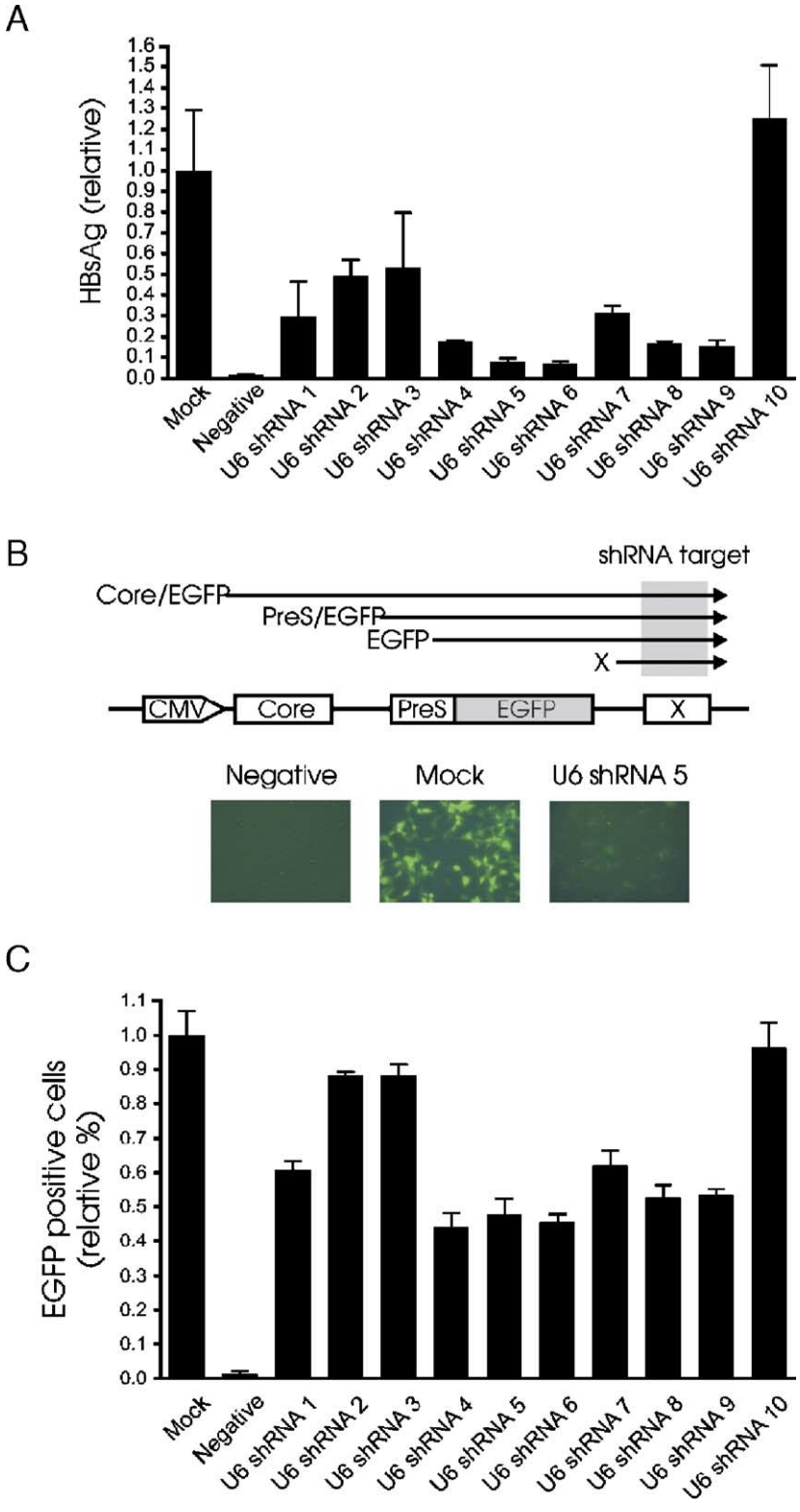


FIG. 2. shRNA-mediated inhibition of HBsAg secretion and HBV–eGFP fusion marker protein expression in transfected cells. (A) Measurement of HBsAg secretion from Huh7 cells cotransfected with indicated shRNA-encoding plasmids together with HBV target plasmid. HBsAg measurements from quantitative ELISA are given as a normalized mean relative to the mock-treated cells. Results are from four independent transfections and the bars indicate the standard error of the mean (SEM). (B) Schematic illustration of plasmid construct pCH-eGFP showing open reading frames, respective transcripts, and sites targeted by shRNAs. The disrupted polymerase ORF is not indicated. Representative fluorescence microscopy fields of Huh7 cells transfected with pCH-eGFP and indicated shRNA-expressing construct are also shown. (C) Quantitative comparison of the percentage of eGFP-positive Huh7 cells detected using flow cytometry after transfection with indicated shRNA-encoding expression vectors. Number of eGFP-positive cells is given as a normalized mean relative to the mock-treated cells, which represents approximately 45% eGFP-positive cells in the total population. Results are depicted as means from four independent transfections (each counting 100,000 events) with the SEM indicated.

Copyright © The American Society of Gene Therapy

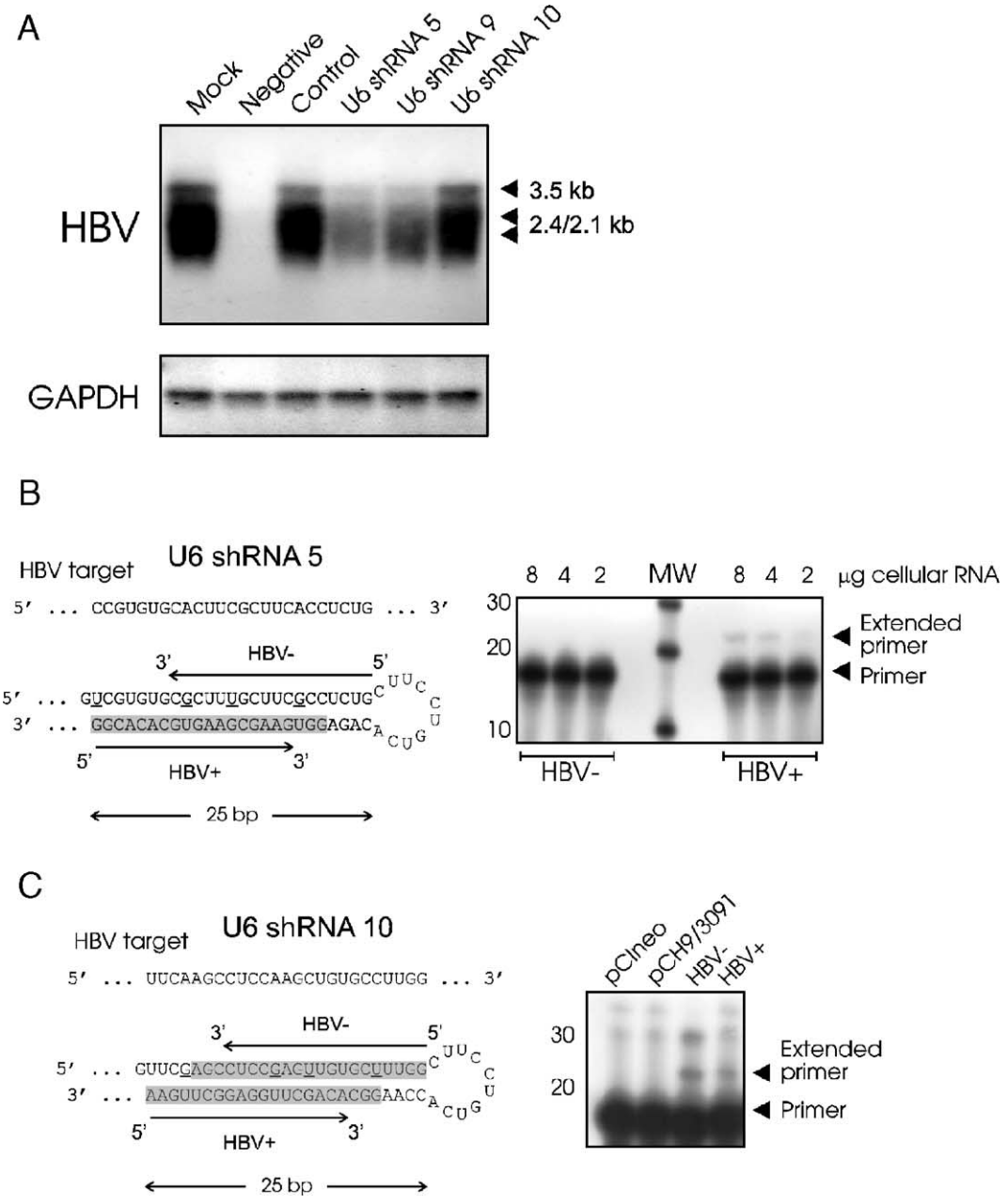


FIG. 3. RNA analysis. (A) Huh7 hepatocytes were transfected with the indicated shRNA-encoding plasmids. Two days after transfection, total RNA was extracted from the cells and analyzed by Northern blot hybridization. The control lane represents analysis of RNA extracted from cells that had been transfected with a plasmid encoding shRNA 5 sequences under transcriptional regulation of the Pol II CMV immediate early promoter/enhancer. Blots were probed for HBV RNA and also GAPDH as a loading control. (B and C) Either radiolabeled HBV^- or radiolabeled HBV^+ oligonucleotides targeting the relevant sequences of shRNA 5 or shRNA 10 were hybridized to total RNA extracted from transfected Huh7 cells and then subjected to primer extension analysis using reverse transcriptase. Sizes of extended fragments were then detected using autoradiography after resolution with denaturing PAGE. The amount of template cellular RNA subjected to reverse transcription is indicated above the lanes and RNA molecular weight marker sizes (nt) are indicated on the left of the autoradiographs.

We radiolabeled oligonucleotide primers that were complementary to the HBV sense or antisense sequence of the hairpin RNA encoded by U6 shRNA 5 or U6 shRNA 10 at their 5′ end, hybridized them to complementary cellular RNA from transfected cells, and then extended them using reverse transcriptase. Extension of end-labeled primers complementary to the U6 shRNA 5 antisense strand generated a 21-nt product that corresponds to the

Copyright © The American Society of Gene Therapy

doi:10.1016/j.ymthe.2005.10.013

putative guide sequence that effects HBV gene silencing (Fig. 3B). A similar primer extension to detect a shRNA-derived *HBx* sense sequence did not generate a signal, and this was confirmed in an overexposed autoradiograph from the same gel. Conversely, when we subjected RNA extracted from U6 shRNA 10-transfected cells to primer extension analysis, both sense and antisense labeled oligonucleotides generated extended products 21 nt in length (Fig. 3C). Moreover, the U6 shRNA 10-encoded sense strand sequence is present at a slightly higher concentration compared to the intended antisense guide. Thus, intracellular processing of the hairpin encoded by U6 shRNA 10 has a slight bias for the nonhybridizing sequence with the same polarity as its viral target. Conversely, the only single-stranded RNA sequence that is detectable from U6 shRNA 5-transfected cells is that which corresponds to the intended antisense guide RNA. Several factors that affect processing and functionality of RNAi effectors have been identified. Included among these is a GC content of 30–52% that is thought to be optimal for efficient unwinding of the duplex while at the same time retaining sufficient stability of interaction of the siRNA guide strand with its target [36–38]. Based on primer extension analysis of shRNA 5, the siRNA derived from this hairpin has 47% GC pairs (9 of 19 pairs in the duplex region). However, the proportion of GC pairs between the shRNA 5-derived guide sequence and the HBV target is higher (62%), and this is a result of the GU mismatch pairs of the shRNA stem that are not present in the hybrid with the HBV target. Thus, it is likely that the relatively lower GC content of the Dicer-processed product facilitates unwinding of the duplex, while the higher GC content of the guide and target pair stabilizes this interaction. Another important factor that determines the processing of RNA duplex is the stability at the 5′ end of the intended guide sequence within the double-stranded RNA [36–38]. With shRNA 5, there is a 5′ GU mismatched base pair at the 5′ end of the antisense strand, and this is likely to facilitate the intended strand bias. Together, these factors are likely to improve processing of shRNA 5 and advance our understanding of the properties of effective anti-HBV RNA sequences.

Efficacy of shRNA-Encoding Plasmids *in Vivo* Using the Murine Hydrodynamic Injection Procedure

To determine anti-HBV efficacy of shRNA *in vivo*, we initially used the hydrodynamic injection procedure to deliver target and shRNA-encoding DNA simultaneously. Using this approach, shRNA 5-encoding plasmid DNA continuously knocked down HBsAg in the serum of mice to a background level over a period of 4 days (Fig. 4A). We also observed an inhibitory effect when we measured HBV core antigen (HBcAg) using immunohistochemical staining in liver sections from mice that had been subjected to hydrodynamic injections (Fig. 4B). The control for DNA delivery efficiency showed that uptake and expression of the *lacZ* marker gene were similar in treated and untreated mice. Comparing efficacies of U6 shRNAs 5, 6, and 10 on day 4 after injection, the production of HBsAg was suppressed completely in mice treated with shRNA 5- or shRNA 6-encoding plasmids (Fig. 4C). However, as was observed in transfected cells, HBsAg concentrations in the serum of mice that were injected with shRNA 10-encoding DNA were not significantly diminished. Similarly, on day 4 HBV viral loads were knocked down to background levels in the mice treated with DNA encoding shRNA 5 or shRNA 6 (Fig. 4D). Again U6 shRNA 10 was less effective, indicating that the knockdown is a sequence-specific phenomenon and is unrelated to generic features of the anti-*HBx* hairpin cassettes. Efficient inhibition of viral replication markers was confirmed when we administered shRNA 5-encoding DNA at a fifth of the molar concentration of HBV target DNA (not shown). Simultaneous injection of 25 μg of synthetic siRNA 5, which has a sequence equivalent to that encoded by U6 shRNA 5, inhibited secretion of HBsAg and viral particle concentration in the serum significantly ($P < 0.05$) (Figs. 4C and 4D). However, the synthetic RNA was also significantly less effective against markers of viral replication than U6 shRNA 5 and U6 shRNA 6 ($P < 0.05$). Sustained production of shRNA from a constitutively active DNA cassette as well as the shorter half-life of RNA compared to plasmid DNA is likely to account for this. Moreover, improved silencing by coupled Dicer processing prior to loading of guide sequences onto the RISC has been reported [39] and may contribute to the enhanced silencing effected by DNA-encoded shRNA compared to synthetic siRNA.

Efficacy of shRNA-Encoding Recombinant Adenovirus Vectors *in Vivo* in HBV Transgenic Mice

We assessed the efficacy of shRNAs against HBV in the context of established constitutive replication of the virus in HBV transgenic mice [40], which mimic natural infection more closely than does the hydrodynamic murine injection model. We incorporated U6 shRNA 5, 6, and 10 expression cassettes into recombinant adenovirus vectors to produce ADV shRNA 5, ADV shRNA 6, and ADV shRNA 10, respectively. Control adenoviruses included a U6 shRNA cassette targeted to the β-galactosidase marker (ADV shRNA LacZ) or no U6 shRNA sequence (ADV eGFP). The recombinant vectors coexpressing eGFP and fluorescence microscopy revealed that approximately 60–80% of hepatocytes expressed adenovirus DNA after tail vein injection with 5×10^9 infectious particles (not shown). Higher doses of adenovirus vectors caused significant hepatic toxicity. Compared to controls and ADV shRNA 10, a single dose of ADV shRNA 5 and ADV shRNA 6 significantly diminished the concentration of HBsAg concentration in the serum over a period of 12

Copyright © The American Society of Gene Therapy

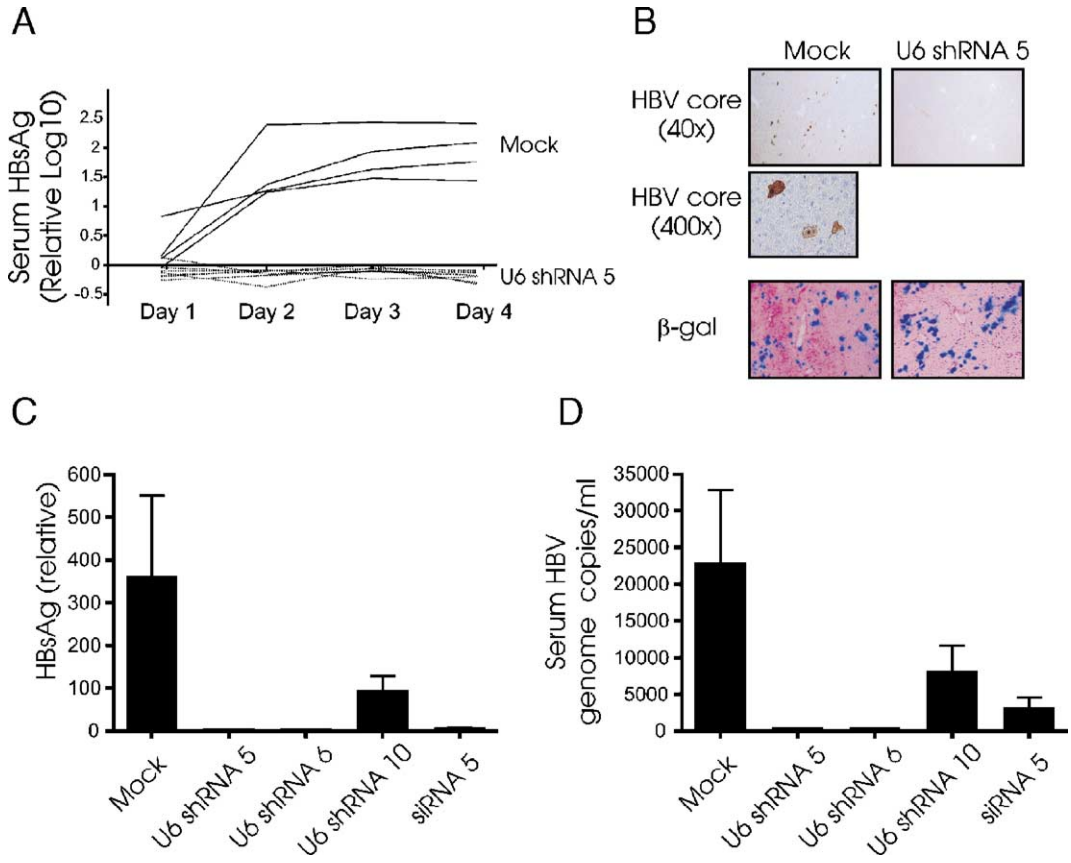


FIG. 4. Effects of shRNA sequences on HBV antigen production in the hydrodynamic injection model of HBV replication. (A) Time course of relative serum HBsAg concentrations, measured using quantitative ELISA, in mice treated with hydrodynamic injection. Graphical depictions of individual measurements of the viral antigen are given on a log scale for four mock- and four U6 shRNA 5-treated animals. (B) Mice subjected to the hydrodynamic injection procedure were sacrificed after 4 days and the livers analyzed using immunohistochemistry to detect the HBcAg. Representative low- and high-power fields are shown for livers from mock- and U6 shRNA 5-treated animals. Frozen sections from the same animals were stained for LacZ activity to confirm similar delivery of DNA to hepatocytes. (C) Serum HBsAg concentrations and (D) viral loads on day 4 after injection of mice using the hydrodynamic injection procedure. Mice were injected with the indicated shRNA-encoding plasmids or synthetic RNA duplex equivalent to shRNA 5 (siRNA 5) together with pCH/9-3091 HBV target DNA. Mock-treated animals received backbone plasmid (pGEM-T Easy) without shRNA-encoding sequences. Viral loads were determined using real-time quantitative PCR and included EuroHep standards to calibrate the virion copy numbers. Groups comprised six to eight animals and the graphs indicate the mean and SEM for each group.

days ($P < 0.05$) (Fig. 5A). Preliminary data also indicate that the inhibition of HBsAg secretion persists for at least 28 days (not shown). This is comparable to a recently reported observation that adenovirus vectors expressing shRNA sequences effected a sustained inhibition of markers of HBV replication [25]. Similarly, compared to control adenovirus vectors, serum HBeAg concentrations were significantly diminished by both ADV shRNA 5 and ADV shRNA 6 at day 12 after administration of the viral vectors ($P < 0.05$) (Fig. 5B). Interestingly, the effects of ADV shRNA 5 and ADV shRNA 6 on HBeAg secretion were less marked than those on HBsAg (approx 2-fold compared to 10-fold inhibition, compare Figs. 5A and 5B). This correlates with the previously reported observation that suggests the 3.5-kb HBV transcript encoding HBeAg is relatively more resistant to RNAi-mediated knockdown [25]. Circulating virion counts were diminished in animals treated with ADV shRNA 5 and ADV shRNA 6, although the effect was less significant than on serum HBeAg and HBsAg concentrations (Fig. 5C). Although target sites of shRNA 5 and shRNA 6 are conserved in the transgenic mice, silencing is less marked than that observed in the hydrodynamic model. There are two possible explanations for this observation. First, levels of HBV in the transgenic mice greatly exceed those of the hydrodynamic injection model (compare viral loads of Figs. 4D and 5C) and complete silencing may be more difficult to achieve when HBV replication is high. Second, under experimental conditions described here, the adenovirus vectors infected 60–80% of hepatocytes. Incomplete delivery of the shRNA-encoding cassettes to all of the HBV-producing cells is likely to account for

Copyright © The American Society of Gene Therapy

doi:10.1016/j.ymthe.2005.10.013

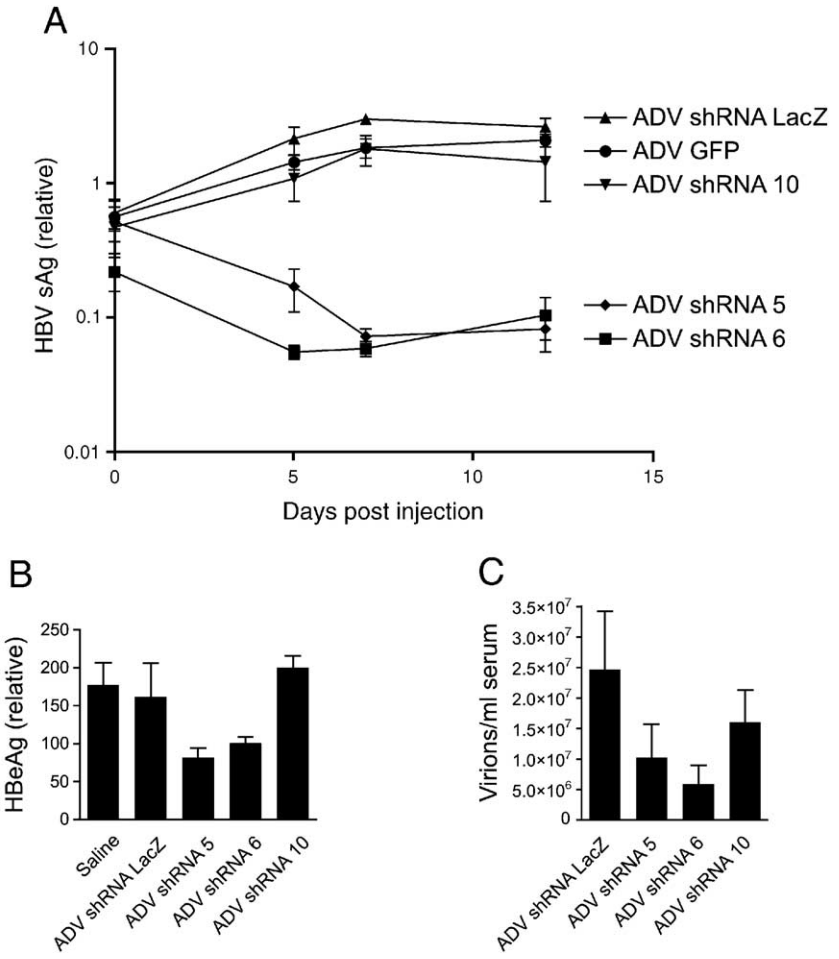


FIG. 5. Effects of recombinant adenovirus-mediated shRNA delivery on viral replication markers in the HBV transgenic mouse model. (A) Time course of relative mouse serum HBsAg concentrations, measured using quantitative ELISA, after tail vein injection of indicated recombinant adenovirus vectors. Relative serum HBsAg concentrations over a period of 12 days are shown. Comparison of (B) serum HBeAg and (C) viral loads at day 12 after injection of animals with saline or indicated recombinant adenovirus.

lower silencing efficiency. Taken together, these data indicate that recombinant adenoviruses incorporating U6 shRNA 5 and U6 shRNA 6 are capable of sustained inhibition of gene expression *in vivo* during constitutive replication of HBV. Moreover, HBV RNA is susceptible to RNAi-mediated silencing and is not protected from silencing by viral proteins.

The demonstration that the anti-*HBx* shRNAs used in this study can successfully inhibit HBV replication indicates that this target sequence is potentially useful for therapeutic application. Effective inhibition of HBV antigen production by U6 shRNA 5 and U6 shRNA 6 is an important advantage over available inhibitors of HBV reverse transcription, which do not reduce viral antigen secretion directly. HBV antigenemia may attenuate the host immune response and compromise eradication of the virus by these drugs [41]. RNAi-based inhibition of viral antigenemia may thus induce a more vigorous anti-HBV immune response to eliminate HBV during chronic infection. Unlike many other viruses, plasticity of the HBV genome is restricted because of its compact arrangement. Target sites of shRNA 5 and shRNA 6 are conserved in most genotypes, suggesting that these RNAi effectors may have broad applicability against different HBV genotypes. Although the results reported here and elsewhere augur well, there are concerns that need to be addressed before effective RNAi-based therapy of HBV infection will be realized. In particular, off-target effects of anti-HBV RNA sequences, which include activation of the interferon response and nonspecific interactions between guide sequences and alternative cellular targets, remain a concern. These effects require further characterization, and optimal therapeutic concentrations need to be defined. An important technical hurdle related to developing RNAi-based antiviral therapy is the efficient delivery of nucleic acid sequences to infected cells in the liver. Although DNA expression cassettes have been shown to be effective in the context of recombinant adenoviruses tested in this study and by others [25], these vectors are unlikely to be suitable for clinical application. Potential toxicity and the limited number of administrations caused by adenovirus immunity are of concern.

Copyright © The American Society of Gene Therapy

Incorporation of U6 shRNA 5 and U6 shRNA 6 into hepatotropic nonviral vectors with limited immunogenicity is an objective of current work.

MATERIALS AND METHODS

shRNA expression cassettes and synthetic siRNA. Conserved target sequences within the *HBx* open reading frame of the HBV A1 subgenotype were identified by aligning sequences of 27 viral isolates of South African origin. To generate the panel of 10 shRNA expression constructs, oligonucleotides were designed to produce Pol III U6 shRNA cassettes from a U6 DNA template [42] in a two-step amplification reaction. The reverse oligonucleotide sequences used during PCR are indicated in Table 1. U6 shRNA X.1 primers were complementary to part of the U6 promoter and included the mismatched *HBx* sense sequences of the short hairpin, together with the hairpin loop. U6 shRNA X.2 primers included the overlapping loop, *HBx* antisense sequence, and transcription termination sequence. Each PCR step was performed with a U6 universal forward primer (5′-CTAACTAGTGGCGCGCCAAGGTCGGGCAGGAAGAGGG-3′). The PCR products from the final amplification step were purified and ligated to a PCR cloning vector (pGEM-T Easy, Promega, WI, USA) to generate pG-U6shRNA plasmids (e.g., pG-U6shRNA 5 and pG-U6shRNA 6). The sequences were confirmed by standard manual or automated sequencing procedures involving dideoxy chain termination. siRNA 5, which has a sequence equivalent to that of the duplex stem of shRNA 5, was synthesized using 2′-O-ACE-RNA phosphoramidites (Dharmacon, CO, USA). The sequences of the oligoribonucleotides were 5′-UCGUGUGCGCUUUGCUUCGCCUCUG-3′ (sense) and 5′-CAGAGGUGAAGCGAAGUGCACACGG-3′ (antisense).

Target vectors. pCH-9/3091 has been described previously [32]. It contains a greater than genome length HBV sequence, which is similar to the HBV A1 subgenotype consensus. pCH-eGFP is derived from pCH-9/3091 and has the eGFP sequence substituting for the preS2/S ORF [33].

Cell culture. Huh7 cells were maintained in RPMI medium supplemented with 2.5% fetal calf serum (FCS), penicillin (50 IU/ml), and streptomycin (50 μg/ml) (Gibco BRL, UK). HEK293 cells were propagated in DMEM supplemented with 10% FCS, penicillin (50 IU/ml), and streptomycin (50 μg/ml) (Gibco BRL). On the day prior to transfection, 250,000 HEK293 cells or 150,000 Huh7 cells were seeded in wells 2 cm in diameter. Transfection was carried out using Lipofectamine (Invitrogen, CA, USA) according to the manufacturer's instructions. To determine the effects of shRNA-encoding plasmids, Huh7 cells were transfected with a combination of 6 μg of pCH-9/3091 and 2 μg of hairpin-encoding pGEM-derived plasmid or control plasmid lacking the shRNA cassette. HBsAg secretion into the culture supernatants was measured daily using the Monolisa (ELISA) immunoassay kit (Bio-Rad, CA, USA). To determine *in situ* effects of the pG-U6 shRNA series of plasmids, Huh7 cells were cotransfected with 6 μg pCH-eGFP instead of pCH-9/3091. Cells labeled with eGFP were detected using flow cytometry and confirmatory fluorescence microscopy 48 h after transfection. The mean number of fluorescent cells as well as the standard error of the mean was calculated from four independent experiments. A plasmid vector that constitutively produces β-galactosidase [43] was included in each cotransfection and equivalent transfection efficiencies were verified by staining for activity of this marker gene [44].

Northern blot hybridization. Huh7 cells were harvested 4 days after transfection and total RNA was extracted using Tri Reagent (Sigma, MI, USA) according to the manufacturer's instructions. The RNA was resolved using formaldehyde agarose gel electrophoresis and blotted onto nylon membranes. An HBV sequence from the surface region was radiolabeled with [α-^{32}P]dCTP using the multiprime technique (Megaprime kit; Amersham, UK) and then hybridized to blotted RNA and detected using autoradiography. As a control for equal loading, the same blot was stripped and rehybridized to a radiolabeled GAPDH-specific probe.

Expression and processing of shRNA. DNA oligonucleotides, which were complementary to 18 nucleotides of each of the strands of the U6-encoded hairpins, were labeled at their 5′ ends with [γ-^{32}P]ATP and T4 polynucleotide kinase. After purification using standard procedures, labeled DNA oligonucleotides were hybridized to 2 to 8 μg of total Huh7 cellular RNA and then extended for 20 min at 42°C with AMV reverse transcriptase (Promega) according to the conditions recommended by the supplier. Products were analyzed by autoradiography after resolution using 8 M urea denaturing 15% polyacrylamide gel electrophoresis. The oligonucleotides used in the primer extension assays were as follows: shRNA 5 HBV+, 5′-CCGTGTGCACTTCGCTTC-3′; shRNA 5 HBV−, 5′-CAGAGGCGAAGCAAAGCG-3′; shRNA 6 HBV+, 5′-TGCACTTCGCTTCACCTC-3′; shRNA 6 HBV−, 5′-ATGTGTAGAGGTGAAGCG-3′; shRNA 10 HBV+, 5′-TTCAAGCCTCCAAGCTGT-3′; shRNA 10 HBV−, 5′-CCAAAGCACAACTCGGAG-3′.

Quantitative PCR. To measure the effects of shRNA sequences on circulating virion DNA (see below), total DNA was isolated from 50 μl of mouse serum using the Total Nucleic Acid Isolation Kit and MagNApure instrument from Roche Diagnostics. Controls included water blanks and HBV-negative serum. DNA extracted from the equivalent of 8 μl of mouse serum was amplified using SYBR Green *Taq* Readymix (Sigma, MO, USA). Crossing-point analysis was used to measure virion DNA concentrations and standard curves were generated using EuroHep calibrators [45]. The HBV surface primer set was HBV surface forward, 5′-TGCACCTGTATTCCATC-3′, and HBV surface reverse, 5′-CTGAAAGCCAAACAGTGG-3′. PCR was carried out using the Roche Lightcycler v.2. Capillary reaction volume was 20 μl and thermal cycling parameters consisted of a hot start for 30 s at 95°C followed by 50 cycles of 57°C for 10 s, 72°C for 7 s, and then 95°C for 5 s. Specificity of the PCR products was verified by melting curve analysis and agarose gel electrophoresis.

Assessment of in vivo efficacy of anti-HBV shRNA constructs. The murine hydrodynamic tail vein injection method was initially employed to determine the effects of shRNA plasmid vectors on the expression of HBV genes *in vivo*. Experiments on animals were carried out in accordance with protocols approved by the University of the Witwatersrand Animal Ethics Screening Committee. A saline solution comprising 10% of the mouse's body mass was injected via the tail vein over 5–10 s. The saline solution included a combination of three plasmid vectors: 10 μg target DNA (pCH-9/3091) or 10 μg pCI-neo plasmid DNA (Promega), which lacks HBV sequences; 10 μg anti HBV sequence (shRNA-encoding plasmid) or mock (pGEM backbone); and 10 μg pLTR β-gal [43] (a control for hepatic DNA delivery, which encodes the β-galactosidase marker gene under control of an LTR promoter). In some investigations, the amount of shRNA-encoding plasmid was reduced to 5 and 1 μg. To test the efficacy of synthetic siRNA 5 against HBV, 25 μg of this duplex was coinjected via the tail vein. Blood was collected daily from the tail vein over a period of 5 days and HBsAg was measured using the electrochemiluminescence assay (ECLIA) from Roche Diagnostics (Mannheim, Germany) according to the manufacturer's instructions. Animals were sacrificed after 4 days. Fixed and unfixed frozen liver sections were processed respectively for immunohistochemical HBcAg detection or for β-galactosidase staining [44]. A rabbit polyclonal antibody against HBcAg (Signet Laboratories, Inc., MA, USA) and horseradish peroxidase-conjugated secondary antibody (Dako, Denmark) were used to detect the viral antigen in paraffin-embedded sections according to standard procedures.

Adenovirus vectors. The procedure described by He *et al*. [46] was followed for the preparation of the ADV shRNA 5, ADV shRNA 6, ADV shRNA 10, ADV eGFP, and ADV shRNA LacZ adenovirus vectors. ADV shRNA LacZ is a control adenovirus that includes a U6 shRNA cassette with hairpin that targets the β-galactosidase reporter gene. ADV eGFP is another control that includes the backbone sequence without U6 hairpin cassette. The pG shLacZ vector was propagated using the two-step PCR procedure described above. The U6 universal forward primer, with 5′-CTGTTTGACAGGAAGAACAAGTATCCGCTAGTCACTTCGACGGTGTTTCGTCCTTTCCACA-3′ and 5′-CCCAGATCTACGCGTAAAAAATCGAAGTGACCAGCGAATACCTGTTTGACAGGAAGAACAA-3′ as reverse primers, was used in sequential amplifications. To generate adenovirus shuttle vectors containing the shRNA cassettes, pG-U6shRNA vectors were

Copyright © The American Society of Gene Therapy

doi:10.1016/j.ymthe.2005.10.013

digested with *Not*I and *Hin*dIII. The U6 shRNA-containing fragment was purified and ligated to equivalent sites of pAdTrack to generate pAd-Track U6 shRNA. After verifying the sequence of the inserts, pAdTrack U6 shRNAs were digested with *Pme*I and homologous recombination with the pAdEasy-1 adenoviral backbone plasmid was carried out in *Escherichia coli* BJ55183 cells. Propagation of the adenovirus in HEK293 cells was then done according to the described procedures [46]. Absence of E1A sequences from each adenovirus was confirmed using PCR. Failure to observe a cytopathic effect in A549 cells, which support adenovirus replication, but which do not provide E1 sequences *in trans*, verified that wild-type revertants were not present in any of the adenovirus preparations.

HBV transgenic mice. HBV transgenic mice with greater than genome length HBV sequence stably integrated into their genomes, which constitutively generates HBV particles [40], were used to assess the antiviral efficacy of shRNA-encoding adenoviral vectors. All procedures were approved by the Animal Care Committee at Stanford University. A dose of 5×10^9 adenovirus infectious particles was injected via the tail vein. Serum HBsAg was measured using a quantitative sandwich ELISA from Abbott Laboratories, and HBeAg was determined using the ECLIA from Roche Diagnostics (Mannheim, Germany) according to the manufacturer's instructions. Viral loads were determined using real-time PCR according to procedures described above. Adenovirus gene transduction, assessed by detection of eGFP, was determined using fluorescence microscopy of liver sections.

Statistical analysis. Data are expressed as the mean ± standard error of the mean. Statistical difference was considered significant when $P < 0.05$ and was determined according to the Dunnett multiple comparison test and calculated with the GraphPad Prism software package (GraphPad Software, Inc., CA, USA).

ACKNOWLEDGMENTS

This work was supported by grants from the South African Innovation Fund, the National Research Foundation, the South African Poliomyelitis Research Foundation, Mellon Trust, and les Ministères Français des Affaires Etrangères et de l'Education Nationale et de la Recherche. We thank the vector core facility of the University Hospital of Nantes supported by the Association Française contre les Myopathies for providing the adenovirus vectors. The pCH-9/3091 plasmid was generously provided by Michael Nassal. We are also grateful to Gladys Gagliardi for providing technical support, to Marjorie Robbins for assistance with the design of primers for the interferon response, and to Anna Kramvis for HBV subgenotype A1 sequence alignments.

RECEIVED FOR PUBLICATION AUGUST 19, 2005; REVISED OCTOBER 8, 2005; ACCEPTED OCTOBER 27, 2005.

APPENDIX A. SUPPLEMENTARY DATA

Supplementary data associated with this article can be found in the online version at doi:10.1016/j.ymthe.2005.10.013.

REFERENCES

1. Arbuthnot, P., Capovilla, A., and Kew, M. (2000). Putative role of hepatitis B virus X protein in hepatocarcinogenesis: effects on apoptosis, DNA repair, mitogen-activated protein kinase and JAK/STAT pathways. *J. Gastroenterol. Hepatol.* **15:** 357–368.
2. Beasley, R. P., and Hwang, L. Y. (1984). Hepatocellular carcinoma and hepatitis B virus. *Semin. Liver Dis.* **4:** 113–121.
3. Szmuness, W., Neurath, A. R., Stevens, C. E., Strick, N., and Harley, E. J. (1981). Prevalence of hepatitis B "e" antigen and its antibody in various HBsAg carrier populations. *Am. J. Epidemiol.* **113:** 113–121.
4. Kramvis, A., Kew, M., and Francois, G. (2005). Hepatitis B virus genotypes. *Vaccine* **23:** 2409–2423.
5. Schaefer, S. (2005). Hepatitis B virus: significance of genotypes. *J. Viral Hepatitis* **12:** 111–124.
6. Kew, M. C., Kramvis, A., Yu, M. C., Arakawa, K., and Hodkinson, J. (2005). Increased hepatocarcinogenic potential of hepatitis B virus genotype A in Bantu-speaking sub-Saharan Africans. *J. Med. Virol.* **75:** 513–521.
7. Hanazaki, K. (2004). Antiviral therapy for chronic hepatitis B: a review. *Curr. Drug Targets Inflammation Allergy* **3:** 63–70.
8. van Nunen, A. B., Janssen, H. L., Wolters, L. M., Niesters, H. G., de Man, R. A., and Schalm, S. W. (2001). Is combination therapy with lamivudine and interferon-alpha superior to monotherapy with either drug? *Antiviral Res.* **52:** 139–146.
9. Tiollais, P., Pourcel, C., and Dejean, A. (1985). The hepatitis B virus. *Nature* **317:** 489–495.
10. Chen, H. S., *et al.* (1993). The woodchuck hepatitis virus X gene is important for establishment of virus infection in woodchucks. *J. Virol.* **67:** 1218–1226.
11. Zoulim, F., Saputelli, J., and Seeger, C. (1994). Woodchuck hepatitis virus X protein is required for viral infection in vivo. *J. Virol.* **68:** 2026–2030.
12. Elbashir, S. M., Harborth, J., Lendeckel, W., Yalcin, A., Weber, K., and Tuschl, T. (2001). Duplexes of 21-nucleotide RNAs mediate RNA interference in cultured mammalian cells. *Nature* **411:** 494–498.
13. Hammond, S. M., Bernstein, E., Beach, D., and Hannon, G. J. (2000). An RNA-directed nuclease mediates post-transcriptional gene silencing in Drosophila cells. *Nature* **404:** 293–296.
14. Sharp, P. A. (2001). RNA interference—2001. *Genes Dev.* **15:** 485–490.
15. Brummelkamp, T. R., Bernards, R., and Agami, R. (2002). A system for stable expression of short interfering RNAs in mammalian cells. *Science* **296:** 550–553.
16. Elbashir, S. M., Lendeckel, W., and Tuschl, T. (2001). RNA interference is mediated by 21- and 22-nucleotide RNAs. *Genes Dev.* **15:** 188–200.
17. Miyagishi, M., and Taira, K. (2002). U6 promoter driven siRNAs with four uridine 3′ overhangs efficiently suppress targeted gene expression in mammalian cells. *Nat. Biotechnol.* **20:** 497–500.
18. Chen, Y., *et al.* (2003). Inhibition of hepatitis B virus replication by stably expressed shRNA. *Biochem. Biophys. Res. Commun.* **311:** 398–404.
19. Giladi, H., Ketzinel-Gilad, M., Rivkin, L., Felig, Y., Nussbaum, O., and Galun, E. (2003). Small interfering RNA inhibits hepatitis B virus replication in mice. *Mol. Ther.* **8:** 769–776.
20. Hamasaki, K., Nakao, K., Matsumoto, K., Ichikawa, T., Ishikawa, H., and Eguchi, K. (2003). Short interfering RNA-directed inhibition of hepatitis B virus replication. *FEBS Lett.* **543:** 51–54.
21. Klein, C., *et al.* (2003). Inhibition of hepatitis B virus replication in vivo by nucleoside analogues and siRNA. *Gastroenterology* **125:** 9–18.
22. Konishi, M., Wu, C. H., and Wu, G. Y. (2003). Inhibition of HBV replication by siRNA in a stable HBV-producing cell line. *Hepatology* **38:** 842–850.
23. McCaffrey, A. P., *et al.* (2003). Inhibition of hepatitis B virus in mice by RNA interference. *Nat. Biotechnol.* **21:** 639–644.
24. Shlomai, A., and Shaul, Y. (2003). Inhibition of hepatitis B virus expression and replication by RNA interference. *Hepatology* **37:** 764–770.
25. Uprichard, S. L., Boyd, B., Althage, A., and Chisari, F. V. (2005). Clearance of hepatitis B virus from the liver of transgenic mice by short hairpin RNAs. *Proc. Natl. Acad. Sci. USA* **102:** 773–778.
26. Wu, H. L., *et al.* (2005). RNA interference-mediated control of hepatitis B virus and emergence of resistant mutant. *Gastroenterology* **128:** 708–716.
27. Ying, C., De Clercq, E., and Neyts, J. (2003). Selective inhibition of hepatitis B virus replication by RNA interference. *Biochem. Biophys. Res. Commun.* **309:** 482–484.
28. Kimbi, G. C., Kramvis, A., and Kew, M. C. (2004). Distinctive sequence characteristics of subgenotype A1 isolates of hepatitis B virus from South Africa. *J. Gen. Virol.* **85:** 1211–1220.
29. Kawasaki, H., and Taira, K. (2003). Short hairpin type of dsRNAs that are controlled by tRNA(Val) promoter significantly induce RNAi-mediated gene silencing in the cytoplasm of human cells. *Nucleic Acids Res.* **31:** 700–707.
30. Akashi, H., Matsumoto, S., and Taira, K. (2005). Gene discovery by ribozyme and siRNA libraries. *Nat. Rev. Mol. Cell Biol.* **6:** 413–422.
31. Matsumoto, S., Miyagishi, M., Akashi, H., Nagai, R., and Taira, K. (2005). Analysis of double-stranded RNA-induced apoptosis pathways using interferon-response noninducible small interfering RNA expression vector library. *J. Biol. Chem.* **280:** 25687–25696.
32. Nassal, M. (1992). The arginine-rich domain of the hepatitis B virus core protein is required for pregenome encapsidation and productive viral positive-strand DNA synthesis but not for virus assembly. *J. Virol.* **66:** 4107–4116.
33. Passman, M., Weinberg, M., Kew, M., and Arbuthnot, P. (2000). *In situ* demonstration of inhibitory effects of hammerhead ribozymes that are targeted to the hepatitis Bx sequence in cultured cells. *Biochem. Biophys. Res. Commun.* **268:** 728–733.
34. Bridge, A. J., Pebernard, S., Ducraux, A., Nicoulaz, A. L., and Iggo, R. (2003). Induction of an interferon response by RNAi vectors in mammalian cells. *Nat. Genet.* **34:** 263–264.
35. Sledz, C. A., Holko, M., de Veer, M. J., Silverman, R. H., and Williams, B. R. (2003). Activation of the interferon system by short-interfering RNAs. *Nat. Cell Biol.* **5:** 834–839.
36. Khvorova, A., Reynolds, A., and Jayasena, S. D. (2003). Functional siRNAs and miRNAs exhibit strand bias. *Cell* **115:** 209–216.
37. Reynolds, A., Leake, D., Boese, Q., Scaringe, S., Marshall, W. S., and Khvorova, A. (2004). Rational siRNA design for RNA interference. *Nat. Biotechnol.* **22:** 326–330.
38. Schwarz, D. S., Hutvagner, G., Du, T., Xu, Z., Aronin, N., and Zamore, P. D. (2003). Asymmetry in the assembly of the RNAi enzyme complex. *Cell* **115:** 199–208.
39. Kim, D. H., Behlke, M. A., Rose, S. D., Chang, M. S., Choi, S., and Rossi, J. J. (2005). Synthetic dsRNA Dicer substrates enhance RNAi potency and efficacy. *Nat. Biotechnol.* **23:** 222–226.

Copyright © The American Society of Gene Therapy

40. Marion, P. L., *et al.* (2003). A transgenic mouse lineage useful for testing antivirals targeting hepatitis B virus. In *Frontiers in Viral Hepatitis*, pp. 197–202. Elsevier, Amsterdam.
41. Rehermann, B., and Chisari, F. V. (1995). The immunology of chronic hepatitis B. In *Hepatitis B Virus: Molecular Mechanisms in Disease and Novel Strategies for Therapy* (R. Koshy, W. Caselmann Eds.), pp. 85–117. Imperial College Press, London.
42. Castanotto, D., Li, H., and Rossi, J. J. (2002). Functional siRNA expression from transfected PCR products. *RNA* **8:** 1454–1460.
43. Wang, C., and Stiles, C. D. (1994). Platelet-derived growth factor alpha receptor gene expression: isolation and characterization of the promoter and upstream regulatory elements. *Proc. Natl. Acad. Sci. USA* **91:** 7061–7065.
44. Sanes, J. R., Rubenstein, J. L., and Nicolas, J. F. (1986). Use of a recombinant retrovirus to study post-implantation cell lineage in mouse embryos. *EMBO J.* **5:** 3133–3142.
45. Heermann, K. H., Gerlich, W. H., Chudy, M., Schaefer, S., and Thomssen, R. (1999). Quantitative detection of hepatitis B virus DNA in two international reference plasma preparations. Eurohep Pathobiology Group. *J. Clin. Microbiol.* **37:** 68–73.
46. He, T. C., Zhou, S., da Costa, L. T., Yu, J., Kinzler, K. W., and Vogelstein, B. (1998). A simplified system for generating recombinant adenoviruses. *Proc. Natl. Acad. Sci. USA* **95:** 2509–2514.

Copyright © The American Society of Gene Therapy

Chapter 4: Specific inhibition of HBV replication *in vitro* and *in vivo* with expressed long hairpin RNA

Weinberg, M. S., Ely, A., Barichievy, S., Crowther, C., Mufamadi, S., Carmona, S. & Arbuthnot, P.

Molecular Therapy 2007;15(3):534-41.

The article describes the use of long hairpin RNAs as an alternative modality to generate multiple short interfering RNAs targeting the *HBx* open reading frame of HBV. The study used two U6 Pol III lhRNAs and the efficacy was compared to a previously characterised shRNA to HBV (shRNA5) and a control lhRNA designed to target HIV TAR site. The findings revealed that targets complementary to sequences close to the base of the hairpin stem resulted in higher concentration of effector molecules and consequently a stronger silencing effect. In conclusion, while some advantages were noted incomplete processing was likely to account for the uneven silencing of the HBV targets.

Contribution by the author:

SC contributed from the onset in conceptualizing the study design. SC performed several pilot experiments to determine the feasibility of using lhRNAs and focused on the *in vivo* work, namely hydrodynamic injections. In addition, worked on northern blot hybridization of small RNA molecules that demonstrated correct processing. Under the supervision of Prof P Arbuthnot, SC contributed to data analysis, drafting of the manuscript and final review.

© The American Society of Gene Therapy

Specific Inhibition of HBV Replication *In Vitro* and *In Vivo* With Expressed Long Hairpin RNA

Marc S Weinberg[1], Abdullah Ely[1], Samantha Barichievy[1], Carol Crowther[1], Steven Mufamadi[1], Sergio Carmona[1] and Patrick Arbuthnot[1]

[1]*Hepatitis B Virus Research Unit, Department of Molecular Medicine and Haematology, University of the Witwatersrand Medical School, Wits, South Africa*

Activating RNA interference to achieve specific gene silencing has shown promise for the development of RNA-based treatment of chronic hepatitis B virus (HBV) infection. To further this approach, we assessed the efficacy of expressed long hairpin RNAs (lhRNAs) that target the conserved *HBx* open reading frame of HBV. As substrates for Dicer, lhRNAs have the potential to generate multiple short interfering RNAs (siRNAs) to enable simultaneous targeting of different sites. Two U6 Pol III vectors were constructed that encode anti-HBV lhRNAs with a 62 base pair stem sequence containing multiple G:U pairings. Assessment in transfected cultured cells and also *in vivo* using the murine hydrodynamic injection model showed that one of the lhRNA vectors (lhRNA 1) diminished markers of virus replication by 70–90% without evidence of interferon response induction. Greatest silencing efficacy was observed for targets that are complementary to sequences located at the base of the hairpin stem and this correlated with a higher concentration of siRNAs derived from this region of the lhRNA. Although lhRNA 1 has the advantage of targeting a greater viral sequence, incomplete cellular processing may result in unequal silencing across the span of the viral target RNA.

Received 28 June 2006; accepted 14 November 2006; published online 9 January 2007. doi:10.1038/sj.mt.6300077

INTRODUCTION

Infection with hepatitis B virus (HBV) is an important global medical problem. Available therapy is only partially effective against the virus[1,2] and development of improved treatment modalities remains an important medical priority. Recent demonstrations that activation of the RNA interference (RNAi) pathway can achieve specific silencing of HBV genes[3–8] have prompted the development of novel RNA-based antiviral agents. RNAi usually involves processing of precursor double-stranded RNA (dsRNA) by Dicer to form short interfering RNA (siRNA) duplexes of 21–23 base pairs (bp).[9,10] The siRNA is incorporated into the RNA-induced silencing complex, where one of the strands is selected and acts as a guide to target degradation of complementary cytoplasmic RNA.[11] Silencing by exogenous potentially therapeutic sequences is typically induced by short synthetic duplex RNA or expressed Pol III-driven short hairpin RNA (shRNA).[12–15] Although several viruses have been shown to be susceptible to knockdown by RNAi effector sequences,[16,17] an important concern is escape from silencing effects by viruses that are prone to a high mutation rate. Selection of RNAi escape mutants has been reported *in vitro* for poliovirus,[18] human immunodeficiency virus 1 (HIV-1),[19,20] and hepatitis C virus (HCV).[21] However, with HCV, resistant viral sequences were susceptible to silencing by siRNAs that targeted alternative sites.[21] Using a vector that produces a Dicer substrate that generates multiple siRNAs would have the advantage of limiting escape and targeting a range of sequences found in different viral genotypes or quasispecies.

Use of dsRNA Dicer substrates with a duplex region greater than 30 bp may be complicated by the induction of the nonspecific type 1 interferon (IFN) response in mammalian cells.[22] This may ultimately cause translation suppression and mRNA degradation, which would be undesirable in a therapeutic context. The IFN response is elicited by interaction of dsRNA with cellular proteins, such as dsRNA-dependent RNA protein kinase (PKR) and triggers activation of interferon-β (*IFN-β*), *Myxovirus A* (*MxA*), and *2′,5′-oligoadenylate synthase 1* (*OAS1*) genes among others. Recent studies showed that expressed hairpins evade activation of the IFN response more efficiently than exogenous synthetic RNA.[23] Also, modified long hairpin RNAs (lhRNAs) comprising 50–100 bp with multiple G:U pairings in the stem sequence have been reported to silence HCV targets in cell culture without an immunostimulatory effect.[24,25] Although promising for therapeutic application, it has not been established whether expressed lhRNA vectors are capable of efficient silencing across the extent of the hairpin duplex and whether specific viral gene silencing can be achieved *in vivo*. To address this, we examined the silencing of HBV replication by expressed lhRNAs targeting *HBx*. This multifunctional sequence encodes the HBx protein, which is required for viral replication and has been implicated in HBV-related hepatocarcinogenesis. We show that an anti-lhRNA cassette is capable of specific inhibition of markers of viral replication.

Correspondence: *Patrick Arbuthnot, Hepatitis B Virus Research Unit, Department of Molecular Medicine and Haematology, University of the Witwatersrand Medical School, Private Bag 3, Wits 2050, South Africa. E-mail: patrick.arbuthnot@wits.ac.za*

RESULTS

lhRNA-encoding cassettes

Two U6 Pol III lhRNA cassettes were generated, which target conserved *HBx* sites of HBV genotype A1 isolates[26] (**Figure 1**). Hairpins were designed to comprise a 62 bp stem with 12 G:U wobble pairs in the stem sequence. The lhRNA antisense sequence was perfectly complementary to the viral target, whereas the sense sequence included mismatches. It has been suggested that inclusion of G:U wobble pairings evades induction of the IFN response by a mechanism that involves structural simulation of endogenous microRNA.[24,25] Although the lhRNAs described here included G:U pairings, they were incorporated primarily as a technical aid to improve the efficiency of the two-step polymerase chain reaction (PCR) method for generating expression cassettes.

lhRNA-mediated target silencing in transfected cells without evidence for induction of an IFN response

Initially, to assess efficacy against HBV *in vitro*, Huh7 cells were co-transfected with lhRNA 1 and lhRNA 2 vectors together with the pCH-9/3091 HBV target plasmid.[27] The *HBx* sequence is common to all HBV transcripts (**Figure 1b**) and inhibition of HBV surface antigen (HBsAg) secretion correlates with RNAi-mediated silencing of HBV replication.[3,28,29] Controls included an shRNA-encoding plasmid (shRNA 5), which we have previously shown to be effective against HBV,[3] and also a long hairpin directed against an unrelated HIV-1 trans-acting response element (TAR) sequence. Compared to mock-treated cells, a knockdown of approximately 90% of viral antigen secretion was achieved by lhRNA 1 and shRNA 5 (**Figure 2a**).

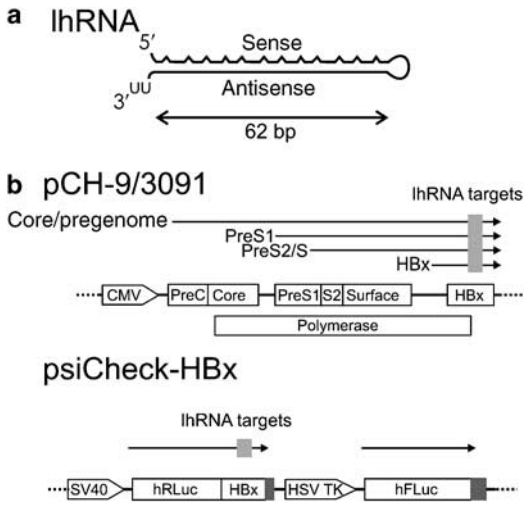


Figure 1 lhRNA sequences and HBV target sites. (**a**) Schematic illustration of lhRNA comprising 62 bp in the stem. G:U pairings are shown as well as a sequence of 2 U residues that are derived from the transcription termination signal. The antisense strand is perfectly complementary to its HBV target. (**b**) Organization of the HBV genome showing ORFs and sites within the pCH-9/3091 target vector that are complementary to antisense components of lhRNA. Four arrows indicate the HBV transcripts, which have common 3′ ends, and include the lhRNA targets. The psiCheck-*HBx* vector includes the entire *HBx* target sequence downstream of the *Renilla* luciferase reporter ORF and firefly luciferase is constitutively produced from a separate expression cassette.

The vector encoding lhRNA 2 caused less impressive inhibition of HBsAg secretion (approximately 50%) and control HIV lhRNA TAR had no significant effect on HBsAg secretion. A series of experiments was also carried out in which psiCheck-*HBx*, a dual luciferase reporter vector (**Figure 1b**), was co-transfected with hairpin plasmids. Firefly luciferase is expressed constitutively in psiCheck-*HBx*, whereas *Renilla* luciferase is susceptible to silencing by hairpin-expressing sequences. A ratio of *Renilla* to firefly luciferase activity was thus used as an indicator of target knockdown. A very similar inhibition of the ratio of *Renilla* to firefly luciferase acivity, and HBsAg secretion was demonstrated (**Figure 2b**). These observations are in accordance with previously reported data, which showed that the viral sequence targeted by lhRNA 1 is particularly susceptible to RNAi-mediated silencing, whereas the downstream lhRNA 2 site is less so.[3]

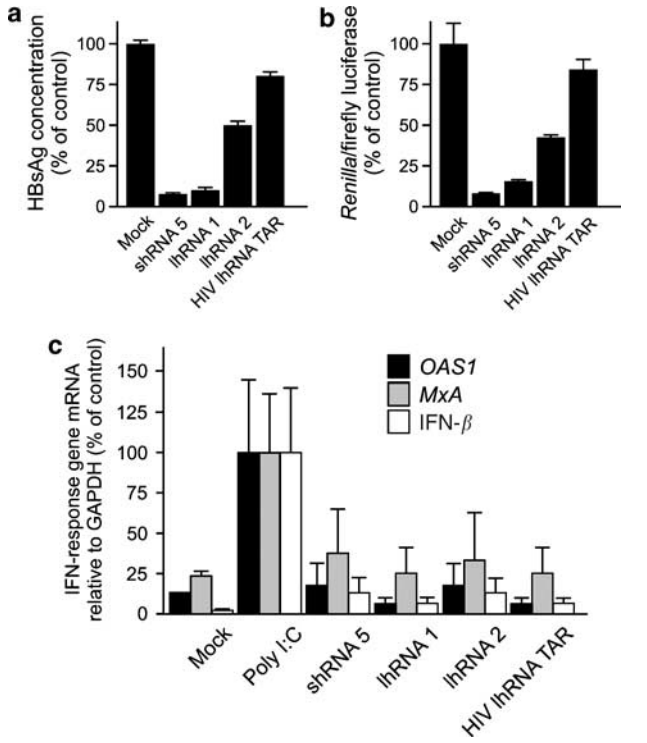


Figure 2 HBsAg secretion and IFN response-related gene expression in transfected cells in culture. (**a**) HBsAg secretion from Huh7 cells co-transfected with indicated hairpin RNA-encoding plasmids together with HBV target plasmid. HBsAg measurements from quantitative ELISA (enzyme-linked immunosorbent assay) are presented as a normalized mean relative to the mock-treated cells. Results are from seven independent transfections and the bars indicate the SEM. (**b**) *Renilla* luciferase reporter gene activity in Huh7 cells co-transfected with indicated hairpin RNA-encoding plasmids together with psiCheck-*HBx* reporter plasmid. Measurements are given as a normalized ratio (±SEM) of *Renilla* to firefly luciferase activity and were determined from three independent experiments. (**c**) Assessing activation of the IFN response in transfected cells. Quantitative real-time PCR was used to measure *IFN-β*, *MxA*, or *OAS1* mRNA. HEK293 cells were transfected with the indicated hairpin RNA-encoding plasmids and the positive control group was transfected with poly (I:C). Means (±SEM) of *IFN-β*, *MxA*, or *OAS1* to *GAPDH* mRNA were calculated from the positive control and were determined from four independent experiments.

© The American Society of Gene Therapy

Activation of the IFN response, which can induce unintended programmed cell death and nonspecific gene silencing, may be effected by duplex RNA in mammalian cells (reviewed in ref. 22). To assess activation of the IFN response in cells that were transfected with lhRNAs, relative levels of cellular *2′,5′-OAS1*, *MxA*, and *IFN-β* mRNA were measured using a sensitive quantitative PCR assay. Data revealed that IFN response genes were not significantly induced in HEK293 cells that had been transfected with lhRNA-encoding sequences (**Figure 2c**), whereas cells treated with poly (I:C) (positive control) mounted an expected IFN response. Activation of *2′,5′-OAS1*, *MxA*, and *IFN-β* was not observed in Huh7 cells after lhRNA vector transfection or poly (I:C) treatment (data not shown), supporting previous findings that the IFN response is attenuated in this liver-derived line.[30] Also, transfection efficiency and cell viability were unaffected by transfection with lhRNA-encoding plasmids (data not shown). Together these data indicate that silencing of reporter gene expression and HBsAg secretion from cells that were co-transfected with lhRNA-encoding cassettes was specific and not a result of induction of the IFN response.

Effects of lhRNA on viral replication *in vivo*

To determine anti-HBV efficacy of shRNA *in vivo*, HBV replication competent plasmid together with lhRNA-encoding vectors were delivered to the liver using the hydrodynamic tail vein injection method. lhRNA 1- and shRNA 5-encoding plasmids knocked down HBsAg in the serum of mice by approximately 90% when measured at day 5 after administering this DNA ($P<0.05$) (**Figure 3a**). lhRNA 2 effected a less significant decrease in HBsAg secretion ($P<0.1$) and HIV lhRNA TAR did not diminish serum HBsAg concentration. These data were supported by measuring the number of viral particle equivalents in the serum at 2 and 5 days after coinjecting HBV target and hairpin-encoding DNA (**Figure 3b**). lhRNA 1 and shRNA 5 inhibited production of viral particle equivalents *in vivo* by 60–70%. Furthermore, measurement of intrahepatic knockdown of HBV gene expression corroborated these findings. Concentrations of HBV mRNA containing core and surface sequences were diminished by lhRNA 1 and shRNA 5 by approximately 60–70% (**Figure 3c**). Three separate lines of evidence, HBsAg concentration determination, viral loads, and intracellular HBV mRNA determination, establish that lhRNA 1 substantially decreases markers of HBV replication *in vivo*.

IFN response *in vivo*

To determine whether lhRNA-induced activation of the IFN response pathway occurs *in vivo*, induction of *OAS1* and *IFN-β* genes in hepatocytes was determined after murine hydrodynamic injection. Expression of both genes was increased at 6 h after injection with poly (I:C), which confirms activation of the IFN response in the positive control (**Figure 4**). This effect was not observed after 5 days and is likely to be a result of the transient nature of the effect of poly (I:C) (data not shown). There was a small increase in *OAS1* mRNA concentration in mock-treated animals at 6 h, which may be due to effects of the hydrodynamic injection procedure itself. Five days after administration of

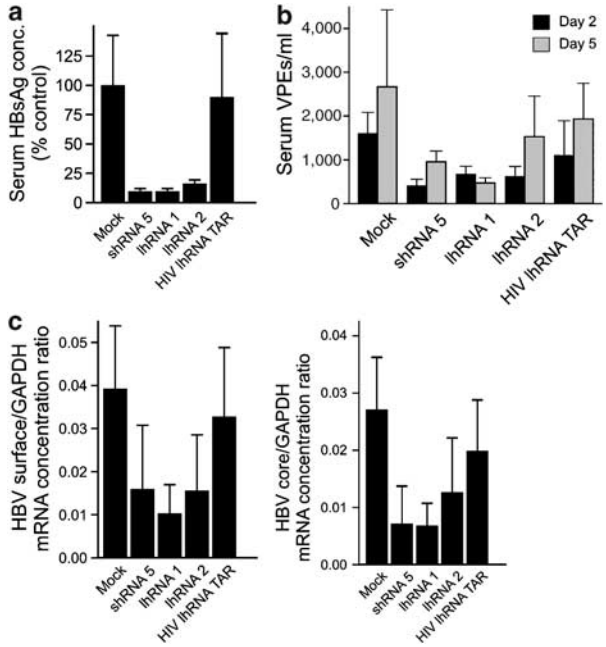


Figure 3 Effects of hairpin sequences on markers of HBV replication in the hydrodynamic injection model of HBV replication. (**a**) Serum HBsAg concentrations were determined at day 5 after hydrodynamic injection of mice with pCH-9/3091 HBV target and indicated hairpin-encoding sequences. Results were normalized relative to the mock-treated mice and are expressed as the mean (±SEM) from at least five mice. (**b**) Serum circulating viral particle equivalents (VPEs) at days 2 and 5 after hydrodynamic injection with the target vector together with hairpin-encoding sequences. (**c**) Hepatocyte concentrations of HBV mRNA from the core and surface regions expressed as a ratio to amount of *GAPDH* mRNA. Total RNA was isolated from liver cells at day 5 after hydrodynamic injection and subjected to quantitative real-time PCR. Groups comprised 5–8 animals and the graphs indicate the mean and SEM for each group.

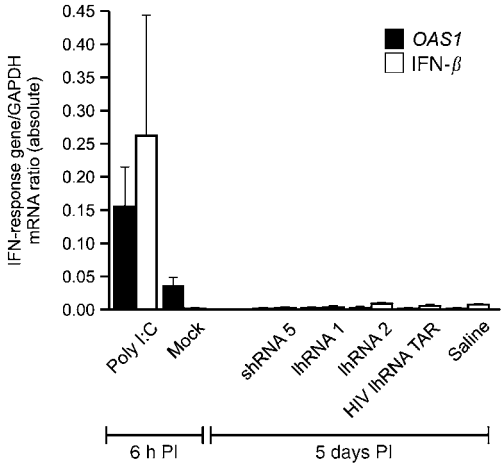


Figure 4 Assessment of *in vivo* IFN response. Mice were mock treated, injected with indicated hairpin-encoding cassettes, or with poly (I:C) using the hydrodynamic procedure. RNA was extracted from the livers and then subjected to quantitative real-time PCR to determine concentrations of *OAS1*, *IFN-β*, and *GAPDH* mRNA. Analysis was carried out after 6 h to verify that an IFN response was induced using the poly (I:C) positive control. In the remaining animals, which had been treated with anti-HBV hairpins, markers of induction of the IFN response were determined after 5 days.

lhRNA-encoding vectors, activation of *OAS1* and *IFN-β* was not observed in any of the groups of mice.

Silencing of mutant targets by lhRNA 1

An advantage of using long hairpin sequences to effect silencing is their potential to serve as substrates for the production of several siRNAs, which can target different viral sequences. This is of importance for inhibition of expression of viral mutants that evade the silencing mechanism. To assess this, we inserted wild-type and mutant targets downstream of the sequence encoding the *Renilla* luciferase gene within the psiCheck2 dual reporter vector. The mutations were located within the target of shRNA 5 (**Figure 5a**). Transfection of cultured cells demonstrated that both lhRNA 1 and shRNA 5 were capable of silencing the normal target (**Figure 5b**). However, the lhRNA sequence silenced mutant targets more effectively than shRNA 5. Interestingly, the shRNA vector remained capable of significant mutant sequence knockdown when compared to the control transfected cells. This may have resulted from translational suppression that did not require perfect complementarity with the HBV cognate. Although lhRNA 1-mediated knockdown of the mutant targets was better than that of shRNA 5, this observation does not establish that there is equally efficient silencing of the target across the extent of the lhRNA 1 duplex.

siRNA guide sequences derived from lhRNA 1

Northern blot hybridization was carried out to determine whether the siRNA guide sequences from lhRNA 1 were produced in equal amounts. RNA extracted from cells transfected with lhRNA 1- and shRNA 5-encoding plasmids was hybridized to each of three labelled oligonucleotide probes (**Figure 6a** and **b**). The sequences of the probes were complementary to, and together spanned the extent of the lhRNA HBV antisense region. Precursor unprocessed shRNA 5 sequences were detectable as a band of approximately 60 nucleotides (nt). Probe A, which is located at the 3′ end of the lhRNA, detected a putative guide sequence of approximately 23 nt in the cells that had been transfected with lhRNA 1, whereas no hybridizing RNA was detectable in cells that had been transfected with shRNA 5. RNA sequences of approximately 23 nt, when detected by probe B, were found in both lhRNA 1- and shRNA 5-transfected cells. As expected, probe C detected a prominent siRNA sequence in shRNA 5-transfected cells. Interestingly, a 23 nt band was not detectable in RNA from lhRNA 1-transfected cells when hybridized to probe C. This was confirmed in a duplicate blot and when hybridized blots were overexposed (data not shown). Thus, siRNAs generated from the loop side of the lhRNA 1 sequences are present in lower concentration than those from the stem base. These observations may reflect initial efficient Dicer cleavage at the stem base of lhRNA 1 and less efficient processing toward the loop side of the hairpin.

Greater silencing efficacy of siRNAs derived from the lhRNA 1 stem base sequence

To determine whether silencing by lhRNA 1 along the extent of the viral target sequence correlated with siRNA concentrations, a tiling assay was performed in which the entire lhRNA 1 target and segments of this sequence spanning from 5′ to 3′

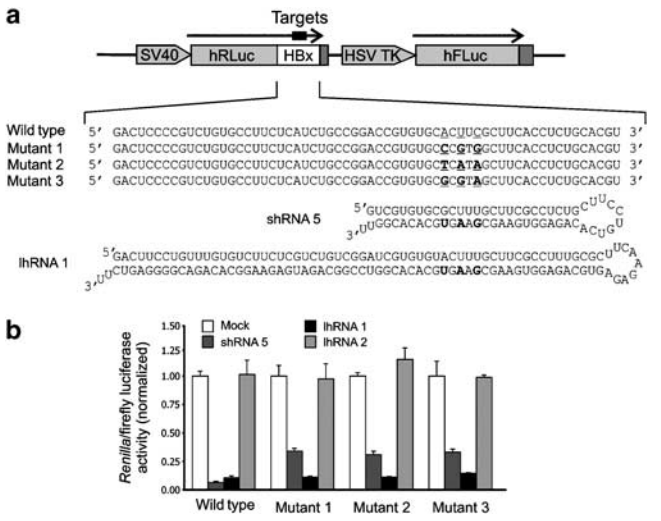


Figure 5 Assessment of silencing efficacy of shRNA 5, shRNA 6, and lhRNA 1 against mutant and wild-type HBV targets. (**a**) HBV sequences were inserted downstream of the *Renilla* luciferase ORF within the psiCheck2 plasmid vector. Nucleotides that are mutated within the targets are indicated in bold as are the affected complementary bases within the putative shRNA 5 and lhRNA 1 structures. (**b**) Knockdown efficiency of shRNA 5 and lhRNA 1 vectors against wild-type and mutant targets. Values are normalized to the ratio of *Renilla* to firefly luciferase activity in the mock transfected cells. Columns indicate the average values from four separate experiments and error bars show the SEM.

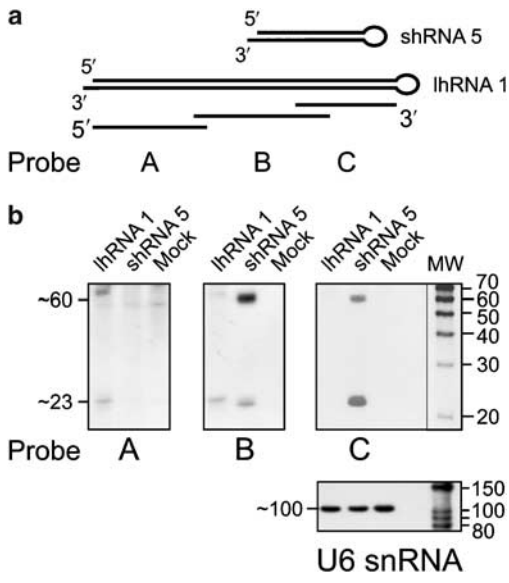


Figure 6 Detection of siRNA sequences produced from expressed lhRNA 1 and shRNA 5. (**a**) Schematic illustration of shRNA 5 and lhRNA 1 with relative positions of probes A, B, and C. These oligonucleotides comprise single-stranded DNA sequences complementary to the HBV antisense strand of the hairpins. (**b**) Hybridization of radiolabelled probes A, B, C, and U6 snRNA (small nuclear RNA) oligonucleotides to RNA from transfected HEK293 cells using Northern blot analysis. Approximate sizes (nt) of hybridizing bands and molecular weight markers are indicated. Blots were sequentially hybridized, stripped, and rehybridized. Repeated hybridization analysis showed data to be reproducible.

© The American Society of Gene Therapy

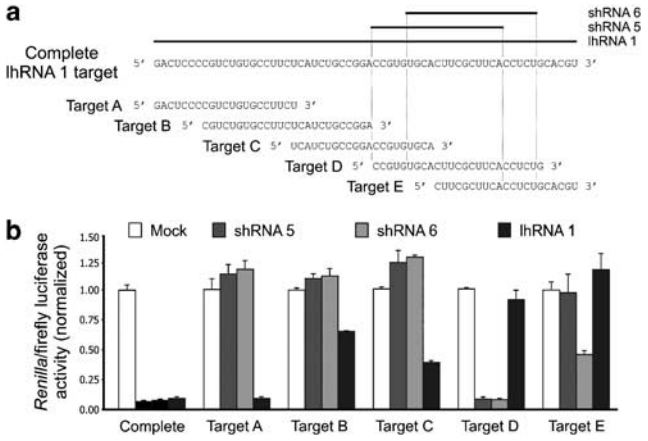


Figure 7 Silencing efficiency across the span of the lhRNA1 target sequence. (**a**) The complete lhRNA1 as well as individual short target sequences (targets A–E) were inserted downstream of the *Renilla* luciferase ORF within the psiCheck2 vector. Areas that are complementary to the sequences located within shRNA 5, shRNA 6, and lhRNA 1 are indicated above. (**b**) Knockdown by shRNA 5, shRNA 6, and lhRNA 1 of individual target sequences. Values are normalized to the ratio of *Renilla* to firefly luciferase activity in the mock-transfected cells. Columns indicate the average values from four separate experiments and error bars show the SEM.

(progressively targets A–E) were inserted downstream of the *Renilla* luciferase open reading frame (ORF) of psiCheck2 (**Figure 7a**). Knockdown of each of the targets was determined according to the ratios of *Renilla* and firefly luciferase activity (**Figure 7b**). Predictably, each of the hairpin-encoding sequences caused knockdown of the complete target. Only lhRNA 1 inhibited *Renilla* luciferase expression when target A was placed downstream of the reporter. Neither shRNA 5 nor shRNA 6 had any effect on *Renilla* luciferase expression when the reporter vector contained targets A, B, or C, whereas lhRNA 1 induced silencing at targets B and C, but with lower efficacy than against target A. Target B straddles the putative initial Dicer cleavage site of lhRNA 1. This means that siRNAs from the long hairpin are likely to have only partial sequence complementarity to target B and poor silencing efficacy against this sequence. More effective lhRNA 1 silencing of target C than target B may be a result of improved hybridization of a putative second Dicer-generated siRNA from the lhRNA 1 sequence. Target D, which encompasses shRNA 5 and shRNA 6 cognates, was a poor substrate for silencing by lhRNA 1, but efficient knockdown was achieved by the shRNA vectors. Target E was also poorly silenced by lhRNA 1 and partially knocked down by shRNA 6. Taken together with the analysis of concentrations of RNA fragments from lhRNA 1 (**Figure 6**), these data suggest that siRNAs from the loop side of the long hairpin are formed less efficiently and are less effective silencers of target RNA than those from the stem base. Similar investigation of knockdown of HIV-1 targets by lhRNAs (data not shown) corroborates this.

DISCUSSION

Several studies have demonstrated that synthetic siRNA and expressed shRNA can be used to silence HBV gene expression.[3–8] A range of different sites within the viral genome has been targeted, and variable efficiency of knockdown has been observed. Although algorithms have been devised that distinguish effective RNAi inducers, predictions that identify optimal targets are often difficult to make.[31] Typically, screening of several candidate silencing sequences and empirical validation is required to aid in identifying the optimal RNAi effector. Use of a combination of siRNAs should thus facilitate the process of achieving successful silencing. This was confirmed in a study which showed that transfecting cells with a panel of siRNAs produced *ex vivo* using recombinant Dicer is a useful means of attaining reliable silencing.[32,33] Generating several siRNAs from one expressed lhRNAs sequence is analogous and should improve the probability of assembling effective silencing complexes.[34] An important concern of applying RNAi to the treatment of virus infections, particularly viruses such as HBV which replicate using error-prone reverse transcriptase, is the evasion of silencing effects as a result of mutation. Selection of poliovirus,[18] HIV-1,[19,20] and HCV[21] RNAi escape mutants has been reported and, in the case of HCV, resistant sequences were susceptible to siRNAs that targeted alternative sites.[21] Using lhRNA to target several sites simultaneously should overcome viral escape and also improve the probability of successful silencing. Although these are important theoretical advantages, our data show that silencing is not equally efficient across the extent of the lhRNA duplex. siRNAs originating from the duplex at the loop terminus side of the hairpin have poor silencing efficacy. Knockdown was most effective by siRNAs derived from the stem base and siRNAs from this part of the lhRNA were also present in higher concentration. Importantly, this bias in knockdown efficiency has implications for design and use of lhRNAs to counter viral escape and optimize target sequence silencing. A likely reason for unequal silencing by lhRNA-derived siRNAs is that Dicer cleavage is initiated at the stem base end of the lhRNA where 2 nt 3′ overhangs are recognized by the enzyme.[9,10] Processing capacity of intracellular Dicer may be incomplete, resulting in a relatively higher concentration of siRNAs arising from the stem base of the lhRNA. The rate of lhRNA transcription and differences in the stability of nascent and partially diced hairpin RNA are also likely to contribute to our findings.

Several properties of RNAi effectors have been described that may cause unwanted activation of an innate immune response. These include duplex sequences that are longer than 30 bp,[35] presence of 5′ triphosphates,[36] "danger" sequence motifs,[37] and lack of 2 nt 3′ overhangs.[38] Induction of immunostimulatory effects, particularly the IFN response, has thus been a concern of using lhRNA sequences to effect gene silencing. Although long dsRNA induces the IFN response through activation of PKR and interaction with endosomal Toll-like receptors, this effect may be of greater significance when using perfectly matched exogenous synthetic RNA to cause gene silencing.[24,25,39] Expressed hairpin RNA does not have the same immunostimulatory properties as synthetic dsRNA.[23] Importantly, RNA that is transcribed within cells does not typically traverse the endosomal compartment and interact with Toll-like receptor 3, Toll-like receptor 7, and Toll-like receptor 8 to stimulate downstream activators of the innate immune response. Moreover, lhRNA products of Dicer

processing have characteristic 2 nt 3′ overhangs, which are a structural feature that suppresses immunostimulation by RIG-I (retinoic-acid-inducible protein I).[38] Collectively, these factors, and possibly the presence of G:U wobbles in the lhRNA duplex, are likely to limit induction of the IFN response in cultured cells or *in vivo*.

Specificity of RNAi effectors for their cognate targets is also critical for development of therapeutic RNA. Minimal or no unintended crossreaction of silencing sequences with cellular RNA will be an important requirement for therapeutic application of lhRNAs. A concern of using lhRNAs is that Dicer may generate multiple overlapping siRNAs with unpredictable guide strand bias, resulting in an increased probability of off-target effects. The length and specific sequences of the duplex are likely to be the major contributors to these nonspecific side effects. Although Dicer predominantly generates duplex siRNAs containing 21 nt RNA strands, the size ranges from approximately 21 to 23 nt.[9,10] Thus, with longer dsRNA substrates, formation of siRNAs is likely to proceed with decreasing precision, which may contribute to off-target effects. In this study, we designed an lhRNA expression cassette that would potentially target three adjacent HBV siRNA targets. This is considerably shorter than the duplex region of other lhRNAs that have been reported to cause specific silencing of target genes.[34] Nevertheless, as with eventual therapeutic application of any RNAi effectors, it is likely that detailed analysis, including use of microarrays, will be required to verify specificity of lhRNA1.

The recent demonstration that saturation of the natural microRNA pathway by exogenous expressed RNA causes toxicity in hepatocytes is a caveat for development of RNAi-based HBV therapy.[40] This is of concern for application of constitutively expressed lhRNAs, and refined transcription control to regulate intracellular concentration of RNAi effectors will be required. Investigations are currently in progress in our laboratory, which are aimed at assessing efficacy of hairpin sequences expressed from liver-specific Pol II promoters.

Results from our study have shown that expressed lhRNA is capable of inhibiting production of markers of viral replication in cell culture and *in vivo* models of HBV. This effect was observed without induction of the IFN response. Although unequal silencing across the extent of the lhRNA duplex was observed, the approach offers promise for the use of expressed sequences containing long duplexes that generate multiple siRNAs to silence HBV gene expression.

MATERIALS AND METHODS

lhRNA expression plasmids. Generation of the Pol III U6 shRNA 5 cassette has been described.[41] A similar two-step PCR approach was used to produce the lhRNA vectors complementary to HBV coordinates 1581–1640 (lhRNA 1) and 1372–1431 (lhRNA 2) (accession J02203). The first amplification was carried out with a universal U6 forward primer and first lhRNA reverse primer with U6 promoter plasmid DNA as template. The amplified product was used as template for a PCR step with a second lhRNA reverse primer and again the universal U6 forward primer. The sequence of the U6 universal forward (F) primer was 5′-CTAACTAGTGGCGCGCCAAGGTCGGGCAGGAAGAGGG-3′. Sequences of the reverse (R) primers for the amplifications were as follows: lhRNA HBV1-R1 5′-ACTCTCTTGAAGCGCAAAGGCGAAGCAAAGTACACAC GATCCGACAGACGAGAAGACACAAACAGGAAGTCGGTGTTTCGTC CTTTCCACAA-3′ (92 nt), lhRNA HBV1-R2 5′-GATCTCTAGAAAAAA GACTCCCCGTCTGTGCCTTCTCATCTGCCGGACCGTGTGCACTTC GCTTCACCTCTGCACTCTCTTGAAGCGCAAAG-3′ (92 nt), lhRNA HBV2-R1 5′-CATCTCTTGAATGCCGGTACGCAAACAACTTACGCC CACAACCTCCCAGCACAAAGACCCTCAACCCAATCGGTGTTTCGT CCTTTCCACAA-3′ (92 nt), lhRNA HBV2-R2 5′-GATCTCTAGAAA AAAGATTAGGTTAAAGGTCTTTGTACTAGGAGGCTGTAGGCATAAA TTGTCTGCGCACCAGCATCTCTTGAATGCCGGTA-3′ (92 nt), lhRNA HIV TAR-R1 5′-CCTCTCTTGAAGAGTCCCCTAAATAACCAGAGAAC CCCCGGACTCAGATCCGGTCCACCCAGAAAGAACCGGTGTTTCGT CCTTTCCACAA-3′ (91 nt), and lhRNA HIV TAR-R2 5′-GATCTCTA GAAAAAAGGGTCTCTCTAGGTAGACCAGATCTGAGCCCGGGAGCT CTCTGGCTATCTAGGGAACCCTCTCTTGAAGAGTCCCC-3′ (91 nt). Each pair of primers had an overlapping sequence of 19 bases that enabled extension of the PCR product to generate a U6 promoter lhRNA cassette with transcription termination signal.[41] Amplified DNA was ligated to a PCR cloning vector (pTZ57R/T, Fermentas, Madison, WI) to generate pTZ-U6 lhRNA plasmids (pTZ-U6 lhRNA HBV 1, pTZ-U6 lhRNA HBV 2, and pTZ-U6 lhRNA TAR). The sequences were confirmed by standard procedures.

Target plasmids. pCH-9/3091 has been described previously.[27] It contains a greater than genome length HBV sequence, which is similar to the HBV A1 subgenotype consensus. The psiCheck-*HBx* target plasmid was prepared by directed insertion of the *Xho*I-*Not*I digested *HBx* fragment from pCI-neo *HBx*[29] into the plasmid psiCheck2 (Promega, Madison, WI) such that the *HBx* ORF is within the 3′ untranslated region of the *Renilla* Luciferase cassette. The lhRNA HBV 1 target sequence was amplified by PCR amplification using HBx lhRNA-1 F (5′-GATCTCGAGGACTCCCCGTCTGTGCCTTCT-3′) and HBx lhRNA-1 R (5′-GATCGCGGCCGCACGTGCAGAGGTGAAGCGAAGT GCACACGG-3′) primer combinations. The mutagenic reverse primer HBx lhRNA-1m R (5′-GATCGCGGCCGCACGTGCAGAGGTGAAGC NANGNGCACACGG-3′), which contains three random nucleotides, was used to generate mutated targets. PCR products were cloned into the PCR cloning vector as described above and, for the mutated targets, a mixed plasmid population was used to extract target fragments for insertion into corresponding *Xho*I-*Not*I sites within the *Renilla* 3′ untranslated region of psiCheck2. To generate multiple short targets that "tile" the entire HBx lhRNA 1 target, complementary oligonucleotides were treated with polynucleotide kinase (Promega, WI), annealed, and cloned directly into the *Xho*I-*Not*I sites of psiCheck2. To facilitate screening, an *Eco*RV site was inserted within each annealed dsDNA insert. The complementary oligonucleotide sequences used were lhRNA 1a F 5′-TCGAGATATCGACTCCCCGTCTGTGCCTTCTGC-3′ and lhRNA 1a R 5′-GGCCGCAGAAGGCACAGACGGGGAGTCGATA TC-3′; lhRNA 1b F 5′-TCGAGATATCCGTCTGTGCCTTCTCATCTG CCGGAGC-3′ and lhRNA 1b R 5′-GGCCGCTCCGGCAGATGAGA AGGCACAGACGGATATC-3′; lhRNA 1c F 5′-TCGAGATATCTCATCTG CCGGACCGTGTGCAGC-3′ and lhRNA 1c R 5′-GGCCGCTGCACACG GTCCGGCAGATGAGATATC-3′; lhRNA 1d F 5′-TCGAGATATCCCGTG TGCACTTCGCTTCACCTCTGGC-3′ and lhRNA 1d R 5′-GGCCGCCA GAGGTGAAGCGAAGTGCACACGGGATATC-3′; and lhRNA 1e F 5′-TCGAGATATCCTTCGCTTCACCTCTGCACGTGC-3′ and lhRNA 1e R 5′-GGCCGCACGTGCAGAGGTGAAGCGAAGGATATC-3′.

Cell culture. Huh7 cells were maintained in Roswell's Park Memorial Institute medium supplemented with 2.5% fetal calf serum, penicillin (50 IU/ml), and streptomycin (50 μg/ml) (Gibco BRL, Paisley, UK). HEK293 cells were propagated in Dulbecco's modified Eagle's medium supplemented with 10% fetal calf serum, penicillin (50 IU/ml), and streptomycin (50 μg/ml) (Gibco BRL, UK). On the day before transfection, 250,000 HEK293 cells or 150,000 Huh7 cells were seeded

© The American Society of Gene Therapy

in wells of 2 cm diameter. Transfection was carried out using Lipofectamine (Invitrogen, Carlsbad, CA) according to the manufacturer's instructions. To determine the effects of lhRNA-encoding plasmids, Huh7 cells were transfected with a combination of 6 μg of pCH-9/3091[27] or psiCheck-*HBx* target vector and 2 μg of long hairpin-encoding pTZ-derived plasmid or plasmid lacking the lhRNA/shRNA cassettes. HBsAg secretion into the culture supernatants was measured using the Monolisa (enzyme-linked immunosorbent assay) immunoassay kit (BioRad, Hercules, CA). A plasmid vector that constitutively produces enhanced green fluorescent protein[28] was included in each co-transfection and equivalent transfection efficiencies were verified by fluorescence microscopy. The activities of *Renilla* and firefly luciferase were measured with the dual luciferase assay kit (Promega, WI) and using the Veritas dual injection luminometer (Turner BioSystems, Sunnyvale, CA).

Assessment of* in vivo *efficacy of lhRNA constructs. The murine hydrodynamic tail vein injection method was employed according to previously described methods to determine the effects of hairpin-encoding plasmid vectors on the expression of HBV genes *in vivo*.[3] Experiments on animals were carried out in accordance with protocols approved by the University of the Witwatersrand Animal Ethics Screening Committee. As a positive control for the activation of the IFN response *in vivo*, mice were injected with 100 μg poly (I:C) (Sigma, St Louis, MO) and killed 6 h thereafter for gene expression analysis. After discarding data from injections that were suboptimal each experimental group comprised 5–8 mice.

Quantitative PCR. To measure the effects of lhRNA sequences on circulating viral particle equivalents, total DNA was isolated from 50 μl of the serum of mice on days 3 and 5 after hydrodynamic injection and viral DNA was determined using quantitative PCR according to previously described methods[3] with EuroHep calibrating standards.[42] To measure concentrations of mRNA encoding HBV and IFN response-related genes, total RNA from HEK293 cells or mouse liver was reverse transcribed using Sensiscript (Qiagen, GmbH, Germany) and oligo d-T primer according to the manufacturer's instructions. HBV mRNA containing core and surface sequences was amplified using the following primer combinations: core F 5′-ACCACCAAATGCCCCTAT-3′, core R 5′-TTCTGCGACGCGGCGA-3′, surface F 5′-GCCAAAATTCGCAGT CC-3′, and surface R 5′-ACGGGCAACATACCTT-3′. The primer combinations listed below were used to amplify IFN response-related mRNA of human (Huh7 and HEK293 cells) origin: *IFN-β* F (h): 5′-TCCAAATTGCTCTCCTGTTGTGCT-3′; *IFN-β* R (h): 5′-CCACAGGA GCTTCTGACACTGAAAA-3′; glyceraldehyde-3-phosphate dehydrogenase (*GAPDH*) F (h): 5′-AGGGGTCATTgATGGCAACAATATCCA-3′; *GAPDH* R (h): 5′-TTTACCAGAGTTAAAAGCAGCCCTGGTG-3′; *OAS1* F (h): 5′-CGAGGGAGCATGAAAACACATTT-3′; *OAS1* R (h): 5′-GCAG AGTTGCTGGTAGTTTATGAC-3′; *MxA* F (h): 5′-CTGGTGCTGAAAC TGAAGAAAC-3′; and *MxA* R (h): 5′-ATCTCAATCTCGTAGTCCTGG TA-3′. To amplify murine *OAS1*, *IFN-β*, and *GAPDH* complementary DNA, the procedures and primer combinations described by Song *et al.*[43] were used. All quantitative PCRs were carried out using the Roche Lightcycler V.2. Controls included water blanks and RNA extracts that were not subjected to reverse transcription. Taq readymix with SYBR green (Sigma, St Louis, MO) was used to amplify and detect DNA during the reaction. Thermal cycling parameters consisted of a hotstart for 30 s at 95°C followed by 50 cycles of 58°C for 10 s, 72°C for 7 s, and then 95°C for 5 s. Specificity of the PCR products was verified by melting curve analysis and agarose gel electrophoresis.

Northern blot analysis. HEK293 cells were harvested 4 days after transfection and total RNA was extracted using Tri Reagent (Sigma, MI) according to the manufacturer's instructions. Twenty-five micrograms of RNA was resolved on urea denaturing 15% polyacrylamide gels and blotted onto nylon membranes. Decade RNA molecular weight markers (Ambion, Austin, TX), which were labelled radioactively as described below, were run alongside the cellular RNA. Blots were hybridized to three DNA oligonucleotides (probes A, B, and C) to detect products of hairpin processing. These were complementary to regions spanning the HBV antisense sequence of the long hairpin. Probes were labelled at their 5′ ends with [γ-^{32}P]ATP and T4 polynucleotide kinase. After purification using standard procedures, they were hybridized to immobilized RNA, exposed to X-ray film and then stripped and reprobed. An oligonucleotide sequence complementary to U6 small nuclear RNA was used as a control to verify equal loading of the cellular RNA. Probe oligonucleotide sequences were as follows: probe A: 5′-GACTCCCC GTCTGTGCCTTCTCA-3′; probe B: 5′-TCATCTGCCGGACCGTGTG CACT-3′; probe C: 5′-TGCACTTCGCTTCACCTCTGCACTC-3′; and U6 small nuclear RNA probe: 5′-TAGTATATGTGCTGCCGAAGCGAG CA-3′.

Statistical analysis. Data are expressed as the mean ± SE of the mean. Statistical difference was considered significant when $P < 0.05$ and was determined according to Dunnett's multiple comparison test and calculated with the GraphPad Prism software package (GraphPad Software, San Diego, CA).

ACKNOWLEDGMENTS

This work was supported by grants from the South African Innovation Fund, National Research Foundation, and Poliomyelitis Research Foundation. The pCH-9/3091 plasmid was generously provided by Michael Nassal. We thank Gladys Gagliardi for providing technical support.

REFERENCES

1. Hanazaki, K (2004). Antiviral therapy for chronic hepatitis B: a review. *Curr Drug Targets Inflamm Allergy* **3**: 63–70.
2. van Nunen, AB, Janssen, HL, Wolters, LM, Niesters, HG, de Man, RA and Schalm, SW (2001). Is combination therapy with lamivudine and interferon-alpha superior to monotherapy with either drug? *Antiviral Res* **52**: 139–146.
3. Carmona, S, Ely, A, Crowther, C, Moolla, N, Salazar, FH and Marion, PL *et al.* (2006). Effective inhibition of HBV replication *in vivo* by anti-HBx short hairpin RNAs. *Mol Ther* **13**: 411–421.
4. McCaffrey, AP, Nakai, H, Pandey, K, Huang, Z, Salazar, FH and Xu, H *et al.* (2003). Inhibition of hepatitis B virus in mice by RNA interference. *Nat Biotechnol* **21**: 639–644.
5. Uprichard, SL, Boyd, B, Althage, A and Chisari, FV (2005). Clearance of hepatitis B virus from the liver of transgenic mice by short hairpin RNAs. *Proc Natl Acad Sci USA* **102**: 773–778.
6. Giladi, H, Ketzinel-Gilad, M, Rivkin, L, Felig, Y, Nussbaum, O and Galun, E (2003). Small interfering RNA inhibits hepatitis B virus replication in mice. *Mol Ther* **8**: 769–776.
7. Klein, C, Bock, CT, Wedemeyer, H, Wustefeld, T, Locarnini, S and Dienes, HP *et al.* (2003). Inhibition of hepatitis B virus replication *in vivo* by nucleoside analogues and siRNA. *Gastroenterology* **125**: 9–18.
8. Shlomai, A and Shaul, Y (2003). Inhibition of hepatitis B virus expression and replication by RNA interference. *Hepatology* **37**: 764–770.
9. Provost, P, Dishart, D, Doucet, J, Frendewey, D, Samuelsson, B and Radmark, O (2002). Ribonuclease activity and RNA binding of recombinant human Dicer. *EMBO J* **21**: 5864–5874.
10. Zhang, H, Kolb, FA, Brondani, V, Billy, E and Filipowicz, W (2002). Human Dicer preferentially cleaves dsRNAs at their termini without a requirement for ATP. *EMBO J* **21**: 5875–5885.
11. Rand, TA, Petersen, S, Du, F and Wang, X (2005). Argonaute2 cleaves the anti-guide strand of siRNA during RISC activation. *Cell* **123**: 621–629.
12. Brummelkamp, TR, Bernards, R and Agami, R (2002). A system for stable expression of short interfering RNAs in mammalian cells. *Science* **296**: 550–553.
13. Elbashir, SM, Harborth, J, Lendeckel, W, Yalcin, A, Weber, K and Tuschl, T (2001). Duplexes of 21-nucleotide RNAs mediate RNA interference in cultured mammalian cells. *Nature* **411**: 494–498.
14. Elbashir, SM, Lendeckel, W and Tuschl, T (2001). RNA interference is mediated by 21- and 22-nucleotide RNAs. *Genes Dev* **15**: 188–200.
15. Miyagishi, M and Taira, K (2002). U6 promoter driven siRNAs with four uridine 3′ overhangs efficiently suppress targeted gene expression in mammalian cells. *Nat Biotechnol* **20**: 497–500.
16. Haasnoot, PC, Cupac, D and Berkhout, B (2003). Inhibition of virus replication by RNA interference. *J Biomed Sci* **10**: 607–616.

17. Saleh, MC, Van Rij, RP and Andino, R (2004). RNA silencing in viral infections: insights from poliovirus. *Virus Res* **102**: 11–17.
18. Gitlin, L, Stone, JK and Andino, R (2005). Poliovirus escape from RNA interference: short interfering RNA-target recognition and implications for therapeutic approaches. *J Virol* **79**: 1027–1035.
19. Boden, D, Pusch, O, Lee, F, Tucker, L and Ramratnam, B (2003). Human immunodeficiency virus type 1 escape from RNA interference. *J Virol* **77**: 11531–11535.
20. Das, AT, Brummelkamp, TR, Westerhout, EM, Vink, M, Madiredjo, M and Bernards, R *et al.* (2004). Human immunodeficiency virus type 1 escapes from RNA interference-mediated inhibition. *J Virol* **78**: 2601–2605.
21. Wilson, JA and Richardson, CD (2005). Hepatitis C virus replicons escape RNA interference induced by a short interfering RNA directed against the NS5b coding region. *J Virol* **79**: 7050–7058.
22. Stark, GR, Kerr, IM, Williams, BR, Silverman, RH and Schreiber, RD (1998). How cells respond to interferons. *Annu Rev Biochem* **67**: 227–264.
23. Robbins, MA, Li, M, Leung, I, Li, H, Boyer, DV and Song, Y *et al.* (2006). Stable expression of shRNAs in human CD34+ progenitor cells can avoid induction of interferon responses to siRNAs *in vitro*. *Nat Biotechnol* **24**: 566–571.
24. Akashi, H, Miyagishi, M, Yokota, T, Watanabe, T, Hino, T and Nishina, K *et al.* (2005). Escape from the interferon response associated with RNA interference using vectors that encode long modified hairpin-RNA. *Mol BioSyst* **1**: 382–390.
25. Watanabe, T, Sudoh, M, Miyagishi, M, Akashi, H, Arai, M and Inoue, K *et al.* (2006). Intracellular-diced dsRNA has enhanced efficacy for silencing HCV RNA and overcomes variation in the viral genotype. *Gene Ther* **13**: 883–892.
26. Kimbi, GC, Kramvis, A and Kew, MC (2004). Distinctive sequence characteristics of subgenotype A1 isolates of hepatitis B virus from South Africa. *J Gen Virol* **85**: 1211–1220.
27. Nassal, M (1992). The arginine-rich domain of the hepatitis B virus core protein is required for pregenome encapsidation and productive viral positive-strand DNA synthesis but not for virus assembly. *J Virol* **66**: 4107–4116.
28. Passman, M, Weinberg, M, Kew, M and Arbuthnot, P (2000). *In situ* demonstration of inhibitory effects of hammerhead ribozymes that are targeted to the hepatitis Bx sequence in cultured cells. *Biochem Biophys Res Commun* **268**: 728–733.
29. Weinberg, M, Passman, M, Kew, M and Arbuthnot, P (2000). Hammerhead ribozyme-mediated inhibition of hepatitis B virus X gene expression in cultured cells. *J Hepatol* **33**: 142–151.
30. Li, K, Chen, Z, Kato, N, Gale, M Jr and Lemon, SM (2005). Distinct poly(I-C) and virus-activated signaling pathways leading to interferon-beta production in hepatocytes. *J Biol Chem* **280**: 16739–16747.
31. Pei, Y and Tuschl, T (2006). On the art of identifying effective and specific siRNAs. *Nat Methods* **3**: 670–676.
32. Myers, JW and Ferrell, JE (2005). Silencing gene expression with Dicer-generated siRNA pools. *Methods Mol Biol* **309**: 93–196.
33. Myers, JW, Jones, JT, Meyer, T and Ferrell, JE Jr (2003). Recombinant Dicer efficiently converts large dsRNAs into siRNAs suitable for gene silencing. *Nat Biotechnol* **21**: 324–328.
34. Strat, A, Gao, L, Utsuki, T, Cheng, B, Nuthalapaty, S and Mathis, JM *et al.* (2006). Specific and nontoxic silencing in mammalian cells with expressed long dsRNAs. *Nucleic Acids Res* **34**: 3803–3810.
35. Caplen, NJ, Parrish, S, Imani, F, Fire, A and Morgan, RA (2001). Specific inhibition of gene expression by small double-stranded RNAs in invertebrate and vertebrate systems. *Proc Natl Acad Sci USA* **98**: 9742–9747.
36. Kim, DH, Longo, M, Han, Y, Lundberg, P, Cantin, E and Rossi, JJ (2004). Interferon induction by siRNAs and ssRNAs synthesized by phage polymerase. *Nat Biotechnol* **22**: 321–325.
37. Judge, AD, Sood, V, Shaw, JR, Fang, D, McClintock, K and MacLachlan, I (2005). Sequence-dependent stimulation of the mammalian innate immune response by synthetic siRNA. *Nat Biotechnol* **23**: 457–462.
38. Marques, JT, Devosse, T, Wang, D, Zamanian-Daryoush, M, Serbinowski, P and Hartmann, R *et al.* (2006). A structural basis for discriminating between self and nonself double-stranded RNAs in mammalian cells. *Nat Biotechnol* **24**: 559–565.
39. Cullen, BR (2006). Enhancing and confirming the specificity of RNAi experiments. *Nat Methods* **3**: 677–681.
40. Grimm, D, Streetz, KL, Jopling, CL, Storm, TA, Pandey, K and Davis, CR *et al.* (2006). Fatality in mice due to oversaturation of cellular microRNA/short hairpin RNA pathways. *Nature* **441**: 537–541.
41. Castanotto, D, Li, H and Rossi, JJ (2002). Functional siRNA expression from transfected PCR products. *RNA* **8**: 1454–1460.
42. Heermann, KH, Gerlich, WH, Chudy, M, Schaefer, S and Thomssen, R (1999). Quantitative detection of hepatitis B virus DNA in two international reference plasma preparations. Eurohep Pathobiology Group. *J Clin Microbiol* **37**: 68–73.
43. Song, E, Zhu, P, Lee, SK, Chowdhury, D, Kussman, S and Dykxhoorn, DM *et al.* (2005). Antibody mediated *in vivo* delivery of small interfering RNAs via cell-surface receptors. *Nat Biotechnol* **23**: 709–717.

Chapter 5: Controlling HBV Replication *in vivo* by intravenous administration of triggered PEGylated siRNA-Nanoparticles

Carmona, S., Jorgensen, M. R., Kolli, S., Crowther, C., Salazar, F. H., Marion, P. L., Fujino, M., Natori, Y., Thanou, M., Arbuthnot, P. & Miller, A. D.

Molecular Pharmaceutics 2009;6(3):706-17.

This report describes the synthesis of a novel hepatotropic non-viral vector assembled from a cationic liposome containing a cholesteryl-amoxyl lipid for chemoselective post-coupling of polyethylene glycol. The oxime linkage in PEGylated siRNA nanoparticle is pH sensitive and was introduced to promote release of the siRNA once it reached the acidic pH of endosomes. The biodistribution, toxicity profile and silencing effect over a 28-day period was favourable.

Contribution by the author:

SC, MRJ, PA and ADM conceptualised the study, defined the hypothesis and designed experiments. SC was trained to conduct the siRNA PEGylation and nanoparticle assembly of the synthetic siRNAs from components synthesised by the collaborators at Imperial College, London, UK. SC conducted cellular culture experiments, hydrodynamic tail vein injections and all the transgenic mice work. SC conducted the toxicity studies at the WITS Faculty of Health Sciences animal facility. SC contributed to data analysis, manuscript drafting and final review.

articles

molecular pharmaceutics

Controlling HBV Replication *in Vivo* by Intravenous Administration of Triggered PEGylated siRNA-Nanoparticles

Sergio Carmona,[†] Michael R. Jorgensen,[‡] Soumia Kolli,[‡] Carol Crowther,[†] Felix H. Salazar,[§,||] Patricia L. Marion,[||] Masato Fujino,[⊥] Yukikazu Natori,[⊥] Maya Thanou,[‡] Patrick Arbuthnot,*[,†] and Andrew D. Miller*[,‡,#]

Antiviral Gene Therapy Research Unit, Department of Molecular Medicine and Haematology, University of the Witwatersrand Medical School, Private Bag 3, WITS 2050, South Africa, Imperial College Genetic Therapies Centre, Department of Chemistry, Flowers Building, Armstrong Road, Imperial College London, London SW7 2AZ, U.K., Stanford University, Stanford, California, Hepadnavirus Testing, Inc., Mountain View, California, RNAi Co., Cosmos Hongo Bldg. 10F, 4-1-4, Hongo, Bunkyo-ku, Tokyo, 113-0033, Japan, and ImuThes Ltd., Flowers Building, Armstrong Road, London SW7 2AZ, U.K.

Received September 9, 2008; Revised Manuscript Received December 4, 2008; Accepted December 11, 2008

Abstract: Harnessing RNA interference (RNAi) to inhibit hepatitis B virus (HBV) gene expression has promising application to therapy. Here we describe a new hepatotropic nontoxic lipid-based vector system that is used to deliver chemically unmodified small interfering RNA (siRNA) sequences to the liver. Anti HBV formulations were generated by condensation of siRNA (A component) with cationic liposomes (B component) to form AB core particles. These core particles incorporate an aminoxy cholesteryl lipid for convenient surface postcoupling of polyethylene glycol (PEG; C component, stealth/biocompatibility polymer) to give triggered PEGylated siRNA-nanoparticles (also known as siRNA-ABC nanoparticles) with uniform small sizes of 80−100 nm in diameter. The oxime linkage that results from PEG coupling is pH sensitive and was included to facilitate acidic pH-triggered release of nucleic acids from endosomes. Nanoparticle-mediated siRNA delivery results in HBV replication knockdown in cell culture and in murine hydrodynamic injection models *in vivo*. Furthermore repeated systemic administration of triggered PEGylated siRNA-nanoparticles to HBV transgenic mice results in the suppression of markers of HBV replication by up to 3-fold relative to controls over a 28 day period. This compares favorably to silencing effects seen during lamivudine treatment. Collectively these observations indicate that our PEGylated siRNA-nanoparticles may have valuable applications in RNAi-based HBV therapy.

Keywords: Cationic lipids; nanoparticles; RNA interference; hepatitis B virus; lamivudine

Introduction

Approximately 6% of the world's population is chronically infected with HBV and between 25% and 40% of carriers of the virus will develop complicating hepatocellular carcinoma (HCC).[1] Licensed therapies for HBV, which include interferon-α (IFN-α), nucleoside (e.g., lamivudine) and nucleotide (e.g., adefovir) analogues, are only partially effective, and the response to treatment may not be durable.[2−4] Development of an effective antiviral therapy thus remains an important global priority.

* Correspondence should be addressed to these authors. P.A.: e-mail, patrick.arbuthnot@wits.ac.za; tel, +27 (0)11 717 2365; fax, +27 (0)11 717 2395; mailing address, Antiviral Gene Therapy Research Unit, Department of Molecular Medicine and Haematology, University of the Witwatersrand Medical School, Private Bag 3, WITS 2050, South Africa. A.D.M.: e-mail, a.miller@imperial.ac.uk; tel, +44 (0)20 7594 5773; fax, +44 (0)20 7594 5803; mailing address, Imperial College Genetic Therapies Centre, Department of Chemistry, Flowers Building, Armstrong Road, Imperial College London, South Kensington, London SW7 2AZ, U.K.

[†] University of the Witwatersrand Medical School.

[‡] Imperial College London.

[§] Stanford University.

[||] Hepadnavirus Testing, Inc.

[⊥] RNAi Co.

[#] ImuThes Ltd.

(1) Beasley, R. P.; Hwang, L. Y. Hepatocellular carcinoma and hepatitis B virus. *Semin. Liver Dis.* **1984**, *4*, 113–121.

(2) Hanazaki, K. Antiviral therapy for chronic hepatitis B: a review. *Curr. Drug Targets: Inflammation Allergy* **2004**, *3*, 63–70.

10.1021/mp800157x CCC: $40.75 © **2009 American Chemical Society**
Published on Web 01/21/2009

Recent demonstration that the RNAi pathway can be exploited to cause silencing of HBV genes has led to enthusiasm for new nucleic acid-based therapies.[5,6] However, the clinical use of therapeutic antiviral sequences is dependent on their incorporation into vectors which can be conveniently generated in large scale and are nontoxic, minimally immunogenic and efficiently hepatotropic. Although recombinant adenoviruses[7,8] and adeno-associated viruses (AAVs)[9,10] have been used successfully to deliver anti-HBV small hairpin RNA (shRNA) expression cassettes to liver cells, problems of toxicity, difficulty with large scale preparation and immunostimulation may limit application of these viral vectors in a clinical setting. As an alternative class of delivery agent nonviral vectors offer many advantages, and this has led to considerable interest in employing this class of vector to advance RNAi-based therapy.[11−14]

In studies carried out by others, liver-targeting siRNA formulations have been generated as cholesterol, α-tocopherol conjugates, apolipoprotein A1 complexes and in association with vitamin A-coupled liposomes.[15−18] "Stabilized nucleic acid−lipid particles" (SNALPs) have also been used to deliver functional siRNA *in vivo*. Stabilized nucleic acid−lipid particles mediate efficient delivery of anti-HBV synthetic siRNAs to liver in a murine hydrodynamic injection (MHI) model of transient HBV replication[19] and have also been used successfully to silence expression of an endogenous hepatic gene.[20] Previously we developed the siFECTamine cationic liposome system[13] to deliver siRNA to cells (siFection) and showed that this approach may be used for RNAi-based gene silencing. This cationic liposome system was formulated from the cationic cholesteryl polyamine N^1-cholesteryloxycarbonyl-3,7-diazanonane-1,9-diamine (CDAN) and the neutral colipid dioleoyl-L-α-phosphatidyl ethanolamine (DOPE) in a 45:55 molar ratio (Figure 1a). Highly efficient siRNA-mediated gene knockdown was routinely achievable without causing toxicity in cultured cells.[13] In order to advance use of nonviral vectors for therapeutic siRNA delivery, our main aim has been to devise a way to upgrade siFECTamine for *in vivo* use by means of a convenient, flexible modular molecular assembly process giving rise to biocompatible nanoparticles for siRNA delivery. Our approach has relied on the recently described synthetic, self-assembly ABCD nanoparticle paradigm that defines critical requirements for successful nonviral vector mediated nucleic acid delivery *in vivo*.[12] In addition, references were made to a number of different molecular conjugates and methodologies used to prepare other nonviral

(3) Jacobson, I. M. Therapeutic options for chronic hepatitis B: considerations and controversies. *Am. J. Gastroenterol.* **2006**, *100*, S13−18.

(4) Liaw, Y. F. The current management of HBV drug resistance. *J. Clin. Virol.* **2005**, *34*, S143−146.

(5) Arbuthnot, P.; Carmona, S.; Ely, A. Exploiting the RNA interference pathway to counter hepatitis B virus replication. *Liver Int.* **2005**, *25*, 9–15.

(6) Grimm, D.; Kay, M. A. Therapeutic short hairpin RNA expression in the liver: viral targets and vectors. *Gene Ther.* **2006**, *13*, 563–575.

(7) Carmona, S.; Ely, A.; Crowther, C.; Moolla, N.; Salazar, F. H.; Marion, P. L.; Ferry, N.; Weinberg, M. S.; Arbuthnot, P. A. Effective inhibition of HBV replication in vivo by anti-HBx short hairpin RNAs. *Mol. Ther.* **2006**, *13*, 411–421.

(8) Uprichard, S. L.; Boyd, B.; Althage, A.; Chisari, F. V. Clearance of hepatitis B virus from the liver of transgenic mice by short hairpin RNAs. *Proc. Natl. Acad. Sci. U.S.A.* **2005**, *102*, 773–778.

(9) Grimm, D.; Streetz, K. L.; Jopling, C. L.; Storm, T. A.; Pandey, K.; Davis, C. R.; Marion, P.; Salazar, F.; Kay, M. A. Fatality in mice due to oversaturation of cellular microRNA/short hairpin RNA pathways. *Nature* **2006**, *441*, 537–541.

(10) Moore, M. D.; McGarvey, M. J.; Russell, R. A.; Cullen, B. R.; McClure, M. O. Stable inhibition of hepatitis B virus proteins by small interfering RNA expressed from viral vectors. *J. Gene Med.* **2005**, *7*, 918–925.

(11) Thanou, M.; Waddington, S.; Miller, A. D. Gene Therapy. In *Comprehensive Medicinal Chemistry II*; Taylor, J. B., Triggle, D. J., Eds.; Elsevier: Oxford, 2007; Vol. 1, pp 297−320.

(12) Kostarelos, K.; Miller, A. D. Synthetic, self-assembly ABCD nanoparticles; a structural paradigm for viable synthetic non-viral vectors. *Chem. Soc. Rev.* **2005**, *34*, 970–994.

(13) Spagnou, S.; Miller, A. D.; Keller, M. Lipidic Carriers of siRNA: Differences in the Formulation, Cellular Uptake, and Delivery with Plasmid DNA. *Biochemistry* **2004**, *43*, 13348–13356.

(14) Keller, M.; Miller, A. D. Intracellular delivery of nucleic acids: differences between transfection and siFection reflect differences between DNA and RNA, and between oligodeoxynucleotides and oligonucleotides. In *Non-viral gene therapy: gene design and delivery*; Taira, K., Kataoka, K., Niidome, T., Eds.; Springer-Verlag: Tokyo, 2005; pp 441−455.

(15) Soutschek, J.; Atkinc, A.; Bramlage, B.; Charisse, K.; Constien, R.; Donoghue, M.; Elbashir, S.; Geick, A.; Hadwiger, P.; Harborth, J.; John, M.; Kesavan, V.; Lavine, G.; Pandey, R. K.; Racie, T.; Rajeev, K. G.; Rohl, I.; Toudjarska, I.; Wang, G.; Wuschko, S.; Bumcrot, D.; Koteliansky, V.; Limmer, S.; Manoharan, M.; Vornlocher, H. P. Therapeutic silencing of an endogenous gene by systemic administration of modified siRNAs. *Nature* **2004**, *432*, 173–178.

(16) Kim, S. I.; Shin, D.; Choi, T. H.; Lee, J. C.; Cheon, G. J.; Kim, K. Y.; Park, M.; Kim, M. Systemic and specific delivery of small interfering RNAs to the liver mediated by apolipoprotein A-I. *Mol. Ther.* **2007**, *15*, 1145–1152.

(17) Nishina, K.; Unno, T.; Uno, Y.; Kubodera, T.; Kanouchi, T.; Mizusawa, H.; Yokota, T. Efficient in vivo delivery of siRNA to the liver by conjugation of α-tocopherol. *Mol. Ther.* **2008**, *16*, 734–740.

(18) Sato, Y.; Murase, K.; Kato, J.; Kobune, M.; Sato, T.; Kawano, Y.; Takimoto, R.; Takada, K.; Miyanishi, K.; Matsunaga, T.; Takayama, T.; Niitsu, Y. Resolution of liver cirrhosis using vitamin A-coupled liposomes to deliver siRNA against a collagen-specific chaperone. *Nat. Biotechnol.* **2008**, *26*, 431–442.

(19) Morrissey, D. V.; Lockridge, J. A.; Shaw, L.; Blanchard, K.; Jensen, K.; Breen, W.; Hartsough, K.; Machemer, L.; Radka, S.; Jadhav, V.; Vaish, N.; Zinnen, S.; Vargeese, C.; Bowman, K.; Shaffer, C. S.; Jeffs, L. B.; Judge, A.; MacLachlan, I.; Polisky, B. Potent and persistent in vivo anti-HBV activity of chemically modified siRNAs. *Nat. Biotechnol.* **2005**, *23*, 1002–1007.

(20) Zimmermann, T. S.; Lee, A. C.; Akinc, A.; Bramlage, B.; Bumcrot, D.; Fedoruk, M. N.; Harborth, J.; Heyes, J. A.; Jeffs, L. B.; John, M.; Judge, A. D.; Lam, K.; McClintock, K.; Nechev, L. V.; Palmer, L. R.; Racie, T.; Rohl, I.; Seiffert, S.; Shanmugam, S.; Sood, V.; Soutschek, J.; Toudjarska, I.; Wheat, A. J.; Yaworski, E.; Zedalis, W.; Koteliansky, V.; Manoharan, M.; Vornlocher, H. P.; MacLachlan, I. RNAi-mediated gene silencing in non-human primates. *Nature* **2006**, *441*, 111–114.

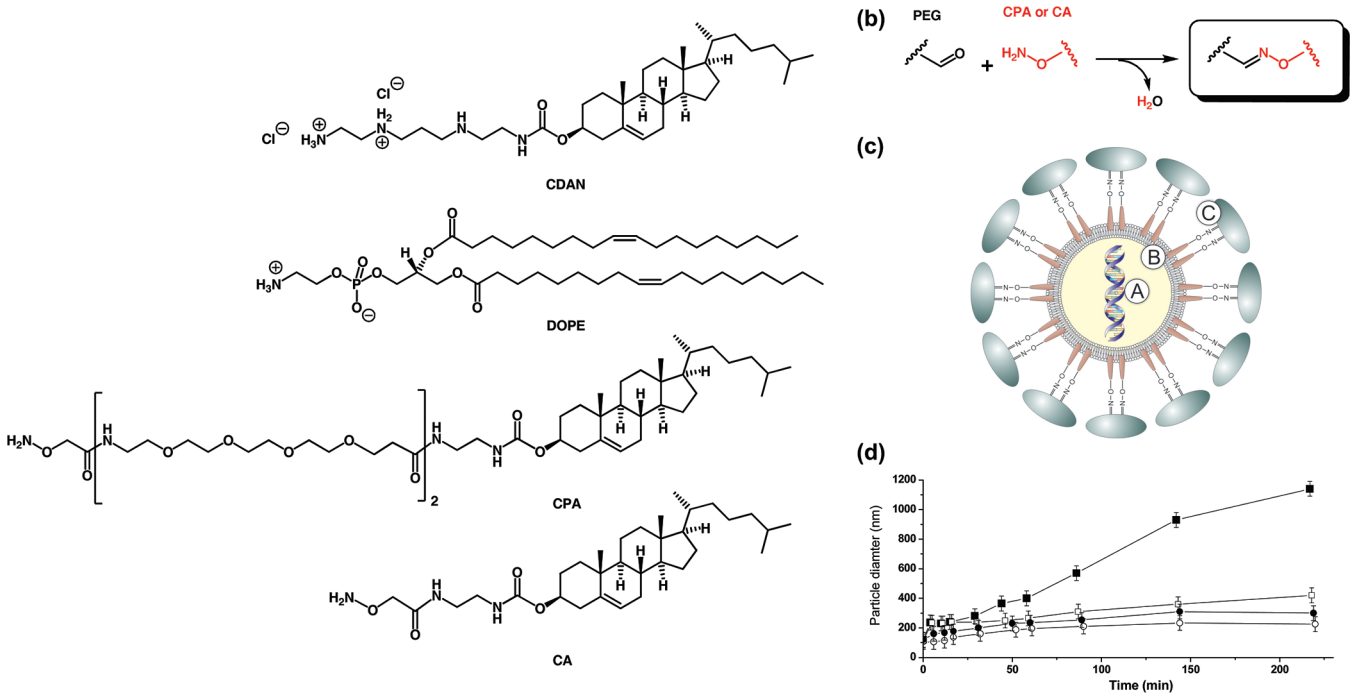


Figure 1. Chemical components and stability of siRNA nanoparticles. (a) Schematic illustration of structures of lipid components. (b) The aminoxy group of CPA or of CA allows for convenient addition of PEG^{2000}-$(CHO)_2$ in order to confer biocompatibility and stealth functions. (c) Schematic illustration of a triggered PEGylated siRNA nanoparticle (siRNA-ABC nanoparticle); siRNA (A component) is likely to be condensed as a multilammellar siRNA-lipoplex encapsulated within a lipid bilayer (B component) for cellular uptake and intracellular delivery of siRNA; PEG^{2000} is added by surface postcoupling to act as a stealth/biocompatibility polymer (C component). (d) Change in particle diameter of siRNA-nanoparticle formulations prepared from CDAN/DOPE/CPA (40:50:10, m/m/m) liposomes containing varying amounts of PEG (■ 0.1 mol %; □ 0.5 mol %; ● 1.0 mol %; ○ 5.0 mol %), as a function of time in the presence of 80% serum.

vector systems.[21−26] ABCD nanoparticles comprise nucleic acids such as plasmid DNA (pDNA) or siRNA (A component), which are condensed with cationic liposomes (B component) to form AB core nanoparticles. An important feature of our assembly approach described here is incorporation of an aminoxy cholesteryl lipid into these AB core nanoparticles to enable quantitative chemoselective postcoupling of biocompatibility polymers (C component) and optional tissue-targeting ligands (D component) to the core nanoparticles. In principle, ABCD nanoparticles thus prepared can be assembled from a variety of chemical components and represent a highly flexible nonviral vector system that is amenable to large-scale preparation. Here we describe the synthesis of novel hepatotropic anti-HBV triggered PEGylated siRNA-nanoparticle (also known as siRNA-ABC nanoparticle) vectors. Good efficacy of these formulations is demonstrated *in vivo*, which compares favorably to inhibition of HBV replication with lamivudine, and indicates that the vectors may have therapeutic use.

Experimental Section

General Synthesis. Boc-amino-oxyacetic acid and HBTU were obtained from Novabiochem (Merck Chemicals Ltd., Nottingham, U.K.). *N*-Fmoc-amido-$dPEG_4$-acid was purchased from Quanta BioDesign Ltd. (Powell, OH). PS-chlorotrityl-Cl resins were obtained from Argonaut Technologies, Inc. (Foster City, CA). All other chemicals were purchased from Sigma Aldrich (Dorset, U.K.) unless otherwise stated. Dried dichloromethane was distilled with phosphorus pentoxide; other solvents were purchased predried or as required from Sigma-Aldrich or BDH Laboratory Supplies (Poole, U.K.). HPLC-grade acetonitrile was pur-

(21) Li, W.; Szoka, F. C., Jr. Lipid-based nanoparticles for nucleic acid delivery. *Pharm. Res.* **2007**, *24*, 438–449.
(22) Oupicky, D.; Ogris, M.; Seymour, L. W. Development of long-circulating polyelectrolyte complexes for systemic delivery of genes. *J. Drug Targeting* **2002**, *10*, 93–98.
(23) Trubetskoy, V. S.; Budker, V. G.; Hanson, L. J.; Slattum, P. M.; Wolff, J. A.; Hagstrom, J. E. Self-assembly of DNA-polymer complexes using template polymerization. *Nucleic Acids Res.* **1998**, *26*, 4178–4185.
(24) Chittimalla, C.; Zammut-Italiano, L.; Zuber, G.; Behr, J. P. Monomolecular DNA nanoparticles for intravenous delivery of genes. *J. Am. Chem. Soc.* **2005**, *127*, 11436–11441.
(25) Dauty, E.; Remy, J. S.; Blessing, T.; Behr, J. P. Dimerizable cationic detergents with a low cmc condense plasmid DNA into nanometric particles and transfect cells in culture. *J. Am. Chem. Soc.* **2001**, *123*, 9227–9234.
(26) Ouyang, M.; Remy, J. S.; Szoka, F. C., Jr. Controlled template-assisted assembly of plasmid DNA into nanometric particles with high DNA concentration. *Bioconjugate Chem.* **2000**, *11*, 104–112.

chased from Fisher Chemicals (Leicester, U.K.) and other HPLC-grade solvents from BDH Laboratory Supplies. Thin layer chromatography (TLC) was performed on precoated Merck-Kieselgel 60 F_{254} aluminum backed plated and revealed with ultraviolet light, iodine, acidic ammonium molybdate(IV), acidic ethanolic vanillin, or other agents as appropriate. Flash column chromatography was accomplished on Merck-Kieselgel 60 (230−400 mesh). Mass spectra were recorded using Bruker (Coventry, U.K.) Esquire 3000, VG-7070B or JEOL SX-102 instruments. ^{1}H- and ^{13}C- NMR were recorded on Advance Bruker 400 Ultrashield machine using residual isotopic solvent as an internal reference (s = singlet, d = doublet, t = triplet, q = quartet, quin = quintet, br = broad singlet). Analytical HPLC (Hitachi-LaChrom L-7150 pump system equipped with a Polymer Laboratories (Varian Ltd, Oxford, U.K.) PL-ELS 1000 evaporative light scattering detector) was conducted with a Vydac C4 peptide column with gradient 0.1% aqueous trifluoroacetic acid (TFA) to 100% acetonitrile (0.1% TFA) [0−15 min], followed by 100% acetonitrile (0.1% TFA) [15−25 min], followed by 100% methanol [25−45 min].

Synthesis of N-Capped PEG^{350} Linker. Chlorotrityl chloride resin (1.27 mmol/g loading, 55 mg, 0.070 mmol) was swollen in dichloromethane for 16 h. The resin was loaded with *N*-Fmoc-amido-dPEG$_4$-acid (102 mg, 0.209 mmol) and assisted by Hünig base (60 μL, 0.349 mmol) in dimethyl formamide (DMF) (15 mL) for 1 h. Fluorenylmethyloxycarbonyl (Fmoc) removal was achieved with piperidine (20% v/v) in DMF (2 × 5 min) followed by extensive washing with DMF. The resulting resin-bound free amine was then reacted again with *N*-Fmoc-amido-dPEG$_4$-acid (102 mg, 0.209 mmol) that was necessarily preactivated with the coupling reagent 2-(1*H*-benzotriazol-1-yl)-1,1,3,3-tetramethyluronium hexafluorophosphate (HBTU) (132.5 mg, 0.209 mmol) and Hünig base (60 μL, 0.349 mmol) in DMF (15 mL). After 1 h a capping by acetic anhydride (10% v/v) in DMF was performed in the presence of Hünig base (3 equiv). Finally, Fmoc was removed once more (as above) yielding resin-bound free amine that was immediately capped by *N*-Boc-amino oxyacetic acid (40 mg, 3 equiv) with the assistance of HBTU (3 equiv) and Hünig base (5 equiv) in DMF (15 mL) to yield the desired resin-bound *N*-capped PEG^{350} linker. This was cleaved in a solution consisting of trifluoroethanol 50% (v/v) in dichloromethane (3 mL) over 4 h to yield the desired *N*-capped PEG^{350} linker (40 mg, 0.058 mmol): ^{1}H NMR (400 MHz, $CDCl_3$) 1.48 (9H, Boc), 2.51 (2H, t, J = 6.1 Hz, −CH_2CO$_2$H), 2.59 (2H, t, J = 6.05, −CH_2CONHCH$_2$−), 3.45 and 3.52 (2H and 2H, m, CONHCH_2CH$_2$), 3.55−3.7 (28H, m, CH_2OCH$_2$ and CH$_2$OCH_2), 3.77 (4H, m, NHCH$_2$CH_2O), 4.34 (2H, s, BocHNOCH_2CONH), 7.0 (1H, m, BocN*H*O), 7.9 (1H, m, CH$_2$N*H*COCH$_2$) and 8.3 (1H, m, CH$_2$N*H*COCH$_2$); ESI-MS 684.30 $(M - H)^+$.

Synthesis of Cholesterylamine. Cholesteryl chloroformate (7.5 g, 0.0167 mol) was dissolved in ethylene-1,2-diamine (180 mL) and the mixture stirred for 18 h. The reaction mixture was then quenched with water and extracted with dichloromethane. The organic extracts were dried ($MgSO_4$) and the solvent was removed *in vacuo* to afford a residue, which was purified by flash column chromatography [CH_2Cl_2:MeOH:NH_3 192:7:1 → CH_2Cl_2:MeOH:NH_3 92:7:1 (v/v)] giving the pure cholesterylamine (5.5 g, 0.0116 mol, 73%) as a white solid (mp 175−177 °C): FTIR (Nujol mull) ν_{max} 3338 (amine), 2977 (alkane), 2830 (alkane), 1692 (carbamate) cm^{-1}; ^{1}H NMR (400 MHz, $CDCl_3$) 0.66 (3 H, s, H-18), 0.838−0.854 (3 H, d, H-27, J = 6.4 Hz), 0.842−0.858 (3 H, d, H-26, J = 6.4 Hz), 0.890−0.906 (3 H, d, H-21, J = 6.4 Hz), 0.922 (3 H, s, H-19), 1.02−1.63 (21 H, m, H-1, H-9, H-11, H-12, H-14, H-15, H-16, H-17, H-20, H-22, H-23, H-24, H-25), 1.76−2.1 (5 H, m, H-2, H-7, H-8), 2.22−2.36 (2 H, m, H-4), 2.79−2.81 (2 H, m, H$_2$NCH_2), 3.197−3.210 (2 H, m, H$_2$NCH$_2$CH_2), 4.52 (1 H, m, H-3), 5.31 (1 H, s, H-6); MS (ESI +ve) 473 (M + H); HRMS (FAB +ve) calcd for $C_{30}H_{53}N_2O_2$ (M + H) 473.4119, found 473.4107.

Synthesis of Boc-Protected CPA. The *N*-capped PEG^{350} linker (40 mg, 0.058 mmol) in anhydrous dichloromethane was combined with 4-dimethylaminopyridine (DMAP) (22 mg, 0.18 mmol), HBTU (24 mg, 0.063 mmol) and cholesterylamine (28 mg, 0.06 mmol) and the mixture stirred at ambient temperature under a nitrogen atmosphere for 15 h. The reaction was quenched with 7% aqueous citric acid and extracted with dichloromethane. The dried ($MgSO_4$) extracts were concentrated *in vacuo* to afford a residue which was purified by flash column chromatography (gradient CH_2Cl_2:MeOH:H_2O) affording *N*-Boc-protected CPA (47 mg, 0.0411 mmol, 71%): ^{1}H NMR (400 MHz, $CDCl_3$:MeOD) 5.32 (m, 1H, Chol C6), 4.35 (m, 1H, Chol C-3), 4.28 (s, 2H, (CO)CH_2ONH), 3.67 (4H, m, NHCH$_2$CH_2O), 3.56−3.61 (24H, m, CH_2OCH$_2$ and CH$_2$OCH_2), 3.56 (2H, m, CH_2CH$_2$CO), 3.50 (2H, m, CH_2CH$_2$CO), 3.35 and 3.43 (2H and 2H, m, CONHCH_2CH$_2$), 3.24 (m, 2H, CholO(CO)-NHCH_2CH$_2$), 3.18 (m, 2H, CholO(CO)NHCH$_2$CH_2), 2.42 (4H, m, −CH_2CONHCH$_2$−), 2.27 (m, 2 H, Chol C-24), 1.46 (s, 3 H, Boc), 0.94 −2.10 (Chol C-1, 2, 4, 7, 8, 9, 11, 12, 14, 15, 16, 17, 20, 22, 23, 25), 1.0 (s, 3 H, Chol C-19), 0.89 (d, 3 H, J = 6.4, Chol C-21), 0.83, 0.82 (2 × d, 6 H, J = 6.5 and 2.0 Hz), 0.68 (s, 3 H, Chol C-18); ESI-MS 1162.40 [M + K].

Synthesis of CPA. *N*-Boc-protected CPA (40 mg, 0.035 mmol) in propan-2-ol (2 mL) was treated with 4 M HCl in dioxane (2 mL) and the mixture stirred at room temperature for 3 h. The solvents were removed *in vacuo* affording CPA (37 mg, 98%): ^{1}H NMR (400 MHz, d_4-MeOD) 5.31 (m, 1H, Chol C6), 4.57 (s, 2H, (CO)CH_2ONH$_2$), 4.38 (m, 1H, Chol C-3), 3.69 (4H, m, NHCH$_2$CH_2O), 3.53−3.62 (28H, m, CH_2OCH$_2$ and CH$_2$OCH_2), 3.37 and 3.43 (2H and 2H, m, CONHCH_2CH$_2$), 3.26 (m, 2H, CholO(CO)NHCH_2CH$_2$), 3.19 (m, 2H, CholO(CO)NHCH$_2$CH_2), 2.45 (4H, m, −CH_2CONH-CH$_2$−), 2.27 (m, 2 H, Chol C-24), 0.94−1.99 (Chol C-1, 2, 4, 7, 8, 9, 11, 12, 14, 15, 16, 17, 20, 22, 23, 25), 0.97 (s, 3 H, Chol C-19), 0.87 (d, 3 H, J = 6.4, Chol C-21), 0.80, 0.82 (2 × d, 6 H, J = 6.5 and 2.0 Hz), 0.64 (s, 3 H, Chol C-18); ^{13}C NMR (100 MHz, $CDCl_3$) 173.3, 172.8 and 170.5 (NH(*C*O)CH$_2$ONH$_2$), 157.6 (O*C*ONH), 140.16 (C-5), 122.94 (C-6), 75.03 (C-3), 71.90 ((CO)*C*H$_2$ONH$_2$), 70.4−70.83 (*C*H$_2$OCH$_2$ and CH$_2$O*C*H$_2$), 69.54 and 70.14 (NHCH$_2$*C*H$_2$O), 67.62 (2 × *C*H$_2$CH$_2$CO overlapping), 57.12 (C-14), 56.56 (C-17), 50.50 (C-9), 42.7 (C-13), 40.54 and 39.91 (CholO(CO)-

NH*C*H$_2$*C*H$_2$) 40.14 (C-4), 39.88 (C-12), 39.38 and 39.65 (CONH*C*H$_2$CH$_2$), 38.94 (C-24), 37.3 (C-1), 36.95 (C-10), 36.87 (−*C*H$_2$CONHCH$_2$−), 36.55 (C-22), 36.17 (C-20), 32.28 (C-8), 32.26 (C-7), 28.5 (C-16 and C-2 overlapping), 28.36 (C-25), 24.6 (C-15), 24.17 (C-23), 22.98 (C-26), 22.73 (C-27), 21.42 (C-11), 19.6 (C-19), 18.96 (C-21) and 12.11 (C-18). ESI-MS 1102.50 $[M + K + Na]^+$. Analytical HPLC: 1 peak, rt 31 min.

Synthesis of CA. *N*-Boc-amino oxyacetic acid (145 mg, 1.5 equiv) in anhydrous CH_2Cl_2 was treated successively with DMAP (292 mg, 4 equiv), HBTU (2 equiv) followed by cholesterylamine (272 mg, 0.576 mmol). The mixture was then stirred at ambient temperature under an inert (N_2) atmosphere for 15 h. The reaction was quenched with citric acid 7% (w/v) and extracted with CH_2Cl_2. The dried ($MgSO_4$) extracts were concentrated *in vacuo* to give a residue, which was purified by flash chromatography, affording white solid *N*-Boc-protected CA (302 mg, 81%): ^{1}H NMR (400 MHz, $CDCl_3$) 8.56 (s, 1H, BocN*H*OCH$_2$), 8.2 (br, CH$_2$CON*H*CH$_2$), 5.5 (m, 1H, Chol C6), 5.4 (m, 1H, Chol-O(CO)N*H*), 4.5 (m, 1H, Chol C-3), 4.3 (s, 2H, (CO)C*H*$_2$ONH), 3.4 (m, 2H, O(CO)NHC*H*$_2$CH$_2$), 3.3 (m, 2H, O(CO)NHCH$_2$C*H*$_2$), 2.32 (m, 2 H, Chol C-24), 1.46 (s, 3 H, Boc), 0.94 −2.10 (Chol C-1, 2, 4, 7, 8, 9, 11, 12, 14, 15, 16, 17, 20, 22, 23, 25), 1.0 (s, 3 H, Chol C-19), 0.89 (d, 3 H, $J = 6.4$, Chol C-21), 0.83, 0.82 (2 × d, 6 H, $J = 6.5$ and 2.0 Hz), 0.68 (s, 3 H, Chol C-18); ESI-MS 646 $[M + H]^+$; HRMS calcd for $C_{37}H_{64}N_3O_6$ 646.479512, found 646.479874.

N-Boc-protected CA (86 mg, 0.067 mmol) in propan-2-ol (3 mL) was treated with 4 M HCl in dioxane (3 mL) after which the mixture was stirred at ambient temperature for 4 h. Solvents were removed *in vacuo* and the residue was redissolved in a minimum of propan-2-ol:dioxane 1:5 (v/v). Thereafter the desired CA was precipitated by the slow addition of diethyl ether and collected as a white solid (28 mg, 84%): ^{1}H NMR (400 MHz, d_4-MeOD) 5.35 (m, 1H, Chol C6), 4.8 (m, 1H, Chol-O(CO)N*H*), 4.5 (s, 2H, (CO)C*H*$_2$ONH$_2$), 4.4 (m, 1H, Chol C-3), 3.3 (m, 2H, O(CO)NHC*H*$_2$CH$_2$), 3.1 (m, 2H, O(CO)NHCH$_2$C*H*$_2$), 2.32 (m, 2 H, Chol C-24), 0.94 −2.10 (Chol C-1, 2, 4, 7, 8, 9, 11, 12, 14, 15, 16, 17, 20, 22, 23, 25), 1.0 (s, 3 H, Chol C-19), 0.89 (d, 3 H, $J = 6.4$, Chol C-21), 0.83, 0.82 (2 × d, 6 H, $J = 6.5$ and 2.0 Hz), 0.68 (s, 3 H, Chol C-18); ^{13}C NMR (100 MHz, $CDCl_3$) 171.4 (NH(*C*O)CH$_2$ONH$_2$), 158.3 (O*C*ONH), 140.55 (C-5), 132.2 (C-6), 75.4 ((CO)*C*H$_2$ONH$_2$), 71.9 (C-3), 57.5 (C-14), 57.0 (C-17), 51.0 (C-9), 43.0 (C-13), 40.2 (C-4), 40.0−40.6 (C-12, C-4 and O(CO)-NH*C*H$_2$*C*H$_2$ overlapping), 39.2 (C-24), 37.8 (C-1), 37.3 (C-10), 36.9 (C-22), 36.6 (C-20), 32.7 (C-8), 32.6 (C-7), 28.9 (C-16), 28.8 (C-2), 28.7 (C-25), 24.9 (C-15), 24.5 (C-23), 23.2 (C-26), 22.9 (C-27), 21.8 (C-11), 19.7 (C-19), 19.2 (C-21) and 12.3 (C-18); ESI-MS 546 $[M + H]^+$.

SiRNA Nanoparticle Formulations. siRNAs were synthesized using standard procedures (Dharmacon, Fisher Scientific, Loughborough, U.K.). Formulation of triggered PEGylated siRNA-nanoparticles (also known as siRNA-ABC nanoparticles) was performed as follows. Appropriate volumes of CDAN·3HCl ([MW 680]; 4 mg/mL in $CHCl_3$), DOPE ([MW 744]; 10 mg/mL in $CHCl_3$) and CPA·HCl ([MW 1075] 5 mg/mL in $CHCl_3$), or CA ([MW 545.8] 10 mg/mL in $CHCl_3$) were combined together in a round-bottomed flask (5 mL) (presilanized by treatment with nitric acid, 10 min, followed by dimethyldichlorosilane, 10 min). Lipid molar ratios were 40:50:10 for CDAN/DOPE/CPA or 40:50:10 for CDAN/DOPE/CA. In each case, organic solvent was evaporated to dryness (rotary evaporator) producing a thin, lipid-film that was rehydrated by addition of water (18 MΩ) (5 mL) and vortex mixing. The multilamellar liposome formulation (pH 3.5−4) was then sonicated at 40 °C for 30 min (Sonomatic water bath, Langford (Coventry, U.K.) Ultrasonics, 33 kHz ultrasound frequency, 150 W electric power output) to produce very small unilamellar vesicles (SUVs) (30−50 nm), giving a final lipid concentration of 3 mg/mL (approximately 4 μmol/mL). Thereafter, an aliquot was removed and an aqueous solution of siRNA (0.28 mg/mL) was added slowly with constant vortex mixing, until a final lipid:siRNA ratio of 10:1 (w/w) was achieved. An appropriate volume of polyethylene glycol 2000-dialdehyde [PEG^{2000}-(CHO)$_2$, SunBio Ltd., Anyang City, South Korea] ([MW 2000] 10 mg/mL in water) was then introduced for postcoupling such that final composition of PEG^{2000}-modified lipid was between 0.1 and 5.0 mol % of total lipid. Mixtures were then incubated for 16 h at ambient temperature, and pH was maintained constant throughout. Thereafter, pH was corrected to 7 and volumes were adjusted with PBS, to give a final siRNA concentration of 0.1 mg/mL, ready for immediate use. Final triggered PEGylated siRNA-nanoparticles were essentially monodisperse with particle sizes that ranged from 80 to 100 nm in diameter (photon correlation spectroscopy, N4 plus Coulter Electronics, Beckman Coulter UK Ltd, High Wycombe, U.K.). For long-term storage, triggered PEGylated siRNA-nanoparticle suspensions were supplemented with trehalose solution (100%, w/v) to give a final trehalose concentration of 5−10% (w/v) and these samples were then flash-frozen in liquid nitrogen and lyophilized for storage. Prior to further use, nanoparticles were resuspended in a 50% (v/v) PBS solution such that the final siRNA concentration was also 0.1 mg/mL (as above). In order to assess the possibility of nanoparticle aggregation, sizes of triggered PEGylated siRNA-nanoparticle formulations were studied as a function of time by means of photon correlation spectroscopy (N4 plus Coulter Electronics), in the presence of 80% fetal calf serum (FCS).

Nanoparticle Biodistribution. These animal experiments were carried out in accordance with protocols approved by the Imperial College, London, U.K., animal ethics committee. The biodistribution of our triggered PEGylated siRNA-nanoparticles was investigated by substituting 0.05 mol % of CDAN with 4-[^{14}C] cholesterol. Labeled triggered PEGylated siRNA-nanoparticles were then administered via the tail vein to mice (3 animals per group and approximately 0.04 μCi per mouse). After 1 h, mice were anesthetized and blood was obtained by cardiac puncture and immediately mixed with heparin (15U). The blood concentration of the

nanoparticles was calculated assuming that the total blood weight is 6% body weight. After cervical dislocation, liver, spleen, kidney, lung and heart were harvested and weighed. Organs were homogenized in PBS and aliquots (200 μL) solubilized with a minimum volume of Solvable (Dupont, Boston, MA) at 60 °C for 1 h. Samples were then treated with EDTA (0.1 M, 0.1 mL), followed by aqueous hydrogen peroxide. Each treated sample was allowed to stand for 15−30 min at ambient temperature, then 1 h at 60 °C, Ultima Gold (10 mL; Perkin-Elmer, Waltham, MA) was added and radioactivity determined using liquid scintillation counting. Detected radioactivity was expressed as a percentage of injected dose per organ (% ID). To determine distribution of Cy3-labeled synthetic oligonucleotides (Dharmacon), mice were treated as described above and the labeled siRNA was detected in frozen sections (5 μm) using fluorescence microscopy.

Transient Transfection of Huh7 Cells. Huh7 liver-derived cells were maintained under standard conditions of cell culture. siFECTamine was used to codeliver either pCH-9/3091 HBV replication competent target plasmid,[27] or a vector constitutively expressing enhanced green fluorescent protein (eGFP),[28] together with relevant siRNA sequences. Briefly, to prepare the complexes, nucleic acid (0.25 pmol of pDNA and 20 pmol of siRNA) (1 μg total) was added to Opti-MEM (100 μL) (Invitrogen, Carlsbad, CA) and in a separate tube siFECTamine (12 μg) as added to 100 μL of Opti-MEM. The two mixtures were then combined and incubated at room temperature for up to 20 min and then added to the Huh7 culture medium. Controls included mock-treated or untransfected cells. Equivalent transfection efficiencies were confirmed by detection of eGFP using fluorescence microscopy.[28] HBsAg secretion into the culture supernatants was measured daily using the Monolisa (ELISA) immunoassay kit (BioRad, Hemel Hempstead, U.K.).

***In Vivo* Assessment of Efficacy of Anti HBV siRNAs.** The MHI method was initially employed to determine the effects of siRNAs on the expression of HBV genes *in vivo*. These experiments were carried out in accordance with protocols approved by the University of the Witwatersrand Animal Ethics Screening Committee. A saline solution comprising 10% of the mouse's body mass was injected via the tail vein over 5−10 s. The saline solution (NaCl 0.9%) included a combination of 1 μg of target DNA (pCH-9/3091) or 10 μg of pLTR β-gal[29] (a control for hepatic DNA delivery, which constitutively expresses β-galactosidase marker gene). Eight hours after MHI, naked siRNAs as indicated or triggered 5 mol % PEGylated siRNA-nanoparticles (known as siFECTplus nanoparticles) were injected iv. Each group of mice comprised 8 animals, and siRNA was administered at a dose of 1 mg/kg body weight. Blood was collected from the tail vein, and animals were sacrificed after 4 days.

HBV transgenic mice[30] were also used to assess anti viral efficacy of formulations. For these experiments, procedures were approved by the Animal Care Committee at Stanford University, CA. Nanoparticle formulations were prepared as described above, and the siRNA dose for each injection was 1 mg/kg animal body weight every 3 days. Groups initially comprised 6 animals. In mice receiving lamivudine, the drug was administered ip daily at a dose of 200 mg/kg mouse body weight.

Markers of HBV Replication *in Vivo*. Measurement of circulating VPEs and intrahepatic HBV mRNA concentrations was carried out using quantitative real time PCR according to previously described methods.[7,31,32] Fixed and unfixed frozen liver sections were processed respectively for immunohistochemical HBV core antigen (HBcAg) detection or for β-galactosidase staining.[7,33] Serum HBsAg was measured using a quantitative sandwich ELISA from Abbott Laboratories (Maidenhead, U.K.), and HBeAg was determined using the electrochemiluminescence assay (ECLIA) from Roche Diagnostics (Mannheim, Germany) according to the manufacturer's instructions.

Experimental Toxicity. NMR1 mice (5 animals per group) were injected with saline, naked siRNAs as indicated or triggered 5 mol % PEGylated siRNA-nanoparticles as previously described above (siRNA was administered as single dose 1 mg/kg per animal). Four days after the injection, the mice were anesthetized, and blood samples were collected by cardiac puncture before sacrifice. The blood samples were submitted for hematological analysis, urea and electrolyte concentration measurement, alanine transaminase (ALT) and lactate dehydrogenase (LDH) activity determination. Assays were performed in the accredited Haematology and Chemical Pathology Department laboratories of the South African National Health Laboratory Services (NHLS) in Johannesburg.

Statistical Analysis. Data are expressed as the mean ± standard error of the mean. Statistical difference was considered significant * when $P < 0.05$ and was determined

(27) Nassal, M. The arginine-rich domain of the hepatitis B virus core protein is required for pregenome encapsidation and productive viral positive-strand DNA synthesis but not for virus assembly. *J. Virol.* **1992**, *66*, 4107–4116.

(28) Passman, M.; Weinberg, M.; Kew, M.; Arbuthnot, P. In situ demonstration of inhibitory effects of hammerhead ribozymes that are targeted to the hepatitis Bx sequence in cultured cells. *Biochem. Biophys. Res. Commun.* **2000**, *268*, 728–733.

(29) Wang, C.; Stiles, C. D. Platelet-derived growth factor alpha receptor gene expression: isolation and characterization of the promoter and upstream regulatory elements. *Proc. Natl. Acad. Sci. U.S.A.* **1994**, *91*, 7061–7065.

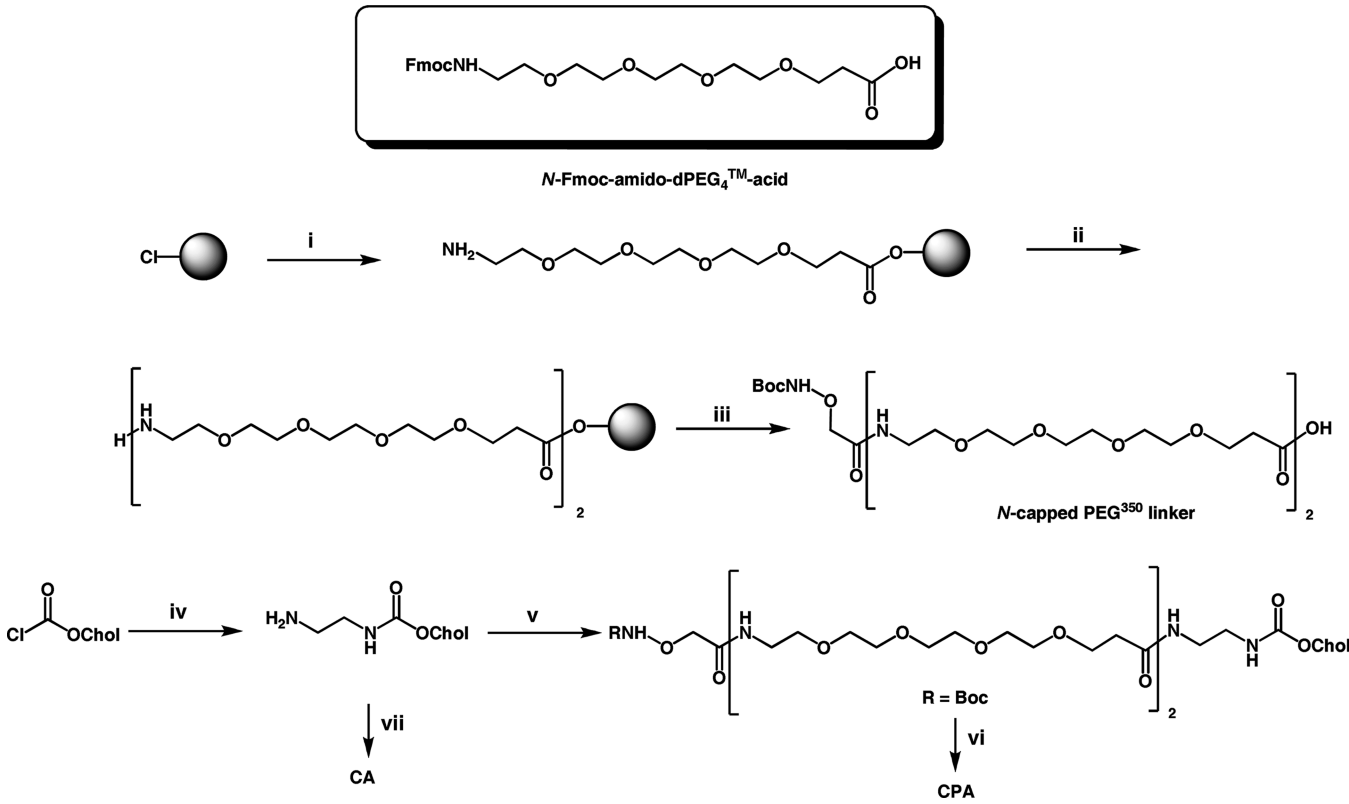
(30) Marion, P. L.; Salazar, F. H.; Liitschwager, K.; Bordier, B. B.; Seegers, C.; Winters, M. A. A transgenic mouse lineage useful for testing antivirals targeting hepatitis B virus. In *Frontiers in Viral Hepatitis*; Schinazi, R. F., Sommadossi, J.-P., Rice, C., Eds.; Elsevier Science: Amsterdam, 2003; pp 197−202.

(31) Ely, A.; Naidoo, T.; Mufamadi, S.; Crowther, C.; Arbuthnot, P. Expressed anti-HBV primary microRNA shuttles inhibit viral replication efficiently in vitro and in vivo. *Mol. Ther.* **2008**, *16*, 1105–1112.

(32) Weinberg, M. S.; Ely, A.; Barichievy, S.; Crowther, C.; Mufamadi, S.; Carmona, S.; Arbuthnot, P. Specific inhibition of HBV replication in vitro and in vivo with expressed long hairpin RNA. *Mol. Ther.* **2007**, *15*, 534–541.

(33) Sanes, J. R.; Rubenstein, J. L.; Nicolas, J. F. Use of a recombinant retrovirus to study post-implantation cell lineage in mouse embryos. *EMBO J.* **1986**, *5*, 3133–3142.

Scheme 1. Reagents and Appropriate Reaction Conditions[a]



[a] (i) (a) *N*-Fmoc-amido-dPEG$_4$-acid (3 equiv), Hünig base (5 equiv) in DMF, 1 h, rt; (b) 20% (v/v) piperidine in DMF (2 × 5 min), rt; (ii) (a) *N*-Fmoc-amido-dPEG$_4$-acid (3 equiv), HBTU (3 equiv), Hünig base (5 equiv) in DMF, 1 h, rt; (b) 20% (v/v) piperidine in DMF (2 × 5 min), rt; (iii) (a) *N*-Boc-amino-oxyacetic acid (3 equiv), HBTU (3 equiv), Hünig base (5 equiv) in DMF, 1 h, rt; (b) 50% (v/v) 1,1,1-trifluoroethanol in dichloromethane, 4 h, rt; (iv) ethylene diamine (large excess), rt, 18 h, 73%; (v) *N*-capped PEG^{350} linker, HBTU (1 equiv), DMAP (3 equiv), dichloromethane, rt, 15 h, 71%; (vi) 4 M HCl, dioxane/propan-2-ol, 3 h, 98%; (vii) (a) *N*-Boc-amino-oxyacetic acid (1.5 equiv), HBTU (2 equiv), DMAP (4 equiv) in dichloromethane, 15 h, rt, 81%; (b) 4 M HCl, dioxane/propan-2-ol, 4 h, rt, 84%.

according to the Dunnett's multiple comparison test and calculated with the GraphPad Prism software package (GraphPad Software Inc.).

Results

Lipid Synthesis. Two new cationic lipids were synthesized according to the procedures outlined in Scheme 1. These cholesterol derivatives were cholesteryl-PEG^{350} aminoxy lipid (CPA) and cholesteryl-aminoxy lipid (CA). CPA contains a short polyethylene glycol 350 (PEG^{350}) moiety with a remote aminoxy functional group. CA is the same as CPA but lacks the PEG^{350}-moiety intervening between the cholesteryl and aminoxy groups (Figure 1a). The two lipids differ according to the length of their spacer arm between the cholesterol and reactive aminoxy functional groups. In brief the synthesis of CPA required the following steps. A short PEG^{175} linker *N*-Fmoc-amido-dPEG$_4$-acid (Quanta BioDesign, Inc.) was loaded onto 2-chlorotrityl polystyrene resin (Argonaut) and then coupled to a second PEG^{175} linker *N*-Fmoc-amido-dPEG$_4$-acid using 2-(1*H*-benzotriazol-1-yl)-1,1,3,3-tetramethyluronium hexafluoro-phosphate (HBTU). The resulting PEG^{350} linker was then *N*-capped with *N*-Boc-amino-oxyacetic acid (Novabiochem, U.K.) and subsequently released from resin for coupling to cholesterylamine to yield Boc-protected CPA (71% yield). Finally, this was treated with 4 M HCl to yield CPA. Cholesterylamine was prepared previously by reaction of cholesterol chloroformate with excess ethylene diamine. The synthesis of CA was much simpler. In brief, cholesterylamine was *N*-capped with *N*-Boc-amino-oxyacetic acid (Novabiochem, U.K.) and then treated with 4 M HCl to yield CA in good yield. CDAN was prepared as indicated previously.[12,13] All other lipids were purchased from Sigma Aldrich (Dorset, U.K.) unless otherwise stated.

siRNA Formulations. In order to prepare siRNA-containing vectors, core AB nanoparticles (70−80 nm in diameter) were initially formulated in aqueous solution by combining selected siRNAs with cationic liposomes comprising CDAN/DOPE/CPA (40:50:10 molar ratio) or CDAN/DOPE/CA (40:50:10 molar ratio). Polyethylene glycol^{2000}-dialdehyde (PEG^{2000}-(CHO)$_2$) (C component), in a range of 0.1−5.0 mol %, was then coupled to AB particles under aqueous acidic conditions (pH 4). This surface postcoupling was enabled by rapid, quantitative chemoselective aminoxy−aldehyde conjugation between the aminoxy functional group of aminoxy lipids CA or CPA (as appropriate) and the aldehyde functional groups of PEG^{2000}-(CHO)$_2$. At pH 4, only aminoxy functional groups remain unprotonated (pK_a approx 4) to combine with free

aldehyde functional groups, hence the amine functional groups of the CDAN cytofectin head groups provide negligible competition in terms of Schiff's base formation through conjugation with PEG^{2000}-$(CHO)_2$. Moreover, the resulting oxime linkages (Figure 1b) are robust at pH 7, but prone to decomposition at pH 5.5 and below. This behavior might be expected to enhance pH-triggered endosome release of the C component polymer and improve efficiency of nucleic acid delivery.[12] Immediately after formulation, our triggered PEGylated siRNA-nanoparticles (schematically illustrated in Figure 1c) had an average diameter of 80−100 nm and narrow poly dispersity index (<0.3), which is suitable for use *in vivo*. By allowing functional group conjugation to be carried out in aqueous solution or organic solvent, the methodology allows for simple, controlled, modular and highly flexible formulations of triggered PEGylated siRNA-nanoparticles.[34] The surface postcoupling to aminoxy groups has the added advantage of enabling the incorporation of ligands to create targeted, triggered PEGylated siRNA-nanoparticles.

In order to assess propensity to aggregate, particle sizes of our triggered PEGylated siRNA-nanoparticles were determined in the presence of 80% serum over a 4 h time period (Figure 1d). With formulations containing 0.1 mol % polyethylene glycol 2000 (PEG^{2000}), average particle diameter rapidly rose above 1000 nm. However, there was little evidence for aggregation when PEG^{2000} content was increased to 5 mol %, which indicates that PEG diminishes siRNA nanoparticle aggregation. Since aggregation is likely to lead to particle susceptibility to clearance by the reticuloendothelial system (RES)[12] and compromise hepatocyte delivery of anti HBV siRNAs, we selected triggered PEGylated siRNA-nanoparticles containing PEG^{2000} at 5 mol % for further analysis.

Vector Hepatotrophism and Experimental Toxicology Assessment. In order to assess hepatotrophism of the vectors, 4-[^{14}C]-labeled cholesterol was included in CDAN/DOPE/CPA cationic liposomes. Thereafter, triggered PEGylated siRNA-nanoparticles were prepared from these cationic liposomes and injected at a dose of 1 mg/kg (siRNA/mouse body weight) via the tail vein of mice. Mice were sacrificed 1 h postinjection and extracts prepared from various tissues. Labeled cholesterol accumulated preferentially in the liver in all cases, and increasing PEG^{2000} content had little effect on nanoparticle hepatotrophism (Figure 2a). Equivalent results were obtained with triggered PEGylated siRNA-nanoparticles prepared from CDAN/DOPE/CA liposomes (not shown). This indicated that the PEG^{350} spacer arm between the cholesteryl and conjugated PEG^{2000} was not significantly affecting either the efficiency of PEG coupling or the extent of nanoparticle biodistribution. We therefore chose to focus only on nanoparticles prepared from CDAN/DOPE/CA cationic liposomes, because CA-containing formulations could be prepared with a higher level of reproducibility and uniformity than was possible with CPA-containing formulations (not shown). However, we also noted that CPA was less prone to compound degradation on storage than CA, therefore we anticipate that some benefit is likely to result should the use of CPA be studied in future formulations.

Hepatotrophic delivery of Cy3-labeled siRNA was examined after systemic iv administration of triggered 5 mol % PEGylated siRNA-nanoparticles to mice. Forty five minutes after injection, livers were removed from mice and frozen sections examined using fluorescence microscopy (Figure 2b). Labeled siRNA was detected primarily in the liver with trace amounts observed in other organs such as the kidneys (data not shown). Cy3-labeled siRNA was predominantly localized in the cytoplasm of 4′,6-diamidino-2-phenylindole-(DAPI-) positive hepatocytes. Large aggregates of Cy3 label, consistent with nanoparticle sequestration by Kupffer cells, were occasionally observed (not shown). We estimated that delivery to approx 60−70% of liver cells had occurred after a single bolus administration.

Potential toxic side effects of triggered 5 mol % PEGylated siRNA-nanoparticles were investigated experimentally *in vivo* using markers of hepatic, renal and hematological damage. In particular, we examined serum activity of lactate dehydrogenase (LDH) a general marker of cell lysis (Figure 2c), and alanine transaminase (ALT) which is a specific indicator of hepatocyte damage (Figure 2d). Activities of these enzymes were not elevated significantly in the sera of any mice 4 days after receiving the these triggered PEGylated siRNA-nanoparticles. Renal function appeared unaffected by the nanoparticles since blood concentrations of urea, creatinine and electrolytes did not differ significantly from those of the control group (Supporting Information Figure 1). Furthermore, morphological assessments of liver sections and peripheral blood smears from animals that received regular doses of triggered 5 mol % PEGylated siRNA-nanoparticles over a 4-week period did not reveal evidence for unintended harmful effects (Supporting Information Figures 2 and 3). Collectively these data indicated that our nanoparticles are passively hepatotrophic without obvious toxic side effects. These properties were considered sufficiently significant to warrant further investigation by using the vector system to silence HBV replication. These triggered 5 mol % PEGylated siRNA-nanoparticles were subsequently renamed siFECTplus nanoparticles.

Antiviral Efficacy of siRNA Nanoparticles in Cell Culture and in Murine Hydrodynamic Injection Models of HBV Replication. Initially anti-HBV efficacy of a panel of 7 different siRNAs was assessed. These siRNAs targeted conserved regions of the HBV genome (Figure 3a and Supporting Information Figure 4)[35,36] and were selected to avoid homologous targets found within the human or mouse genomes. Their design was according to the predicted susceptibility of HBV targets to RNAi-mediated silencing.[35,36] siRNAs (Table 1) were delivered using by means of siFECTamine and gene knock-down effects determined in cultured liver-derived Huh7 cells that had been transfected with a HBV replication competent plasmid. Of the panel, siRNA 1407 and siRNA 1794 were reliably capable of achieving inhibition of HBV s-antigen

(34) Perouzel, E.; Jorgensen, M. R.; Keller, M.; Miller, A. D. Synthesis and formulation of neoglycolipids for the functionalization of liposomes and lipoplexes. *Bioconjugate Chem.* **2003**, *14*, 884–898.

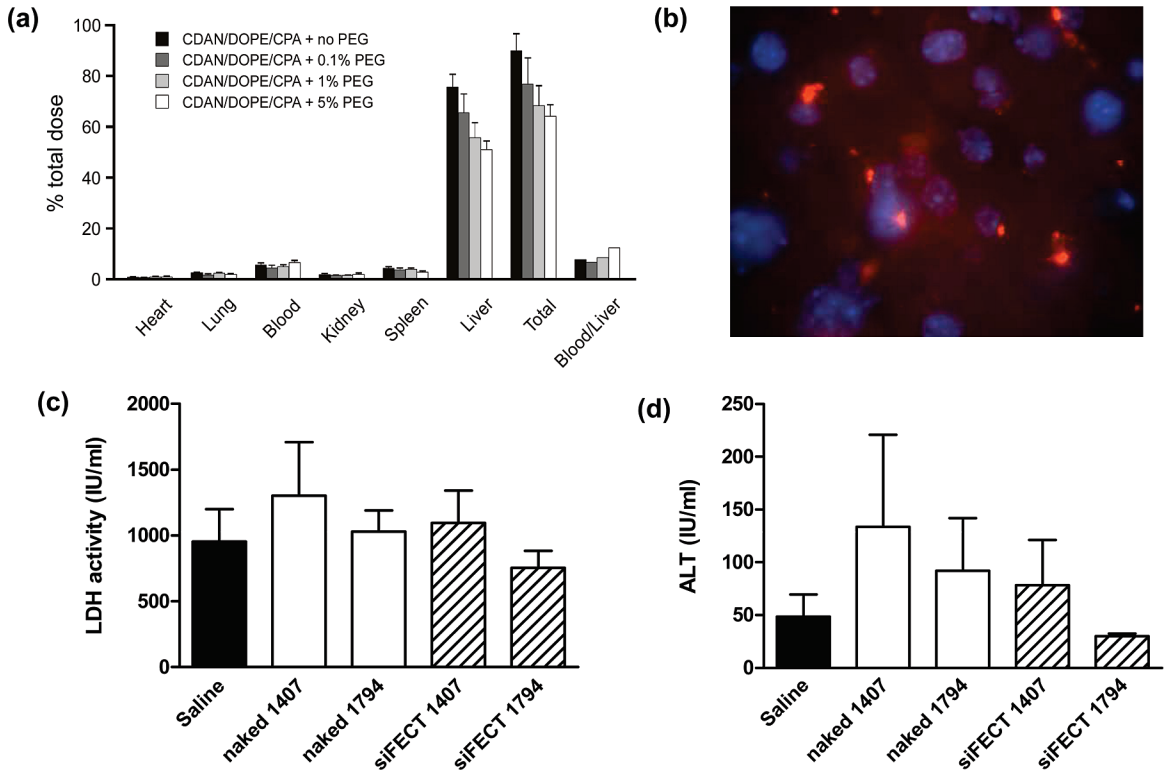


Figure 2. Biodistribution and experimental toxicity assessment of siRNA nanoparticle formulations. (a) Triggered PEGylated siRNA nanoparticle formulations (0.1−5.0 mol % PEG) containing 4-[^{14}C]-labeled cholesterol were administered iv to mice. Animals were sacrificed after 1 h, and radioactivity present in heart, lung, blood, liver, spleen, kidney and blood in the liver (blood/liver) was determined. (b) Frozen section of liver examined using microscopy (100× magnification). Labeled Cy3-siRNA was incorporated into triggered 5 mol % PEGylated siRNA nanoparticles (siFECTplus nanoparticles) and administered intravenously. Cy3 labeled siRNA (red) is noted in the liver parenchyma 45 min after injection. For histological assessment, liver sections have been counter stained with DAPI (blue) to delineate the nuclei. Serum concentrations of LDH (c) and ALT (d) at 4 d after iv administration of saline, naked siRNA-1407 (naked 1407) and naked siRNA-1794 (naked 1794) or siFECTplus nanoparticles delivering functional siRNA-1407 and siRNA-1794 (siFECT 1407 and siFECT 1794 respectively).

(HBsAg) by 40% to 50% (Figure 3b), and were selected for further studies *in vivo*.

Initially, to assess HBV gene knockdown *in vivo*, a murine hydrodynamic injection (MHI) model of viral replication was employed. A saline solution comprising 10% of mouse body weight, which contained a HBV replication-competent plasmid, was injected over 5−10 s via the tail vein. Equivalent efficiency of hepatotropic delivery using this method was confirmed by staining for activity of β-galactosidase, which was expressed from a coinjected reporter plasmid.[7] At 8 h post MHI, siFECTplus nanoparticles were administered iv at a dose of 1 mg/kg (siRNA/mouse body weight). Serum concentrations of HBsAg and VPEs were measured thereafter. Compared to controls, siFECTplus nanoparticle-mediated administration of siRNA1407 or siRNA1794 resulted in significant knockdown of HBsAg at time points of 2 and 4 days (Figure 3c). Our observations were similar to those reported when an equivalent dose of chemically modified siRNA was delivered by means of stabilized nucleic acid−lipid particles.[19] Morrissey et al. were also able to demonstrate a more efficient knockdown of HBsAg with daily iv administrations of stabilized nucleic acid−lipid particles using a higher siRNA dose of 2.5 mg/kg (siRNA/mouse body weight) for 6 days after MHI. In our case, functional siRNAs were administered earlier after hydrodynamic injection when HBV replication may have been higher and more difficult to silence. Based on these positive observations, and in order to assess HBV gene knockdown in a setting that simulates the condition of chronic HBV infection, further investigations with siFECTplus nanoparticles were carried out on HBV transgenic mice.

Antiviral Efficacy of siRNA Nanoparticle Formulations in HBV Transgenic Mice. The HBV transgenic mouse line used here was propagated after stable integration of greater than genome length HBV sequences.[30] In this model of chronic

(35) Naito, Y.; Yamada, T.; Ui-Tei, K.; Morishita, S.; Saigo, K. siDirect: highly effective, target-specific siRNA design software for mammalian RNA interference. *Nucleic Acids Res.* **2004**, *32*, W124−129.

(36) Ui-Tei, K.; Naito, Y.; Takahashi, F.; Haraguchi, T.; Ohki-Hamazaki, H.; Juni, A.; Ueda, R.; Saigo, K. Guidelines for the selection of highly effective siRNA sequences for mammalian and chick RNA interference. *Nucleic Acids Res.* **2004**, *32*, 936–948.

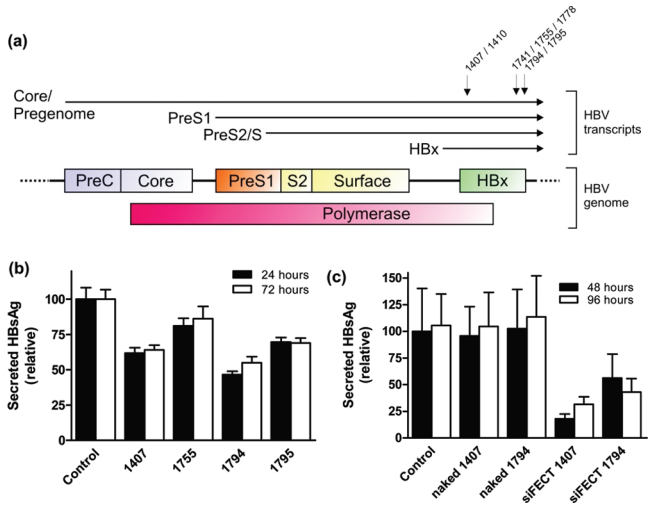


Figure 3. Effect of siFECTplus nanoparticles on markers of HBV replication in cell culture and MHI models. (a) Schematic illustration of HBV genome to indicate the siRNA target sites. (b) HBsAg was determined in the cell culture supernatant at times of 24 and 72 h after siFECTamine-mediated delivery of the indicated siRNAs (see Table 1) to Huh7 liver-derived cells, including an irrelevant, nonfunctional siRNA (control).[13] (c) Serum concentrations of HBsAg measured in MHI-treated mice at 48 and 96 h after the iv administration of naked siRNA-1407 (naked 1407) and naked siRNA-1794 (naked 1794), or siFECTplus nanoparticles delivering either an irrelevant, nonfunctional siRNA (control)[13] [equivalent result obtained with saline injection], or functional siRNAs 1407 and 1794 (siFECT 1407 and siFECT 1794 respectively).

Table 1. Designed Anti-HBV siRNAs and Their HBV Target Sequences[a]

siRNA	HBV target sequence	siRNA sequence[b]
1407	1407−1429	5′-GCGGGACGUCCUUUGUUUACG **AGCGCCCUGCAGGAAACAAAU**-5′
1410	1410−1432	5′-GGACGUCCUUUGUUUACGUCC **GCCCUGCAGGAAACAAAUGCA**-5′
1741	1741−1783	5′-GGGGAGGAGAUUAGGUUAAAG **ACCCCCUCCUCUAAUCCAAUU**-5′
1755	1755−1777	5′-GUUAAAGGUCUUUGUAUUAGG **UCCAAUUUCCAGAAACAUAAU**-5′
1778	1778−1800	5′-GCUGUAGGCAUAAAUUGGUCU **UCCGACAUCCGUAUUUAACCA**-5′
1794	1794−1816	5′-GGUCUGCGCACCAUCAUCAUG **AACCAGACGCGUGGUAGUAGU**-5′
1795	1795−1817	5′-GUCUGCGCACCAUCAUCAUGC **ACCAGACGCGUGGUAGUAGUA**-5′

[a] See *Supporting Information* Figure 1 for sequence alignments. [b] The siRNA antisense strands are in bold font.

infection, HBV particles are constitutively produced and the number of circulating VPEs is typically in the range from 0.5 to 1.0 × 10^7 per mL. siFECTplus nanoparticle formulations were administered iv at a dose of 1 mg/kg (siRNA/mouse body weight) every third day over a 4 week period. Nanoparticles effected a statistically significant decrease in HBsAg blood concentrations at day 28 when compared to controls. This inhibition was equivalent to the effect produced by daily intraperitoneal (ip) administration of lamivudine at a dose of 200 mg/kg mouse body weight (Figure 4a). Similar but diminished trends were also observed when measuring hepatitis B e-antigen (HBeAg) (Figure 4b). In mice receiving siRNA 1407 or siRNA 1794 containing nanoparticles, we also observed that circulating VPEs were diminished significantly by approximately 3-fold relative to controls at 28 days (Figure 4c). Furthermore, compared to lamivudine administration, siFECTplus nanoparticle mediated delivery of siRNA 1407 or siRNA 1794 appeared to have up to twice the inhibitory effect on VPEs (Figure 4c). A similar decrease in HBsAg mRNA was observed relative to controls in livers of mice receiving nanoparticles (Figure 4d).

Interferon Response *in Vivo.* Oligoadenylate synthase-1 (*OAS-1*) and interferon-β (*IFN-*β) mRNA concentrations were measured to determine whether induction of the interferon (IFN) response caused by siRNA administration had occurred (Figure 4e). Comparisons with controls revealed that siFECTplus nanoparticles delivering siRNA 1407 or siRNA 1794 were not inducing significant activation of the IFN response genes. These data support an interpretation that inhibitory effects on markers of HBV replication were unlikely to be due to any unintended toxic immunostimulatory mechanisms. Silencing of HBV replication in a stringent mouse model of chronic HBV infection without obvious signs of IFN stimulations indicate that our triggered PEGylated siRNA-nanoparticles have potential RNAi therapeutic use.

Discussion

The application of RNAi to developing new HBV treatment is very promising. Replication of the virus is susceptible to RNAi-mediated inhibition and unlike HIV-1 or hepatitis C virus, HBV is not prone to mutation with escape from silencing by antiviral siRNAs. This is primarily because HBV has a very compact genome with overlapping reading frames (Figure 3a) that limit its sequence plasticity. Accordingly, the HBV genome is a good target for anti-HBV RNAi-based therapies and HBV is also an excellent disease model to assess the feasibility of therapy that is based on systemic administration of siRNA. One of the most important challenges facing development of RNAi-based HBV therapy is achieving safe, convenient and efficient delivery of siRNAs to hepatocytes *in vivo*. In this study, we report on the use of nonviral vectors that can be used to deliver anti HBV sequences efficiently. Although viral vectors have been used successfully to deliver expressed anti HBV sequences, convenience of large-scale chemical synthesis and modifications to alter biological properties seem likely to make nonviral vectors the preferred class of vector for therapeutic use.

Thus far, a number of nonviral vector approaches have been employed to deliver siRNAs to the liver after systemic injections. These include use of cholesterol-conjugation, apolipoprotein AI complexes, α-tocopherol conjugates, and vitamin A coupled liposomes.[15−18] Silencing of markers of HBV replication in the MHI model[19] and also the endogenous ApoB gene in monkeys[20] were achieved with stabilized nucleic acid−lipid particle vector systems. In the study reported here, we have extended the range of synthetic,

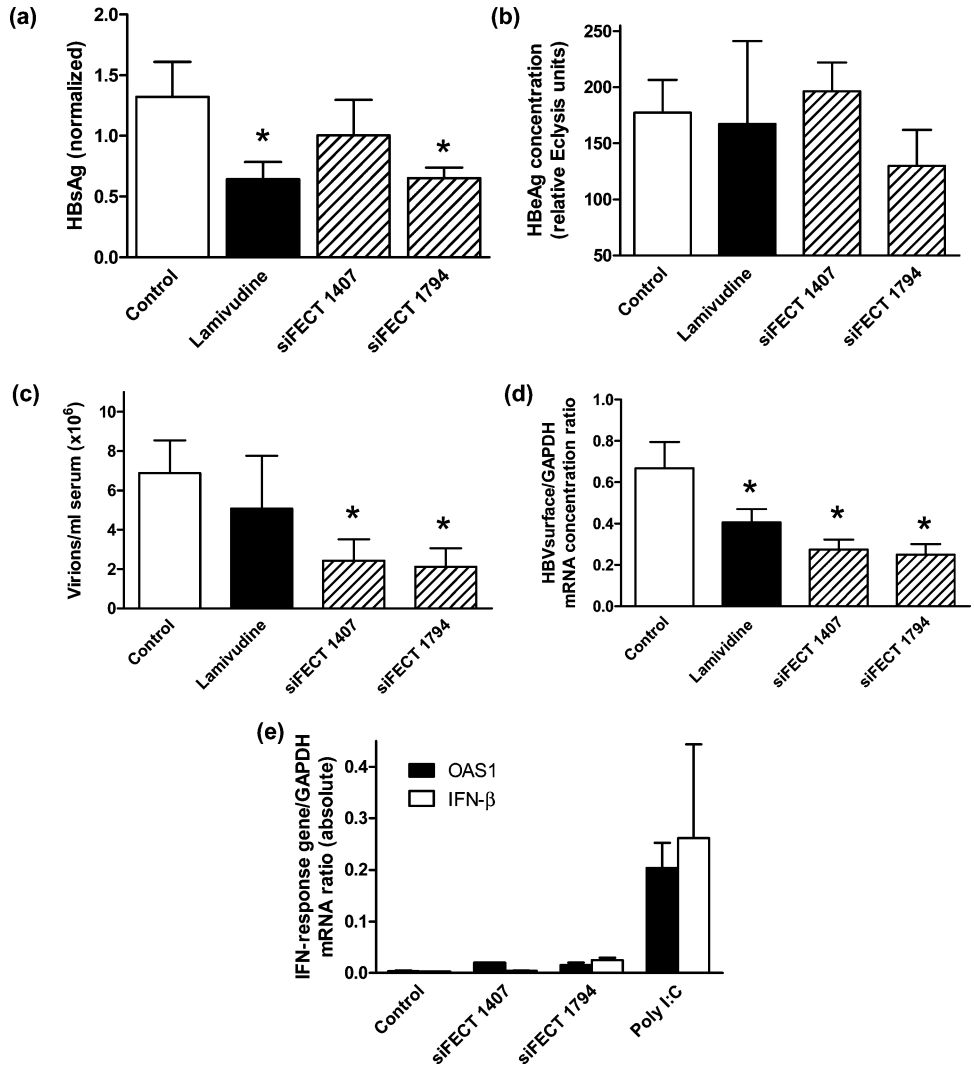


Figure 4. Markers of viral replication and immunostimulation in HBV transgenic mice. (a) HBsAg concentrations measured at 28 days in HBV transgenic mice treated every 3 days by iv administration of siFECTplus nanoparticles delivering either an irrelevant, nonfunctional control siRNA (control)[13] [equivalent result obtained with saline injection], or functional siRNAs 1407 and 1794 (siFECT 1407 and siFECT 1794 respectively), Positive control lamivudine was administered daily. (b) HBeAg concentrations measured at 28 d in HBV transgenic mice treated as described in (a). (c) Circulating VPEs (d) HBV mRNA and (e) *OAS-1* and *IFN-β* mRNA measured at 28 days in HBV transgenic mice treated as described in (a). As positive control for induction of the IFN response, mice were treated with poly I:C using MHI at 6 h before sacrifice.

nonviral hepatotropic vectors to include novel triggered 5 mol % PEGylated siRNA-nanoparticles (also known as siFECTplus nanoparticles). After peripheral iv administration, these vectors appear capable of safely delivering chemically unmodified siRNAs to murine livers to achieve inhibition of markers of HBV replication. Importantly siRNA-mediated silencing of HBV replication with siRNA 1407 or siRNA 1794 was more effective than the inhibition of viral proliferation achieved with lamivudine, which is a licensed HBV drug. The observed suppression of HBV (Figures 3 and 4) is significant and our data compare well with reported results obtained using higher doses of chemically modified siRNA or expressed RNAi effectors.[37,38]

Our triggered PEGylated siRNA-nanoparticles (siRNA-ABC nanoparticles) are prepared using a rapid, quantitative chemoselective reaction for the postcoupling of PEG stealth/biocompatibility polymer to the outer surface of core siRNA-nanoparticles (siRNA-lipoplexes)[12,13] (Figure 1c). Bioconjugation gives rise to oxime bonds that are themselves stable at pH 7 but can be expected to be labile at pH 5.5 and below. To the best of our knowledge the data described here provide a first demonstration of applying a modular surface post-coupling approach to produce simultaneously a pH-triggerable vector system.[12] Moreover this methodology should

(37) Morrissey, D. V.; Blanchard, K.; Shaw, L.; Jensen, K.; Lockridge, J. A.; Dickinson, B.; McSwiggen, J. A.; Vargeese, C.; Bowman, K.; Shaffer, C. S.; Polisky, B. A.; Zinnen, S. Activity of stabilized short interfering RNA in a mouse model of hepatitis B virus infection. *Hepatology* **2005**, *41*, 1349–1356.

enable large-scale preparation, which would be appropriate for pharmaceutical applications.

The potential advantage of such a pH triggerable vector system should be as follows. Successful functional delivery of siRNA to liver by passive (biophysical) targeting, without the requirement for a targeting ligand, has also been demonstrated by others using stabilized nucleic acid−lipid particles.[19,20] In fact passive targeting to hepatocytes occurs because of a natural trophism of nanoparticles for the liver post iv administration where capillary fenestrations (approximately 100 nm in diameter) allow nanoparticles to leave the main circulation and enter the hepatic space of Disse. Once there, Kupffer cells (of the reticuloendothelial system) would be expected to engulf nanoparticles unless protected by PEGylation.[12] Consequently, triggered PEGylated nanoparticles (<100 nm in diameter) would appear to remain largely free to enter hepatocytes. We have noted previously that PEGylation does not necessarily impair uptake into cells by endocytosis.[12] However, we have also noted previously that release of nucleic acids after endocytosis may be substantially limited unless there is some form of in-built triggereability (such as a pH-dependent trigger) in the nanoparticle. This pH-triggerability in particular is needed to enable PEG release, overall particle destablization and associated escape from early endosomes of functional nucleic acids once the internal endosome pH has dropped from an initial pH 7 to approximately pH 5.5.[12]

In this study we report on a partial analysis of immune stimulation by our triggered PEGylated siRNA-nanoparticles. The rationale behind this focused study was to determine whether nanoparticle-mediated siRNA delivery provoked an innate immune response. This nonspecific innate response could be a direct result of effects of siRNA sequence, concentration and method of delivery. *OAS-1* and *IFN-β* gene expression are useful and well-characterized indicators of the activation of this pathway. The analysis of these markers (Figure 4e) indicates that observed inhibitory effects on HBV replication were unlikely to be a result of any unintended toxic immunostimulatory mechanisms, but rather the direct consequence of RNAi mediated effects.

In summary, the major distinguishing features of our triggered PEGylated siRNA-nanoparticles compared with other lipid-nanoparticle systems described elsewhere are the modular assembly process, the use of a postcoupling methodology to include PEG, and the simultaneous incorporation of pH-triggerability by through the formation of a pH-labile oxime bond. Going forward in order to develop our triggered PEGylated siRNA-nanoparticles for therapeutic applications, comprehensive characterization and further refinement is being carried out. Dose optimization, detailed evaluation of non specific effects, assessment of stability, pharmacokinetic analysis and metabolite profiling are being undertaken. We are also carrying out studies to improve silencing efficiency of the formulations by introducing stabilizing modifications to the siRNAs. Although challenges remain, we believe that our data together with those reported by others[19,20,37,38] are encouraging and support the notion that synthetic nonviral siRNA delivery technologies can be used to advance HBV therapy as well as for treatment of other hepatic diseases where silencing of pathology-causing diseases is indicated.

Abbreviations Used

RNAi, RNA interference; HBV, hepatitis B virus; siRNA, small interfering RNA; VPEs, viral particle equivalents; HCC, hepatocellular carcinoma; IFN-α, interferon-α; AAVs, adeno-associated viruses; shRNA, small hairpin RNA sequences; shRNAi, small hairpin interfering RNA; pDNA, plasmid DNA; SNALP, stabilized nucleic acid−lipid particle; MHI, murine hydrodynamic injection; CDAN, N^1-cholesteryloxycarbonyl-3,7-diazanonane-1,9-diamine; DOPE, dioleoyl-L-α-phosphatidylethanolamine; CPA, cholesteryl-PEG^{350}-aminoxy lipid; CA, cholesteryl-aminoxy lipid; PEG^{175}, polyethylene glycol 175; PEG^{350}, polyethylene glycol 350; PEG^{2000}, polyethylene glycol 2000; PEG^{2000}-$(CHO)_2$, polyethylene glycol 2000-dialdehyde; Fmoc, 9-fluorenylmethyloxycarbonyl; Boc, *t*-butyloxycarbonyl; HBTU, 2-(1*H*-benzotriazol-1-yl)-1,1,3,3-tetramethyluronium hexafluorophosphate; DAPI, 4′,6-diamidino-2-phenylindole; LDH, lactate dehydrogenase; ALT, alanine transaminase; HBsAg, hepatitis B s-antigen; HBeAg, hepatitis B e-antigen; OAS-1, oligoadenylate synthase-1; IFN-β, interferon-β.

Acknowledgment. Financial support from ImuThes Ltd., Mitsubishi Chemical Corporation, the South African Innovation Fund, National Research Foundation and the South African Poliomyelitis Research Foundation is gratefully acknowledged. The pCH-9/3091 plasmid was generously provided by Michael Nassal (The University Hospital Freiberg, Germany).

Note Added after ASAP Publication. Michael Keller has been removed as an author on this paper. The article was reposted on January 30, 2009.

Supporting Information Available: Figures depicting urea, creatinine and electrolyte levels in blood post iv administration to NMR-1 mice of saline, naked siRNAs 1794 and 1407, or siFECTplus nanoparticles formulated with siRNAs 1794 and 1407; representative smears of murine blood post iv administration to NMR-1 mice of saline, naked siRNAs 1794 and 1407, or siFECTplus nanoparticles formulated with siRNAs 1794 and 1407; histological examination of NMR-1 murine liver post iv administration of saline control and siFECTplus nanoparticles; and alignment of siRNAs with representative HBV genotype sequences. This material is available free of charge via the Internet at http://pubs.acs.org.

MP800157X

(38) McCaffrey, A. P.; Nakai, H.; Pandey, K.; Huang, Z.; Salazar, F. H.; Xu, H.; Wieland, S. F.; Marion, P. L.; Kay, M. A. Inhibition of hepatitis B virus in mice by RNA interference. *Nat. Biotechnol.* **2003**, *21*, 639–644.

Chapter 6: DODAG; a versatile new cationic lipid that mediates efficient delivery of pDNA and siRNA

Mevel, M., Kamaly, N., Carmona, S., Oliver, M. H., Jorgensen, M. R., Crowther, C., Salazar, F. H., Marion, P. L., Fujino, M., Natori, Y., Thanou, M., Arbuthnot, P., Yaouanc, J. J., Jaffres, P. A. & Miller, A. D.

Journal of Controlled Release. 2010;143(2):222-32.

This study described the synthesis of new cationic lipids, first the substitution of the polyamine functional head with guanidinium moieties and similarly the replacement of the cholesteryl hydrophobic moiety with a long-chain hydrocarbon moiety. The cationic lipid DODAG in combination with the neutral lipid DOPE showed high levels of transfection and minimal toxicity *in vitro*. We reported on the delivery properties of the cationic lipid DODAG in HBV transgenic mice, using previously characterised siRNAs targeting HBV. siRNA-DODAG nanoparticles delivering siRNA-1407 had a more pronounced effect compared to lamivudine treatment on markers of HBV infection.

Contribution by the author:

SC contributed with all other authors to the hypothesis to be tested and the functional experiments that assess the *in vivo* efficacy of these lipids. SC conducted the final assembly of the nanoparticles and transgenic mice experiments at the animal facility of Stanford University, CA, USA. SC conducted toxicity studies to determine haematological, hepatic and renal potential undesirable effects. SC contributed to data analysis, manuscript writing and final review

Journal of Controlled Release 143 (2010) 222–232

Contents lists available at ScienceDirect

Journal of Controlled Release

journal homepage: www.elsevier.com/locate/jconrel

DODAG; a versatile new cationic lipid that mediates efficient delivery of pDNA and siRNA

Mathieu Mével [a], Nazila Kamaly [a], Sergio Carmona [b], Morag H. Oliver [a], Michael R. Jorgensen [a], Carol Crowther [b], Felix H. Salazar [c,d], Patricia L. Marion [d], Masato Fujino [e], Yukikazu Natori [e], Maya Thanou [a], Patrick Arbuthnot [b], Jean-Jacques Yaouanc [f], Paul Alain Jaffrès [f], Andrew D. Miller [a,g,*]

[a] Imperial College Genetic Therapies Centre, Department of Chemistry, Flowers Building, Armstrong Road, Imperial College London, London, SW7 2AZ, UK
[b] Antiviral Gene Therapy Research Unit, Department of Molecular Medicine and Haematology, University of the Witwatersrand Medical School, Private Bag 3, WITS 2050, South Africa
[c] Stanford University, Stanford CA, USA
[d] Hepadnavirus Testing, Inc. Mountain View CA, USA
[e] RNAi Co., Cosmos Hongo Bldg. 10F. 4-1-4, Hongo, Bunkyo-ku, Tokyo, 113-0033, Japan
[f] CEMCA, UMR CNRS 6521, Faculté des Sciences et Techniques, Université de Brest, Université Européenne de Bretagne, IFR ScinBios 148, 6 avenue Le Gorgeu, 29238 Brest, France
[g] ImuThes Ltd., Flowers Building, Armstrong Road, London SW7 2AZ, UK

ARTICLE INFO

Article history:
Received 18 November 2009
Accepted 1 December 2009
Available online 5 December 2009

Keywords:
Cationic lipids
Nucleic acid delivery
Liposomes
Nanoparticles
Guanidinium lipids
Polyamines
Transfection
RNA interference

ABSTRACT

We report the syntheses of novel cationic lipids comprised of cholesteryl-moieties linked to guanidinium functional groups, and also cationic lipids comprising a dialkylglycylamide moiety conjugated with a polyamine or a guanidinium functional group. In plasmid DNA (pDNA) transfection studies, these cationic lipids were formulated into cationic liposomes with the neutral co-lipid dioleoyl-L-α-phosphatidylethanolamine (DOPE) or with a recently reported neutral lipophosphoramidate derivative of histamine (MM27). We observe that cationic liposomes prepared from the cationic lipid *N′,N′*-dioctadecyl-*N*-4,8-diaza-10-aminodecanoylglycine amide (DODAG) and DOPE frequently mediate the highest levels of transfection *in vitro* in all three different cell lines studied (OVCAR-3, IGROV-1 and HeLa) both in the presence or absence of serum. In addition, *in vitro* cellular toxicity was found to be minimal. Alternatively, we observe that DODAG alone forms lipoplex nanoparticles with small interfering RNA (siRNA) that are able to mediate the functional delivery of two previously validated anti-hepatitis B virus (HBV) — siRNAs to murine liver *in vivo* with minimal observable liver toxicity and immune stimulation. Specific knock-down of HBV infection parameters (virion and hepatic mRNA levels) is observed that is at least equivalent to the impact of extensive treatment with lamivudine (a licensed antiviral drug).

© 2009 Elsevier B.V. All rights reserved.

1. Introduction

Gene delivery has numerous potential applications both clinically and for basic science research. Typically, the term gene therapy refers to the delivery of nucleic acids by means of a vector to a patient for some therapeutic purpose. The vector is the means of carriage of the nucleic acid from site of administration to site of action. Most current vector technologies can be divided into two groups; viral and nonviral, with both having their intrinsic advantages and disadvantages. Despite the high transfection efficiency of viral vectors, safety concerns have been raised in clinical trials because of their highly toxic nature [1]. Nonviral vectors, such as cationic liposome and polymer-based systems, are considered to be less toxic, less immunogenic, and easier to prepare than viral vectors and are potentially more attractive vectors for clinical applications [2–4].

Cationic liposomes/micelles and cationic polymers have been utilized since Felgner et al.[5] and Wu et al.[6] respectively demonstrated their use for nucleic acid delivery *in vitro*. Over the

Abbreviations: pDNA, plasmid DNA; DOPE, dioleoyl-L-α-phosphatidylethanolamine; DODAG, *N′,N′*-dioctadecyl-*N*-4,8-diaza-10-aminodecanoylglycine amide; HBV, hepatitis B virus; siRNA, small interfering RNA; Chol, cholesterol; CTAP, N^{15}-Cholesteryloxycarbonyl-3,7,12-triazapentadecane-1,15-diamine; CDAN, N^1-cholesteryloxycarbonyl-3,7-diazanonane-1,9-diamine; CEAG, N^1-cholesteryloxycarbonyl ethylene-1-amino-2-guanidinium chloride; CAPG, N^1-cholesteryloxycarbonyl-3-aza-pent-1-amino-5-guanidinium chloride; DOAG, *N′,N′*-dioctadecylamido-*N*-methyl-guanidinium chloride; DOGS, dioctadecylamidoglycylspermine; Z, benzyloxycarbonyl; *t*BOC, *t*-Butyloxy-carbonyl; HBTU, 2-(1*H*-benzotriazol-1-yl)-1,1,3,3-tetramethyluronium hexafluorophosphate; DMAP, 4-dimethylaminopyridine; TFA, trifluoroacetic acid; DIPEA, diisopropylethylamine; PCS, photon correlation spectroscopy; LDH, lactate dehydrogenase; GFP, green fluorescent protein; PEG, polyethylene glycol; ALT, alanine transaminase; VPEs, Viral Particle Equivalents; HBsAg, hepatitis B s-antigen; OAS-1, oligoadenylate synthase-1; IFN-β, interferon-β; RNAi, RNA interference; HCC, hepatocellular carcinoma; IFN-α, interferon-α; AAVs, adeno-associated viruses; shRNA, small hairpin RNA sequences; shRNAi, small hairpin interfering RNA; SNALPs, stabilized nucleic acid-lipid particles.

* Corresponding author. Postal address: Imperial College Genetic Therapies Centre, Department of Chemistry, Flowers Building, Armstrong Road, Imperial College London, London, SW7 2AZ, UK. Tel.: +44 20 7594 5773; fax: +44 20 7594 5803.
E-mail address: a.miller@imperial.ac.uk (A.D. Miller).

0168-3659/$ – see front matter © 2009 Elsevier B.V. All rights reserved.
doi:10.1016/j.jconrel.2009.12.001

last twenty years various cationic liposome/micelle formulations have been formulated using a succession of novel cationic lipids to assist nucleic acid delivery *in vitro* and even *in vivo* with generally disappointing results [7–16]. Most cationic liposome/micelle systems for nucleic acid delivery involve the formulation of a cationic lipid (cytofectins) and a neutral co-lipid such as dioleoyl-L-α-phosphatidylethanolamine (DOPE) **1** or cholesterol **2** (Fig. 1). The role of the cationic lipid is to facilitate nucleic acid binding and condensation leading to cationic liposome/micelle–nucleic acid complex (lipoplex) nanoparticles. The cationic lipids also facilitate nanoparticle interactions with cell wall membranes to trigger internalization (typically by endocytosis) and if well designed, endosomolysis (endosome escape) in order that nucleic acids may enter the cytosol post-nanoparticle internalization [15,16]. The neutral co-lipid DOPE **1** is a natural fusogenic lipid with a tendency to adopt the inversion hexagonal phase, H_{II}, over a wide range of temperatures, a characteristic typically expected to aid endosomolysis and improve intracellular trafficking of nucleic acids post nanoparticle internalization [17–24]. However, DOPE **1** has potentially limited utility *in vivo* because although the fusogenic nature helps to promote transfection *in vitro*, this also renders lipoplex nanoparticles unstable with respect to aggregation in more complex *in vivo* environments [25]. In order to overcome this problem, fluorinated phosphatidylethanolamine co-lipids were recently developed by Boussif et al. [26,27]. Alternatively, a series of dialkynoyl DOPE analogues has been developed [28,29]. Most recently, Jaffrès and Midoux et al. described the synthesis of a new neutral co-lipid lipophosphoramidate derivative of histamine (MM27) **3** that appears to enhance transfection up to 100-fold above levels achieved using cationic liposome/micelles formulated with DOPE **1** (Fig. 1) [30,31]. This effect may be due to the low pK_a (approximately 6) value of the imidazole ring nitrogen atoms [14,29,32]. As a result of this low pK_a value, imidazole rings should be unprotonated at pH 7 prior to nanoparticle entry into cells, but would be expected to become protonated when endosome compartments are acidified to around pH 5.5, post endocytosis. Protonation is associated typically with an increase in endosome ionic strength that is widely considered to cause endosomolysis by an osmotic shock type mechanism assisted by co-lipid fusogenic characteristics [32].

In previous research, cationic lipids have been prepared frequently by the conjugation of a variety of hydrophobic moieties to a variety of polyamine structures. This approach to cationic lipid design has been used widely. The polyamine employed can have a small and fully defined structure such as spermine–lipid conjugates [33,34] or spermine–lipophosphoramides [35]. Conversely, lipidic moieties may also be conjugated with monodisperse polymers such as PEI [36,37] or PLL [38]. In our case, two cationic lipids each with a cholesteryl hydrophobic moiety, namely N^{15}-Cholesteryloxycarbonyl-3,7,12-triazapenta-decane-1,15-diamine (CTAP) **4** and N^{1}-cholesteryl-oxycarbonyl-3, 7-diazanonane-1, 9-diamine (CDAN) **5**, have proven particularly useful for *in vitro* and *in vivo* delivery of plasmid DNA (pDNA) and small interfering RNA (siRNA) [32,39–44]. However, in spite of the apparently high level of utility in both cases, we have considered that **4** and **5** may in fact not be optimal structures for all requirements. Therefore, we became interested in exploring the structures of other cationic lipids in an attempt to find cationic lipids with potentially further improved and/or more versatile properties. In particular we were intrigued to investigate the effects of substituting the polyamine functional head group with guanidinium functional

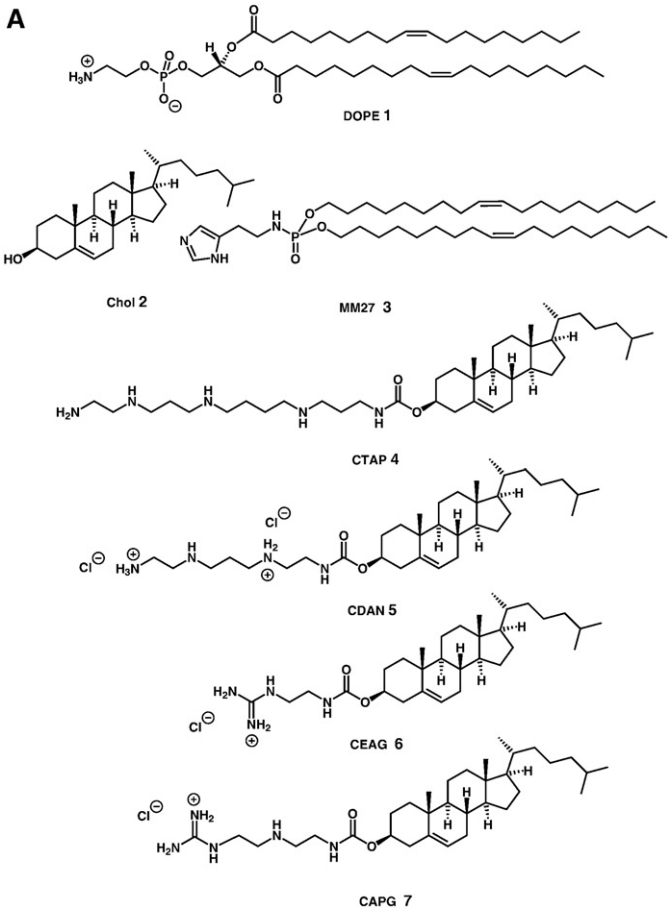


Fig. 1. Schematic illustration of structures of cationic lipids and neutral co-lipids constituents synthesized or used in transfection studies.

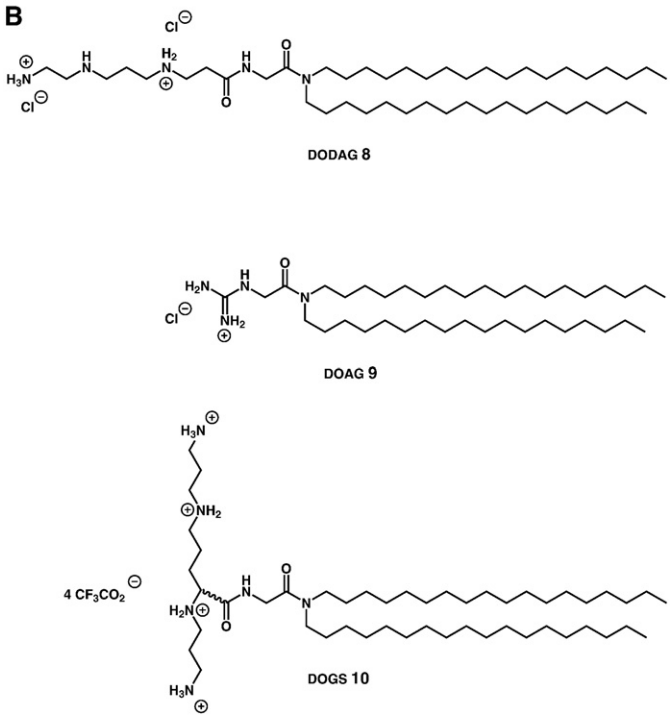


Fig. 1 (*continued*).

moeities. Conversely we wished to explore the consequences of replacing the cholesteryl hydrophobic moiety of **5** with a long-chain hydrocarbon moiety. Guanidinium functional groups have a pK_a value of approximately 14, and so are easily protonated at physiological pH. Different complexes between guanidinium groups and anionic phosphate have already been observed [45,46] that can facilitate the formation of lipoplex nanoparticles with pDNA. Therefore, besides applications in the anti-trypanosome agent synthaline [47] guanidinium groups have also been used by a number of different groups to originate cationic lipids for pDNA transfection [48–51].

Accordingly, we now report on the syntheses and nucleic acid delivery properties of novel cationic lipids comprised of cholesteryl hydrophobic moieties linked to guanidinium functional groups (**6** and **7**). At the same time we report on the syntheses and nucleic acid delivery properties of novel cationic lipids with a polyamine or guanidinium functional group conjugated (**8** and **9** respectively) to a long-chain hydrocarbon dialkylglycylamide moiety of the type that was first described in the structure of the spermine–lipid conjugate dioctadecylamido-glycylspermine (DOGS) **10** (Fig. 1). We observe the important co-lipid characteristics of the lipophosphoramidate derivative of histamine (MM27) **3** in partnering guanidinium functional group containing cationic lipids. We also observe the surprising versatility of the dialkyl glycylamide polyamine cationic lipid, *N′,N′*-dioctadecyl-*N*-4, 8-diaza-10-aminodecanoylglycine amide (DODAG), **8** in helping to mediate functional pDNA delivery to cells *in vitro* and siRNA delivery to liver *in vivo*.

2. Materials and methods

2.1. General synthesis

All chemicals and reagents were purchased from Sigma Aldrich (Dorset, UK) or Avanti Lipids (USA) or Invitrogen (UK) unless stated otherwise. Solvents were typically prepared as freshly distilled from appropriate drying agents (CH_2Cl_2 was distilled over P_2O_5, diisopropylethylamine (DIPEA) was distilled over NaOH) and reactions were run under a nitrogen atmosphere. Other solvents were purchased predried or as required from Sigma-Aldrich (Dorset, UK) or BDH Laboratory Supplies (Poole, UK). HPLC-grade acetonitrile was purchased from Fisher Chemicals (Leicester, UK) and other HPLC-grade solvents from BDH Laboratory Supplies (Poole, UK). Thin layer chromatography (TLC) was performed on pre-coated Merck–Kieselgel 60 F_{254} aluminium backed plated and revealed with ultraviolet light, iodine, acidic ammonium molybdate (IV), acidic ethanolic vanillin, or other agents as appropriate. Flash column chromatography was accomplished on Merck–Kieselgel 60 (230–400 mesh). Mass spectra were recorded using Bruker Esquire 3000, VG-7070B or JEOL SX-102 instruments. ^{1}H NMR spectra were recorded on an Advance Brucker 400 Ultrashield ^{TM} machine using residual isotopic solvent as an internal reference. Coupling constants *J* are given in Hz (The following abbreviations were used: s = singlet, d = doublet, t = triplet, q = quartet, quin = quintet, br = broad singlet). Analytical HPLC (Hitachi-LaChrom L-7150 pump system equipped with a Polymer Laboratories PL-ELS 1000 evaporative light scattering detector) was conducted with a Vydac C4 peptide column and HPLC gradient mixes assigned as follows: gradient mix A = H_2O/0.1%TFA; mix B = MeCN/0.1%TFA; mix C = MeOH. Liposomes were sized using a DynaPro particle sizer (Protein Solutions; Piscataway, NJ) and employing the Dynamics data collection and analysis software. Detailed syntheses are reported in supplementary information.

2.2. Formulation of cationic liposomes

All lipids were stored as stock solutions in anhydrous organic solvents ($CHCl_3$, MeOH, or a mixture of both), at −20 °C under argon. Liposomes were made with cationic lipids and co-lipids (DOPE **1** or MM27, **3**) at a standard ratio of 1:1 (molar ratio) to give a cationic liposome suspension with a fixed total lipid concentration of 3 mg mL^{-1} in water. Fluorescent labeled liposomes always contained 0.5 mol % of DOPE-Rhodamine (Avanti Polar Lipids Inc., USA). Appropriate volumes of each lipid stock were placed in a round-bottom flask (typically 5 mL). The solvent was slowly removed *in vacuo* to ensure production of an even lipid film. The film was rehydrated with water at a defined volume (hydration time of 5 min). The resulting

solution was sonicated for 30 min at 30 °C to form liposomes of appropriate size. The size of the liposomes was determined by photon correlation spectroscopy (PCS). In each experiment the liposomal preparation (20 μL) was diluted with PBS to a final volume of 200 μL. The mean average diameter of the vesicles was determined at 25 °C as the result of at least three reliable readings.

2.3. Preparation of lipoplex nanoparticles

The plasmid pEGFP-Luc, which encodes for an enhanced green fluorescence protein (GFP), was amplified in *Escherichia coli* and purified using GIGA prep Purification protocol. Purity of the plasmid was checked by electrophoresis on 1.0% agarose gel [pDNA], and was estimated spectroscopically by measuring the $A^{0.1}{}_{260}$ and confirmed by gel electrophoresis. The plasmid preparations showing a value of $A_{260}/A_{280} > 1.8$ were considered essentially free of background protein contamination and used immediately. Cationic liposome-pDNA complexes (lipoplex nanoparticles) were prepared at 1:2, 1:4, 1:8 and 1:12 (pDNA:lipid w/w) with pDNA; pDNA (1 μg) was diluted with sterile pyrogen-free deionized water and added to an aliquot of cationic liposome (2, 4, 8 or 12 μg) in a vial. Lipofectamine 2000 was used as per manufacturers instructions (Invitrogen) and lipoplex nanoparticles were prepared at a pDNA:lipid ratio of 1:2.5 (w/w). After vortex mixing (30 s), the resulting samples of lipoplex nanoparticles were kept at room temperature for 30 min before being used in transfection experiments. Lipoplex nanoparticle sizes were determined in parallel by PCS. In each experiment the nanoparticle suspensions (20 μL) were diluted with PBS to a final volume of 200 μL. The mean average diameter of the vesicles was determined at 25 °C as the result of at least three reliable readings.

2.4. Formulation of siRNA-DODAG nanoparticles

Anti-HBV and control siRNA [42] was dispersed in deionized water (1 mg/ml) at ambient temperature, and then combined with an appropriate aliquot of DODAG **8** (2 mg/ml) in deionized water under conditions of rapid vortex mixing; followed by bath sonication (15 min) in the presence of the osmolyte trehalose (5% w/v final concentration). This procedure typically resulted in the formation of siRNA-DODAG **8** nanoparticles (70 ± 20 nm) with a final siRNA:lipid ratio was 1:3 (w/w).

2.5. Transfection experiments in vitro

Cationic liposome mediated transfection studies were performed using three cancer cell lines: HeLa, OVCAR-3 and IGROV-1. These cells were grown in D-MEM media (Gibco-BRL, UK) and supplemented with 10% fetal calf serum (FCS) (Gibco-BRL, UK) and 100 U/mL of penicillin/streptomycin. All the cells were maintained in a humidified incubator with 5% CO_2 at 37 °C. Cells were seeded 24 h before transfection onto a 24-well plate at a density of 60,000 cells per well and incubated overnight in a humidified 5% CO_2 atmosphere at 37 °C. The cells were grown until 80% confluence was reached, then washed twice with PBS solution before incubation with lipoplex nanoparticles. Lipoplex nanoparticles in OptiMem or OptiMem with FCS 10% (w/v) (about 500 μL) were added to each well (with 1 μg of pDNA per well). After 4 h transfection time at 37 °C, the media was removed, cells were washed twice with PBS solution and fresh media was added. Following a further 48 h of incubation at 37 °C, the cells were assayed for luciferase expression using a chemiluminescent assay (Promega). After transfection the medium was aspirated and the wells were washed briefly with PBS solution. Post removal of PBS the cells were lysed by adding 80 μL of lysis buffer (Promega) to each well. The cell lysate was collected and used for luciferase and protein assays. For the luciferase assay, 20 μL of cell lysate was transferred to a test tube and assessed directly by means of a Monolight 2010 luminometer (Analytical Luminescence Laboratory, San Diego, CA) using a luciferase assay kit (Promega). The luminescence was recorded for 5 s after addition of luciferin (100 μL). Cellular protein content per well was quantified using a bicinchoninic acid (BCA) assay (Pierce; Rockford, IL). The BCA assay was prepared as specified in its manufacturer's instructions. An amount of 20 μL of cell lysate was treated with 200 μL of BCA reagent. The solution was incubated for 30 min at 37 °C, and absorbance at A_{570} was measured by means of a Beckman DU-600 UV–vis spectrometer (Palo Alto, CA). Thereafter, the protein content was estimated by comparison to BSA standards, and the luciferase activity was normalized by protein content and data was expressed as relative luciferase units per microgram of protein (RLU/μg protein). Results are reported as means ± SEM.

2.6. Cellular toxicity in vitro

The cytotoxicity of different lipoplex nanoparticles was evaluated using three different cancer cell lines, HeLa, OVCAR-3 and IGROV-1. Cells were grown in the same conditions as described before, and then seeded for 24 h prior to experimentation on a 96-well plate at a density of 15,000 cells per well and incubated overnight in a humidified 5% CO_2 atmosphere at 37 °C. Normal *in vitro* transfections were performed as described above using lipoplex nanoparticles prepared at 1:2, 1:4, 1:8 and 1:12 (pDNA:lipid w/w) with pDNA (pEGFP-Luc, 0.5 μg). All nanoparticles were prepared in OptiMEM. At 24 h after post-transfection an aliquot of supernatant (100 μL) from each well was collected and transferred to a fresh 96 well assay plate. Cells in the original assay plate were then washed two times with PBS after which 5× reporter lysis buffer (Promega) was added (100 μL per well) and the plates were incubated for 30 min at 37 °C. Aliquots (50 μL) of LDH kit solution were added to the wells of the supernatant and cell lysis assay plates. After 30 min of incubation at room temperature an aliquot (50 μL) of stop solution was added to each well. Light absorption at A_{450} was measured by means of a Beckman DU-600 UV–vis spectrometer (Palo Alto, CA). The complete LDH assay was carried out using the CytoTox 96 non-radioactive cytotoxicity assay (Promega, USA).

2.7. Fluorescence microscopy of in vitro transfection

Adherent HeLa cells were seeded then grown for 24 h in a 6-well (2.5×10^5 cells per well, 3 mL of complete medium) plate fitted with plastic microscopy slides, in a wet (37 °C) 10% CO_2/90% air atmosphere. The cells were grown until 80% confluent. Cells were then treated with either naked pDNA, DODAG **8**/DOPE **1** cationic liposome or DODAG **8**/DOPE **1** lipoplex nanoparticles (pDNA:lipid 1:4, w/w) in OptiMEM, and then incubated in a wet (37 °C) 10% CO_2/90% air atmosphere for 4 h. Media was then removed, and the cells were washed with PBS (2×), then treated with paraformaldehyde (PFA, 1× (20 min at 37 °C), PBS (2×), glycine (1 × 20 mM, 20 min at 37 °C), PBS (2×). Thereafter slides were then removed from their wells and fixing was performed using Vectashield (molecular probes, UK). Microscopy images were obtained on an Olympus 251 scope.

2.8. DODAG mediated delivery of anti-HBV siRNAs in vivo

HBV transgenic mice were also used to assess anti viral efficacy of formulations as described previously [42]. The Animal Care Committee at Stanford University, CA USA approved of all these procedures for all these experiments. SiRNA-DODAG **8** nanoparticle formulations were prepared as described above and the siRNA dose for each injection was 1 mg/kg animal body weight at the indicated days. Groups initially comprised 6 animals. In mice receiving lamivudine, the drug was administered IP daily at a dose of 200 mg/kg mouse body weight. The main markers of viral replication (VPEs in serum, HBsAg mRNA in liver) were assayed as described previously [42]. A complete

experimental toxicity was also carried out in exactly the same manner as described previously including analysis of blood [42]. The blood samples were submitted for haematological analysis, urea and electrolyte concentration determination, ALT and LDH activity determination. Assays were performed in the accredited Haematology and Chemical Pathology Department laboratories of the South African National Health Laboratory Services (NHLS) in Johannesburg.

2.9. Statistical analysis

Data are expressed as the mean ± standard error of the mean. Statistical difference was considered significant * when $P<0.05$ and was determined according to the Dunnett's multiple comparison test and calculated with the GraphPad Prism software package (GraphPad Software Inc., CA, USA).

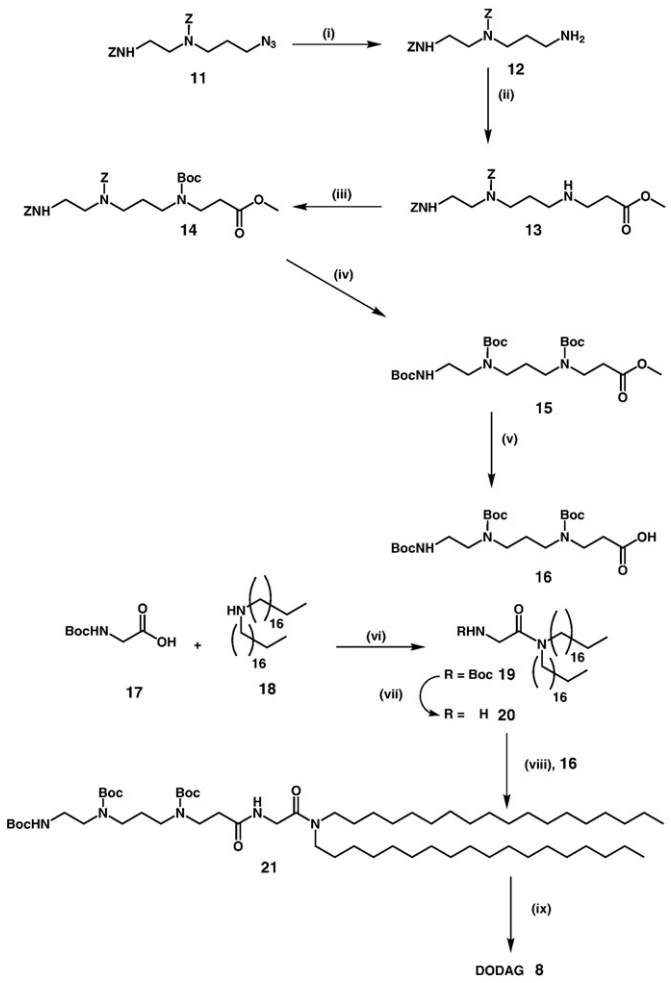
3. Results

3.1. Synthesis

DODAG **8** (Fig. 1) was designed to be a structural chimera involving the CDAN **5** polar head group and the dialkylglycine amide moiety found in micelle forming cationic lipid dioctadecylamido glycylspermine (DOGS) **10** (Fig. 1) [10,14]. The synthesis of DODAG **8** was accomplished in two main stages as shown (Scheme 1). Starting azide **11** was synthesized as reported previously [39] and subsequently smoothly converted into polyamine **12** using a trimethylphosphine adaptation of the Staudinger reaction (Scheme 1). Afterwards, a Michael addition of polyamine **12** to methylacrylate was used to give methyl ester **13** in moderate yield. *N*-Boc protection of the methyl ester then resulted in a fully protected methyl aminodecanoate **14**. This methyl aminodecanoate **14** was then subject to protecting group exchange resulting in a uniformly protected ester **15**, which was then subjected to methyl ester hydrolysis to give the protected aminodecanoic acid **16**. In the second stage of DODAG **8** synthesis, *N*-Boc-glycine **17** was converted, using dioctadecylamine **18**, into tertiary *N*-Boc-glycine amide **19** and then α-*N*-deprotection was carried out to give the key tertiary glycine amide intermediate **20**, in excellent yield. Conjugation of this final intermediate with uniformly protected aminodecanoic acid **16** gave fully protected DODAG **21**. Final deprotection resulted in >98% pure DODAG **8** in excellent yield. This was lyophilized in several cycles from aqueous acetonitrile giving the desired compound as a mixed acid/free base. Thereafter, we synthesized two cholesteryl guanidinum lipids N^1-cholesteryloxycarbonyl ethylene-1-amino-2-guanidinium chloride (CEAG) **6** and N^1-cholesteryloxycarbonyl-3-aza-pent-1-amino-5-guanidinium chloride (CAPG) **7** in the following way. Cholesteryl chloroformate **22** was combined with large excesses of ethylenediamine or diethylentriamine yielding cholesteryl amine intermediates **23** and **24** respectively (Scheme 2). Next, the resulting intermediate compounds **23** and **24** were each treated using the procedure of Matsueda et al. [52] that makes use of ^{1}H-pyrazole-1-carboxamidine monohydrochloride in ethanol as a guanidinylation reagent (Scheme 2) to produce compounds CEAG **6** and CAPG **7** in 70% and 63% yields. Finally desired compound *N*′,*N*′-dioctadecylamido-*N*-methylguanidinium chloride (DOAG) **9** was also synthesized from key tertiary glycine amide intermediate 20 using the same conditions with 58% yield (Scheme 2).

3.2. Cationic liposome/micelle formulations

Liposome formulations were prepared using the thin-film technique and sonicated [53]. The formulations were made in the ratio of 50 mol% cationic and 49.5 mol% neutral helper lipid each time (0.5 mol% of DOPE-Rhodamine was also included for fluorescence microscopy) at a total concentration of 3 mg mL^{-1} in water. The size

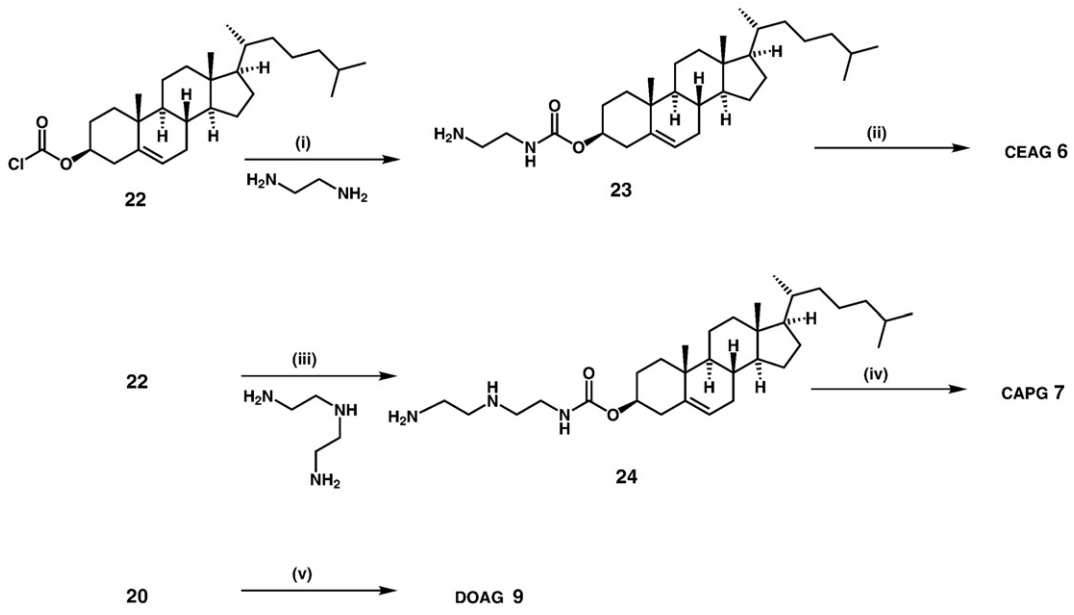


Scheme 1. Reagents and conditions: i) PMe_3 plus H_2O in TMF, r.t., 2.5 h., 82%; ii) Methylacrylate, MeOH, r.t., 12 h., 54%; iii) Boc_2O, NEt_3, CH_2Cl_2, r.t., 12 h, 70%; iv) Pd/C-10%, Boc_2O, MeOH, H_2, r.t., 12 h, 92%; v) LiOH, THF, 0 °C, 12 h., 97%; vi) HBTU, DMAP, $CHCl_3$, r.t., 12 h, 70%; vii) TFA, CH_2Cl_2, N_2, r.t., 2 h, 92%; viii) HBTU, DMAP, $CHCl_3$, r.t., 24 h, 62%; ix) TFA, CH_2Cl_2, r.t., 3 h, 97%.

of the liposomes and the lipoplexes was measured by PCS (Table 1). Suitable lipoplexes were not formed with DOAG **9** when formulated with either DOPE **1** or the novel co-lipid MM27 **3**. PCS size measurements for these particles were around 1000 nm with both co-lipids and as such transfection results were equally poor. The other liposomes were formulated with sizes between 200 and 500 nm, and for their corresponding lipoplexes their size was measured to be between 155 and 423 nm. DODAG (50 nm particle size) were prepared in water at pH 7 by dispersal of DODAG **8** alone in water.

3.3. Plasmid DNA transfection in vitro

Transfections of three cancer cell lines OVCAR-3, IGROV-1 and HeLa were performed with a range of cationic liposomes [either (1:2), (1:4), (1:8), (1:12) pDNA:lipid w/w (Lipofectamine 2000, pDNA:lipid 1:2.5, w/w)] in the absence and presence (10% v/v) of serum. OVCAR-3 transfection data (Fig. 2(A)) are interesting. DODAG **8**/DOPE **1** or DODAG **8**/MM27 **3** cationic liposomes were the most effective agents of transfection at a pDNA:lipid 1:4 w/w ratio, over and above commercially available Lipofectamine 2000, with and without the presence of serum. The DODAG **8**/MM27 **3** cationic liposome combination was also prominent at a pDNA:lipid 1:8 w/w ratio, with and without the presence of serum. In the case of IGROV-1 cell



Scheme 2. i) Excess of amine (20.2 equivalents), H_2O, 8 h, 65%, ii) 1H-pyrazole-1-carboxamidine.mono chlorohydrate, DIPEA, EtOH, 78 °C, 16 h, 70%, iii) excess of amine (10 equivalents), H_2O, 8 h, 54%, iv) 1H-pyrazole 1-carboxamidine.monochlorohydrate, DIPEA, EtOH, 78 °C, 16 h, 67%, v) 1H-pyrazole-1-carboxamidine.monochlorohydrate, DIPEA, EtOH, 78 °C, 48 h, 58%.

line transfection (Fig. 2(B)), DODAG **8**/DOPE **1** cationic liposomes were comparable agents of transfection with Lipofectamine 2000 in the presence of serum, at pDNA:lipid ratios of 1:4 and 1:8 w/w. In the absence of serum, CAPG **7**/MM27 **3** and CDAN **5**/DOPE **1** cationic liposomes combined at pDNA:lipid ratios of 1:12 w/w, and DODAG **8**/DOPE **1** cationic liposomes combined at a pDNA:lipid ratio of 1:4 w/w, appeared modestly more effective than Lipofectamine 2000. Finally in the case of HeLa transfection (Fig. 2(C)), DODAG **8**/DOPE **1** cationic liposome mediated pDNA-transfection was the most effective at low pDNA:lipid 1:4 or 1:2 w/w ratios in the presence of serum, closely followed by DODAG **8**/MM27 **3** cationic liposome mediated transfection. In the absence of serum, DODAG **8**/DOPE **1** cationic liposomes formulated at low pDNA:lipid 1:4 or 1:2 w/w ratios were also found more effective than Lipofectamine 2000 for transfection, alongside CAPG **7**/MM27 **3** and CEAG **6**/MM27 **3** cationic liposomes formulated at high pDNA:lipid ratios of 1:12 w/w. These data in total suggest that DODAG **8** /DOPE **1** and DODAG **8** /MM27 **3** cationic liposomes formulated at pDNA:lipid 1:4 w/w ratios may have utility as a broad-band transfection agent, comparable with Lipofectamine 2000, for different cell lines *in vitro* (suitable for use both with and without serum in cell growth medium). There are also indications that CAPG **7**/MM27 **3** cationic liposomes formulated at a pDNA:lipid ratios of 1:12 w/w, may be an alternative niche transfection system.

Table 1
Liposome and lipoplex nanoparticle sizes with included polydispersity indices.

Liposomes	DOPE 1 Size (nm)	Polydispersity index	MM27 3 Size (nm)	Polydispersity index
CDAN 5	183.3 ± 78.1	0.66	204.2 ± 69.5	0.216
CEAG 6	160.1 ± 64.9	0.481	378.8 ± 160.6	0.678
CAPG 7	190.4 ± 72.6	0.347	218.4 ± 63.5	0.128
DODAG 8	233.6 ± 60.2	0.23	516.8 ± 178.3	0.227
DOAG 9	623.1 ± 274.2	0.859	430.1 ± 177.4	0.531
Lipofectamine 2000	Liposome size: 114.8 ± 32.1		Polydispersity index: 0.29	
Lipoplex nanoparticles				
CDAN 5	290.7 ± 105	0.290	155.4 ± 64.3	0.542
CEAG 6	233.4 ± 94.3	0.460	423.7 ± 150.8	0.257
CAPG 7	229.9 ± 89.3	0.387	311.2 ± 122.2	0.403
DODAG 8	301.5 ± 111.2	0.298	307.2 ± 107.5	0.240
DOAG 9	1365.6 ± 396.5	0.127	818.9 ± 351.2	0.696
Lipofectamine 2000	Lipoplex size: 442.3 ± 81.2		Polydispersity index: 0.41	

3.4. In vitro cellular toxicity

Our own previously published data [40] and reports of Uchida et al. [54] have described extensively the cytotoxicity of Lipofectamine 2000 that results in upwards of 20% lactate dehydrogenase (LDH) release (equivalent to cell death) in the LDH cytotoxicity assay applied to immortalized adherent cell lines. Therefore, we elected to benchmark the cytotoxicity of the different cationic liposomes and their corresponding lipoplex nanoparticles reported here against the published Lipofectamine 2000 mark using the same LDH cytotoxicity assay. Results are illustrated (Fig. 3 (A–C)). Overall there is a general indication in IGROV-1 and HeLa cells that cytotoxicity increases with pDNA/lipid ratio consistent with an increase in cationic charge mediated cytotoxicity. Also co-lipid MM27 **3** appears to confer more cytotoxicity than DOPE **1** in IGROV-1 and OVCAR-3 cells. Otherwise, DODAG **8**/DOPE **1** — pDNA 1:4 w/w lipoplex nanoparticles were found consistently to exhibit the lowest or close to lowest cytotoxicity (approximately 5% LDH release) in all three cell lines. These data are important and gratifying considering the general effectiveness of DODAG **8**/DOPE **1** cationic liposome mediated transfection reported above with a pDNA:lipid ratio1:4 w/w (see Fig. 2). Hence DODAG **8**/DOPE **1** cationic liposomes appear to be overall the most versatile cationic liposomes for efficient transfection with minimal toxicity. Accordingly we would suggest this cationic liposome system represents a potentially valuable alternative to Lipofectamine 2000 as a broad-band transfection agent for adherent cells *in vitro*.

3.5. Fluorescence microscopy

Transfection of HeLa cells by DODAG **8**/DOPE **1** cationic liposomes which were the most efficient transfecting lipid pair was observed by light microscopy in order to verify the process of transfection. Cells

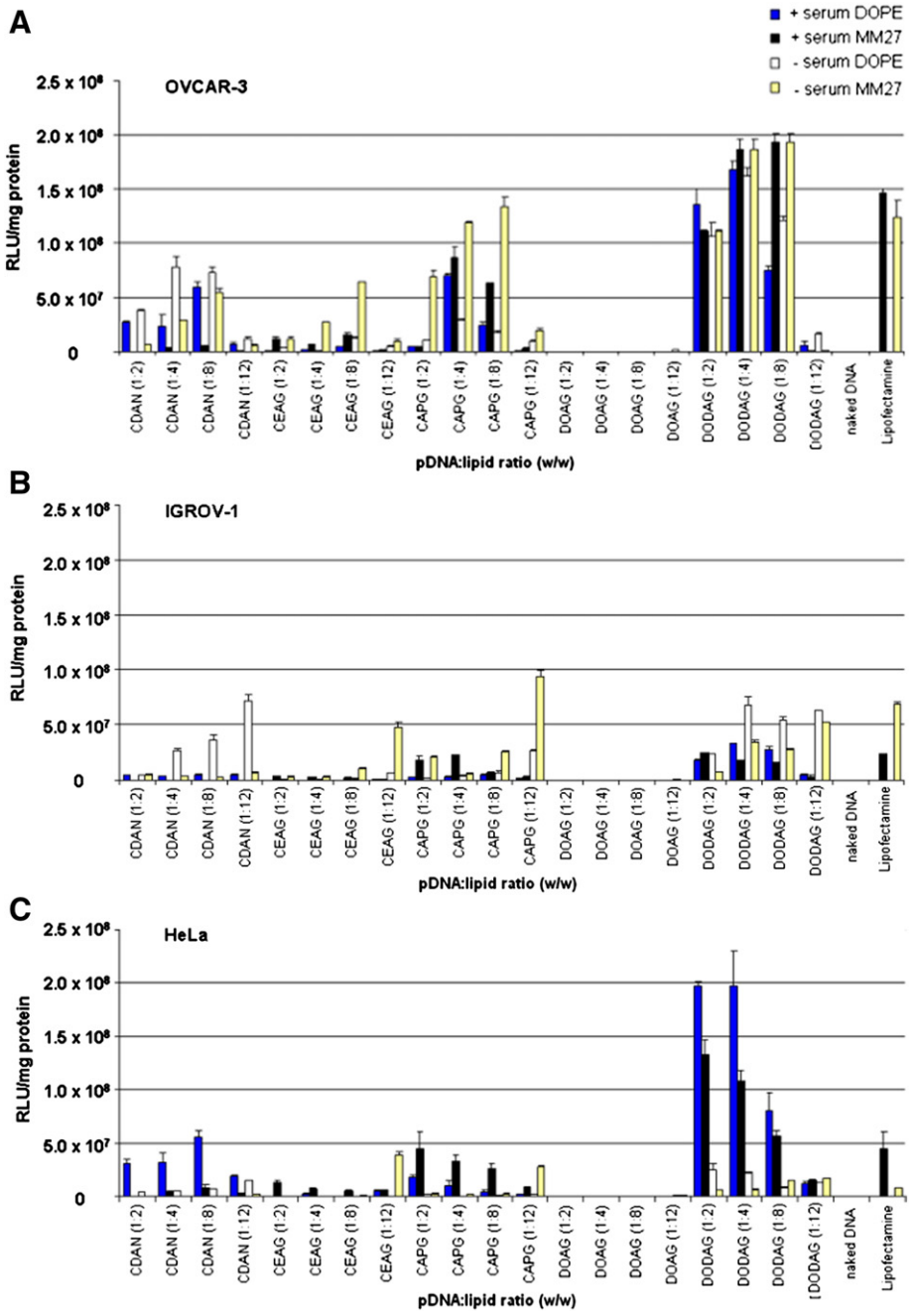


Fig. 2. Transfection data for three cell lines and 20 different lipoplex nanoparticle systems with Lipofectamine2000 transfection as positive control (pDNA:lipid ratio: 1:2.5, w/w). The indicated cationic lipids were mixed with the indicated co-lipids in 1:1 m/m ratio to generate cationic liposomes. Transfections were then performed using pEGFP-luc pDNA expressing both enhanced GFP (EGFP) and luciferase (luc). For each transfection well, different cationic liposomes were combined with pEGFP-luc (1 μg/well) at the indicated pDNA: lipid w/w ratios in order to form lipoplex nanoparticles that were administered to cells for 4 h transfections. The black bars for Lipofectamine represent transfections in the presence of serum and the yellow bars represent lack of serum respectively (A–C).

were incubated with DODAG **8**/DOPE **1** lipoplex nanoparticles for 4 h, washed and fixed for microscopy post incubation. From the images, cell entry and endosomolysis is clearly apparent (Fig. 4), consistent with a high level of efficient transfection. In all other cases of cationic liposome mediated transfection studied here by microscopy, intracellular access was found to be far less effective (as judged by Rhodamine fluorescence microscopy) than that mediated by DODAG **8**/DOPE **1** cationic liposomes. Furthermore, intracellular/nuclear localized green fluorescent protein (GFP) expression was seen at 4 h only post DODAG **8**/DOPE **1** cationic liposome-mediated transfection (Fig. 4) which is itself unusual but indicative of highly efficient transfection.

3.6. Functional delivery of anti-HBV siRNA in vivo

Efficient functional nonviral delivery of pDNA to the liver *in vivo* can only currently be accomplished by physical means using hydrodynamic delivery [55]. However, functional delivery of small interfering RNA (siRNA) to liver appears more tractable although with quite complex multi-component nanoparticles systems as we demonstrated previously [42]. In initial experiments, we were surprised to observe that DODAG **8** alone was able to form nanoparticles with siRNA. The formation of siRNA-DODAG **8** nanoparticles was achieved with relative ease at a lipid:siRNA ratio (3:1, w/w) . This translates into a cationic lipid to nucleotide molar ratio, [cyt]/[nt], of 1.25, and

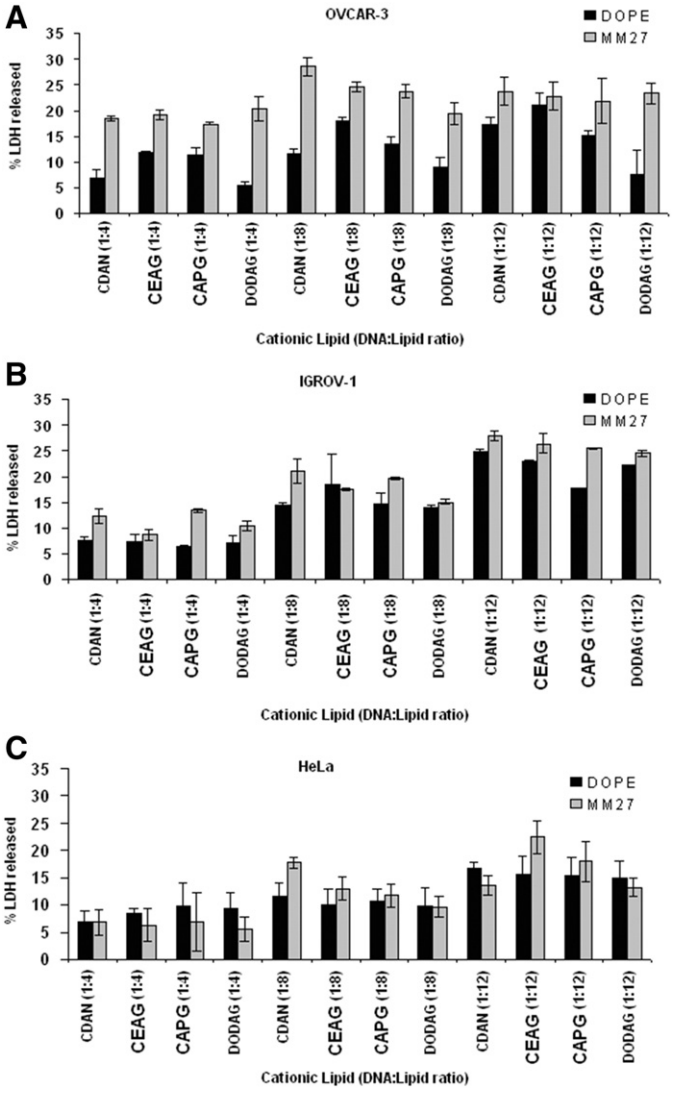


Fig. 3. Percentage LDH cytotoxicity data for lipoplex nanoparticles formulated with cationic lipids DODAG **8**, CDAN **5**, CEAG **6** and CAPG **7** with either DOPE **1** or MM27 **3** as helper co-lipids. The indicated cationic lipids were mixed with the indicated co-lipids in 1:1 m/m ratio to generate cationic liposomes. LDH toxicity experiments were then performed using pEGFP-luc as above. For each toxicity experiment, different cationic liposomes were combined with pEGFP-luc (0.5 μg/well) at the indicated pDNA:lipid w/w ratios in order to form lipoplex nanoparticles that were administered to cells for 30 min toxicity experiments. All toxicity data are normalized to the % LDH release observed with pDNA administration alone (typically near zero).

hence an N/P ratio of approximately 1.8 assuming that each DODAG **8** molecule possesses a cationic charge of approximately 1.5 at neutral pH, in line with the behavior of the original parent molecule CDAN **5** [14,40]. Agarose gel retardation assays showed that at an N/P ratio of 1.8 the movement of siRNA was entirely retarded according to our gel electrophoresis data, consistent with complete interaction with DODAG **8** (Fig. 5A).

Lipoplex siRNA-nanoparticle sizes are dependent on the duration of sonication, but typically a size of 70 ± 20 nm (as determined by photon correlation spectroscopy post preparation) was selected given the target organ preference [42]. Lipoplex siRNA nanoparticles were prepared fresh and then immediately administered in the presence of the trisaccharide osmolyte known as trehalose, intended to shield nanoparticles from immediate serum effects post IV injection thereby giving sufficient time for particles to reach the liver and avoid excessive sequestration by Kupffer cells. Potential toxic side effects of siRNA-DODAG **8** nanoparticles were investigated experimentally *in vivo* (as reported previously) [42] using identical markers of hepatic, renal and haematological damage as previously without the discovery of any obvious signs of toxicity even of LDH and alanine transaminase (ALT) levels (Table 2).

Previously, we reported how anti-HBV siRNA sequences had been screened *in vitro* and two chemically naked sequences were selected and validated for *in vivo* analysis [42,56,57]. Therefore, siRNA-DODAG **8** nanoparticles were prepared as above with the same validated siRNAs, namely siRNA-1407 and siRNA-1794. Lipoplex siRNA-nanoparticles were then administered IV to HBV transgenic mice [58] every 3 days for 4 weeks. The siRNA dose at every IV injection was 1 mg/kg of murine body weight. Compared with controls, nanoparticle-mediated administration of siRNA-1407 or siRNA-1794 resulted in a 2–3 fold fall in viral particle equivalent (VPE) levels in serum, together with a similar decrease in HBV s-antigen (HBsAg) mRNA levels in liver relative to controls after 4 weeks (Fig. 5B, C). Overall, siRNA-DODAG **8** nanoparticle mediated administration of siRNA-1407 or siRNA-1794 appeared to result in comparable inhibitory anti-viral effects to those observed after lamivudine treatment (Fig. 5B, C). Indeed, siRNA-DODAG **8**-nanoparticle administration of siRNA-1407 appeared to promote an even more pronounced anti-viral inhibitory effect than lamivudine. Moreover the antiviral effects were also comparable to the effects produced delivering siRNA-1407 or siRNA-1794 using the much more complex multi-component. pH-triggerable, siRNA-nanoparticle system that we had designed previously for functional delivery of siRNA to liver [42]. As in our previous study, interferon response genes for oligoadenylate synthase-1 (OAS-1) and interferon-β (IFN-β) were found not stimulated by siRNA-DODAG **8** nanoparticle administration suggesting that our observed anti-HBV effects here (Fig. 5B, C) are the consequence of an RNA interference (RNAi) mechanism, as observed previously [42].

4. Discussion

Our premise in this paper was to evolve cationic lipid design through a simple functional group swap of hydrophilic polyamine side chains for guanidinium side chains and/or an exchange of hydrophobic cholesteryl for *N′, N′*-dialkyl glycylamide moieties. In addition, the list of potential co-lipid partners was extended to include the latest

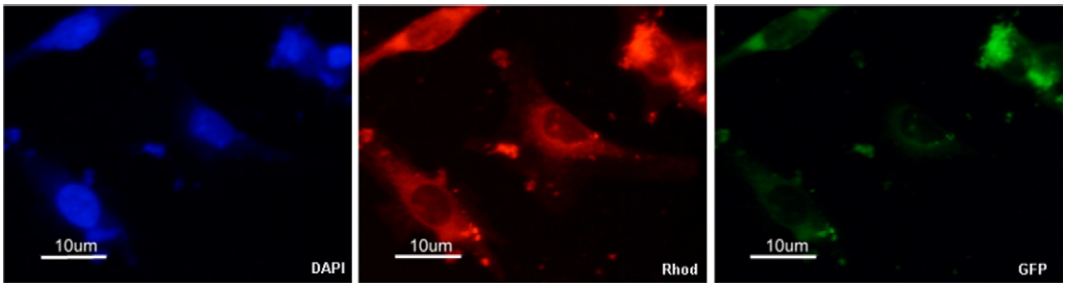


Fig. 4. Fluorescence microscopy of HeLa cells post transfection with DODAG **8**/DOPE **1** cationic liposome–pDNA complexes (lipoplexes, ×400 magnification). Cells are stained with DAPI (left) to illustrate nuclei, visualized for GFP expression (right) and visualized for rhodamine fluorescence (middle).

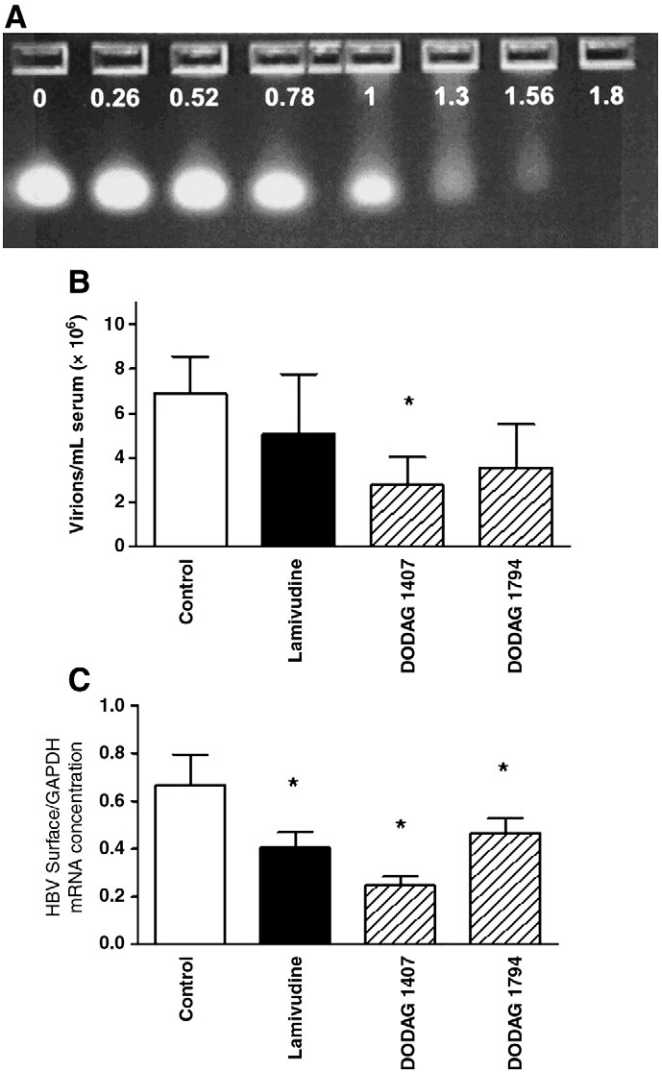


Fig. 5. Formulation and experimental assessment of siRNA-DODAG **8** nanoparticle formulations. (A) Gel retardation experiment showing variation of siRNA (1 μg) retardation viewed by agarose gel electrophoresis as a function of DODAG **8**:siRNA ratio (w/w); Effect of siRNA-DODAG **8** nanoparticle formulations on markers of HBV replication: (B) Circulating VPEs measured at 28 days in HBV transgenic mice treated every 3 days with a siRNA-DODAG **8** nanoparticle formulation delivering non-functional control siRNA (**Control**) [equivalent result obtained with saline injection], or siRNA-DODAG **8** nanoparticle formulations delivering functional siRNA-1407 or siRNA-1794 (**DODAG 1407** or **DODAG 1794** respectively), in comparison with lamivudine. (C) HBsAg mRNA measured at 28 days in HBV transgenic mice treated exactly as in (B).

neutral co-lipid reported, namely the lipophosphoramidate derivative of histamine (MM27) **3** (Fig. 1). Our initial interest was to test out whether the new combinations of structural elements could lead to enhanced *in vitro* pDNA transfections of different cell lines, under different conditions, consistently on a par with or in excess of a lipofectamine 2000 positive control transfection. This was achieved and on balance DODAG **8**/DOPE **1** cationic liposomes formulated at a low pDNA:lipid 1:4 w/w ratio compared well with lipofectamine 2000 both in terms of transfection efficiency (with and without the presence of serum) and cellular cytotoxicity (Figs. 2 and 3). The CAPG **7**/MM27 **3** cationic liposome combination may have some utility at a higher pDNA:lipid 1:12 w/w ratio in the absence of serum and at the lower pDNA:lipid ratios in the presence of serum (Fig. 2).

The utility and mechanism of CDAN **5**/DOPE **1** cationic liposome mediated delivery has been noted and described in detail previously [32,39]. In comparison, the advent of CAPG **7**/MM27 **3** cationic liposomes indicates the explicit sense of pairing a cationic lipid that has a hydrophilic side chain possessing a high pK_a (basic), with a neutral co-lipid with a hydrophilic side chain, that is mildly acidic in character, in order to promote transfection efficiency. In this pairing we would suggest that the cationic lipid provides for nucleic acid binding and cell binding/entry; the co-lipid for endosomolysis and intracellular trafficking (as described in the Introduction above). By contrast, the clear efficacy of the DODAG **8**/DOPE **1** cationic liposome mediated delivery appears to suggest the involvement of other additional physical properties that could contribute towards the observed efficacy. In terms of the cationic lipid and the co-lipid, the hydrophilic head group of DODAG **8** is borrowed from CDAN **5** that has been described to exhibit both basic and mildly acidic characteristics [32,39]. Hence we would suggest by extrapolation that such a head group should have the capacity for involvement in all aspects of nucleic acid delivery including nucleic acid binding itself, cell binding/entry, endosomolysis (possibly involving osmotic shock) and intracellular trafficking in association with DOPE **1**. However, these effects could be further enhanced by cationic liposome and lipoplex nanoparticle metastability. Indeed cationic liposome and corresponding lipoplex metastability with respect to aggregation and colloidal instability has already been reported to be helpful to promote CDAN **5**/DOPE **1** cationic liposome-mediated transfection *in vitro* [39]. In the case of DODAG **8**/DOPE **1** cationic liposomes, we would like to suggest that cationic liposome and lipoplex metastability may also be important for efficient transfection and could be related in this case to considerations about lipid molecular shape.

DOPE **1** is regarded classically as having an inverse-conical molecular shape that is wide at the termini of the dioleoyl fatty acid side chains and narrow at the polar head group. This molecular shape is perceived to be a critical reason that DOPE **1** shows preference for inverse hexagonal, H_{II}, macromolecular lipid phase structures and is more abundantly present into the inner cytoplasmic leaflet of plasma membranes. On the other hand, given the close correlation between the molecular shape of DOGS **10** and DODAG **8**, then DODAG **8** like DOGS **10** should possess a conical molecular shape that is narrow at the termini of the dioleyl alkyl side chains and wide at the polar head group. In which case DODAG **8** like DOGS **10** might also be expected to show a preference for normal hexagonal, H_I, macromolecular lipid phase structures such as normal lipid micelles. Accordingly, in combination with each other in cationic liposomes or in corresponding lipoplex nanoparticles, DODAG **8** and DOPE **1** would thus appear to be of opposite steric character and lamellar phase structures thus formed by both lipids in combination would exhibit inevitable instability with respect to phase change, a characteristic that could be regarded as favorable for efficient transfection of cells *in vitro*. We have some circumstantial evidence in support of this proposed phase metastability in that fluorescence microscope images of cellular transfection using DODAG **8**/DOPE **1** cationic liposomes

Table 2
Experimental toxicity and inflammation markers. Details concerning the measurement of these parameters are described elsewhere [42]. OAS-1 and IFN-β are early interferon (IFN) response genes. Units of expression are IFN response gene/GAPDH mRNA ratio (absolute). Pro-inflammatory poly-IC treatment results in values of approximately 0.2 and 0.25 for OAS-1 and IFN-β respectively. All abbreviations are explained in the main text as appropriate.

Toxicity/ inflammationmarker	Saline	Naked siRNA 1794	Naked siRNA 1407	DODAG 1794	DODAG 1407
ALT (IU/l)	300 ± 200	600 ± 300	900 ± 600	200 ± 50	500 ± 200
LDH (IU/ml)	950 ± 200	1000 ± 100	1250 ± 450	750 ± 50	1300 ± 200
Urea (mmol/l)	9.5 ± 0.5	9.5 ± 0.5	10 ± 1.0	9.0 ± 0.5	9.0 ± 0.5
Creatinine (μmol/l)	8.0 ± 0.5	9.0 ± 0.5	8.5 ± 0.5	7.0 ± 0.5	8.0 ± 0.5
Na+ (mmol/l)	150 ± 5	150 ± 5	150 ± 5	150 ± 5	150 ± 5
Cl− (mmol/l)	115 ± 5	110 ± 5	115 ± 5	115 ± 5	115 ± 5
K+ (mmol/l)	120 ± 5	130 ± 5	120 ± 5	100 ± 5	120 ± 5
OAS-1	<0.01	<0.02	<0.02	<0.02	<0.02
IFN-β	<0.01	<0.02	<0.02	<0.02	<0.02

show that lipoplex nanoparticles have completely disintegrated in the cell post entry and are spread throughout the cellular cytoplasm without a pronounced appearance of endosome entrapment (Fig. 4). Moreover, this ease of entry is reflected in very early GFP expression at 4 h post transfection (instead of a more typical time period of 8–12 h) (Fig. 4), an observation not made readily with any other cationic liposome system studied here.

The efficacy of DODAG **8**/DOPE **1** cationic liposome mediated plasmid DNA delivery *in vitro* appears usefully high and accompanied by only modest cytotoxicity, but the cationic liposome system was expected to have only limited utility *in vivo*, especially for systemic applications, in view of the general metastability of lipoplex nanoparticles [28,29]. However, the implication that DODAG **8** has a conical lipid structure suggested to us that DODAG **8** alone might be able to form lipoplex nanoparticles with siRNA that in turn might be stable enough for limited *in vivo* applications. This proposition was tested here and appears to be the case. Simple siRNA-DODAG **8** nanoparticles were formulated and appeared to be stable when delivered IV in a high concentration of trehalose, to mediate functional delivery of validated anti-HBV siRNAs (chemically unmodified), to livers of HBV-transgenic mice [58] in sufficient quantity to modulate both viral particle equivalents and liver HBV mRNA levels downward by 2–3 fold (Fig. 5). Importantly this siRNA-mediated silencing of HBV replication with nanoparticle delivered anti-HBV sequences (siRNA-1407 or siRNA-1794) was at least as effective as the inhibition of viral proliferation observed with the licensed HBV drug lamivudine. Our observed suppression of HBV parameters (Fig. 5) are significant. Also our data compare well with results reported following the use of higher doses of chemically modified siRNA or expressed RNAi effectors [59,60].

Previously we developed the siFECTamine^{TM} cationic liposome system [40] to deliver siRNA to cells (siFection) and showed that this approach may be used for RNAi-based gene silencing *in vitro*. This cationic liposome system was formulated from CDAN **5** and DOPE **1** in a 45:55 molar ratio (Fig. 1). Highly efficient siRNA-mediated gene knockdown was routinely achievable without causing toxicity in cultured cells [40]. A number of siRNA loaded hepatotrophic formulations have since been generated for *in vivo* use that comprise molecular conjugates involving cholesterol or α-tocopherol conjugation, complexation with apolipoprotein A1 or association with vitamin A-coupled liposomes [61–64]. 'Stabilized nucleic acid-lipid particles' (SNALPs) have also been used to deliver functional siRNA *in vivo* [65,66] and we have recently described the use of multi-component, pH triggered, PEGylated siRNA nanoparticles (also known as siRNA–**ABC** nanoparticles) to treat HBV infection in a severe, chronic animal model of human HBV infection (*i.e.,* the HBV transgenic mouse model) [42]. In this study here, we have extended the range of synthetic, non-viral hepatotrophic vectors to include very simple siRNA-DODAG **8** nanoparticles. To the best of our knowledge, siRNA-DODAG **8** nanoparticles provide a first demonstration of a single cationic lipid-based vector system that can be used for siRNA delivery *in vivo*. The methodology that we describe here would certainly enable large-scale preparation, an essential prerequisite for pharmaceutical applications. Further refinements of nucleic acid-DODAG **8** nanoparticles will be required and nanoparticles will also need to be comprehensively characterized under a variety of different conditions to understand and appreciate fully the mechanisms of delivery. We are also investigating dose optimization, detailed evaluation of non-specific effects, together with an assessment of stability, pharmacokinetic analysis and metabolite profiling. Furthermore, we expect to carry out studies to improve silencing efficiency of the formulations by introducing stabilizing modifications to the siRNAs. Although challenges remain, we believe that our data together with those reported by ourselves and others [59,60,65–68], are encouraging and support the proposition that siRNA-DODAG **8** lipoplex nanoparticles may be of use for the treatment of HBV infection and other hepatic diseases where silencing of pathology-causing symptoms are required for disease treatment.

5. Conclusion

We have synthesized a number of novel cationic lipids of which one, DODAG **8** in combination with neutral co-lipid DOPE **1**, forms DODAG **8**/DOPE **1** cationic liposomes that appear to have the capacity to act as a broad band agent for transfection *in vitro* under various conditions. We suggest that cationic liposome and corresponding lipoplex nanoparticle metastability due to lipid molecular shape differences may be a key factor to ensure highly efficient transfection *in vitro*. In contrast, we observe that DODAG **8** mixed with siRNA forms siRNA-DODAG **8** lipoplex nanoparticles that mediate multiple, efficient delivery of anti-HBV siRNAs *in vivo* to the livers of HBV transgenic mice leading to a partial treatment of HBV infection over a period of 28 days.

Acknowledgements

EPSRC is gratefully acknowledged for a grant to Mathieu Mével. General financial support is greatly appreciated from ImuThes Ltd and from Mitsubishi Chemical Corporation prior to that. Financial support comes from the South African Innovation Fund, National Research Foundation, Sixth Research Framework Programme of the European Union, Project RIGHT (LSHB-CT-2004-005276), CANSA and the South African Poliomyelitis Research Foundation.

References

[1] S.E. Raper, N. Chirmule, F.S. Lee, N. Wivel, A. Bagg, et al., Fatal systemic inflammatory response syndrome in a ornithine transcarbamylase deficient patient following adenoviral gene transfer, Mol. Genet. Metab. 80 (2003) 48–158.
[2] L. Huang, S. Li, Liposomal gene delivery: a complex package, Nat. Biotechnol. 15 (1997) 620–621.
[3] M. Hashida, M. Nishikawa, F. Yamashita, Y. Takakura, Cell-specific delivery of genes with glycosylated carriers, Adv. Drug Deliv. Rev. 52 (1997) 187–196.
[4] G.J. Nabel, E.G.Z.Y. Yang, A.B. Fox, Direct gene transfer with DNA-liposome complexes in melanoma: expression, biologic activity, and lack of toxicity in humans, Proc. Natl Acad. Sci. USA 90 (1993) 11307–11311.
[5] P.L.G. Felgner, T.R. Gadek, M. Holm, R. Roman, H.W. Chan, M. Wenz, J.P. Northrop, M.G. Ringold, M. Danielsen, Lipofection: a highly efficient lipid-mediated DNA transfection procedure, Proc. Natl Acad. Sci. USA 84 (1987) 7413–7417.
[6] G.Y. Wu, C.H. Wu, Receptor-mediated in vitro gene transformation by a soluble DNA carrier system, J. Biol. Chem. 262 (1987) 4429–4432.
[7] X.H. Gao, L. Huang, A novel cationic liposome reagent for efficient transfection of mammalian cells, Biochem. Biophys. Res. Comm. 179 (1991) 280–284.
[8] E.R. Lee, J. Marshall, C.S. Siegel, C. Jiang, N.S. Yew, M.R. Nichols, J.B. Nietupsky, R.J. Ziegler, M.B. Lane, K.X. Wang, N.C. Wan, R.K. Scheule, D.J. Harris, A.E. Smith, S.H. Cheng, S.H., Detailed analysis of structures and formulations of cationic lipids for efficient gene transfer to the lung, Hum. Gen. Ther. 7 (1996) 1701–1717.
[9] J.P. Vigneron, N. Oudrhiri, M. Fauquet, L. Vergely, J.C. Bradley, et al., Guanidinium-cholesterol cationic lipids: efficient vectors for the transfection of eukaryotic cells, Proc. Natl Acad. Sci. USA 93 (1996) 9682–9686.
[10] A.D. Miller, Cationic liposomes for gene therapy, Angew. Chem. Int. Ed. 37 (1998) 1768–1785.
[11] A.D. Miller, The problem with cationic liposome/micelle-based non-viral vector systems for gene therapy, Curr. Med. Chem. 10 (2003) 1195–1211.
[12] M. Thanou, S. Waddington, A.D. Miller, Gene therapy, in: J.B Taylor, D.J. Triggle (Eds.), Comprehensive Medicinal Chemistry II, Elsevier, Oxford, 2007, pp. 297–320.
[13] A.D. Miller, Nonviral liposomes, Meth. Mol. Med. 90 (2004) 107–138.
[14] K. Kostarelos, A.D. Miller, Synthetic, self-assembly ABCD nanoparticles; a structural paradigm for viable synthetic non-viral vectors, Chem. Soc. Rev. 34 (2005) 970–994.
[15] A.D. Miller, Towards safe nanoparticle technologies for nucleic acid therapeutics, Tumori 94 (2004) 234–245.
[16] B. Martin, M. Sainlos, A. Aissaoui, N. Oudrhiri, M. Hauchecorne, J.M. Vigneron, J.M. Lehn, P. Lehn, The design of cationic lipids for gene delivery, Curr. Pharm. Des. 11 (2005) 375–394.
[17] J. Zabner, A.J. Fasbender, T. Moninger, K.A. Poellinger, K. A., Cellular and molecular barriers to gene transfer by a cationic lipid, J. Biol. Chem. 270 (1995) 18997–19007.
[18] I. Wrobel, D. Collins, Fusion of cationic liposomes with mammalian cells occurs after endocytosis, Biochim. Biophys. Acta 1235 (1995) 296–304.
[19] X. Gao, L. Huang, Cationic liposome-mediated gene transfer, Gene Ther. 2 (1995) 710–722.

[20] C.R. Safinya, Structures of lipid-DNA complexes: supramolecular assembly and gene delivery, Curr. Opin. Struct. Biol. 11 (2001) 440–448.
[21] R. Koynova, L. Wang, R.C. MacDonald, An intracellular lamellar-nonlamellar phase transition rationalizes the superior performance of some cationic lipid transfection agents, Proc. Natl Acad. Sci. USA 103 (2006) 14373–14378.
[22] A. Noguchi, T. Furuno, C. Kawaura, M. Nakanishi, Membrane fusion plays an important role in gene transfection mediated by cationic liposomes, FEBS Lett. 422 (1998) 169–173.
[23] H. Farhood, N. Serbina, L. Huang, The role of dioleoyl phosphatidylethanolamine in cationic liposome mediated gene transfer, Biochim. Biophys. Acta 1235 (1995) 289–295.
[24] A.L. Bailey, P.R. Cullis, Membrane fusion with cationic liposomes: effects of target membrane lipid composition, Biochemistry 36 (1997) 1628–1634.
[25] S. Li, M.A. Rizzo, S. Bhattacharya, L. Huang, Characterization of cationic lipid-protamine-DNA (LPD) complexes for intravenous gene delivery, Gene Ther. 5 (1998) 930–937.
[26] O. Boussif, J. Gaucheron, C. Boulanger, C. Santaella, H.V.J. Kolbe, et al., Enhanced in vitro and in vivo cationic lipid-mediated gene delivery with a fluorinated glycerophosphoethanolamine helper lipid, J. Gene Med. 3 (2001) 109–114.
[27] J. Gaucheron, C. Boulanger, C. Santaella, N. Sbirrazzuoli, O. Boussif, et al., In vitro cationic lipid-mediated gene delivery with fluorinated glycerophosphoethanolamine helper lipids, Bioconjug. Chem. 12 (2001) 949–963.
[28] S. Fletcher, A. Ahmad, E. Perouzel, M.R. Jorgensen, A.D. Miller, A dialkynoyl analogue of DOPE improves gene transfer of lower-charged, cationic lipoplexes, Org. Biomol. Chem. 4 (2006) 196–199.
[29] S. Fletcher, A. Ahmad, W.S. Price, M.R. Jorgensen, A.D. Miller, Biophysical properties of CDAN/DOPE-Analogue lipoplexes account for enhanced gene delivery, Chem. BioChem. 9 (2008) 455–463.
[30] M. Mével, G. Breuzard, J.J. Yaouanc, J.C. Clement, P. Lehn, et al., Synthesis and transfection activity of new cationic phosphoramidate lipids: high efficiency of an imidazolium derivative, Chem. Biochem. 9 (2008) 1462–1471.
[31] M. Mével, C. Neveu, C. Goncalves, J.J. Yaouanc, C. Pichon, P.A. Jaffrès, P. Midoux, Novel neutral imidazole-lipophosphoramides for transfection assays, Chem. Commun. 21 (2008) 3124–3126.
[32] L. Stewart, M. Manvell, E. Hillery, C.J. Etheridge, R.G. Cooper, et al., Physico-chemical analysis of cationic liposome–DNA complexes (lipoplexes) with respect to in vitro and in vivo gene delivery efficiency, J. Chem. Soc., Perkin Trans. 2 (2001) 624–632.
[33] J.P. Behr, B. Demeneix, J.P. Loeffler, J. Perez-Mutul, Efficient gene transfer into mammalian primary endocrine cells, Proc. Natl Acad. Sci. USA 86 (1989) 6982–6986.
[34] P. Hawley-Nelson, V. Ciccarone, J. Gebeyehu, J. Jessee, P.L. Felgner, Lipofectamine reagent : a new, higher efficiency polycationic liposome transfection reagent, Focus 15 (1993) 73–79.
[35] F. Lamarche, M. Mével, T. Montier, L. Burel-Deschamps, P. Giamarchi, et al., Lipophosphoramidates as lipidic part of lipospermines for gene delivery, Bioconjug. Chem. 18 (2007) 1575–1582.
[36] A. Alshamsan, A. Haddadi, V. Incani, J. Samuel, A. Lavasanifar, et al., Formulation and delivery of siRNA by oleic acid and stearic acid modified polyethylenimine, Mol. Pharmaceutics 6 (2009) 121–133.
[37] Y.T. Ko, A. Kale, A.W.C. Hartner, B. Papahadjopoulos-Sternberg, V.P. Torchilin, Self-assembling micelle-like nanoparticles based on phospholipid-polyethyleneimine conjugates for systemic gene delivery, J. Control. Release 133 (2009) 132–138.
[38] M. Abbasi, H. Uludag, V. Incani, C.Y.M. Hsu, A. Jeffery, Further investigation of lipid-substituted poly(L-lysine) polymers for transfection of human skin fibroblasts, Biomacromolecules 9 (2008) 1618–1630.
[39] M. Keller, M.R. Jorgensen, E. Perouzel, A.D. Miller, Thermodynamic aspects and biological profile of CDAN/DOPE and DC-Cho1/DOPE lipoplexes, Biochemistry 42 (2003) 6067–6077.
[40] S. Spagnou, A.D. Miller, M. Keller, Lipidic carriers of siRNA: differences in the formulation, cellular uptake, and delivery with plasmid DNA, Biochemistry 43 (2004) 13348–13356.
[41] R.G. Cooper, C.J. Etheridge, L. Stewart, J. Marshall, S. Rudginsky, et al., Polyamine analogues of 3β-[N-(N′, N′-dimethylaminoethane)carbamoyl]cholesterol (DC-Chol) as agents for gene delivery, Chem. Eur. J. 4 (1998) 137–151.
[42] S. Carmona, M.R. Jorgensen, S. Kolli, C. Crowther, F.H. Salazar, P.L. Marion, M. Fujino, Y. Natori, M. Thanou, P. Arbuthnot, A.D. Miller, Controlling HBV replication in vivo by intravenous administration of triggered PEGylated siRNA nanoparticles, Mol. Pharmaceutics 6 (2009) 706–717.
[43] T. Tagawa, M. Manvell, N. Brown, M. Keller, E. Perouzel, et al., Characterisation of LMD virus-like nanoparticles self-assembled from cationic liposomes, adenovirus core peptide μ (mu) and plasmid DNA, Gene Ther. 9 (2002) 564–576.
[44] M. Oliver, M.R. Jorgensen, A. Miller, The facile solid-phase synthesis of cholesterol-based polyamine lipids, Tet. Lett. 45 (2004) 3105–3107.
[45] N. Sakai, S. Matile, Anion-mediated transfer of polyarginine across liquid and bilayer membranes, J. Am. Chem. Soc. 125 (2003) 14348–14356.
[46] N. Sakai, T. Takeuchi, S. Futaki, S. Matile, Direct observation of anion-mediated translocation of fluorescent oligoarginine carriers into and across bulk liquid and anionic bilayer membranes, Chem. Biochem. 6 (2005) 114–122.
[47] C. Dardonville, R. Brun, Bisguanidine, bis(2-aminoimidazoline), and polyamine derivatives as potent and selective chemotherapeutic agents against *Trypanosoma brucei rhodesiense*, synthesis and in vitro evaluation, J. Med. Chem. 47 (2004) 2296–2307.
[48] C.L. Densmore, T.H. Giddings, J.C. Waldrep, B.M. Kinsey, V. Knight, Gene transfer by guanidinium-cholesterol: dioleoylphosphatidyl-ethanolamine liposome-DNA complexes in aerosol, J. Gene Med. 1 (1999) 251–264.
[49] D. Luton, N. Oudrhiri, P. de Lagausie, A. Aissaoui, M. Hauchecorne, et al., Gene transfection into fetal sheep airways in utero using guanidinium-cholesterol cationic lipids, J. Gene Med. 6 (2004) 328–336.
[50] B.E. Yingyongnarongkul, M. Howarth, T. Elliott, M. Bradley, Solid-phase synthesis of 89 polyamine-based cationic lipids for DNA delivery to mammalian cells, Chem. Eur. J. 10 (2004) 463–473.
[51] J. Sen, A. Chaudhuri, Design, syntheses, and transfection biology of novel non-cholesterol-based guanidinylated cationic lipids, J. Med. Chem. 48 (2005) 812–820.
[52] M.S. Bernatowicz, Y. Wu, G.S. Matsueda, H-Pyrazole-1-carboxamidine hydrochloride an attractive reagent for guanylation of amines and its application to peptide synthesis, J. Org. Chem. 57 (1992) 2497–2502.
[53] N. Kamaly, T. Kalber, A. Ahmad, M.H. Oliver, P.W. So, A.H. Herlihy, J.D. Bell, M.R. Jorgensen, A.D. Miller, Bimodal paramagnetic and fluorescent liposomes for cellular and tumor magnetic resonance imaging, Bioconjug. Chem. 19 (2008) 118–129.
[54] E. Uchida, H. Mizuguchi, A. Ishii-Watabe, T. Hayakawa, Comparison of the efficiency and safety of non-viral vector-mediated gene transfer into a wide range of human cells, Biol. Pharm. Bull. 25 (2002) 891–897.
[55] O. Argyros, S.P. Wong, M. Niceta, S.N. Waddington, S.J. Howe, et al., Persistent episomal transgene expression in liver following delivery of a scaffold/matrix attachment region containing non-viral vector, Gene Ther. 15 (2008) 1593–1605.
[56] Y. Naito, T. Yamada, K. Ui-Tei, S. Morishita, K. Saigo, siDirect: highly effective, target-specific siRNA design software for mammalian RNA interference, Nucleic Acids Res. 32 (2004) W124–W129.
[57] K. Ui-Tei, Y. Naito, F. Takahashi, T. Haraguchi, H. Ohki-Hamazaki, et al., Guidelines for the selection of highly effective siRNA sequences for mammalian and chick RNA interference, Nucleic Acids Res. 32 (2004) 936–948.
[58] P.L. Marion, F.H. Salazar, K. Liittschwager, B.B. Bordier, C. Seegers, M.A. Winters, M. A. Frontiers in Viral Hepatitis, in: R. Schinazi, R.F. Sommadossi, J.P. Rice, (Eds.), Elsevier Science, Amsterdam, pp. 197–202.
[59] D.V. Morrissey, K. Blanchard, L. Shaw, K. Jensen, J.A. Lockridge, et al., Activity of stabilized short interfering RNA in a mouse model of hepatitis B virus replication, Hepatology 41 (2005) 1349–1356.
[60] A.P. McCaffrey, H. Nakai, K. Pandey, Z. Huang, F.H. Salazar, et al., Inhibition of hepatitis B virus in mice by RNA interference, Nat. Biotechnol. 21 (2003) 639–644.
[61] J. Soutschek, A. Akinc, B. Bramlage, K. Charisse, R. Constien, et al., Therapeutic silencing of an endogenous gene by systemic administration of modified siRNAs, Nature (2004) 173–178.
[62] S.I. Kim, D. Shin, T.H. Choi, J.C. Lee, G.J. Cheon, et al., Systemic and specific delivery of small interfering RNAs to the liver mediated by apolipoprotein A-I, Mol. Ther. 15 (2007) 1145–1152.
[63] K. Nishina, T. Unno, Y. Uno, T. Kubodera, T. Kanouchi, et al., Efficient in vivo delivery of siRNA to the liver by conjugation of α-tocopherol, Mol. Ther. 16 (2008) 734–740.
[64] Y. Sato, K. Murase, J. Kato, M. Kobune, T. Sato, et al., Resolution of liver cirrhosis using vitamin A-coupled liposomes to deliver siRNA against a collagen-specific chaperone, Nat. Biotechnol. 26 (2008) 431–442.
[65] D.V. Morrissey, J.A. Lockridge, L. Shaw, K. Blanchard, K. Jensen, et al., Potent and persistent in vivo anti-HBV activity of chemically modified siRNAs, Nat. Biotechnol. 23 (2005) 1002–1007.
[66] T.S. Zimmermann, A.C.H. Lee, A. Akinc, B. Bramlage, D. Bumcrot, et al., RNAi-mediated gene silencing in non-human primates, Nature 441 (2006) 111–114.
[67] W. Li, F.C. Szoka, Lipid-based nanoparticles for nucleic acid delivery, Pharm. Res. 24 (2007) 438–449.
[68] Y. Chen, G. Cheng, R.I. Mahato, RNAi for treating hepatitis B viral infection, Pharm. Res. 25 (2008) 72–86.

Chapter 7: Discussion and Conclusion

Currently licensed therapies have limited efficacy in eradication of HBV in chronic carriers of the virus, and there remains an urgent need to find new therapeutic modalities. Harnessing the RNAi pathway for the provision of a clinically sound intervention depends on rigorously considering three key elements: safety, efficacy and delivery. The findings described in this body of work contribute to the field by having addressed the following aims: firstly, to identify novel RNAi effectors targeting *HBx* that inhibit HBV replication and viral gene expression; secondly, deliver synthetic siRNAs with lipid-based vectors to the liver and evaluate viral inhibition using *in vitro* and *in vivo* models of HBV infection. Lastly, to ensure that RNAi effectors and vectors induced minimal off-target effects.

7.1 Design and efficacy of RNAi effectors

shRNAs were designed as a 25-bp stem with mismatches in the sense strand while the anti-sense strand had perfect complementarity to the viral target. The mismatches were incorporated to facilitate cloning, and aid selection of the guide RNA by RISC. The loop was derived from miR-23, based on design parameters available at the initiation of the study that indicated that a miR-23 scaffold would facilitate nuclear export. This is further supported by the notion that evolutionary conserved miRs derived from precursors result in optimal processing and have structures that are likely to minimise non-specific effects (232-235). Using a similar model, others have tailored hairpins to contain features that mimic naturally occurring miR-30 or included bulges to the passenger strand to avert induction of interferon response, with outcomes that concur with data presented in this thesis (233, 236). Similarly, incorporating alternative backbones derived from miR-122 (understood to favour intrahepatic processing (237)), and

miR-31 (for the efficient processing by Drosha (124)) have been highly effective in suppressing HBV replication *in vitro* and *in vivo* (233). The effective processing of shRNA 5 and 6 using miR-23 as a backbone extended the available repertoire of expressed RNAi effectors (41).

The RNAi-induced silencing of HBV gene expression and replication, which was shown in cultured cells and *in vivo* to be specific, was induced by the guide sequences processed from shRNAs 5 and 6 as intended (Chapter 3). shRNA 5 and 6 yielded robust and lasting inhibition which was free of any detectable IFN response. The discrepant effect shRNA 10 had on HBV markers of replication was confirmed to be as a result of inadequate processing of the hairpin (Appendix 8.5). Processing of this effector favoured a guide sequence with the same polarity of the HBV target, consequently inducing no silencing effect. Although all short hairpins had a common loop sequence, the sense and anti-sense strands differed by spanning distinct areas of the *HBx* gene. There have been various factors identified that determine processing and functionality of RNAi effectors (137, 238, 239). For example, an optimal GC content of the dsRNA is needed to provide a balance between efficient unwinding of the duplex and retention of adequate stability between the guide sequence and its target. Examination of the GC content of the duplex generated from the processing of shRNA 5 is aligned with the proposed optimal GC content, in that it favours Dicer processing and guide strand stability with the HBV target. Processing of the duplex may be determined by 5' stability of the desired guide sequence. Notably, instability at the 5'-end of the antisense strand of shRNA 5, from a GU mismatched base pair, is likely to favour the intended strand bias. The disparate silencing effect among the shRNAs targeting *HBx* derived from a common backbone is significant and confirms that processing and functionality of the RNAi effectors are dependent on a multitude of factors which should be considered carefully in the design of these agents.

shRNAs and lhRNAs (Chapters 3 and 4) were under the transcriptional control of the U6 small nuclear RNA promoter, a Pol III promoter. This promoter induces high levels of expression, is relatively short in length and has distinct initiation and termination sites, hence enabling abundant and predictable RNAi effector synthesis. These may saturate the endogenous miR pathway and displace essential miRs that also depend on exportin-5 (240) for nuclear export and RISC-loading for processing (241). Vigorous over expression of VV-mediated RNAi expression, in small and large animals, may evoke severe side effects, from cytotoxicity, severe tissue damage, organ failure and death (242). Evidence from our laboratory indicates that U6-driven shRNAs targeting HBV induced saturation of exogenous miRs in a dose-dependent manner (233). However, our findings were not associated with any cytotoxic or histological evidence of hepatic damage. These differences may be related to study design: we employed an Ad vector at a low multiplicity of infection, and not a scAAV, thereby likely introducing a lower shRNA dose. Nevertheless, for this therapeutic strategy to develop clinically, further work is required to enhance the efficiency and potency of shRNAs to ensure maximal inhibition at a reduced dose (as described in (243)). Our attempts to generate shRNAs directly from a CMV promoter had no silencing effect on HBV. We postulate that the most likely reason for these findings was that the RNA transcripts expressed were not suitable substrates for processing (supporting data is provided in appendix 8.6). To correct this approach, effective shRNA sequences identified here may be expressed in the context of endogenous miR (244, 245). The advantage of this modality is that endogenous miRs are predominantly under transcriptional regulation of more versatile, tissue-specific Pol II promoters. Reported evidence of this strategy is available from a model of cell proliferation, where pri-miR-based shRNA under the transcriptional control of Pol II promoters, produced potent, stable and controlled target inhibition (246). Similarly, observations from our laboratory using miR scaffolds (miR-

31 and -122) against HBV show efficacy with no interference of exogenous artificial miR-31-derived sequences on endogenous miR-16 function (159, 233). These findings demonstrate that shRNAs in the context of miR scaffolds are less likely to cause saturation of the miR pathway. This underscores the need for development of controllable shRNA expression systems which are under regulation of moderate promoters with compatible miR shuttles.

7.2 Delivery of RNAi effectors

Ad vectors are attractive VVs for the delivery of expressed RNAi effectors to the liver. They bear numerous features that have supported their extensive use, but they may elicit strong immune responses, thereby compromising their effectiveness. The use of these vectors in clinical settings raised many concerns, especially following the death of a patient four days after the administration of an Ad vector (247, 248) and the failure of an HIV-1 vaccine using an Ad5 vector (249, 250). In contrast, Ad vectors have been successfully used in correcting clotting factor deficiency in haemophiliacs (251). The work presented here made use of Ad5-derived vectors primarily for their inherent hepatotropism. These vectors were used to deliver anti-HBV shRNAs and resulted in significant HBV suppression relative to a control group and provided proof-of-concept in a stringent animal model of chronic HBV infection (41). However, these VV have many barriers that have hampered widespread utilisation in clinical settings.

Advances in vectors to deliver DNA or RNA to hepatocytes are pivotal to the success of RNAi-based therapy for the treatment of chronic HBV. Hence, the need for continued development and optimisation of NVV for this specific application remains. Our work adds to a growing body of knowledge in the field by describing the synthesis of PEGylated siRNA-nanoparticles, inclusion of a pH-labile oxime bond and by extending the range of cationic lipids to be used in

NVV (Chapters 5 and 6). These vectors successfully delivered unmodified siRNA to mouse livers and induced inhibition of HBV replication without any observed toxic effects. The nanoparticles employed are unique in the manner in which they were assembled and formulated. A pH-sensitive lipid vector promotes early escape from the acidic endosomal environment (pH 6) by protonation of the amino groups which promotes fusion with endosomal phospholipids. This destabilises the endosomal membrane after endocytosis and releases the nucleic acids (siRNA or shRNA plasmid) into the cytoplasm. There is sufficient evidence that NVV containing ionisable cationic lipids *in vivo* accumulate in hepatocytes by endocytosis, following adsorption of ApoE (219), this is further supported by our findings (Chapter 5). It is proposed that cationic lipid based NVV are processed as chylomicrons, which are able to adsorb ApoE. This confers hepatotropism to several receptors with ApoE binding ligands (215). Although NVV showed promising results, efficacy could be further enhanced. Future work should aim to modify NVV to improve on liver-directed nucleic acid delivery. To achieve this, several liver-specific ligands may be incorporated. Galactose is a promising monosaccharide and hepatocytes possess a vast number of asialoglycoprotein receptors that recognise this molecule in oligosaccharide chains of glycoproteins. Improved hepatotropism may be achieved by synthesising galactosylated lipoplexes (252). The safety profile of NVVs, synthesis methodology and scalability make these a more favourable delivery option for clinical implementation of RNAi strategies.

Alternatives to lipid-based NVV delivery strategies are being developed to exploit the RNAi pathway to target HBV. siRNAs have been conjugated effectively to lipids, polymers, peptides and aptamers to improve delivery (253-255). For example, conjugation of cholesterol to the 3'-end of the sense strand of the siRNA duplex facilitates receptor-driven endocytosis. Soutschek *et al*. used this approach to deliver siRNAs targeted against Apo B to the liver and jejunum

following systemic administration and demonstrated significant localisation of this conjugate in the liver (172). This study confirms that systemic delivery to specific organs such as the liver can be accomplished by direct conjugation of siRNAs with ligands that promote targeted cellular intake. Similarly, using a polymer-based Dynamic PolyConjugate (DPC), Wooddell *et al*., demonstrated targeted delivery of siRNAs to hepatocytes (256). Remarkably, a single dose of this conjugated siRNA, resulted in a sustained and potent inhibition of HBV viral RNA, DNA and proteins, both in a transient and transgenic HBV mouse model (256). The outcomes of an early phase clinical trial delivering this RNAi effector (ARC-520) yielded two types of responses. HBeAg positive treatment-naïve patients benefited from a strong inhibition while HBeAg-negative patients who had prior exposure to nucleoside or nucleotide inhibitors, had a diminished inhibition of HBsAg. Further investigations elucidated the source of surface antigen expression to be from episomal cccDNA minichromosome and viral DNA integrated into the host genome. These unanticipated findings are of significance to the field in that they elucidate a source of HBsAg. The data also provide a viral mechanism to support chronic HBV in the presence of host immunosurveillance (257).The importance of cccDNA and integrated viral DNA for elimination of the virus using wider strategies to cover all possible sources of viral transcripts is also emphasised. The work presented in this thesis was limited to targeting *HBx* which may only achieve elimination of HBV transcripts but not of cccDNA. However, would the potential reduction in HBx function suffice to diminish the stability it confers to cccDNA and eradicate the persistent episomal viral genome? (96, 97). HBx promotes degradation of Smc5/6, hence stabilising cccDNA and promoting continued transcription. Consequently, by targeting HBx, inhibition of cccDNA transcription would be expected. This remains to be determined in experiments of longer duration using chimeric humanised uPA SCID mice that support cccDNA formation that allows for hepatocyte turnover. It is clear that elimination of cccDNA would result in HBV eradication. How this can be achieved remains an enormous

challenge. Perhaps adopting an alternative approach to elimination or epigenetic modification of cccDNA may be needed.

Direct RNAi-based strategies alone do not target the HBV DNA reservoir, thus the use of novel engineered sequence-specific nucleases as an adjuvant therapeutic modality is promising. The recent engineering of programmable nucleases such as, zinc-finger nucleases, transcription activator-like effectors nucleases (TALENs), and the clustered regularly interspaced palindromic repeats (CRISPR) - CRISPR-associated (Cas) (CRISPR/Cas) system has provided a new approach for gene therapy of clinical disorders from haemophilia (258), primary immunodeficiency (259) as well as high burden infectious diseases like HIV (260). The safety and efficacy of gene-editing interventions, both *ex vivo* and *in vivo* are under evaluation in clinical trials (261). There is growing evidence of the successful use of TALENs to target chronic HBV (32). Recently, the inhibition of HBV gene expression was demonstrated in a combined approached of gene editing and silencing (262). Dreyer *et al*. used TALENs directed to *core* and *surface* genes of HBV to introduce double stranded breaks and through homology-directed DNA recombination, integrate pri-miRs against HBV into the viral genome. The constructed mutant HBV genome could then generate multiple RNAi effectors to its own transcripts (262). This complementary approach proved to be effective, has the potential to be long-lasting and makes use of different pathways to avoid potential toxic effects from saturation. Likewise, combining a strategy aimed at inhibition of cccDNA by epigenetic modification could open other avenues for a functional cure if not eradication of HBV in chronic infection (263).

7.3 RNAi effector off-target effects

The use of RNAi for clinical purposes is limited by specificity and therefore safety of gene silencing. This has the potential to induce non-specific silencing of unintended transcripts (264). This has major implications for high throughput screening of RNAi effector candidates with the identification of false positive candidates (265, 266). Off-target transcript silencing may be induced by limited target sequence complementarity to the seed region (nucleotides at position 2-8 from the 5' end) of the siRNA guide strand (173-175). This "off-target" effect is milder and results in mRNA destabilisation rather than shRNA-induced mRNA cleavage. In addition, there is evidence that the sense strand may also be loaded into RISC, contributing further to a reduction of target specificity (267, 268). Careful sequence selection using bioinformatics tools may not entirely eliminate this unintended effect and would still require evidence generated through empirical testing. A comprehensive bioinformatics analysis of the RNAi effectors described here was beyond the scope of this work. To illustrate possible off-target effects, sequence alignment was performed (Blast query: https://blast.ncbi.nlm.nih.gov) on the predicted 21 nt passenger strand sequence of shRNA 5 (appendix 8.7). Although, 53 sequences were identified to produce significant alignment, some of the identified targets are from either computer predicted pseudo-genes or sequences of unknown function. Furthermore, since the essence of RNAi rests on sequence recognition, particularly of a mere 7 nt of the seed region of the guide strand, the mathematical (as opposed to biological) probability of off-target effects is significantly higher than that expected from a 21 nt siRNA. However, off-target effects may be mitigated by employing several strategies. Introducing chemically modified nucleotides at specific positions within the seed region may increase siRNA specificity. 2'-*O*-methyl ribosyl modifications of the nucleotide at the second position from the 5'-end of the guide strand (and not the first nucleotide) may diminish position-dependent off-target silencing (269). Potency,

specificity and safety profile of expressed shRNAs may be improved by blocking the sense-strand to limit off-target gene regulation by co-expression of decoy RNAs to the sense strand (201). RNAi-based therapies would require in-depth assessment of unintentional transcript silencing prior to becoming a clinical tool.

7.4 Conclusion

In conclusion, the data presented in this thesis provide a substantial body of evidence that different RNAi modalities can suppress HBV replication and gene expression in cell culture and animal models of acute and chronic HBV infection. This is true for VV-expressing hairpin sequences, or with NVV-delivering synthetic siRNAs. In addition, the *HBx* ORF was shown to be highly suitable target for RNAi-based therapy. Despite these optimistic findings, several challenges still remain for RNAi-based therapies to reach the clinic. The biggest hurdle remains the safe implementation of RNAi *in vivo*; identifying a safe and effective dose for the desired delivery strategy is an important future objective. In this thesis, both viral and non-viral delivery strategies were shown to be effective options, but a final therapy will have to ponder the advantages of robust liver-directed transduction and single-intervention application of viral therapies with the superior safety considerations of non-viral approaches. As research on RNAi enters its third decade since discovery of the pathway, the advent of clinically approved RNAi therapies is upon us. It is highly likely that an RNAi-based solution for chronic HBV infection is imminent.

Chapter 8: Appendices

8.1 Ethics certificates

Ethics clearance was granted by the University of the Witwatersrand Animal Ethics Screening Committee:

2005/1/4 “Assessing efficacy of sifectamine-mediated delivery of anti HBV RNA”

2006/14/03 “Establishing a HB virus transgenic mice colony for use as a model to test efficacy of antiviral agents”

UNIVERSITY OF THE WITWATERSRAND, JOHANNESBURG

STRICTLY CONFIDENTIAL

ANIMAL ETHICS SCREENING COMMITTEE (AESC)

CLEARANCE CERTIFICATE NO. 2006/14/03

APPLICANT: Professor PB Arbuthnot

SCHOOL: Molecular Medicine and Haematology
DEPARTMENT:
LOCATION: Medical School

PROJECT TITLE: Establishing a HB virus transgenic mouse colony for use as a model to test antiviral efficacy of antiviral therapy

Number and Species

576 transgenic mice

Approval was given for to the use of animals for the project described above at an AESC meeting held on 20060228 and subsequent meetings on 20060328 and 20060425. This approval remains valid until 20080424.

The use of these animals is subject to AESC guidelines for the use and care of animals, is limited to the procedures described in the application form and to the following additional conditions:

Approval is based on adherence to the attached SOP's

Signed: D. A. Gray (Chairperson, AESC) Date: 11/05/06

I am satisfied that the persons listed in this application are competent to perform the procedures therein, in terms of Section 23 (1) (c) of the Veterinary and Para-Veterinary Professions Act (19 of 1982)

Signed: _____ (Registered Veterinarian) Date: 11/05/06

cc: Supervisor:
Director: CAS

Works 2000/Iain0015/AESCCert.wps

AESC 3

STRICTLY CONFIDENTIAL

UNIVERSITY OF THE WITWATERSRAND, JOHANNESBURG

ANIMAL ETHICS SCREENING COMMITTEE

CLEARANCE CERTIFICATE NO:

2005	1	4

APPLICANT: Professor PB Arbuthnot

DEPARTMENT: Molecular Medicine & Haematology

PROJECT TITLE: Assessing efficacy of sifectamine-mediated delivery of anti HBV nucleic acids

Species	Number	Expiry Date
Mouse	480	January 2007

i) Approval is hereby given for the experiment described in the above application.

The use of these animals is subject to AESC Guidelines for the use and care of animals, is limited to the procedures specified in the application form, and to:

SIGNED D.A. Gray DATE: 25/01/2005
(Chairman: ~~Animal~~ Ethics Screening Committee)

ii) I am satisfied that the persons listed in this application are competent to perform the procedures therein, in terms of Section 23(1)(c) of the Veterinary and Para-veterinary Professions Act (19 of 1982)

SIGNED _____ DATE: 25/01/2005
(Registered Veterinarian)

NOTE:

First-time users of the CAS should contact the Director of the CAS in order to familiarise themselves with the facilities available, and the procedures required by the CAS for the carrying out of experiments.

AESC 3

UNIVERSITY OF THE WITWATERSRAND, JOHANNESBURG

STRICTLY CONFIDENTIAL

ANIMAL ETHICS SCREENING COMMITTEE (AESC)

CLEARANCE CERTIFICATE NO. 2007/47/3

APPLICANT: Dr P Arbuthnot

SCHOOL: Molecular medicine and Haematology
DEPARTMENT:
LOCATION: Medical School

PROJECT TITLE: **Assessment of efficacy of anti hepatitis B virus RNA interference expression cassettes using the murine hydrodynamic injection model**

Number and Species

384 male and female mice

Approval was given for to the use of animals for the project described above at an AESC meeting held on 20071127. This approval remains valid until 20091127

The use of these animals is subject to AESC guidelines for the use and care of animals, is limited to the procedures described in the application form and to the following additional conditions:

Report % of animal deaths under this protocol, volume injected must be in proportion to body size with 3ml maximum, retro-orbital bleeds twice only, liaison with CAS vet for injections and retro orbital bleeds, all animals that die other than euthanasia for experimental procedure must be made available to the CAS in line with normal procedure.

Signed: _____ Date: 30/11/2007
(Chairperson, AESC)

I am satisfied that the persons listed in this application are competent to perform the procedures therein, in terms of Section 23 (1) (c) of the Veterinary and Para-Veterinary Professions Act (19 of 1982)

Signed: _____ Date: 30/11/2007
(Registered Veterinarian)

cc: Supervisor:
Director: CAS

Works 2000/Iain0015/AESCCert.wps

UNIVERSITY OF THE WITWATERSRAND, JOHANNESBURG

STRICTLY CONFIDENTIAL

ANIMAL ETHICS SCREENING COMMITTEE (AESC)

CLEARANCE CERTIFICATE NO. 2008/24/03

APPLICANT: Prof P Arbuthnot

SCHOOL: Molecular Medicine & Haematolgy
DEPARTMENT:
LOCATION:

PROJECT TITLE: **Testing anti hepatitis B virus (HBV) efficacy of RNA interference activators in a transgenic mouse model of viral replication**

Number and Species

834 6-weeks Mice

Approval was given for the use of animals for the project described above at an AESC meeting held on 20080527. This approval remains valid until 20100527

The use of these animals is subject to AESC guidelines for the use and care of animals, is limited to the procedures described in the application form and to the following additional conditions:

Inject lamivudine IP, provide dosage amounts and route of delivery in bed letters, the CAS will test the procedure using the saphenous vein, and if successful, the researcher will be guided on how to perform the technique for the study

Signed: _____ Date: 09/06/2008
(Chairperson, AESC)

I am satisfied that the persons listed in this application are competent to perform the procedures therein, in terms of Section 23 (1) (c) of the Veterinary and Para-Veterinary Professions Act (19 of 1982)

Signed: _____ Date: 09/06/2008
(Registered Veterinarian)

cc: Supervisor:
Director: CAS

Works 2000/lain0015/AESCCert.wps

8.2 Chapter 3 - Supplementary data

8.2.1 Interferon Response.

Huh7 and HEK293 cells were transfected with plasmids encoding shRNA sequences or poly I:C (Sigma, MO, USA) according to the procedures described. RNA was isolated 24 hours after transfection using an automated nucleic acid extraction system (MagNA Pure, Roche Diagnostics (Mannheim, Germany). To measure concentrations of mRNA encoding interferon response-related genes, total RNA was reverse transcribed using Sensiscript (Qiagen, GmbH, Germany), and oligo d-T according to the manufacturer's instructions. Real time PCR was carried out in a volume of 20 µl using the Roche Lightcycler V.2 with equivalent amounts of template cDNA from each of the transfections. Controls included water blanks and RNA extracts that were not subjected to reverse transcription. SYBR green Taq readymix (Sigma, MO, USA) was used to amplify and detect DNA during the reaction. PCR was carried out in a 20 µl volume and thermal cycling parameters consisted of a hotstart for 30 sec 95°C followed by 50 cycles of 57°C for 10 sec, 72°C for 7 sec and then 95°C for 5 sec. The primer sets used to amplify DNA after reverse transcription were:

interferon-β (IFN-β) forward: 5'-TCCAAATTGCTCTCCTGTTGTGCT-3', IFN-β reverse: 5'-ccacaggagcttctgacactgaaaa-3',

GAPDH forward: 5'- AggggTCATTgATggCAACAATATCCA -3',

GAPDH reverse 5'- TTTACCAgAgTTAAAAgCAgCCCTggTg -3',

OAS1 forward: 5'-CGAGGGAGCATGAAAACACATTT-3',

OAS1 reverse: 5'-GCAGAGTTGCTGGTAGTTTATGAC-3',

MxA forward: 5'-CTGGTGCTGAAACTGAAGAAAC-3' and

MxA reverse: 5'-ATCTCAATCTCGTAGTCCTGGTA-3'. Specificity of the PCR products was verified by melting curve analysis and agarose gel electrophoresis. Ratios of crossing points of IFN-b, MxA or OAS1 to GAPDH were used to quantitate mRNA.

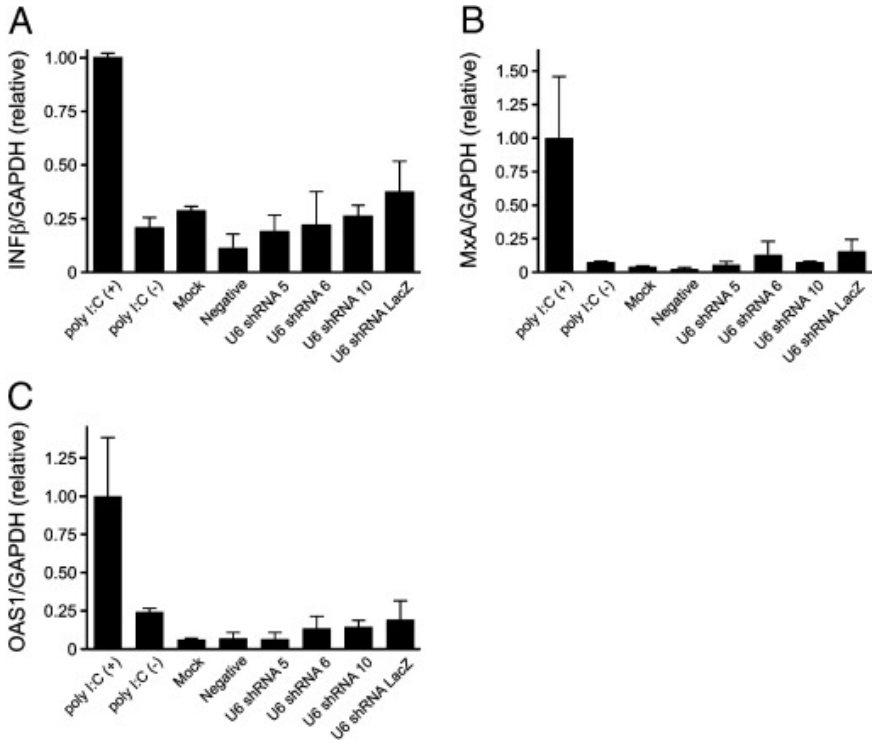


Figure 8.1 Assessing activation of the interferon response –

Quantitative real time PCR was used to measure IFN-β (A), MxA (B) or OAS1 (C) mRNA. Means (±SEM) of the normalized ratios of IFN-β, MxA or OAS1 to GAPDH are indicated from 3 independent experiments. Cells were transfected with the indicated shRNA-encoding plasmids and controls included poly I:C transfected cells (poly I:C (+)) or cells that were incubated with poly I:C in the culture medium without transfection reagent (poly I:C (-)).

8.3 Chapter 4 - Supplementary data

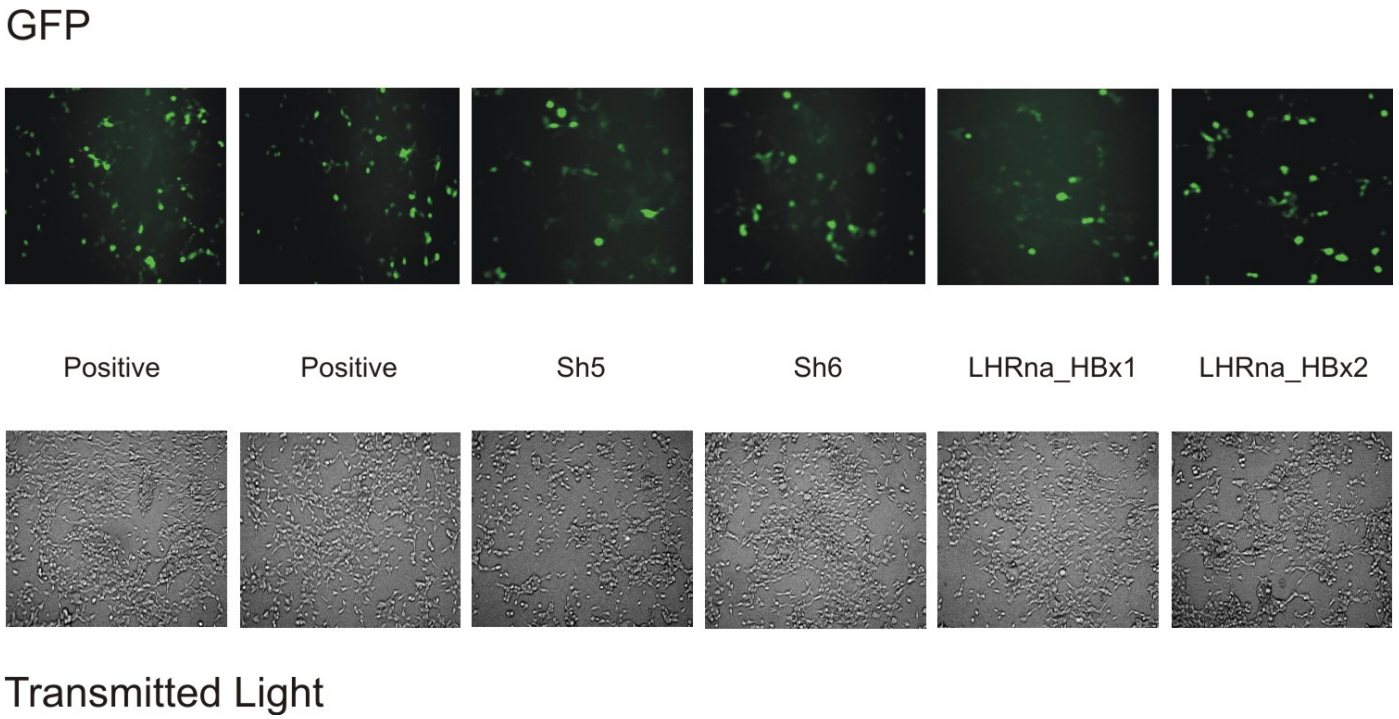


Figure 8.2: Representative fields of transfected Hek293 cells transfected with an HBV GFP reporter plasmid.

Top Panels represent fields examined under fluorescence microscopy and demonstrate the effect of several effectors in relation to positive controls (Left). Bottom panels display the equivalent field examined under transmitted light only, these depict cell number and cytomorphology.

8.4 Chapter 5 - Supplementary data

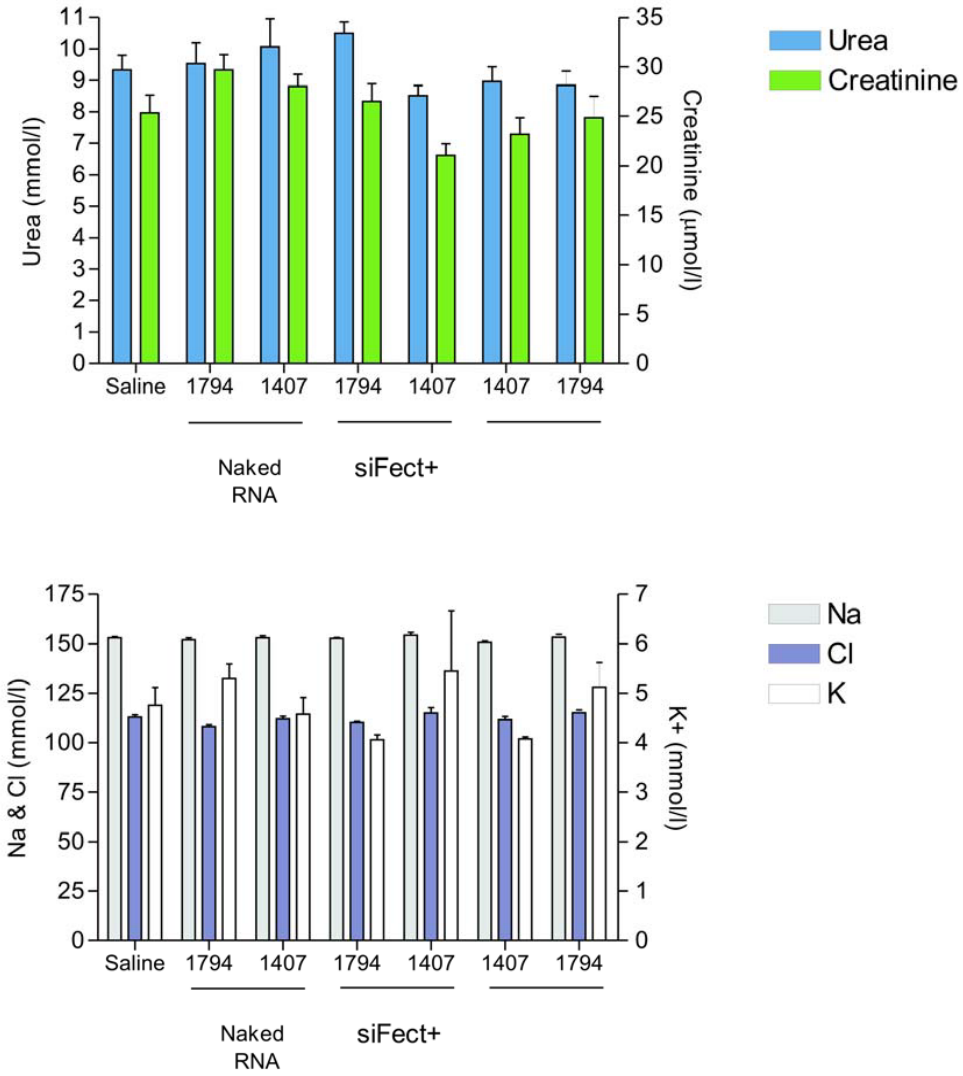


Figure 8.3 Urea, creatinine and electrolyte levels in blood post IV administration

Urea, creatinine and electrolyte levels in blood post IV administration to NMR-1 mice of saline, naked siRNAs 1794 and 1407, or siFECTplusTM nanoparticles formulated with siRNAs 1794 and 1407 (in each case siRNA was administrated as single dose 1mg/kg per animal body weight). Data suggest that renal function is unaffected by either naked siRNA or nanoparticle administration

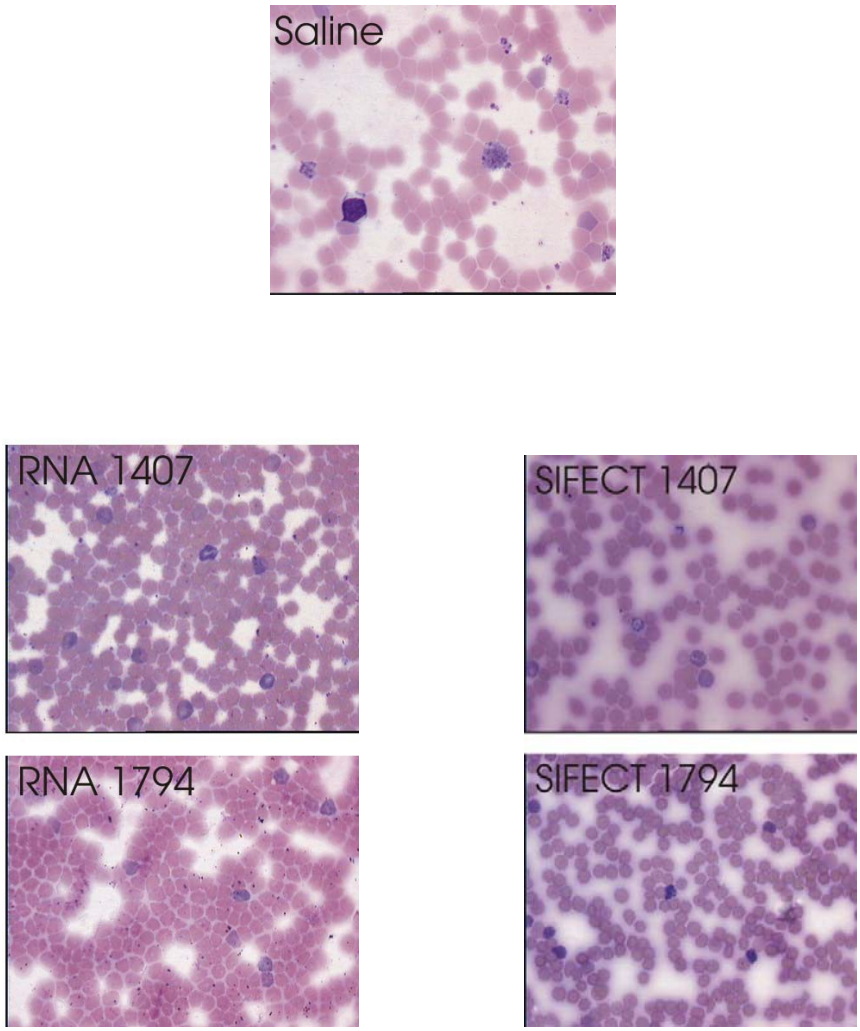


Figure 8.4 Representative smears of murine blood post IV administration

NMR-1 mice were administered with either, saline, naked siRNAs 1794 and 1407, or siFECTplusTM nanoparticles formulated with siRNAs 1794 and 1407. siRNA were administered as single dose 1mg/kg per animal body weight. Data suggest that blood is unaffected by either naked siRNA or nanoparticle administration. Similar effects were seen following a multiple dose regime of naked siRNA or siFECTplusTM nanoparticle administration (as defined in Figure 3)

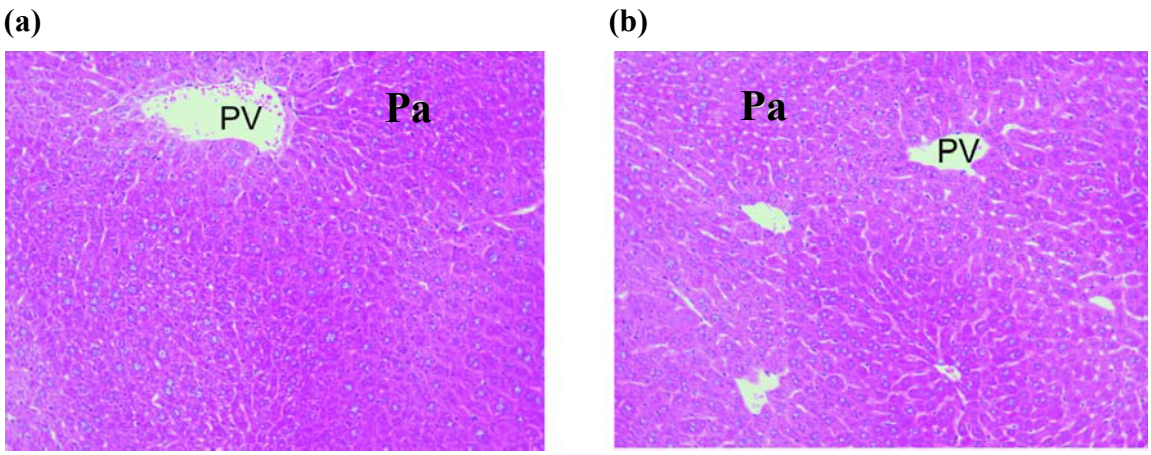


Figure 8.5 Histological examination of NMR-1 murine liver sections post administration of control and siRNA

Histological examination of NMR-1 murine liver post IV administration of saline control (a) and siFECTplusTM nanoparticles (siRNA13 was introduced at a dose of 1 mg/kg animal body weight for each injection every 3 days for 4 weeks) (b). Representative sections are Haematoxalin and Eosin stained (200x magnification). Control and siFECTplusTM nanoparticle-treated mice show no histological evidence of inflammatory changes that might suggest toxic effects in either case. Portal vein (PV), liver parenchyma (Pa)

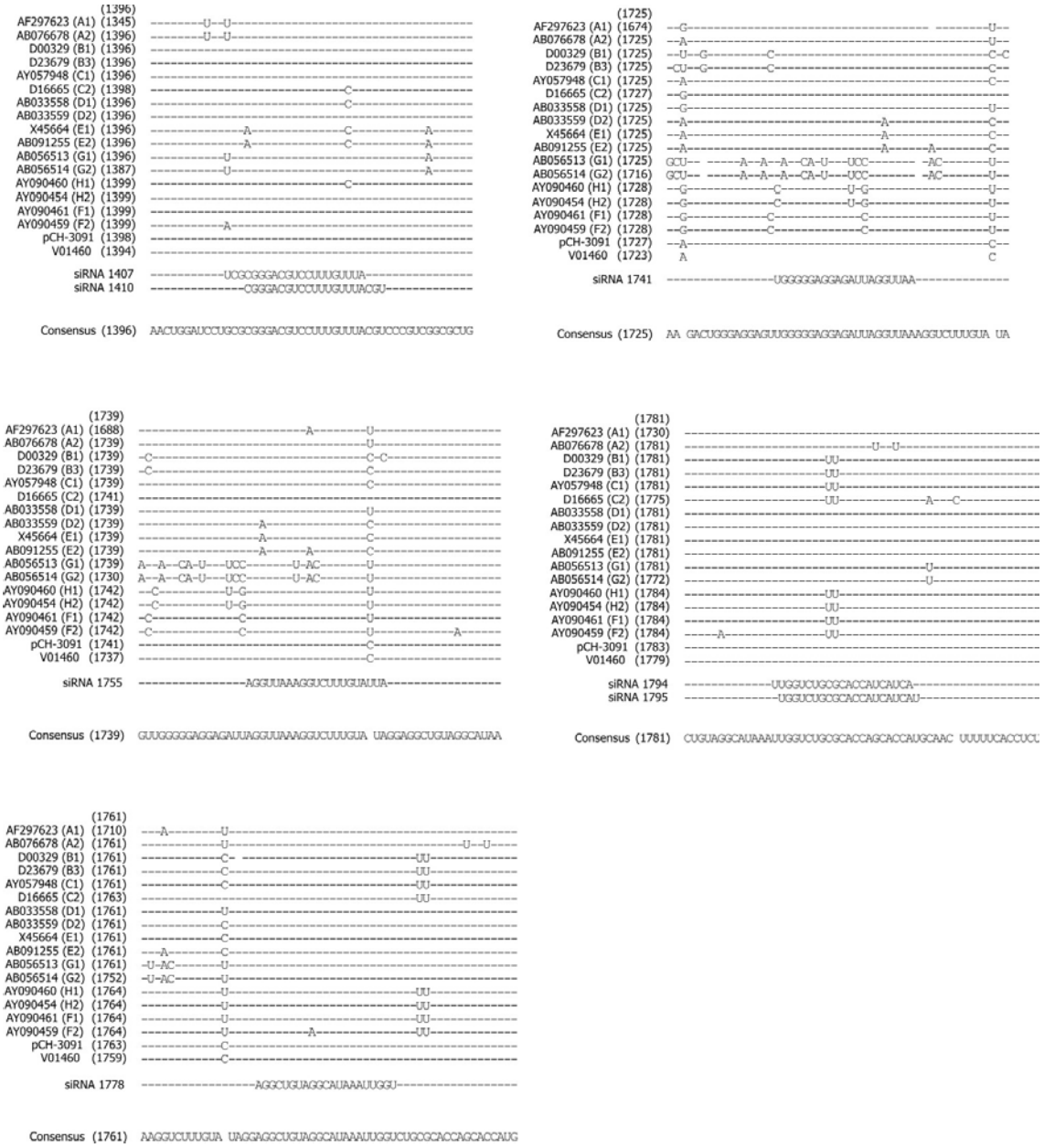


Figure 8.6 Alignment of siRNAs with representative HBV genotype sequences.

The numbering of the siRNA corresponds to the first nucleotide complementary to the guide strand and is relative to the HBV A2 reference sequence (AB076678). The alignment demonstrates sequence conservation along multiple genotypes, including the HBV expression plasmid (pCH-3091) and the HBV transgenic mouse sequence (V01460)

8.5 Processing of shRNA 6 and shRNA 10

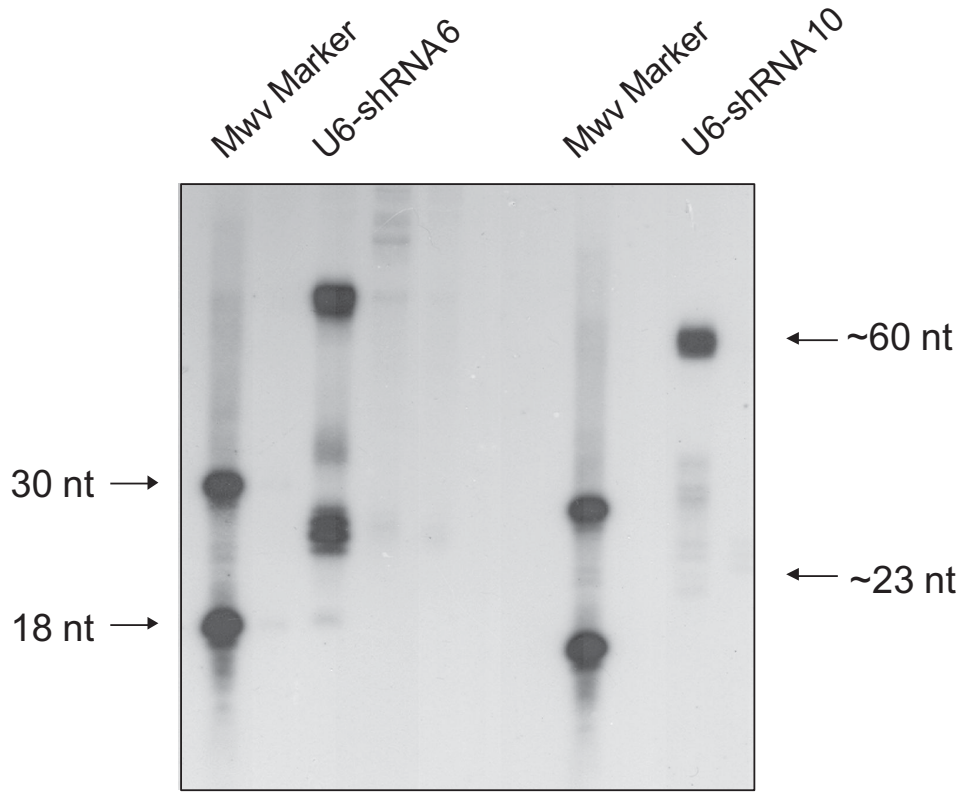


Figure 8.7 Northern blot hybridisation analysis of processed shRNA 6 and 10 mRNA Expressed from U6 promoter.
U6-shRNA6 expression yields an expected ± 21-23 nt long RNA. In contrast, U6-shRNA10 expression shows no discernible processing of effector RNA sequences.

8.6 Pol II and Pol III promoter driven expression of anti HBV shRNAs

Table 8-1 Nucleotide sequences of overlapping oligonucleotides used to generate CMV shRNA-encoding sequences.

HBV Target*	Name	Primer sequence
1575-1596	CMV shRNA 5 F	5'-GATCGAATTCACTAGTGCGACGTGTGTACTTCGCTTCGCCCTGTGAAGCCACAGATGG -3'
	CMV shRNA 5 R	5'-GATCCCCGGGTCTAGAGCA**CCGTGTGCACTTCGCTTCACC**CCCATCTGTGGCTTCACA -3'
1863-1883	CMV shRNA 10 F	5'-GATCGAATTCACTAGTGCGCTCAGGCCTCCAAGTTGTGCCCTGTGAAGCCACAGATGG -3'
	CMV shRNA 10 R	5'-GATCCCCGGGTCTAGAGCA**TTCAAGCCTCCAAGCTGTGCC**CCCATCTGTGGCTTCACA -3'

*HBV coordinates are relative to the single *Eco* RI site as indicated in Fig. 1
Complementary overlapping sequences are underlined
Sequences encoding *HBx* antisense RNA are bold

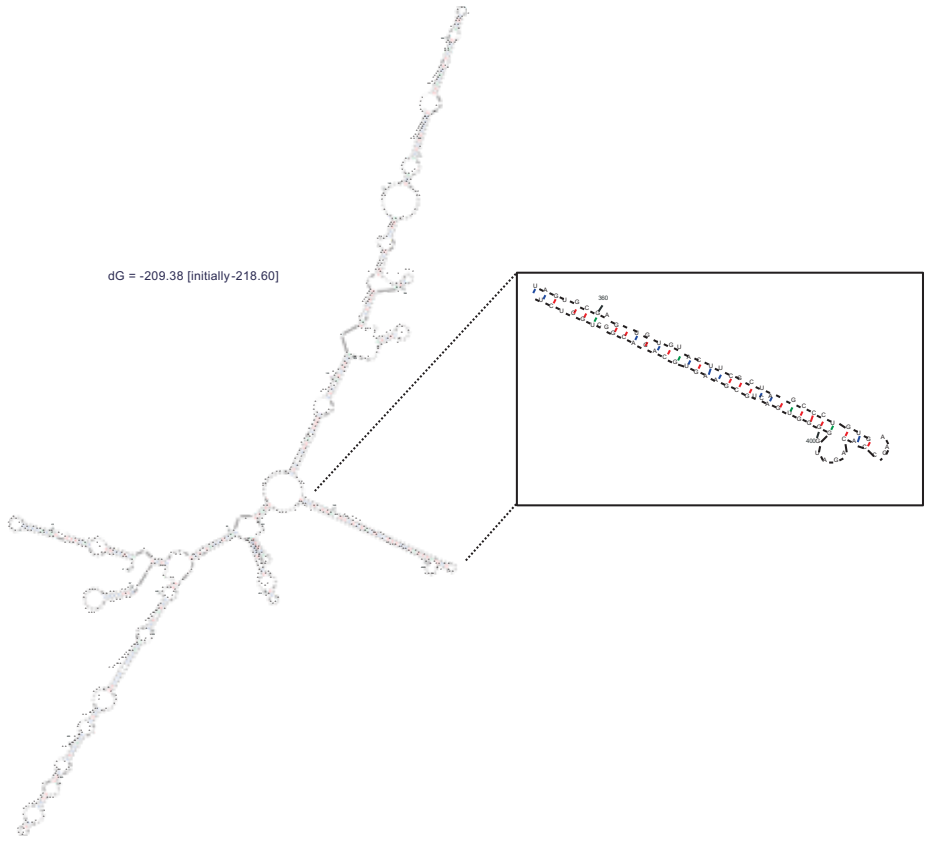


Figure 8.8 Predicted - CMV shRNA 6 - RNA secondary structure

Mfold (Genetics Computer Group, Madison, WI) dG = -209.38 [initially -218.60]

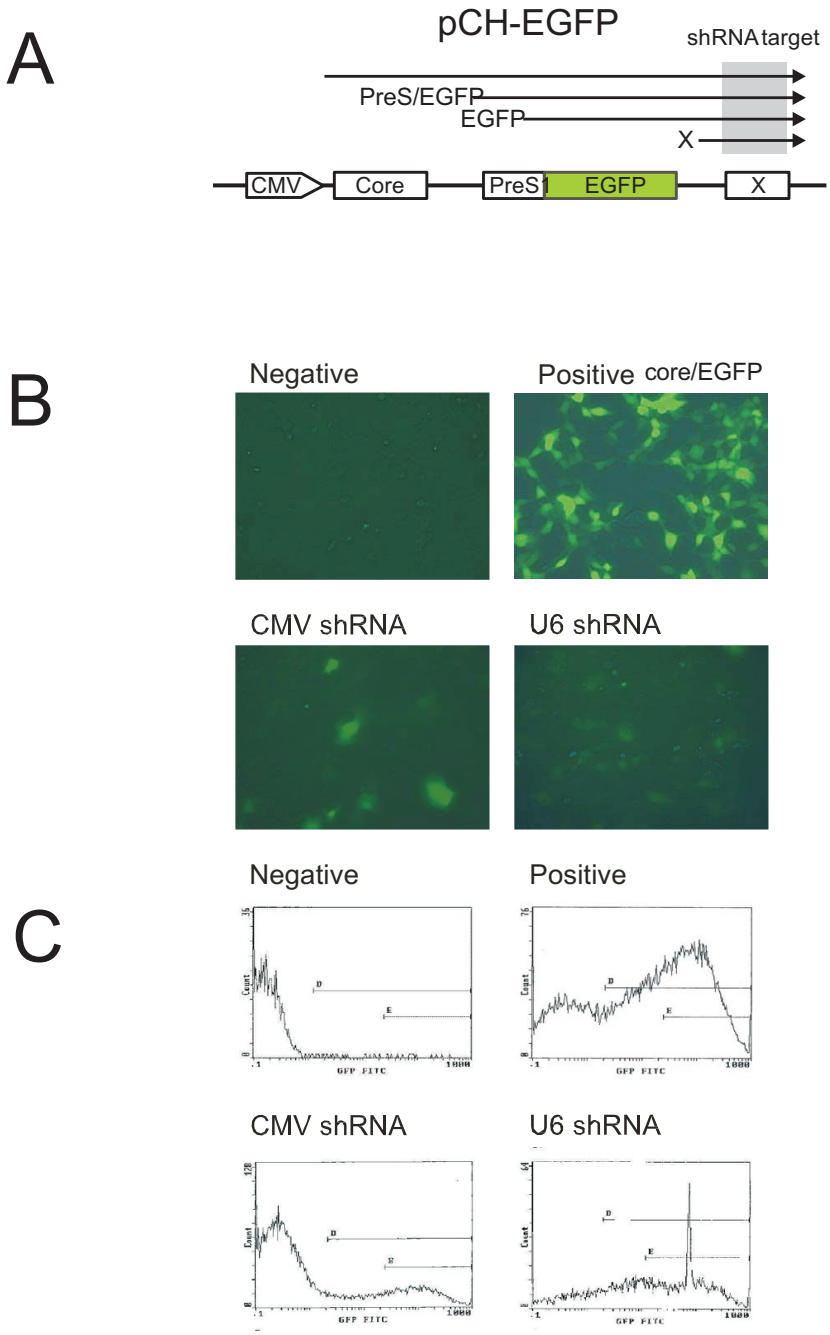


Figure 8.9 Silencing effect of shRNAs expressed from CMV and U6 promoters

Schematic representation of the Green Fluorescent Protein report plasmid and the *HBx* ORF (A), Representative fluorescent microscopy fields demonstrating GFP expression following transfection with RNAi effectors under the control of either CMV or U6 promoters (B), Corresponding flow cytometry enumeration of fluorescent events.

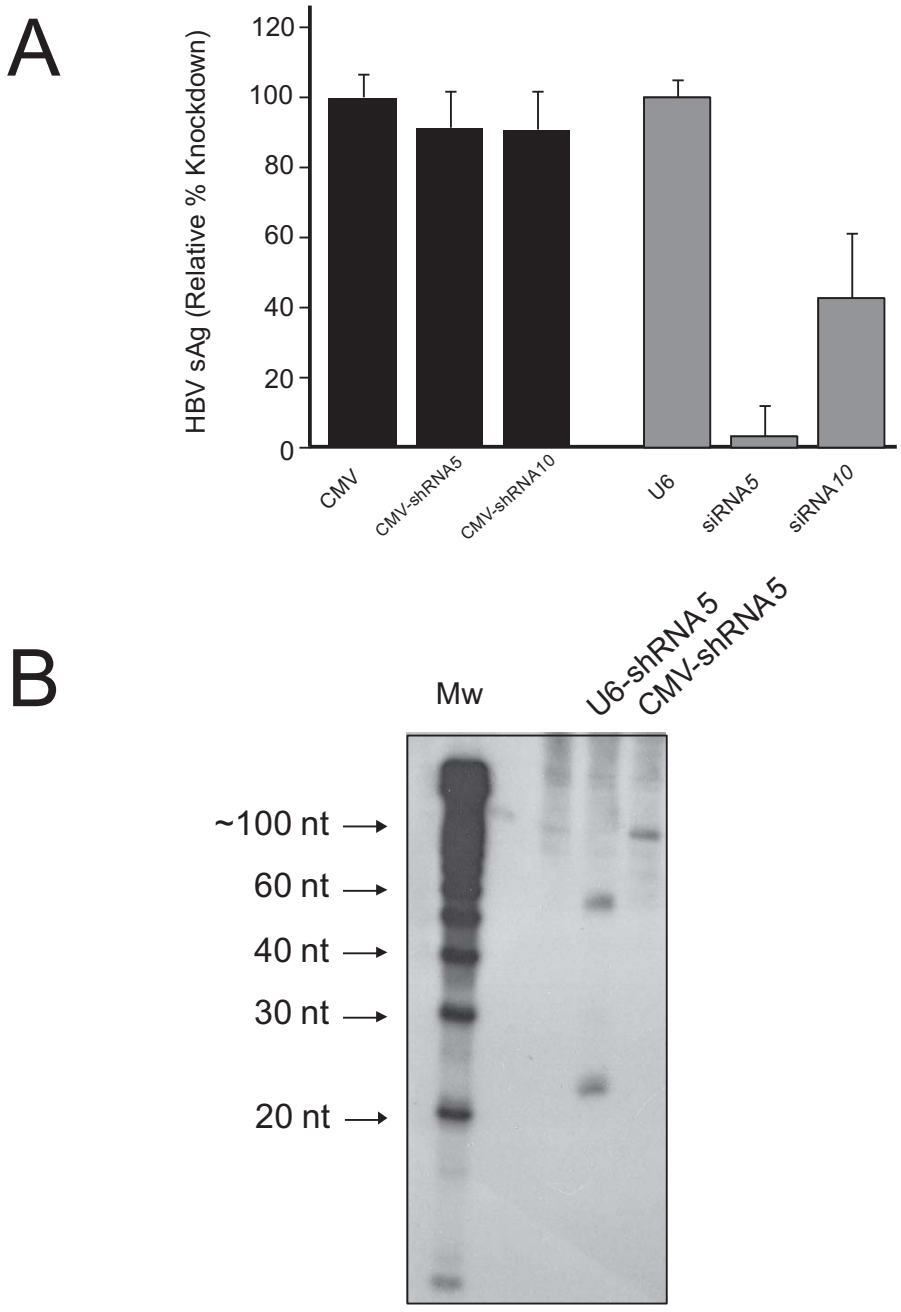


Figure 8.10 Pol II and Pol III promoter driven expression of anti HBV shRNAs.

Huh7 cells were co-transfected with pCH-3091 (HBV plasmid) and either a Pol III (pCMV-shRNA5 and pCMV-shRNA10) or Pol III (pU6-shRNA5 and pU6-shRNA10) driven construct which targeted the HBV X open reading frame. The parental pCMV or pU6 plasmids served as controls. Hepatitis B Virus surface antigen was determined 48 hours post-transfection. Each bar represents the mean of n=4 ± SD and have been normalised against the corresponding control. (**A**) Northern blot hybridisation analysis of processed mRNA expressed from either U6 or CMV promoter. U6 expression yields an expected ± 21-23 nt long RNA. In contrast, CMV expression shows no sign of discernible expression is noted (**B**).

8.7 Sequence alignment of U6 shRNA 5 passenger strand

Sequence: U6 shRNA 5

Sequence query: 5' GUG UGC GCU UUG CUU CGC UC '3

Blast search date: 27 Mar. 18

Number of hits reported: 53

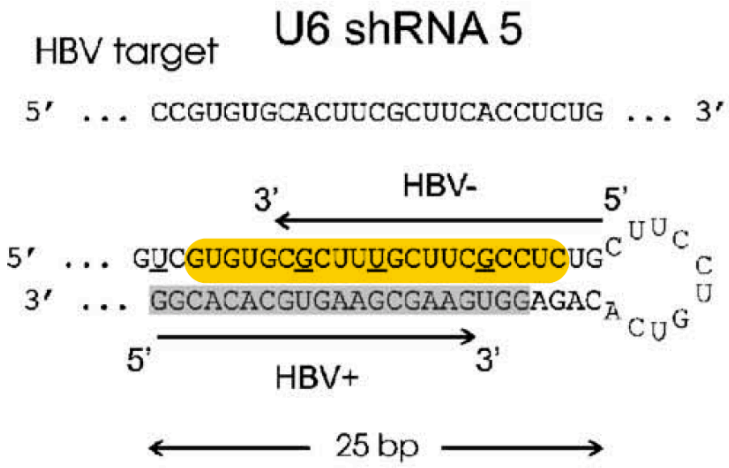


Figure 8.11 Schematic representation of the predicted hairpin structure of shRNA 5

Highlighted in yellow is the predicted 21 nt sequence that represents the passenger strand produced after Dicer processing.

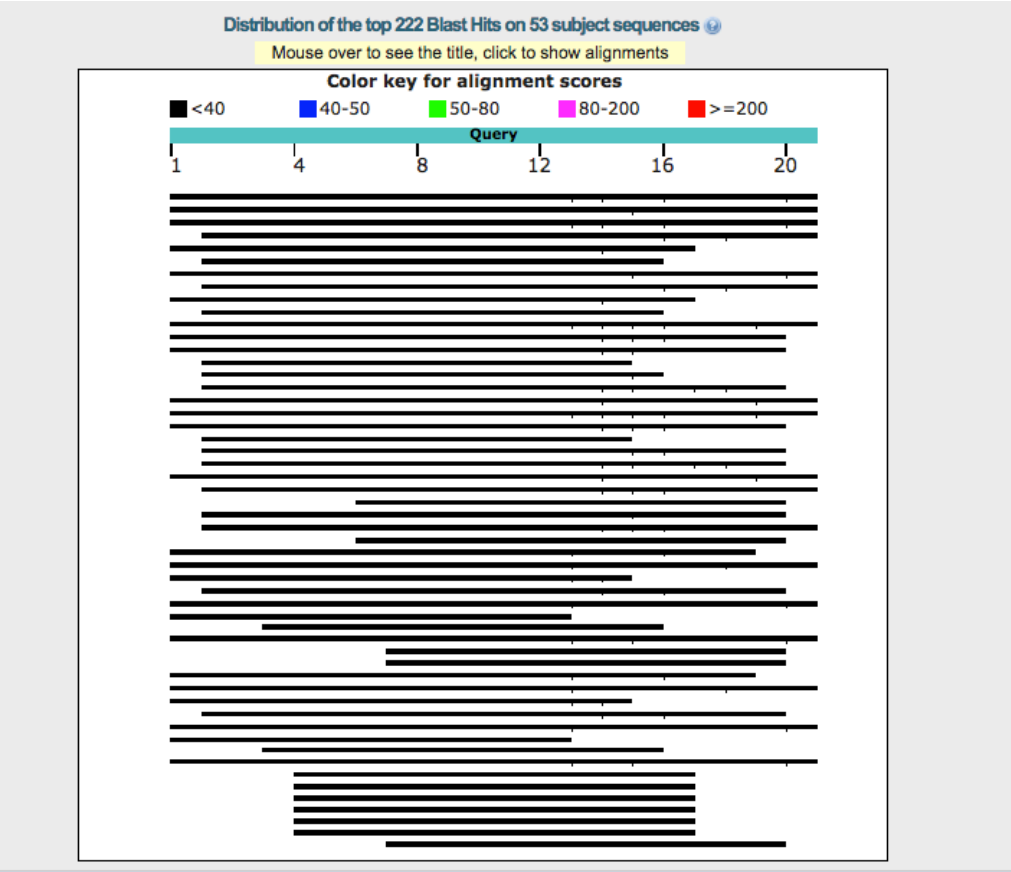


Figure 8.12 Graphic summary of blast search using the passenger strand of U6 shRNA 5 as the search string.

Sequences producing significant alignments:

Select: All None Selected:1

Alignments Download GenBank Graphics Distance tree of results

Description	Max score	Total score	Query cover	E value	Ident	Accession
Homo sapiens chromosome 1, alternate assembly CHM1_1.1	32.2	242	100%	5.0	100%	NC_018912.2
Homo sapiens chromosome 4, alternate assembly CHM1_1.1	32.2	171	100%	5.0	95%	NC_018915.2
Homo sapiens chromosome 1, GRCh38.p7 Primary Assembly	32.2	242	100%	5.0	100%	NC_000001.11
Homo sapiens chromosome 16, alternate assembly CHM1_1.1	30.2	111	95%	20	100%	NC_018927.2
Homo sapiens chromosome 17, alternate assembly CHM1_1.1	30.2	84.7	80%	20	100%	NC_018928.2
Homo sapiens chromosome 20, alternate assembly CHM1_1.1	30.2	56.5	71%	20	100%	NC_018931.2
Homo sapiens chromosome 4, GRCh38.p7 Primary Assembly	30.2	139	100%	20	95%	NC_000004.12
Homo sapiens chromosome 16, GRCh38.p7 Primary Assembly	30.2	111	95%	20	100%	NC_000016.10
Homo sapiens chromosome 17, GRCh38.p7 Primary Assembly	30.2	84.7	80%	20	100%	NC_000017.11
Homo sapiens chromosome 20, GRCh38.p7 Primary Assembly	30.2	56.5	71%	20	100%	NC_000020.11

Figure 8.13 Sequences producing hits against the U6 shRNA passenger strand ranked by maximum score.

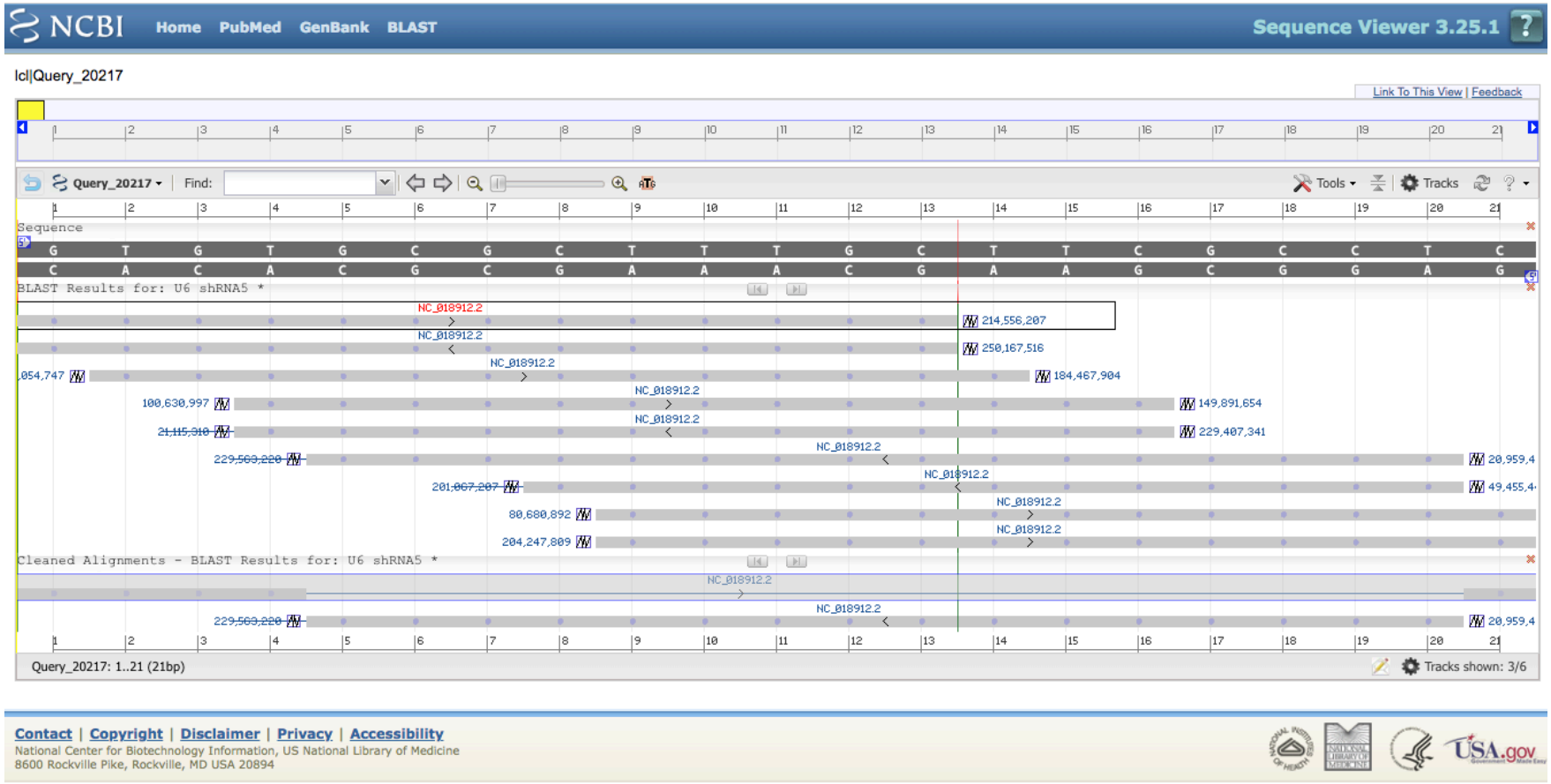


Figure 8.14 Representative alignment of the U6 shRNA 5 passenger strand on chromosome 1

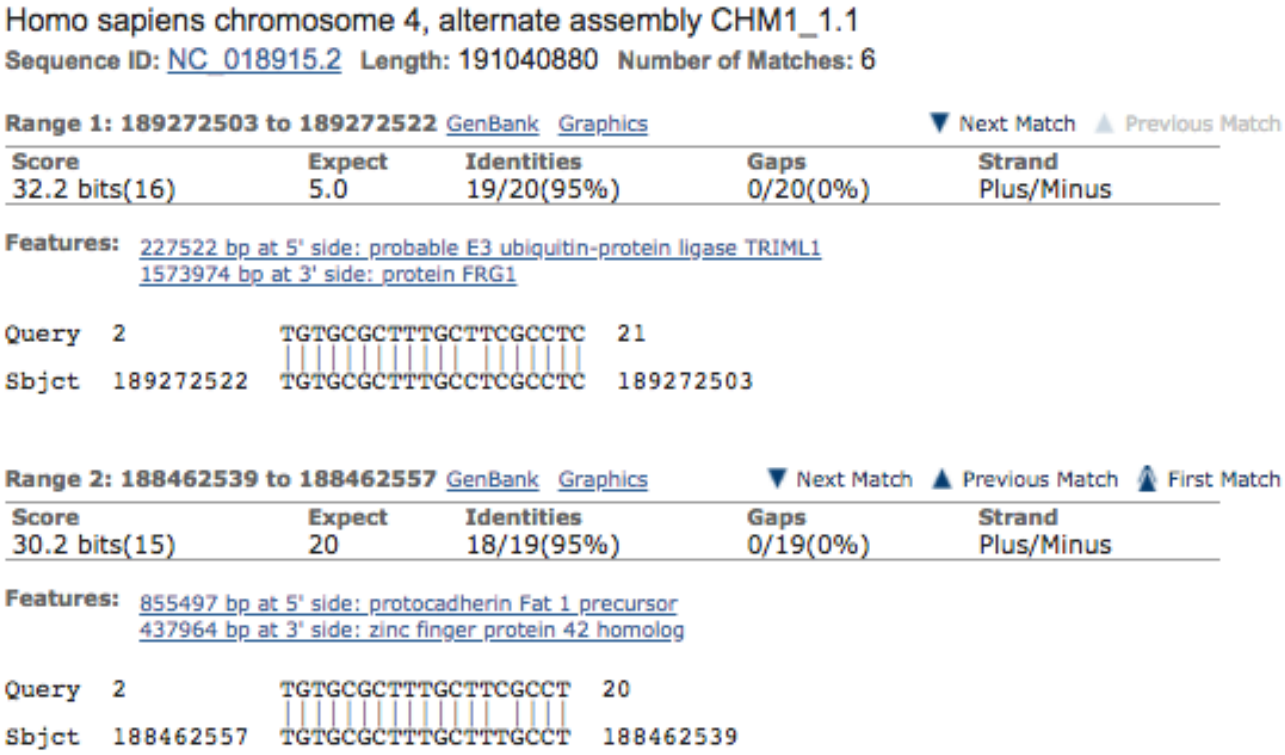


Figure 8.15 Detailed alignment of the U6 shRNA 5 passenger strand on two hits on chromosome 4

8.8 Related additional Publication

Silencing of HIV-1 subtype C primary isolates by expressed small hairpin RNAs targeted to gag.

Cave E, Weinberg MS, Cilliers T, **Carmona S**, Morris L, Arbuthnot P.

AIDS Res Hum Retroviruses. 2006; **22**(5): 401-10

AIDS RESEARCH AND HUMAN RETROVIRUSES
Volume 22, Number 5, 2006, pp. 401–410
© Mary Ann Liebert, Inc.

Silencing of HIV-1 Subtype C Primary Isolates by Expressed Small Hairpin RNAs Targeted to *gag*

ELEANOR CAVE,[1,2] MARC S. WEINBERG,[1] TONIE CILLIERS,[2] SERGIO CARMONA,[1] LYNN MORRIS,[2] and PATRICK ARBUTHNOT[1]

ABSTRACT

Discovery of sequence-specific silencing by activating the RNA interference (RNAi) pathway has led to exciting new strategies for treating infection with human immunodeficiency virus type 1 (HIV-1). Of the HIV-1 subtypes, C is especially common in areas of the world that are worst affected. Although prone to mutation, genome plasticity of this subtype is limited in functionally important regions. We identified conserved sequences within the HIV-1 subtype C *gag* open reading frame and assessed whether they are suitable targets for inhibition of viral replication by RNA Pol III-driven small hairpin RNAs (shRNAs). Initially, the efficacy of each of a panel of 10 shRNAs against HIV-1 was determined using a reporter assay. shRNAs A and B, which targeted the 5′ end of *gag*, were most effective and were used to assess inhibition of replication in cultured cells of two R5 isolates (Du151 and Du422) and one X4 virus (SW7). These shRNAs diminished intracellular HIV-1 *gag* RNA and HIV-1 protein concentrations as well as p24 secretion by up to 80% without inducing an interferon response. However, shRNA-mediated knockdown efficacy against each of these viral isolates varied slightly. These data show successful activation of RNAi to inhibit the replication of biologically distinct HIV-1 subtype C isolates. The effector shRNAs described here are potential candidates for gene therapy applications against the most common global subtype of HIV-1.

INTRODUCTION

EFFECTIVELY TREATING human immunodeficiency virus type 1 (HIV-1) infection presents one of the greatest health challenges facing the world. In many of the worst affected African countries, infection with HIV-1 subtype C is particularly common.[1] Current therapy aimed at inhibiting HIV replication includes the use of drugs that target reverse transcriptase (RT) and protease (PR) enzymes. These agents, particularly in combinations of two or more, have had an important positive impact on the morbidity and mortality of HIV-related illness.[2] However, drug toxicity and resistance remain a concern, which has prompted the search for novel antiretrovirals.

Discovery of the RNA interference (RNAi) pathway has led to exciting new strategies for developing HIV treatment. The endogenous mechanism of RNAi involves processing of larger dsRNA by Dicer to form 21- to 23-bp short interfering RNA (siRNA) duplexes that have 2-nt 3′-OH overhangs.[3,4] One of the strands of the siRNA is incorporated into the RNA-induced silencing complex (RISC) and acts as a guide to target Argonaut 2 (Ago2)-mediated degradation of complementary cytoplasmic RNA.[5] Exogenous silencing is typically induced by synthetic RNA or transcripts produced from U6 or H1 RNA Pol III promoters.[3,6,7] Pol III promoters are constitutively active in most tissues and have the advantage of enabling the transcription of precisely defined RNA sequences. Potent and sustained silencing can be achieved in human cells expressing short hairpin RNAs (shRNAs)[6] and other duplexes that mimic naturally occurring microRNA precursors (pre-miRNAs).[8] These expressed RNA duplexes act as Dicer substrates and can be processed into functional siRNAs without inducing a nonspecific interferon response associated with long (>30 bp) dsRNAs.[9]

RNAi effectors have been successfully targeted to several HIV sequences, resulting in the silencing of genomic and subgenomic viral RNAs of HIV-1 to block both early and late replicative stages of the HIV-1 infection cycle.[8,10–20] Successful inhibition of viral replication has also been achieved by targeting

[1]HBV Research Unit, Department of Molecular Medicine and Haematology, University of the Witwatersrand, Wits 2050, Johannesburg, South Africa.
[2]AIDS Virus Research Unit, National Institute for Communicable Diseases, Sandringham 2131, Johannesburg, South Africa.

host cell HIV-1 receptors and accessory proteins.[21–23] The large HIV-1 sequence diversity may limit the number of conserved sites that are accessible and functional siRNA target sequences, thus representing a significant hurdle to developing successful RNAi-based therapy against the virus.[18] Subtype C alone possesses significant variability,[24] and mutations in target RNA may abolish RNAi activity. Thus, to find sites that are of potential therapeutic importance, we have identified conserved sequences within HIV-1 subtype C *gag* that are sensitive to silencing by Pol III-driven shRNAs.

MATERIALS AND METHODS

shRNA expression vectors

Ten sites (A–J) corresponding to highly conserved regions of the subtype C *gag* open reading frame (ORF) were selected (Fig. 1A) after alignment of 32 HIV-1 subtype C sequences from South Africa (Los Alamos HIV database, http://hiv-web.lanl.gov/content/hiv-db/mainpage.html). All shRNAs were designed to encode guide RNA of 20–22 nucleotides (nt) spanning 1251 bp of the approximately 1500 bp of the *gag* ORF (Fig. 1B). The genetic diversity within these sites was examined with a larger number of sequences from Los Alamos. This included *gag* sequences from subtypes A (≥500), B (≥1,027), C (≥505), D (≥88), and AE (≥149). To generate DNA sequences encoding shRNAs from a human U6 Pol III promoter, a two-step PCR approach was used.[25] The procedure made use of a universal U6 forward primer (5′-GCGCTCGAGTCTAGAAAGGTCGGGCAGGAAGAGGG-3′) for both reactions. shRNA-specific reverse primers for the two rounds of PCR are listed in Table 1. PCR products were cloned into the TA plasmid pDRIVE (Qiagen, Hilden, Germany). Correct sequence and orientation of all clones were verified by automated chain termination sequencing (Inqaba Biotech, Pretoria, South Africa). shRNAs A and D incorporated mismatches in the sense strands within the hairpin, and this is indicated in Table 1.

HIV-1 subtype C viral isolates

Three primary virus strains were used. Du151 and Du422 are R5 viruses and were isolated from female sex workers within 4 months of infection.[26] SW7 is an X4 virus derived from a patient with advanced AIDS.[27] All three viruses have been fully sequenced and shown to be HIV-1 subtype C throughout their genomes.[24,28] Du151 and Du422 are representative South African isolates being used in vaccine development.[26]

HIV-1 subtype C gag-eGFP *reporter plasmid*

The entire *gag* ORF of the HIV-1 subtype C viral isolate Du422 was amplified by PCR and cloned into the pDRIVE TA Cloning vector (Qiagen, Chatsworth, CA) to generate pDRIVE-*gag*. A *Hin*dIII restriction endonuclease site was incorporated into the forward primer upstream of the ORF (5′-GATCAAGCTTATGGGTGCGAGAGCGTCATTAT-3′) and, similarly, an *Xba*I site was added downstream of the *gag* ORF (5′-GATCTCTAGATTATTGAGACAAGGGGTCGCTG-3′). The ORF for enhanced green fluorescent protein (eGFP) was amplified from the previously constructed vector pCH 3091-eGFP,[29] using forward (5′-GATCGGATCCATGGTGAG-

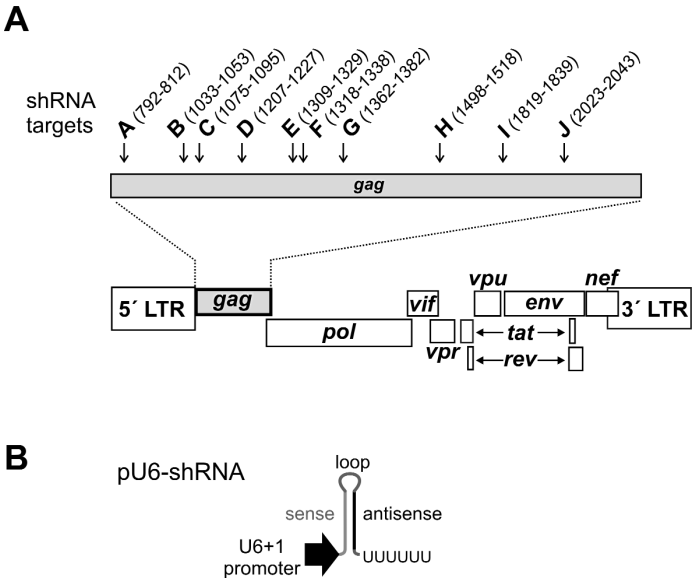


FIG. 1. HIV-1 subtype C genome and shRNA sequences. (**A**) Organization of HIV-1 subtype C genome, with the sites targeted by shRNAs. Open reading frames (ORFs) together with the 5′ and 3′ long terminal repeats (LTRs) are indicated. Arrows above the enlarged *gag* ORF show the sites of shRNAs A–J, and exact coordinates (HBX2 sequence numbering) are given in parentheses. (**B**) Schematic illustration of the expression cassette encoding the predicted shRNAs from the U6+1 promoter. The expressed transcript, which forms a hairpin, is shown below and is indicated as a 20- to 22-bp stem with loop and two U residues following transcriptional termination.

Table 1. Nucleotide Sequences of PCR Reverse Primers Used to Generate HIV U6 shRNA Cassettes[a]

HIV target[b]	*Name*	*Primer sequence*
792–812	Gag-shRNA-1A	5′-ATATTACTACACAAATAATATTGACGTTCTCGCACCC*GGTGTTTCGTCCTTTCCACAAG*-3′
	Gag-shRNA-2A	5′-GATCCTCGAGACTAGTAAAAAA**GGGTGCGAGAGCGTCAATATTAC**TACACAAATAATAT-3′
1033–1053	Gag-shRNA-1B	5′-TGTGTACTACACAAATACACAATAGAGAGTTGCTAC*GGTGTTTCGTCCTTTCCACAAG*-3′
	Gag-shRNA-2B	5′-GATCCTCGAGACTAGTAAAAAA**GTAGCAACTCTCTATTGTGTAC**TACACAAATACACA-3′
1075–1095	Gag-shRNA-1C	5′-TTAGACCTACACAAAGTCTAAGGCTTCCTTGGTGTC*GGTGTTTCGTCCTTTCCACAAG*-3′
	Gag-shRNA-2C	5′-GATCCTCGAGACTAGTAAAAAA**GACACCAAGGAAGCCTTAGAC**CTACACAAAGTCTAA-3′
1207–1227	Gag-shRNA-1D	5′-CAGGCCCTACACAAAGGCATGGTGTACCATCTGCAC*GGTGTTTCGTCCTTTCCACAAG*-3′
	Gag-shRNA-2D	5′-GATCCTCGAGACTAGTAAAAAA**GGGCAAATGGTACACCAGGCC**CTACACAAAGGCCTG-3′
1309–1329	Gag-shRNA-1E	5′-GCCACCCTACACAAAGGTGGCTCCAACTGATAATGC*GGTGTTTCGTCCTTTCCACAAG*-3′
	Gag-shRNA-2E	5′-GATCCTCGAGACTAGTAAAAAA**GCATTATCAGAAGGTGCCACC**CTACACAAAGGTGGC-3′
1318–1338	Gag-shRNA-1F	5′-ACAAGACTACACAAATCTTGTGGGGTGGCTCCTTC*GGTGTTTCGTCCTTTCCACAAG*-3′
	Gag-shRNA-2F	5′-GATCCTCGAGACTAGTAAAAAA**GAAGGAGCCACCCCACAAGAC**TACACAAATCTTGT-3′
1362–1382	Gag-shRNA-1G	5′-GCCATGCTACACAAACATGACTGCTTAATCCCCCCCCC*GGTGTTTCGTCCTTTCCACAAG*-3′
	Gag-shRNA-2G	5′-GATCCTCGAGACTAGTAAAAAA**GGGGGGGGATTAAGCAGTCATGC**TACACAAACATGGC-3′
1498–1518	Gag-shRNA-1H	5′-CCCTTCCTACACAAAGAAGGGTACTAGTAGTTCCTGC*GGTGTTTCGTCCTTTCCACAAG*-3′
	Gag-shRNA-2H	5′-GATCCTCGAGACTAGTAAAAAA**GCAGGAACTACTAGTACCCTTC**CTACACAAAGAAGGG-3′
1819–1839	Gag-shRNA-1I	5′-GATGTCCTACACAAAGACATGCTGTCATCATTTCTTC*GGTGTTTCGTCCTTTCCACAAG*-3′
	Gag-shRNA-2I	5′-GATCCTCGAGACTAGTAAAAAA**GAAGAAATGATGACAGGATGTC**CTACACAAAGACATG-3′
2023–2043	Gag-shRNA-1J	5′-GGAAAGCTACACAAACTTTCCACATTTCCTTCTGCC*GGTGTTTCGTCCTTTCCACAAG*-3′
	Gag-shRNA-2J	5′-GATCCTCGAGACTAGTAAAAAA**GGCAGAAGGAAATGTGGAAAG**CTACACAAACTTTCC-3′

[a]Overlapping sequences are underlined; mismatches incorporated into the sense strand of the hairpin stems are indicated with a double underline; the region complementary to the U6 promoter is italicized; sequences encoding HIV-1 subtype C RNA are in boldface.

[b]HIV-1 subtype C coordinates are given according to HSB2 numbering.

CAAGGGCGAGGA-3′) and reverse (5′-GATCAAGCTTCT-TACTTGTACAGCTCGTCC-3′) primers that included *Bam*HI and *Hin*dIII sites, respectively. The eGFP-encoding PCR product was cloned into the TA vector pDRIVE to generate pDRIVE-*eGFP*. Both Gag- and eGFP-encoding plasmids were sequenced (Inqaba Biotech). The common *Hin*dIII restriction endonuclease site was used to fuse the eGFP- and Gag-encoding sequences and generate pDRIVE-*eGFP-gag*. The *eGFP-gag* sequence was then excised with *Xba*I and *Bam*HI and inserted at corresponding sites in pTRE2hyg (Invitrogen, Carlsbad, CA) to generate the pCMV-*eGFP-gag* reporter plasmid. In this vector, transcription of the fusion sequence is under the control of a modified cytomegalovirus (CMV) promoter.

Transfection and infection of cells in culture

Huh7 cells were maintained in ISE-RPMI with 2.5% fetal calf serum (FCS) and supplemented with penicillin (50 IU/ml) and streptomycin (50 μg/ml) (GIBCO BRL, Paisley, UK). Twenty-four hours before transfection, cells were seeded to 80% confluency in six-well tissue culture plates. Two micrograms of reporter plasmid (pCMV-*eGFP-gag*), 2 μg of the shRNA expression plasmid, and 1 μg of a β-galactosidase-expressing transfection control plasmid (pβactin-βgal)[30] were transfected into cells, using LipofectAMINE 2000 reagent (Invitrogen) according to the manufacturer's instructions. For the mock control, an empty pDRIVE plasmid (2 μg) was included. Equivalent transfection efficiency was verified by staining a duplicate sample set for β-galactosidase.[31] All experiments were conducted in triplicate and, 48 hr posttransfection, the number of cells expressing eGFP was quantified by flow cytometry with confirmatory fluorescence microscopy.

To assess effects of shRNA-expressing plasmids on viral replication, shRNAs A–D were transiently transfected into U87-CD4$^+$CXCR4$^+$ and U87-CD4$^+$CCR5$^+$ cells (NIH AIDS Research and Reference Reagent Program, NIAID, Bethesda, MD), which were maintained in RPMI supplemented with 10% FCS, with penicillin and streptomycin as described above. Twenty-four hours before transfection, cells were seeded to 80% confluency in 24-well tissue culture plates. Cells were infected 24-hr after transfection with the R5 viruses Du151, Du422, and the X4 virus SW7 at 1000 TCID50. Cells were washed on the day after transfection to remove unbound virus. p24 antigen concentration in the culture supernatants was measured 4, 7, and 11 days thereafter as described.[27] On day 11 postinfection, total intracellular RNA was extracted with a MagNA Pure LC RNA isolation kit (Roche, Mannheim, Germany). Cell lysates were also prepared from duplicate plates to measure HIV-1 proteins (see below).

gag *quantitative RT-PCR*

To measure concentrations of HIV-1 *gag* RNA, total RNA (1 μg) was reverse transcribed and then amplified with a QuantiTect one-step RT-PCR kit (Qiagen) according to the manufacturer's instructions. Thereafter, real-time PCR was carried out in a volume of 20 μl, using the Roche Lightcycler 2, with equivalent amounts of template RNA from each of the transfections.[32] Controls included water blanks and RNA extracts that were not subjected to reverse transcription. Thermal cycling parameters consisted of a hot start for 30 sec at 95°C followed by 50 cycles of 57°C for 10 sec, 72°C for 7 sec, and then 95°C for 5 sec. Specificity of the PCR products was verified by melting curve analysis and agarose gel electrophoresis. Crossing point determination was used to quantitate HIV RNA and sample input was normalized, using independent qRT-PCR, to detect *GAPDH* mRNA and analyzed with the Lightcycler relative monocolor software (Roche). Sequences of *gag*- and *GAPDH*-specific primers were as follows: Gag forward (SKT 145), 5′-ACAT-CAAGAAGCCATGCAAAT-3′; Gag reverse (SKT 150), 5′-TGTCACTTCCCCTTGGTTCACTC-3′; GAPDH forward 5′-GAAGGTGAAGGTCGGAGTC-3′; and GAPDH reverse 5′-GAAGATGGTGATGGGATTTC-3′.

Detection of HIV antigens by Western blot analysis

Lysates from U87-CD4$^+$CCR5$^+$ cells (normalized to cell number), which had been infected with the Du422 R5 HIV-1 subtype C isolate, were resolved by 10% PAGE. After transblotting onto a nitrocellulose membrane, HIV proteins were detected with serum from an HIV-1-infected individual and alkaline phosphatase-conjugated goat anti-human secondary antibody (Sigma-Aldrich, Taufkirchen, Germany) according to standard procedures.

TABLE 2. PERCENTAGE INTRA- AND INTERSUBTYPE GENETIC DIVERSITY WITHIN SITES TARGETED BY ANTI-*GAG* SHRNAS

Targeted shRNA	*Subtype A*	*Subtype B*	*Subtype C*[a]	*Subtype D*	*Subtype A_E*
U6-shRNA A	5.9	1.4	**1.2**	5.7	5.5
U6-shRNA B	10.2	13.7	**3.1**	7.4	22.5
U6-shRNA C	7.5	6.4	**1.9**	5.9	5.4
U6-shRNA D	12.5	7.6	**4.9**	4.4	11.4
U6-shRNA E	2.8	1.4	**1.3**	1.5	5.4
U6-shRNA F	3.2	1.3	**2.1**	2.6	5.3
U6-shRNA G	14.2	1.7	**1.7**	4.0	14.3
U6-shRNA H	4.5	2.5	**5.4**	2.1	1.4
U6-shRNA I	4.1	2.7	**2.7**	1.8	10.0
U6-shRNA J	1.6	4.0	**1.5**	2.1	5.1

[a]Subtype C values are given in boldface.

Interferon response

HEK293 cells were propagated in DMEM supplemented with 10% FCS, penicillin (50 IU/ml), and streptomycin (50 μg/ml) (GIBCO-BRL). On the day before transfection, cells were seeded to 80% confluency in 12-well plates. Transfection was carried out with LipofectAMINE (Invitrogen) according to the manufacturer's instructions with a combination of 1 μg of reporter plasmid, pCMV-*eGFP-gag*, 100 ng of poly (I:C) (Sigma, St. Louis, MO), 1 μg of the shRNA expression plasmid, and 1 μg of control plasmid (pTZ-U6+1) lacking the shRNA cassette. RNA was isolated 24 h after transfection, using an automated nucleic acid extraction system (MagNA Pure; Roche Diagnostics, Mannheim, Germany). To measure concentrations of mRNA encoding interferon response-related genes, total RNA was reverse transcribed with Sensiscript (Qiagen), and oligo(dT) according to the manufacturer's instructions. Real-time PCR was carried out in a volume of 20 μl, using the Roche Lightcycler 2, with equivalent amounts of template cDNA from each of the transfections. Controls included water blanks and RNA extracts that were not subjected to reverse transcription. A SYBR green Lightcycler FastStart DNA Master-plus kit (Roche Diagnostics) was used to amplify and detect DNA during the reaction. PCR was carried out in a 20-μl volume and thermal cycling parameters consisted of a hot start for 10 min at 95°C followed by 50 cycles of 57°C for 10 sec, 72°C for 10 sec, and then 95°C for 10 sec. The primer sets used to amplify DNA after reverse transcription were as follows: interferon-β (IFN-β) forward, 5′-TCCAAATTGCTC-TCCTGTTGTGCT-3′; IFN-β reverse, 5′-CCACAGGAGCTT-CTGACACTGAAAA-3′; GAPDH forward, 5′-AGGGGTCA-TTGATGGCAACAATATCCA-3′; GAPDH reverse, 5′-TTT-ACCAGAGTTAAAAGCAGCCCTGGTG-3′; OAS1 forward, 5′-CGAGGGAGCATGAAAACACATTT-3′; OAS1 reverse, 5′-GCAGAGTTGCTGGTAGTTTATGAC-3′; MxA forward, 5′-CTGGTGCTGAAACTGAAGAAAC-3′; and MxA reverse, 5′-ATCTCAATCTCGTAGTCCTGGTA-3′. Specificity of the PCR products was verified by melting curve analysis and agarose gel electrophoresis. Ratios of crossing points of *IFN-β*, *MxA*, or *OAS1* to *GAPDH* were used to quantitate mRNA.

Statistical analysis

Data are expressed as means with standard errors of the mean (SEM). Statistical significance ($p < 0.05$) was determined by one-way ANOVA and Dunnett's multiple comparison test, using the GraphPad Prism software package (GraphPad Software, San Diego, CA).

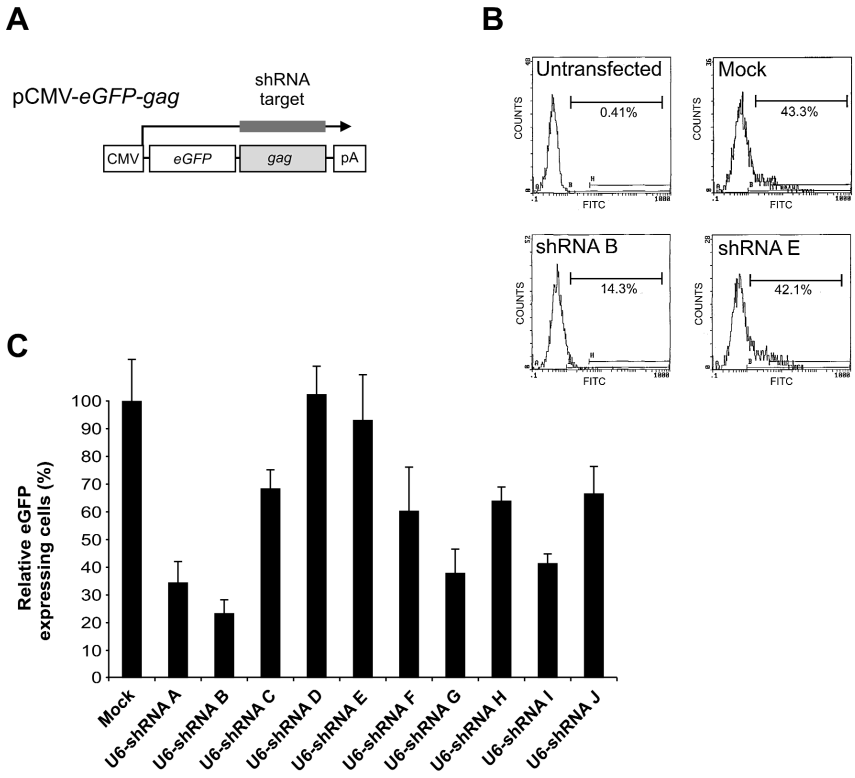


FIG. 2. Inhibition of marker gene expression from *gag-eGFP* fusion reporter vector. (**A**) Schematic illustration of plasmid construct pCMV-*eGFP-gag*. The fused *eGFP-gag* ORF is illustrated together with CMV promoter, fusion sequence transcript (arrow), transcription termination signal (pA), and region targeted by shRNAs A–J. (**B**) Representative flow cytometry histograms indicating the number of cells detected with an FITC filter in the region gated for eGFP. (**C**) shRNA-mediated inhibition of eGFP-Gag fusion marker protein expression in transfected cells. Shown is the percentage of eGFP positive Huh7 cells detected by flow cytometry after transfection with plasmids encoding the indicated shRNAs. In each assay 100,000 events were counted. Results are depicted as means with SEM from four independent transfections.

RESULTS

Identifying shRNA-accessible sites on HIV-1 gag

Ten conserved sites spanning the entire *gag* gene, and identified from the HIV-1 subtype C *gag* ORF isolates of South African origin (Fig. 1A), were used as targets to determine susceptibility to shRNA-mediated inhibition. The variation within these sites among different genetic subtypes was analyzed and the genetic distance for each of the 10 shRNAs was calculated (Table 2). In general, the lowest diversity was found in subtype C isolates, as expected as these shRNAs were designed on subtype C sequences from South Africa. Subtypes D and B showed less variation compared with subtypes A and A_E. Six of the shRNAs showed less than 10% variation across all subtypes.

Initially, to screen for antiviral efficacy, a plasmid containing an *eGFP-gag* fusion sequence (pCMV-*eGFP-gag*) was used in a reporter gene assay. The *gag* ORF of isolate Du422 was placed 3′ of *eGFP* and under the transcriptional control of a CMV promoter such that transcripts from pCMV-*eGFP-gag* contained both *eGFP* and *gag* sequences (Fig. 2A). Flow cytometry and confirmatory fluorescence microscopy were used to detect *eGFP* marker gene expression and to assess the efficacy of anti-*gag* shRNAs by measuring any reduction in the number of eGFP-expressing cells. Equivalent staining for β-galactosidase in duplicate cells verified similar transfection efficiency. This analysis revealed that the number of transfected cells expressing eGFP diminished significantly ($p < 0.05$) when cotransfected with pU6-shRNA A and pU6-shRNA B (Fig. 2B and C). Compared with mock-transfected cells, knockdown of 70% (shRNA A) and 80% (shRNA B) was achieved. shRNAs D and E had no detectable effect on the number of cells expressing eGFP, while shRNA C and shRNA F through J induced only a modest inhibitory effect. Thus, from the panel of shRNA vectors tested, the *gag* sites targeted by shRNA A and shRNA B are most susceptible to RNAi-mediated gene knockdown.

shRNA knockdown of p24 antigen secretion and intracellular viral protein production

shRNAs A, B, C, and D were selected for further analysis based on the knockdown data obtained against the eGFP-Gag reporter. This limited panel included the two optimally acting shRNAs (shRNA A and shRNA B), together with a sequence that had modest (shRNA C) or no (shRNA D) effect according to the reporter gene assay. U87-CD4$^+$CCR5$^+$ and U87-CD4$^+$CXCR4$^+$ cells expressing either CCR5 or CXCR4 coreceptors, respectively, were transiently transfected with shRNA vectors A, B, C, or D, and infected with three different HIV-1

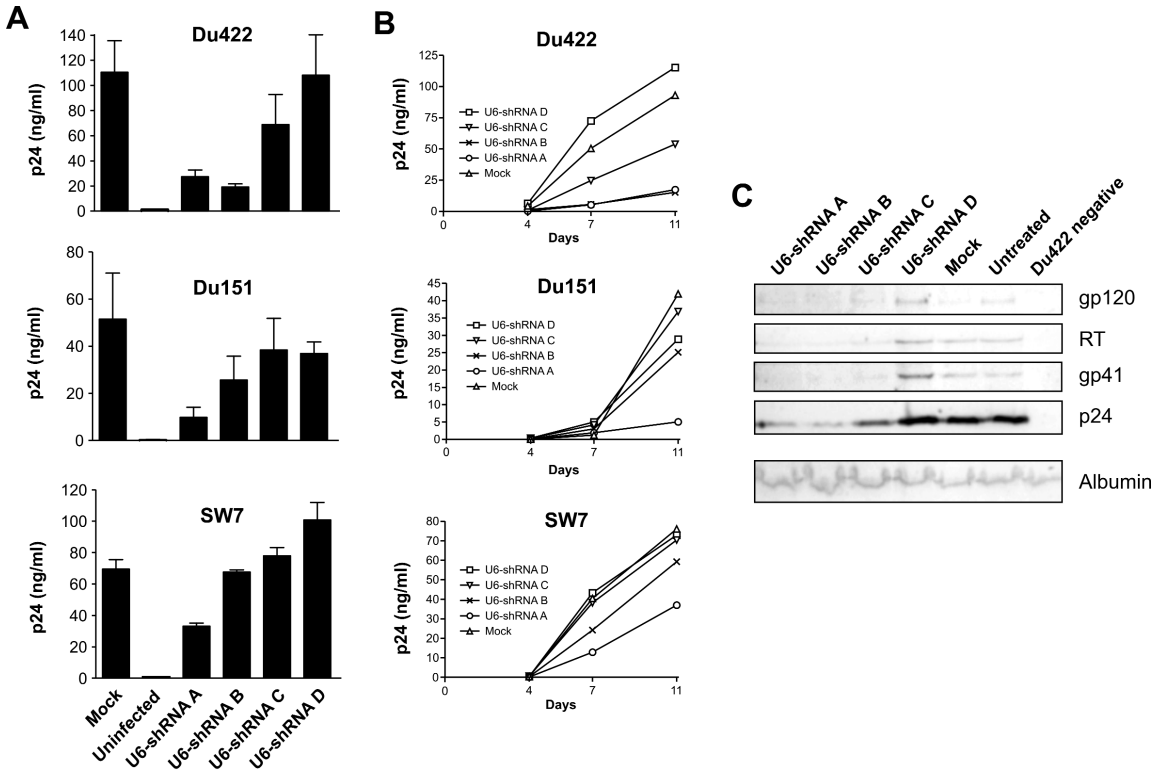
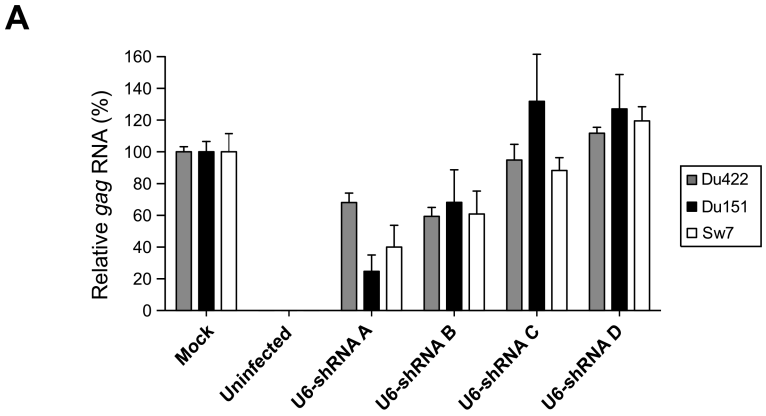


FIG. 3. shRNA-mediated inhibition of HIV-1 subtype C protein production. (**A**) p24 secretion from U87-CD4$^+$ cells expressing either CCR5 or CXCR4 that were transfected with plasmids encoding shRNA A, shRNA B, shRNA C, and shRNA D followed by infection with Du422, Du151, or SW7 HIV-1 subtype C isolates. Values (means and SEM; $n = 3$) are given as nanograms of p24 per milliliters of culture supernatant. (**B**) Replication kinetics of a representative experiment included in (**A**). (**C**) Western blot detection of cellular HIV-1 proteins after transfection with shRNA-encoding plasmids followed by HIV-1 infection with Du422 as described above.

subtype C primary viral isolates. To assess suppression of p24 antigen secretion, culture supernatants were collected 11 days postinfection and p24 antigen concentration was determined by ELISA. shRNA A and shRNA B proved to be the most effective suppressors of p24 secretion and shRNAs C and D did not inhibit p24 secretion relative to control (Fig. 3A). Varying degrees of suppression of p24 secretion was observed, which depended on the viral isolate targeted. A 5-fold knockdown of p24 was observed for shRNA B targeted to isolate Du422, as opposed to a 2-fold and undetected reduction in p24 secretion when targeted to isolates Du151 and SW7, respectively. shRNA A reduced p24 antigen levels significantly in all three isolates ($p < 0.05$), and relative to controls, a 5-fold inhibition was observed for isolates Du151 and Du422, and 2-fold for SW7. The replication kinetics for a single experiment for each of the 3 isolates is shown in Fig. 3B. Viral isolates replicated to varying levels, however there was no difference in the kinetics of replication in presence or absence of shRNA on days 7 or 11. Western blot analysis was used to determine the inhibitory effect of shRNAs on intracellular Du422 HIV-1 subtype C proteins (Fig. 3C). These results showed that major viral proteins gp120, RT, gp41, and p24 were inhibited by shRNAs A and B and not by mock or untreated controls, which further confirmed our previous observations.

shRNA-mediated decrease in gag *RNA concentration in HIV-1-infected cells*

Relative quantitative RT-PCR was used to assess any effect on intracellular *gag* RNA (Fig. 4A). The efficacy of each shRNA against viral infection was generally similar to knockdown of *eGFP-gag* reporter expression and p24 secretion. shRNA D did not diminish *gag* RNA concentration in any of the three isolates when measured relative to mock-treated cells. shRNA C showed a slight inhibitory effect on RNA production from Du422 and SW7 strains that was not significant. No effect was observed for shRNA C when targeted to SW7. The knockdown of RNA elicited by shRNA A varied depending on the viral isolate. Interestingly, shRNA A diminished by up to 75% the viral RNA concentrations in cells infected with Du151 and SW7 ($p < 0.05$) whereas RNA production from isolate Du422 was reduced to a much lesser extent (30%). shRNA A target sequences of all three viral isolates were complementary to the shRNA A antisense strand and match the HIV-1 subtype C consensus (Fig. 4B). Intracellular HIV-1 *gag* RNA concentrations from all isolates were diminished by shRNA B (approximately 40%; $p < 0.05$). The shRNA B-encoded *gag* antisense sequence is complementary to targets of Du422 and SW7, but has a mismatch at position 1047 of Du151 (Fig. 4B). In-



B

	shRNA A		shRNA B	
Subtype C	792	812	1033	1053
consensus:	GGGTGCGAGAGCGTCAATATT		GTAGCAACTCTCTATTGTGTA	
Du422:	---------------------		---------------------	
Du151:	---------------------		----------T----------	
Sw7:	---------------------		---------------------	

	shRNA C		shRNA D	
Subtype C	1075	1095	1207	1227
consensus:	GACACCAAGGAAGCCTTAGAC		GGGCAAATGGTACACCAGGCC	
Du422:	--------------------T-		----------T---------	
Du151:	--------------------T-		----------T---------	
Sw7:	--------------------T-		----------T---------	

FIG. 4. Intracellular *gag* RNA concentrations and HIV-1 subtype C sequences targeted by shRNAs. (**A**) Effect of shRNA-encoding plasmids on *gag* RNA concentrations. Cells were transfected with plasmids encoding shRNA A, shRNA B, shRNA C, and shRNA D and then infected with Du422, Du151, and SW7 HIV-1 subtype C isolates. Total RNA was extracted from the cells 24 hr thereafter. *GAPDH* and *gag* RNA was measured by qRT-PCR. All values are given as a ratio of *gag* to *GAPDH* crossing points and are relative to the mock-treated group (100%). Means and SEMs from four independent experiments are shown. (**B**) HIV-1 consensus sequences and sequences of Du422, Du151, and SW7 isolates in the regions targeted by shRNA A, shRNA B, shRNA C, and shRNA D. Dashes indicate homology and sequence differences are indicated by the nucleotide letter.

terestingly, shRNA B knockdown of Du151 *gag* RNA was not compromised, although the efficacy against SW7 was limited. Mismatches between all viral isolates and shRNA C at position 1095 and shRNA D at position 1219 may have affected RNA knockdown efficacy. However, mismatches at peripheral sites of HIV-1 target sites, such as is found with shRNA C, are usually well tolerated.[18]

Interferon response

Activators of the RNAi pathway can potentially stimulate nonspecific inflammatory effects by activating the interferon response, which in turn is capable of inducing cell death by apoptosis. Double-stranded RNA has been shown to activate the interferon response directly[9] or by interaction with RNA-binding Toll-like receptors (TLR3 and TLR7).[33] Thus, to verify whether induction of the dsRNA-mediated nonspecific interferon response resulted in the observed silencing, we measured mRNA from three genes that are key components of the interferon response: *IFN-β*, *OAS1*, and *MxA* (Fig. 5).[9] Expression of interferon response genes was not increased in HEK293 cells that were transfected with shRNA-expressing plasmids. These observations indicate that the antiviral knockdown induced by the expression of shRNAs A and B was specific to activation of RNAi and not a result of causing interferon response-mediated programmed cell death.

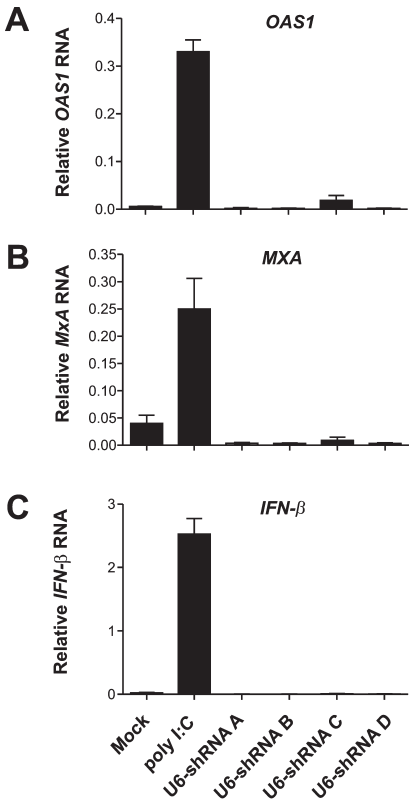


FIG. 5. Assessing shRNA-mediated activation of the interferon response. Quantitative real-time PCR was used to measure *OAS1* (**A**), *MXA* (**B**), or *IFN-β* (**C**). Means (±SEM) of the normalized ratios of *IFN-β*, *MxA*, or *OAS1* to *GAPDH* are indicated from three independent experiments. Cells were transfected with the indicated shRNA-encoding plasmids and poly (I:C) control.

DISCUSSION

The use of RNAi to inhibit HIV-1 represents a novel and potentially powerful antiviral strategy. In this study, we sought to identify candidate shRNAs that were capable of inhibiting gene expression and replication of HIV-1 subtype C viruses isolated from infected South African patients. HIV-1 subtype C infection is particularly common in sub-Saharan Africa, and poses a significant public health problem in the region. Although prone to mutation, the HIV-1 subtype C genome contains conserved sequences within the *gag* ORF.[24] We assessed whether these sequences were good targets for RNAi-mediated inhibition of viral gene expression and replication. From an initial screen of 10 shRNAs, 2 candidate shRNAs (A and B), which both target sites at the 5′ end of the gag^{p17} gene, proved to be the most effective inhibitors of markers of viral replication in cultured cells. Minor differences in knockdown efficacy were observed between the shRNAs, suggesting that different degrees of susceptibility to shRNA-mediated targeting exist between the different viral isolates. shRNA D was found to be largely ineffective, and sequence features of the hairpin and target are likely to contribute to this. First, shRNA D has a high GC content of 63% in the duplex region of the putative siRNA. Previous work has correlated a GC content in the targeted region of between 40 and 52% with efficient silencing.[34] Second, processing of siRNA duplexes with appropriate strand bias is facilitated by weaker H bonding at the 5′ end of the intended guide strand, which correlates with at least 3 A/U base pairs at positions 15–19 of the sense strand. The shRNA D duplex is GC rich at both ends of the putative siRNA duplex, which is likely to inhibit strand separation and incorporation of the HIV-1 antisense guide into RISC. Third, there is a mismatch between shRNA D and the HIV-1 sequences targets of Du422, Du151, and SW7 at position 1219 (nt position 7 on the antisense strand) (Fig. 4B). Single or multiple nucleotide changes in the HIV-1 target sequence may cause variation in shRNA efficacy. Generally, mismatches in central positions of the targeted sequence compromise knockdown significantly, which may be the case for shRNA D. Previously it was shown that a single mutation of the scissile nucleotide necessary for Ago2 cleavage resulted in HIV-1 escape.[35] However, other studies have shown that several sequence mismatches can be tolerated without losing knockdown efficacy,[14,18,36] which suggests that complete viral escape is not always likely. Unlike shRNA D, shRNA A works efficiently against HIV-1 subtype C. This hairpin has a GC content of 52% in the putative siRNA duplex and is AT rich at the 5′ end of the intended anti-HIV-1 guide sequence. Moreover, the sequences of all three subtype C isolates used here match the shRNA A antisense sequence perfectly. Differences in replication kinetics and gene expression rates of the different isolates potentially modulate susceptibility to shRNA knockdown. Also, variation in secondary structures of viral RNAs may affect accessibility of sites to siRNA-mediated attack.[18,37] A combination of these factors is likely to account for the differences in anti-HIV-1 efficacy of each of the antiviral shRNAs.

Anti-*gag* siRNAs have previously been used successfully to inhibit viral pregenomic RNA (before reverse transcription) and also *gag* mRNA, showing that both early and late stages of the infection life cycle can be inhibited.[11,18,38] In this study, we have shown that intracellular *gag* RNA, HIV proteins, and secreted p24 are diminished by shRNA effects. The exact stage(s) of the HIV-1 life cycle when inhibition of viral gene expression occurs is not defined. However, viral RNA and protein production occurs after provirus integration, and inhibition of these markers of replication indicates that shRNAs are effective against HIV-1 after reverse transcription. It is also likely that early stages of the virus life cycle, which include incoming viral RNA, are inhibited by shRNA-mediated silencing.[14] The RNAi pathway acts within the cytoplasm and pregenomic RNA traverses this subcellular compartment during initial stages of viral infection.

Presently little is known about the impact of HIV-1 subtype and biotype diversity on both the short-term and long-term effects of RNAi-mediated inhibition. To date, most studies using RNAi to counter HIV-1 have targeted standard laboratory viral isolates, which are mostly subtype B. Globally, however, HIV-1 subtype C is the predominant strain and this was our rationale for targeting this subtype. However, an analysis of the genetic variation within the shRNA target sequence suggested some conservation across subtypes. In particular, shRNA A target sequence was highly conserved in subtype B; however, at position 807 the A nucleotide was replaced by a G in more than 91% of the sequences. The impact that this may have on efficacy would need to be assessed with subtype B isolates. shRNA B target sequence was far less conserved across subtypes and whether or not shRNA B would show efficacy against viral isolates other than subtype C remains to be tested. Within subtype C, variability of shRNA A and B target sequences was low, at 1.2 and 3.1% respectively. The ability to use RNAi therapeutically for HIV-1 subtype C is contingent on ensuring that isolates diverse in sequence, pathogenesis, and transmissibility are successfully inhibited without inducing significant off-target effects.[39] By targeting expressed shRNAs to *gag*, we have shown specific inhibition of markers of HIV-1 subtype C replication. This effect was observed on viruses with different biological phenotypes and that had been isolated from patients with different disease profiles. These shRNAs represent potential candidates for gene therapy applications against the most prevalent HIV-1 subtype.

ACKNOWLEDGMENTS

We thank Maria Papathanasopoulos for providing the cloned Du422 *gag* gene, Carol Crowther for technical assistance, Marjorie Robbins for the design of primers for the interferon response, and Penny Moore for help with sequence analysis. Financial support for this work from the Carnegie Trust, the South African Innovation Fund, the Cancer Association of South Africa, the South African Poliomyelitis Research Foundation, and the Medical Research Council is gratefully acknowledged. L.M. is an International Senior Research Fellow of the Wellcome Trust, UK. This work formed part of a master's dissertation awarded by the University of the Witwatersrand to E.C.

REFERENCES

1. Esparza J and Bhamarapravati N: Accelerating the development and future availability of HIV-1 vaccines: Why, when, where, and how? Lancet 2000;355:2061–2066.
2. Palella FJ Jr, Delaney KM, Moorman AC, Loveless MO, Fuhrer J, Satten GA, Aschman DJ, and Holmberg SD: Declining morbidity and mortality among patients with advanced human immunodeficiency virus infection. HIV Outpatient Study Investigators. N Engl J Med 1998;338:853–860.
3. Elbashir SM, Harborth J, Lendeckel W, Yalcin A, Weber K, and Tuschl T: Duplexes of 21-nucleotide RNAs mediate RNA interference in cultured mammalian cells. Nature 2001;411:494–498.
4. Hammond SM, Bernstein E, Beach D, and Hannon GJ: An RNA-directed nuclease mediates post-transcriptional gene silencing in *Drosophila* cells. Nature 2000;404:293–296.
5. Liu J, Carmell MA, Rivas FV, Marsden CG, Thomson JM, Song JJ, Hammond SM, Joshua-Tor L, and Hannon GJ: Argonaute2 is the catalytic engine of mammalian RNAi. Science 2004;305: 1437–1441.
6. Brummelkamp TR, Bernards R, and Agami R: A system for stable expression of short interfering RNAs in mammalian cells. Science 2002;296:550–553.
7. Miyagishi M and Taira K: U6 promoter-driven siRNAs with four uridine 3′ overhangs efficiently suppress targeted gene expression in mammalian cells. Nat Biotechnol 2002;20:497–500.
8. Boden D, Pusch O, Silbermann R, Lee F, Tucker L, and Ramratnam B: Enhanced gene silencing of HIV-1 specific siRNA using microRNA designed hairpins. Nucleic Acids Res 2004;32:1154–1158.
9. Sledz CA and Williams BR: RNA interference and double-stranded-RNA-activated pathways. Biochem Soc Trans 2004;32: 952–956.
10. Banerjea A, Li M, Bauer G, Remling L, Lee N, Rossi J, and Akkina R: Inhibition of HIV-1 by lentiviral vector-transduced siRNAs in T-lymphocytes differentiated in SCID-hu mice and $CD34^+$ progenator cell-derived macrophages. Mol Ther 2003;8:62–70.
11. Capodici J, Kariko K, and Weissman D: Inhibition of HIV-1 infection by small interfering RNA-mediated interference. J Immunol 2002;169:5196–5201.
12. Carmichael GG. Medicine: Silencing viruses with RNA. Nature 2002;418:379–380.
13. Coburn GA and Cullen BR: Potent and specific inhibition of human immunodeficiency virus type 1 replication by RNA interference. J Virol 2002;76:9225–9231.
14. Jacque JM, Triques K, and Stevenson M: Modulation of HIV-1 replication by RNA interference. Nature 2002;418:435–438.
15. Laurence J: RNA silencing: A new therapeutic strategy against HIV. AIDS Reader 2003;13:52–53.
16. Lawrence D: RNAi could hold promise in the treatment of HIV. Lancet 2002;359:2007.
17. Lee NS, Dohjima T, Bauer G, Li H, Li MJ, Ehsani A, Salvaterra P, and Rossi J: Expression of small interfering RNAs targeted against HIV-1 *rev* transcripts in human cells. Nat Biotechnol 2002;20:500–505.
18. Lee SK, Dykxhoorn DM, Kumar P, Ranjbar S, Song E, Maliszewski LE, Francois-Bongarcon V, Goldfeld A, Swamy MN, Lieberman J, and Shankar P: Lentiviral delivery of short hairpin RNAs protects CD4 T cells from multiple clades and primary isolates of HIV. Blood 2005;106:818–826.
19. Nelson R: Small interfering RNAs target HIV. Lancet 2003;361: 2214.
20. Qin XF, An DS, Chen IS, and Baltimore D: Inhibiting HIV-1 infection in human T cells by lentiviral-mediated delivery of small interfering RNA against CCR5. Proc Natl Acad Sci USA 2003; 100:183–188.

21. Anderson J and Akkina R: HIV-1 resistance conferred by siRNA cosuppression of CXCR4 and CCR5 coreceptors by a bispecific lentiviral vector. AIDS Res Ther 2005;2:1.
22. Chiu YL, Cao H, Jacque JM, Stevenson M, and Rana TM: Inhibition of human immunodeficiency virus type 1 replication by RNA interference directed against human transcription elongation factor P-TEFb (CDK9/CyclinT1). J Virol 2004;78:2517–2529.
23. Kameoka M, Nukuzuma S, Itaya A, Tanaka Y, Ota K, Ikuta K, and Yoshihara K: RNA interference directed against poly(ADP-ribose) polymerase 1 efficiently suppresses human immunodeficiency virus type 1 replication in human cells. J Virol 2004; 78:8931–8934.
24. van Harmelen J, Williamson C, Kim B, Morris L, Carr J, Karim SS, and McCutchan F: Characterization of full-length HIV type 1 subtype C sequences from South Africa. AIDS Res Hum Retroviruses 2001;17:1527–1531.
25. Castanotto D, Li H, and Rossi JJ: Functional siRNA expression from transfected PCR products. RNA 2002;8:1454–1460.
26. Williamson C, Morris L, Maughan MF, Ping L-H, Dryga SA, Thomas R, Reap EA, Cilliers T, van Harmelen J, Pascual J, Ramjee G, Gray G, Johnston R, Abdool-Karim S, and Swanstron R: Characterization and selection of HIV-1 subtype C isolates for use in vaccine development. AIDS Res Hum Retroviruses 2003;19: 133–144.
27. Cilliers T, Nhlapho J, Coetzer M, Orlovic D, Ketas T, Olson W, Moore J, Trkola A, and Morris L: The CCR5 and CXCR4 coreceptors are both used by human immunodeficiency virus type 1 primary isolates from subtype C. J Virol 2003;77:4449–4456.
28. Papathanasopoulos MA, Cilliers T, Morris L, Mokili JL, Dowling W, Birx DL, and McCutchan FE: Full-length genome analysis of HIV-1 subtype C utilizing CXCR4 and intersubtype recombinants isolated in South Africa. AIDS Res Hum Retroviruses 2002;18: 879–886.
29. Passman M, Weinberg M, Kew M, and Arbuthnot P: *In situ* demonstration of inhibitory effects of hammerhead ribozymes that are targeted to the hepatitis Bx sequence in cultured cells. Biochem Biophys Res Commun 2000;268:728–733.
30. Wang C and Stiles CD: Platelet-derived growth factor α receptor gene expression: Isolation and characterization of the promoter and upstream regulatory elements. Proc Natl Acad Sci USA 1994; 91:7061–7065.
31. Sanes JR, Rubenstein JL, and Nicolas JF: Use of a recombinant retrovirus to study post-implantation cell lineage in mouse embryos. EMBO J 1986;5:3133–3142.
32. Rekhviashvili N, Stevens G, Scott L, and Stevens W: FluorogenicLUX primer for quantitation of HIV-1 by real-time RT-PCR. Mol Biotechnol 2006;32:101–110.
33. Sen GC and Sarkar SN: Transcriptional signaling by double-stranded RNA: role of TLR3. Cytokine Growth Factor Rev 2005; 16:1–14.
34. Khvorova A, Reynolds A, and Jayasena D: Functional siRNAs and miRNAs exhibit strand bias. Cell 2003;115:209–216.
35. Boden D, Pusch O, Silbermann R, Lee F, Tucker L, and Ramratnam B: Human immunodeficiency virus type 1 escape from RNA Interference. J Virol 2003;77:11531–11535.
36. Amarzguioui M, Holen T, Babaie E, and Prydz H: Tolerance for mutations and chemical modifications in a siRNA. Nucleic Acids Res 2003;31:589–595.
37. Westerhout EM, Ooms M, Vink M, Das AT, and Berkhout B: HIV-1 can escape from RNA interference by evolving an alternative structure in its RNA genome. Nucleic Acids Res 2005;33:796–804.
38. Pusch O, Boden D, Silbermann R, Lee F, Tucker L, and Ramratnam B: Nucleotide sequence homology requirements of HIV-1–specific short hairpin RNA. Nucleic Acids Res 2003;31: 6444–6449.
39. Hannon GJ and Rossi JJ: Unlocking the potential of the human genome with RNA interference. Nature 2004;431:371–378.

Address reprint requests to:
Marc S. Weinberg
HBV Research Unit
Department of Molecular Medicine and Haematology
University of the Witwatersrand
Private Bag X3
Wits 2050, Johannesburg, South Africa

E-mail: weinbergms@pathology.wits.ac.za

8.9 Similarity Report

turnitin

Digital Receipt

This receipt acknowledges that Turnitin received your paper. Below you will find the receipt information regarding your submission.

The first page of your submissions is displayed below.

Submission author:	Sergio Carmona
Assignment title:	PhD thesis
Submission title:	00200208:Intro_&_Discussion_The..
File name:	c-9f74f198e27e_Intro___Discussi...
File size:	6.85M
Page count:	47
Word count:	11,184
Character count:	64,474
Submission date:	29-Mar-2018 06:31AM (UTC+0200)
Submission ID:	938022210



Chapter 1: INTRODUCTION

1.1 Chronic hepatitis B virus infection, a global burden of disease

Copyright 2018 Turnitin. All rights reserved.

00200208:Intro_&_Discussion_Thesis_Final_Turn_version.docx

by Sergio Carmona

Submission date: 29-Mar-2018 06:31AM (UTC+0200)
Submission ID: 938022210
File name: c-9f74f198e27e_Intro___Discussion_Thesis_Final_Turn_version.docx (6.85M)
Word count: 11184
Character count: 64474

Chapter 1: INTRODUCTION

1.1 Chronic hepatitis B virus infection, a global burden of disease

In 2015, an estimated 257 million people were living with chronic hepatitis B virus (HBV) infection and 2.7 million are co-infected with HIV {WHO, 2017 #1}. Worldwide, it is estimated that approximately two billion people have evidence of present or past infection with HBV. The prevalence of chronic infection, defined as persistence of HBV surface antigen (HBsAg) for at least six months, varies markedly by age and by geographic distribution (Figure 1.1), with the highest burden of disease observed in sub-Saharan Africa and East Asia {WHO, 2016 #2}. The large burden of chronic HBV infection is exacerbated by the inadequate efficacy of available licensed antivirals and limited access in highly endemic areas. Developing new strategies to target chronic HBV infection thus remains critical.

00200208:Intro_&_Discussion_Thesis_Final_Turn_version.do…

ORIGINALITY REPORT

11%	5%	9%	0%
SIMILARITY INDEX	INTERNET SOURCES	PUBLICATIONS	STUDENT PAPERS

PRIMARY SOURCES

1	Piero L. Almasio. "Management of hepatitis B virus infection in the underprivileged world : Editorial", Liver International, 07/2011 Publication	2%
2	who.int Internet Source	2%
3	"Hepatitis B virus infection: Understanding its epidemiology, course, and diagnosis", Cleveland Clinic Journal of Medicine, 12/01/2008 Publication	1%
4	id-ea.org Internet Source	1%
5	www.perinatology.com Internet Source	1%
6	www.hifazat.org Internet Source	1%
7	www.fsk.it Internet Source	1%

8	Yameng Pei, Chunting Wang, S. Frank Yan, Gang Liu. "Past, Current, and Future Developments of Therapeutic Agents for Treatment of Chronic Hepatitis B Virus Infection", Journal of Medicinal Chemistry, 2017 Publication	1%
9	Dieter Glebe, Alexander König. "Molecular Virology of Hepatitis B Virus and Targets for Antiviral Intervention", Intervirology, 2014 Publication	1%
10	Advances in Experimental Medicine and Biology, 2015. Publication	1%

Exclude quotes	On	Exclude matches	< 5 words
Exclude bibliography	On		

8.10 Declarations and co-authors agreement

Declaration: Student's contribution to article(s) and agreement of co-author(s)

I, Sergio Carmona, student number 91133988E, declare that this Thesis is my own work and that I contributed adequately towards research findings published in the articles stated below which are included in my Thesis.

Signature of Student ..... Date 19 Feb, 2018

Name of Primary Supervisor: Prof. Patrick Arbuthnot

Signature of Primary Supervisor ..... Date 29 March 2018

Agreement by co-authors: By signing this declaration, the co-authors listed below agree to the use of the article(s) by the student as part of his Thesis. In cases where the student is not the 1st author of a published article, the primary supervisor must explain (under comments) why the student is entitled to use the paper for his degree purposes.

1. **Article 1:**

   Title: Exploiting the RNA interference pathway to counter hepatitis B virus replication.

   Liver Int. 2005;25(1):9-15.

   Authors: Arbuthnot, P., S. Carmona, and A. Ely.

Authors	Name	Signature	Date
1st author	Arbuthnot, P.		29/3/18
2nd author	Carmona, S.		19.Feb 18
3rd author	Ely, A.		23/02/18

Comments by primary supervisor: FULLY ENDORSED

2. **Article 2:**

Title: Effective inhibition of HBV replication in vivo by anti-HBx short hairpin RNAs.

Mol Ther. 2006; 13(2): 411-21.

Carmona, S., A. Ely, C. Crowther, N. Moolla, F. H. Salazar, P. L. Marion, N. Ferry, M. S. Weinberg, and P. Arbuthnot.

Authors	Name	Signature	Date
1st author	Carmona, S.	S. Qetil	19 Feb. 18
2nd author	Ely, A.		23/02/18
3rd author	Crowther, C.		24/02/18
4th author	Moolla, N.		19.02.18
5th author	Weinberg, M. S.	approved provided by email	28.2.18
6th author	Arbuthnot, A.P.	Patrick Arbuthnot	29/3/2018

Comments by primary supervisor: FULLY ENDORSED

3. **Article 3:**

Title: Specific inhibition of HBV replication in vitro and in vivo with expressed long hairpin RNA.

Mol Ther. 2007; 15(3): 534-41.

Weinberg, M. S., A. Ely, S. Barichievy, C. Crowther, S. Mufamadi, S. Carmona, and P. Arbuthnot.

Authors	Name	Signature	Date
1st author	Weinberg, M. S	Agreement provided electronically	28.2.18
2nd author	Ely, A.		23/02/18
3rd author	Crowther, C.		24/02/18
4th author	Mufamadi, S.	covered by senior author	
5th author	Carmona, S.	S. Qetil	19 Feb. 18
6th author	Arbuthnot, P.	Patrick Arbuthnot	29/3/18

Comments by primary supervisor: FULLY ENDORSED

4. **Article 4:**

Title: Controlling HBV replication in vivo by intravenous administration of triggered PEGylated siRNA-nanoparticles.

Mol Pharm. 2009; 6(3): 706-17.

Carmona, S., Jorgensen, M. R., Kolli, S., Crowther, C., Salazar, F. H., Marion, P. L., Fujino, M., Natori, Y., Thanou, M., Arbuthnot, P. and Miller, A. D.

Authors	Name	Signature	Date
1st author	Carmona, S.	S. Jorril	19 Feb. 18
4th author	Crowther, C.		24/02/18
10th author	Arbuthnot, P.		29/3/18
Senior author	Miller, A. D.	Agreement provided (email)	

Comments by primary supervisor: FULLY ENDORSED

5. **Article 5:**

Title: DODAG; a versatile new cationic lipid that mediates efficient delivery of pDNA and siRNA.

J Control Release. 2010; 143(2): 222-32.

Mevel, M., Kamaly, N., Carmona, S., Oliver, M. H., Jorgensen, M. R., Crowther, C., Salazar, F. H., Marion, P. L., Fujino, M., Natori, Y., Thanou, M., Arbuthnot, P., Yaouanc, J. J., Jaffres, P. A. and Miller, A. D.

Authors	Name	Signature	Date
1st author	} Agreement provided by A.D. Miller as senior Author.		
2nd author			
3rd author	Carmona, S.	S. Jorril	19 Feb. 18
6th author	Crowther, C.		24/02/18

12th author	Arbuthnot, P.	[signature]	29/3/2014
Senior author	Miller, A. D.	Agreement provided (email)	

Comments by primary supervisor:

FULLY ENDORSED

SENIOR AUTHOR, PROF ANDREW MILLER, PROVIDED AGREEMENT ON BEHALF OF UNAVAILABLE AUTHORS.

UNIVERSITY OF THE WITWATERSRAND, JOHANNESBURG

FACULTY OF HEALTH SCIENCES

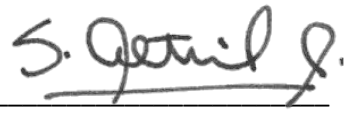
PLAGIARISM DECLARATION TO BE SIGNED BY ALL HIGHER DEGREE STUDENTS

SENATE PLAGIARISM POLICY: APPENDIX ONE

I Sergio Carmona (Student number: 9113398E) am a student registered for the degree of PhD in the academic year 2018.

I hereby declare the following:

- I am aware that plagiarism (the use of someone else's work without their permission and/or without acknowledging the original source) is wrong.
- I confirm that the work submitted for assessment for the above degree is my own unaided work except where I have explicitly indicated otherwise.
- I have followed the required conventions in referencing the thoughts and ideas of others.
- I understand that the University of the Witwatersrand may take disciplinary action against me if there is a belief that this is not my own unaided work or that I have failed to acknowledge the source of the ideas or words in my writing.
- I have included as an appendix a report from "Turnitin" (or other approved plagiarism detection) software indicating the level of plagiarism in my research document.

Signature:  Date: 16 March, 2018

Chapter 9: References

1. WHO. Hepatitis B Fact Sheet July 20172017 [Available from: http://www.who.int/mediacentre/factsheets/fs204/en/.

2. WHO. GLOBAL HEALTH SECTOR STRATEGY ON VIRAL HEPATITIS, 2016–2021. In: Global Hepatitis Programme DoHA, editor. Geneva: WHO; 2016.

3. Schmidt RM, Middleman AB. The importance of hepatitis B vaccination among adolescents. J Adolesc Health. 2001;29(3):217-22.

4. Rich JD, Ching CG, Lally MA, Gaitanis MM, Schwartzapfel B, Charuvastra A, et al. A review of the case for hepatitis B vaccination of high-risk adults. Am J Med. 2003;114(4):316-8.

5. Hilleman MR. Plasma derived hepatitis B vaccine-a breakthrough

in preventive medicine. In: R E, editor. Hepatitis B vaccines in

clinical practice. New York: Marcel Dekker; 1992. p. 17-39.

6. Vryheid RE, Kane MA, Muller N, Schatz GC, Bezabeh S. Infant and adolescent hepatitis B immunization up to 1999: a global overview. Vaccine. 2000;19(9-10):1026-37.

7. WHO. Expanded programme on immunization.

Global advisory group. Part 1. 1992.

8. Ott JJ, Stevens GA, Groeger J, Wiersma ST. Global epidemiology of hepatitis B virus infection: new estimates of age-specific HBsAg seroprevalence and endemicity. Vaccine. 2012;30(12):2212-9.

9. WHO. Hepatitis B vaccines: WHO position paper – July 2017 2017 [Available from: http://apps.who.int/iris/bitstream/10665/255841/1/WER9227.pdf?ua=1.

10. Franco E, Bagnato B, Marino MG, Meleleo C, Serino L, Zaratti L. Hepatitis B: Epidemiology and prevention in developing countries. World J Hepatol. 2012;4(3):74-80.

11. Lavanchy D. Hepatitis B virus epidemiology, disease burden, treatment, and current and emerging prevention and control measures. J Viral Hepat. 2004;11(2):97-107.

12. McMahon BJ. The natural history of chronic hepatitis B virus infection. Semin Liver Dis. 2004;24 Suppl 1:17-21.

13. Hoofnagle JH, Doo E, Liang TJ, Fleischer R, Lok AS. Management of hepatitis B: summary of a clinical research workshop. Hepatology. 2007;45(4):1056-75.

14. Prince AM, Lee DH, Brotman B. Infectivity of blood from PCR-positive, HBsAg-negative, anti-HBs-positive cases of resolved hepatitis B infection. Transfusion. 2001;41(3):329-32.

15. Brunetto MR, Giarin MM, Oliveri F, Chiaberge E, Baldi M, Alfarano A, et al. Wild-type and e antigen-minus hepatitis B viruses and course of chronic hepatitis. Proc Natl Acad Sci U S A. 1991;88(10):4186-90.

16. Carman WF, Jacyna MR, Hadziyannis S, Karayiannis P, McGarvey MJ, Makris A, et al. Mutation preventing formation of hepatitis B e antigen in patients with chronic hepatitis B infection. Lancet. 1989;2(8663):588-91.

17. Kramvis A, Bukofzer S, Kew MC, Song E. Nucleic acid sequence analysis of the precore region of hepatitis B virus from sera of southern African black adult carriers of the virus. Hepatology. 1997;25(1):235-40.

18. Alonso S, Guerra AR, Carreira L, Ferrer JA, Gutierrez ML, Fernandez-Rodriguez CM. Upcoming pharmacological developments in chronic hepatitis B: can we glimpse a cure on the horizon? BMC Gastroenterol. 2017;17(1):168.

19. Terrault NA, Bzowej NH, Chang KM, Hwang JP, Jonas MM, Murad MH, et al. AASLD guidelines for treatment of chronic hepatitis B. Hepatology. 2016;63(1):261-83.

20. WHO. Guidelines for the prevention, care and treatment of persons with chronic hepatitis B infection. 2015.

21. Janssen HL, van Zonneveld M, Senturk H, Zeuzem S, Akarca US, Cakaloglu Y, et al. Pegylated interferon alfa-2b alone or in combination with lamivudine for HBeAg-positive chronic hepatitis B: a randomised trial. Lancet. 2005;365(9454):123-9.

22. Marcellin P, Lau GK, Bonino F, Farci P, Hadziyannis S, Jin R, et al. Peginterferon alfa-2a alone, lamivudine alone, and the two in combination in patients with HBeAg-negative chronic hepatitis B. N Engl J Med. 2004;351(12):1206-17.

23. Seeger C ZF, Mason WS. Hepadnaviruses. In: Knipe DM HP, Cohen JI, Griffin DE, Lamb RA, Martin MA, Racaniello VR, Roizman B, editor. Fields virology. II. 6th ed. Philadelphia, PA.: Lippincott Williams & Wilkins; 2013. p. p 2185–221.

24. Schinazi RF, Ehteshami M, Bassit L, Asselah T. Towards HBV curative therapies. Liver International. 2018;38:102-14.

25. Bogomolov P, Alexandrov A, Voronkova N, Macievich M, Kokina K, Petrachenkova M, et al. Treatment of chronic hepatitis D with the entry inhibitor myrcludex B: First results of a phase Ib/IIa study. J Hepatol. 2016;65(3):490-8.

26. Wang XJ, Hu W, Zhang TY, Mao YY, Liu NN, Wang SQ. Irbesartan, an FDA approved drug for hypertension and diabetic nephropathy, is a potent inhibitor for hepatitis B virus entry by disturbing Na(+)-dependent taurocholate cotransporting polypeptide activity. Antiviral Res. 2015;120:140-6.

27. Agarwal K, Cheng, W., Sievert, W., et al., editor Bi-weekly dosing of ARB-1467 LNP siRNA in HBeAg negative, virally suppressed patients with chronic HBV infection leads to deeper declines in HBsAg and potential association with IL28b. The Liver Meeting; 2017 21 October; Washington, DC, USA.

28. Mueller H, Wildum S, Luangsay S, Walther J, Lopez A, Tropberger P, et al. A novel orally available small molecule that inhibits hepatitis B virus expression. Journal of Hepatology.68(3):412-20.

29. Han KKJ ER, Oliver S, et al, editor Safety, tolerability and pharmacokinetics of GSK3389404, an antisense oligonucleotide for the treatment of chronic hepatitis B (CHB) infection: a randomized, double infection: a randomized, double-blind, placebo-controlled, dose-escalation, first time in human study. The Liver Meeting; 2017 21 October; Washington, DC. USA.

30. Moyo B, Bloom K, Scott T, Ely A, Arbuthnot P. Advances with using CRISPR/Cas-mediated gene editing to treat infections with hepatitis B virus and hepatitis C virus. Virus Res. 2018;244:311-20.

31. Kennedy EM, Bassit LC, Mueller H, Kornepati AV, Bogerd HP, Nie T, et al. Suppression of hepatitis B virus DNA accumulation in chronically infected cells using a bacterial CRISPR/Cas RNA-guided DNA endonuclease. Virology. 2015;476:196-205.

32. Bloom K, Ely A, Mussolino C, Cathomen T, Arbuthnot P. Inactivation of hepatitis B virus replication in cultured cells and in vivo with engineered transcription activator-like effector nucleases. Mol Ther. 2013;21(10):1889-97.

33. Weber ND, Stone D, Sedlak RH, De Silva Feelixge HS, Roychoudhury P, Schiffer JT, et al. AAV-mediated delivery of zinc finger nucleases targeting hepatitis B virus inhibits active replication. PLoS One. 2014;9(5):e97579.

34. Bazinet M, Pantea V, Cebotarescu V, Cojuhari L, Jimbei P, Albrecht J, et al. Safety and efficacy of REP 2139 and pegylated interferon alfa-2a for treatment-naive patients with chronic hepatitis B virus and hepatitis D virus co-infection (REP 301 and REP 301-LTF): a non-randomised, open-label, phase 2 trial. Lancet Gastroenterol Hepatol. 2017;2(12):877-89.

35. Cai D, Mills C, Yu W, Yan R, Aldrich CE, Saputelli JR, et al. Identification of disubstituted sulfonamide compounds as specific inhibitors of hepatitis B virus covalently closed circular DNA formation. Antimicrob Agents Chemother. 2012;56(8):4277-88.

36. Gane E, Gaggar A, Nguyen AH, Subramanian GM, McHutchison JG, Schwabe C, et al. A phase1 study evaluating anti-PD-1 treatment with or without GS-4774 in HBeAg negative chronic hepatitis B patients. Journal of Hepatology.66(1):S26-S7.

37. Sprinz M, editor Phase 1b clinical trial of TG1050 a novel HBV-targeted immunotherapy in NUC suppressed chronic hepatitis B (CHB) patients: safety and early immunological data following single administration. The Liver Meeting; 2017 21 October; Washington, DC. USA.

38. Boni C, Vecchi A, Rossi M, Laccabue D, Giuberti T, Alfieri A, et al. TLR7 Agonist Increases Responses Of HBV-Specific T Cells And Natural Killer Cells In Patients With Chronic Hepatitis B Treated With Nucleos(T)Ide Analogues. Gastroenterology. 2018.

39. Locarnini S, Wong, D., Jackson, K. et al. , editor Novel anti-viral activity of SB 9200, a RIGI agonist; results from Cohort 1 of the ACHIEVE trial. The American Association for the Study of Liver Diseases; 2017 21 October; Washington, DC, USA.

40. Summers J, Mason WS. Replication of the genome of a hepatitis B--like virus by reverse transcription of an RNA intermediate. Cell. 1982;29(2):403-15.

41. Carmona S, Ely A, Crowther C, Moolla N, Salazar FH, Marion PL, et al. Effective inhibition of HBV replication in vivo by anti-HBx short hairpin RNAs. Mol Ther. 2006;13(2):411-21.

42. Ou JH, Laub O, Rutter WJ. Hepatitis B virus gene function: the precore region targets the core antigen to cellular membranes and causes the secretion of the e antigen. Proc Natl Acad Sci U S A. 1986;83(6):1578-82.

43. Takahashi K, Machida A, Funatsu G, Nomura M, Usuda S, Aoyagi S, et al. Immunochemical structure of hepatitis B e antigen in the serum. J Immunol. 1983;130(6):2903-7.

44. Okamoto H, Yotsumoto S, Akahane Y, Yamanaka T, Miyazaki Y, Sugai Y, et al. Hepatitis B viruses with precore region defects prevail in persistently infected hosts along with seroconversion to the antibody against e antigen. J Virol. 1990;64(3):1298-303.

45. Ganem D, Prince AM. Hepatitis B virus infection--natural history and clinical consequences. N Engl J Med. 2004;350(11):1118-29.

46. Heermann KH, Goldmann U, Schwartz W, Seyffarth T, Baumgarten H, Gerlich WH. Large surface proteins of hepatitis B virus containing the pre-s sequence. J Virol. 1984;52(2):396-402.

47. Fields BN, Knipe DM, Howley PM. Fields' virology. 5th ed. / editors-in-chief, David M. Knipe, Peter M. Howley ; associate editors, Diane E. Griffin ... [et al.]. ed. Philadelphia, Pa. ; London: Wolters Kluwer/Lippincott Williams & Wilkins; 2007. 2 v. (xix, 3091, I-86 p.) p.

48. Kamimura T, Yoshikawa A, Ichida F, Sasaki H. Electron microscopic studies of Dane particles in hepatocytes with special reference to intracellular development of Dane particles and their relation with HBeAg in serum. Hepatology. 1981;1(5):392-7.

49. Guo WT, Bell KD, Ou JH. Characterization of the hepatitis B virus EnhI enhancer and X promoter complex. J Virol. 1991;65(12):6686-92.

50. Sugata F, Chen HS, Kaneko S, Purcell RH, Miller RH. Analysis of the X gene promoter of woodchuck hepatitis virus. Virology. 1994;205(1):314-20.

51. Slagle BL, Bouchard MJ. Hepatitis B Virus X and Regulation of Viral Gene Expression. Cold Spring Harb Perspect Med. 2016;6(3):a021402.

52. Tang H, Oishi N, Kaneko S, Murakami S. Molecular functions and biological roles of hepatitis B virus x protein. Cancer Sci. 2006;97(10):977-83.

53. Schek N, Bartenschlager R, Kuhn C, Schaller H. Phosphorylation and rapid turnover of hepatitis B virus X-protein expressed in HepG2 cells from a recombinant vaccinia virus. Oncogene. 1991;6(10):1735-44.

54. Urban S, Hildt E, Eckerskorn C, Sirma H, Kekule A, Hofschneider PH. Isolation and molecular characterization of hepatitis B virus X-protein from a baculovirus expression system. Hepatology. 1997;26(4):1045-53.

55. Kim YH, Kang SK, Lee YI. Functional analysis of hepatitis B virus transactivator X: implication of the leucine zipper-like region and C-terminal seven conserved amino acids in functional regions. Biochem Biophys Res Commun. 1993;197(2):894-903.

56. Kumar V, Jayasuryan N, Kumar R. A truncated mutant (residues 58-140) of the hepatitis B virus X protein retains transactivation function. Proc Natl Acad Sci U S A. 1996;93(11):5647-52.

57. Misra KP, Mukherji A, Kumar V. The conserved amino-terminal region (amino acids 1-20) of the hepatitis B virus X protein shows a transrepression function. Virus Res. 2004;105(2):157-65.

58. Murakami S, Cheong JH, Kaneko S. Human hepatitis virus X gene encodes a regulatory domain that represses transactivation of X protein. J Biol Chem. 1994;269(21):15118-23.

59. Dandri M, Petersen J, Stockert RJ, Harris TM, Rogler CE. Metabolic labeling of woodchuck hepatitis B virus X protein in naturally infected hepatocytes reveals a bimodal half-life and association with the nuclear framework. J Virol. 1998;72(11):9359-64.

60. Doria M, Klein N, Lucito R, Schneider RJ. The hepatitis B virus HBx protein is a dual specificity cytoplasmic activator of Ras and nuclear activator of transcription factors. EMBO J. 1995;14(19):4747-57.

61. Hoare J, Henkler F, Dowling JJ, Errington W, Goldin RD, Fish D, et al. Subcellular localisation of the X protein in HBV infected hepatocytes. J Med Virol. 2001;64(4):419-26.

62. Bouchard MJ, Schneider RJ. The enigmatic X gene of hepatitis B virus. J Virol. 2004;78(23):12725-34.

63. Wei C, Ni C, Song T, Liu Y, Yang X, Zheng Z, et al. The hepatitis B virus X protein disrupts innate immunity by downregulating mitochondrial antiviral signaling protein. J Immunol. 2010;185(2):1158-68.

64. Gearhart TL, Bouchard MJ. The hepatitis B virus HBx protein modulates cell cycle regulatory proteins in cultured primary human hepatocytes. Virus Res. 2011;155(1):363-7.

65. Martin-Vilchez S, Lara-Pezzi E, Trapero-Marugan M, Moreno-Otero R, Sanz-Cameno P. The molecular and pathophysiological implications of hepatitis B X antigen in chronic hepatitis B virus infection. Rev Med Virol. 2011;21(5):315-29.

66. Tong S, Revill P. Overview of hepatitis B viral replication and genetic variability. Journal of Hepatology.64(1):S4-S16.

67. Kramvis A. Genotypes and genetic variability of hepatitis B virus. Intervirology. 2014;57(3-4):141-50.

68. Toh H, Hayashida H, Miyata T. Sequence homology between retroviral reverse transcriptase and putative polymerases of hepatitis B virus and cauliflower mosaic virus. Nature. 1983;305(5937):827-9.

69. Zheng YW, Riegler J, Wu J, Yen TS. Novel short transcripts of hepatitis B virus X gene derived from intragenic promoter. J Biol Chem. 1994;269(36):22593-8.

70. Treinin M, Laub O. Identification of a promoter element located upstream from the hepatitis B virus X gene. Mol Cell Biol. 1987;7(1):545-8.

71. Zhang P, Raney AK, McLachlan A. Characterization of the hepatitis B virus X- and nucleocapsid gene transcriptional regulatory elements. Virology. 1992;191(1):31-41.

72. Leistner CM, Gruen-Bernhard S, Glebe D. Role of glycosaminoglycans for binding and infection of hepatitis B virus. Cell Microbiol. 2008;10(1):122-33.

73. Yan H, Zhong G, Xu G, He W, Jing Z, Gao Z, et al. Sodium taurocholate cotransporting polypeptide is a functional receptor for human hepatitis B and D virus. Elife. 2012;1:e00049.

74. Hagenbuch B, Meier PJ. Molecular cloning, chromosomal localization, and functional characterization of a human liver Na+/bile acid cotransporter. J Clin Invest. 1994;93(3):1326-31.

75. Inuzuka T, Takahashi K, Chiba T, Marusawa H. Mouse Models of Hepatitis B Virus Infection Comprising Host-Virus Immunologic Interactions. Pathogens. 2014;3(2):377.

76. Watashi K, Urban S, Li W, Wakita T. NTCP and beyond: opening the door to unveil hepatitis B virus entry. Int J Mol Sci. 2014;15(2):2892-905.

77. Li H, Zhuang Q, Wang Y, Zhang T, Zhao J, Zhang Y, et al. HBV life cycle is restricted in mouse hepatocytes expressing human NTCP. Cell Mol Immunol. 2014;11(2):175-83.

78. Glebe D, Urban S. Viral and cellular determinants involved in hepadnaviral entry. World J Gastroenterol. 2007;13(1):22-38.

79. Li W, Urban S. Entry of hepatitis B and hepatitis D virus into hepatocytes: Basic insights and clinical implications. J Hepatol. 2016;64(1 Suppl):S32-S40.

80. Ely A, Moyo B, Arbuthnot P. Progress With Developing Use of Gene Editing To Cure Chronic Infection With Hepatitis B Virus. Mol Ther. 2016;24(4):671-7.

81. Wang GH, Seeger C. The reverse transcriptase of hepatitis B virus acts as a protein primer for viral DNA synthesis. Cell. 1992;71(4):663-70.

82. Beck J, Bartos H, Nassal M. Experimental confirmation of a hepatitis B virus (HBV) epsilon-like bulge-and-loop structure in avian HBV RNA encapsidation signals. Virology. 1997;227(2):500-4.

83. Nassal M, Schaller H. Hepatitis B virus replication--an update. J Viral Hepat. 1996;3(5):217-26.

84. Tavis JE, Perri S, Ganem D. Hepadnavirus reverse transcription initiates within the stem-loop of the RNA packaging signal and employs a novel strand transfer. J Virol. 1994;68(6):3536-43.

85. Beck J, Nassal M. Hepatitis B virus replication. World J Gastroenterol. 2007;13(1):48-64.

86. Nassal M, Schaller H. Hepatitis B virus replication. Trends Microbiol. 1993;1(6):221-8.

87. Benhenda S, Ducroux A, Riviere L, Sobhian B, Ward MD, Dion S, et al. Methyltransferase PRMT1 is a binding partner of HBx and a negative regulator of hepatitis B virus transcription. J Virol. 2013;87(8):4360-71.

88. Melegari M, Scaglioni PP, Wands JR. Cloning and characterization of a novel hepatitis B virus x binding protein that inhibits viral replication. J Virol. 1998;72(3):1737-43.

89. Sitterlin D, Lee TH, Prigent S, Tiollais P, Butel JS, Transy C. Interaction of the UV-damaged DNA-binding protein with hepatitis B virus X protein is conserved among mammalian hepadnaviruses and restricted to transactivation-proficient X-insertion mutants. J Virol. 1997;71(8):6194-9.

90. Lee TH, Elledge SJ, Butel JS. Hepatitis B virus X protein interacts with a probable cellular DNA repair protein. J Virol. 1995;69(2):1107-14.

91. Sitterlin D, Bergametti F, Transy C. UVDDB p127-binding modulates activities and intracellular distribution of hepatitis B virus X protein. Oncogene. 2000;19(38):4417-26.

92. Sitterlin D, Bergametti F, Tiollais P, Tennant BC, Transy C. Correct binding of viral X protein to UVDDB-p127 cellular protein is critical for efficient infection by hepatitis B viruses. Oncogene. 2000;19(38):4427-31.

93. Li T, Robert EI, van Breugel PC, Strubin M, Zheng N. A promiscuous alpha-helical motif anchors viral hijackers and substrate receptors to the CUL4-DDB1 ubiquitin ligase machinery. Nat Struct Mol Biol. 2010;17(1):105-11.

94. McCall CM, Hu J, Xiong Y. Recruiting substrates to cullin 4-dependent ubiquitin ligases by DDB1. Cell Cycle. 2005;4(1):27-9.

95. Schrofelbauer B, Hakata Y, Landau NR. HIV-1 Vpr function is mediated by interaction with the damage-specific DNA-binding protein DDB1. Proc Natl Acad Sci U S A. 2007;104(10):4130-5.

96. Decorsiere A, Mueller H, van Breugel PC, Abdul F, Gerossier L, Beran RK, et al. Hepatitis B virus X protein identifies the Smc5/6 complex as a host restriction factor. Nature. 2016;531(7594):386-9.

97. Murphy CM, Xu Y, Li F, Nio K, Reszka-Blanco N, Li X, et al. Hepatitis B Virus X Protein Promotes Degradation of SMC5/6 to Enhance HBV Replication. Cell Rep. 2016;16(11):2846-54.

98. Reifenberg K, Nusser P, Lohler J, Spindler G, Kuhn C, von Weizsacker F, et al. Virus replication and virion export in X-deficient hepatitis B virus transgenic mice. J Gen Virol. 2002;83(Pt 5):991-6.

99. Xu Z, Yen TS, Wu L, Madden CR, Tan W, Slagle BL, et al. Enhancement of hepatitis B virus replication by its X protein in transgenic mice. J Virol. 2002;76(5):2579-84.

100. Chen HS, Kaneko S, Girones R, Anderson RW, Hornbuckle WE, Tennant BC, et al. The woodchuck hepatitis virus X gene is important for establishment of virus infection in woodchucks. J Virol. 1993;67(3):1218-26.

101. Zoulim F, Saputelli J, Seeger C. Woodchuck hepatitis virus X protein is required for viral infection in vivo. J Virol. 1994;68(3):2026-30.

102. Keasler VV, Hodgson AJ, Madden CR, Slagle BL. Enhancement of hepatitis B virus replication by the regulatory X protein in vitro and in vivo. J Virol. 2007;81(6):2656-62.

103. Fire A, Xu S, Montgomery MK, Kostas SA, Driver SE, Mello CC. Potent and specific genetic interference by double-stranded RNA in Caenorhabditis elegans. Nature. 1998;391(6669):806-11.

104. Hammond SM, Bernstein E, Beach D, Hannon GJ. An RNA-directed nuclease mediates post-transcriptional gene silencing in Drosophila cells. Nature. 2000;404(6775):293-6.

105. Hamilton AJ, Baulcombe DC. A species of small antisense RNA in posttranscriptional gene silencing in plants. Science. 1999;286(5441):950-2.

106. Baulcombe D. RNA silencing in plants. Nature. 2004;431(7006):356-63.

107. Elbashir SM, Harborth J, Lendeckel W, Yalcin A, Weber K, Tuschl T. Duplexes of 21-nucleotide RNAs mediate RNA interference in cultured mammalian cells. Nature. 2001;411(6836):494-8.

108. Meister G, Landthaler M, Patkaniowska A, Dorsett Y, Teng G, Tuschl T. Human Argonaute2 mediates RNA cleavage targeted by miRNAs and siRNAs. Mol Cell. 2004;15(2):185-97.

109. Bartel DP. MicroRNAs: genomics, biogenesis, mechanism, and function. Cell. 2004;116(2):281-97.

110. Bushati N, Cohen SM. microRNA functions. Annu Rev Cell Dev Biol. 2007;23:175-205.

111. Eulalio A, Huntzinger E, Izaurralde E. Getting to the root of miRNA-mediated gene silencing. Cell. 2008;132(1):9-14.

112. Stefani G, Slack FJ. Small non-coding RNAs in animal development. Nat Rev Mol Cell Biol. 2008;9(3):219-30.

113. Trajkovski M, Hausser J, Soutschek J, Bhat B, Akin A, Zavolan M, et al. MicroRNAs 103 and 107 regulate insulin sensitivity. Nature. 2011;474(7353):649-53.

114. Adams BD, Kasinski AL, Slack FJ. Aberrant regulation and function of microRNAs in cancer. Curr Biol. 2014;24(16):R762-76.

115. Weinberg MS, Morris KV. Transcriptional gene silencing in humans. Nucleic Acids Res. 2016;44(14):6505-17.

116. Bracht J, Hunter S, Eachus R, Weeks P, Pasquinelli AE. Trans-splicing and polyadenylation of let-7 microRNA primary transcripts. RNA. 2004;10(10):1586-94.

117. Cai X, Hagedorn CH, Cullen BR. Human microRNAs are processed from capped, polyadenylated transcripts that can also function as mRNAs. RNA. 2004;10(12):1957-66.

118. Gottwein E, Cullen BR. Viral and cellular microRNAs as determinants of viral pathogenesis and immunity. Cell Host Microbe. 2008;3(6):375-87.

119. Denli AM, Tops BB, Plasterk RH, Ketting RF, Hannon GJ. Processing of primary microRNAs by the Microprocessor complex. Nature. 2004;432(7014):231-5.

120. Gregory RI, Yan KP, Amuthan G, Chendrimada T, Doratotaj B, Cooch N, et al. The Microprocessor complex mediates the genesis of microRNAs. Nature. 2004;432(7014):235-40.

121. Han J, Lee Y, Yeom KH, Kim YK, Jin H, Kim VN. The Drosha-DGCR8 complex in primary microRNA processing. Genes Dev. 2004;18(24):3016-27.

122. Landthaler M, Yalcin A, Tuschl T. The human DiGeorge syndrome critical region gene 8 and Its D. melanogaster homolog are required for miRNA biogenesis. Curr Biol. 2004;14(23):2162-7.

123. Lee Y, Ahn C, Han J, Choi H, Kim J, Yim J, et al. The nuclear RNase III Drosha initiates microRNA processing. Nature. 2003;425(6956):415-9.

124. Zeng Y, Yi R, Cullen BR. Recognition and cleavage of primary microRNA precursors by the nuclear processing enzyme Drosha. EMBO J. 2005;24(1):138-48.

125. Lund E, Guttinger S, Calado A, Dahlberg JE, Kutay U. Nuclear export of microRNA precursors. Science. 2004;303(5654):95-8.

126. Okada C, Yamashita E, Lee SJ, Shibata S, Katahira J, Nakagawa A, et al. A high-resolution structure of the pre-microRNA nuclear export machinery. Science. 2009;326(5957):1275-9.

127. Yi R, Qin Y, Macara IG, Cullen BR. Exportin-5 mediates the nuclear export of pre-microRNAs and short hairpin RNAs. Genes Dev. 2003;17(24):3011-6.

128. Arbuthnot P. Viral Vectors for Delivery of Antiviral Sequences. Gene therapy for viral infections. Amsterdam: Elsevier/AP, Academic Press is an imprint of Elsevier; 2015. p. 95-126.

129. Chendrimada TP, Gregory RI, Kumaraswamy E, Norman J, Cooch N, Nishikura K, et al. TRBP recruits the Dicer complex to Ago2 for microRNA processing and gene silencing. Nature. 2005;436(7051):740-4.

130. Forstemann K, Tomari Y, Du T, Vagin VV, Denli AM, Bratu DP, et al. Normal microRNA maturation and germ-line stem cell maintenance requires Loquacious, a double-stranded RNA-binding domain protein. PLoS Biol. 2005;3(7):e236.

131. Hutvagner G, McLachlan J, Pasquinelli AE, Balint E, Tuschl T, Zamore PD. A cellular function for the RNA-interference enzyme Dicer in the maturation of the let-7 small temporal RNA. Science. 2001;293(5531):834-8.

132. Jiang F, Ye X, Liu X, Fincher L, McKearin D, Liu Q. Dicer-1 and R3D1-L catalyze microRNA maturation in Drosophila. Genes Dev. 2005;19(14):1674-9.

133. Ketting RF, Fischer SE, Bernstein E, Sijen T, Hannon GJ, Plasterk RH. Dicer functions in RNA interference and in synthesis of small RNA involved in developmental timing in C. elegans. Genes Dev. 2001;15(20):2654-9.

134. Lee Y, Hur I, Park SY, Kim YK, Suh MR, Kim VN. The role of PACT in the RNA silencing pathway. EMBO J. 2006;25(3):522-32.

135. Saito K, Ishizuka A, Siomi H, Siomi MC. Processing of pre-microRNAs by the Dicer-1-Loquacious complex in Drosophila cells. PLoS Biol. 2005;3(7):e235.

136. Filipowicz W, Jaskiewicz L, Kolb FA, Pillai RS. Post-transcriptional gene silencing by siRNAs and miRNAs. Curr Opin Struct Biol. 2005;15(3):331-41.

137. Khvorova A, Reynolds A, Jayasena SD. Functional siRNAs and miRNAs exhibit strand bias. Cell. 2003;115(2):209-16.

138. Noland CL, Ma E, Doudna JA. siRNA repositioning for guide strand selection by human Dicer complexes. Mol Cell. 2011;43(1):110-21.

139. Hutvagner G, Zamore PD. A microRNA in a multiple-turnover RNAi enzyme complex. Science. 2002;297(5589):2056-60.

140. Liu J, Carmell MA, Rivas FV, Marsden CG, Thomson JM, Song JJ, et al. Argonaute2 is the catalytic engine of mammalian RNAi. Science. 2004;305(5689):1437-41.

141. Martinez J, Tuschl T. RISC is a 5' phosphomonoester-producing RNA endonuclease. Genes Dev. 2004;18(9):975-80.

142. Okamura K, Ishizuka A, Siomi H, Siomi MC. Distinct roles for Argonaute proteins in small RNA-directed RNA cleavage pathways. Genes Dev. 2004;18(14):1655-66.

143. Grimson A, Farh KK, Johnston WK, Garrett-Engele P, Lim LP, Bartel DP. MicroRNA targeting specificity in mammals: determinants beyond seed pairing. Mol Cell. 2007;27(1):91-105.

144. Brummelkamp TR, Bernards R, Agami R. A system for stable expression of short interfering RNAs in mammalian cells. Science. 2002;296(5567):550-3.

145. Paddison PJ, Caudy AA, Bernstein E, Hannon GJ, Conklin DS. Short hairpin RNAs (shRNAs) induce sequence-specific silencing in mammalian cells. Genes Dev. 2002;16(8):948-58.

146. Amarzguioui M, Rossi JJ, Kim D. Approaches for chemically synthesized siRNA and vector-mediated RNAi. FEBS Lett. 2005;579(26):5974-81.

147. Bertrand E, Castanotto D, Zhou C, Carbonnelle C, Lee NS, Good P, et al. The expression cassette determines the functional activity of ribozymes in mammalian cells by controlling their intracellular localization. Rna. 1997;3(1):75-88.

148. Baer M, Nilsen TW, Costigan C, Altman S. Structure and transcription of a human gene for H1 RNA, the RNA component of human RNase P. Nucleic Acids Res. 1990;18(1):97-103.

149. Kim DH, Rossi JJ. Strategies for silencing human disease using RNA interference. Nat Rev Genet. 2007;8(3):173-84.

150. Grimm D, Streetz KL, Jopling CL, Storm TA, Pandey K, Davis CR, et al. Fatality in mice due to oversaturation of cellular microRNA/short hairpin RNA pathways. Nature. 2006;441(7092):537-41.

151. Grimm D, Wang L, Lee JS, Schurmann N, Gu S, Borner K, et al. Argonaute proteins are key determinants of RNAi efficacy, toxicity, and persistence in the adult mouse liver. J Clin Invest. 2010;120(9):3106-19.

152. Valdmanis PN, Gu S, Chu K, Jin L, Zhang F, Munding EM, et al. RNA interference-induced hepatotoxicity results from loss of the first synthesized isoform of microRNA-122 in mice. Nat Med. 2016;22(5):557-62.

153. Gupta S, Schoer RA, Egan JE, Hannon GJ, Mittal V. Inducible, reversible, and stable RNA interference in mammalian cells. Proceedings of the National Academy of Sciences. 2004;101(7):1927-32.

154. Wiznerowicz M, Szulc J, Trono D. Tuning silence: conditional systems for RNA interference. Nat Methods. 2006;3(9):682-8.

155. van de Wetering M, Oving I, Muncan V, Pon Fong MT, Brantjes H, van Leenen D, et al. Specific inhibition of gene expression using a stably integrated, inducible small-interfering-RNA vector. EMBO Rep. 2003;4(6):609-15.

156. Zeng Y, Wagner EJ, Cullen BR. Both natural and designed micro RNAs can inhibit the expression of cognate mRNAs when expressed in human cells. Mol Cell. 2002;9(6):1327-33.

157. Aagaard LA, Zhang J, von Eije KJ, Li H, Saetrom P, Amarzguioui M, et al. Engineering and optimization of the miR-106b cluster for ectopic expression of multiplexed anti-HIV RNAs. Gene Ther. 2008;15(23):1536-49.

158. Liu YP, Haasnoot J, ter Brake O, Berkhout B, Konstantinova P. Inhibition of HIV-1 by multiple siRNAs expressed from a single microRNA polycistron. Nucleic Acids Res. 2008;36(9):2811-24.

159. Ely A, Naidoo T, Arbuthnot P. Efficient silencing of gene expression with modular trimeric Pol II expression cassettes comprising microRNA shuttles. Nucleic Acids Res. 2009;37(13):e91.

160. Shabalina SA, Spiridonov AN, Ogurtsov AY. Computational models with thermodynamic and composition features improve siRNA design. BMC Bioinformatics. 2006;7:65.

161. Huesken D, Lange J, Mickanin C, Weiler J, Asselbergs F, Warner J, et al. Design of a genome-wide siRNA library using an artificial neural network. Nat Biotechnol. 2005;23(8):995-1001.

162. Fellmann C, Lowe SW. Stable RNA interference rules for silencing. Nat Cell Biol. 2014;16(1):10-8.

163. Chang CI, Kim HA, Dua P, Kim S, Li CJ, Lee DK. Structural diversity repertoire of gene silencing small interfering RNAs. Nucleic Acid Ther. 2011;21(3):125-31.

164. Shukla S, Sumaria CS, Pradeepkumar PI. Exploring chemical modifications for siRNA therapeutics: a structural and functional outlook. ChemMedChem. 2010;5(3):328-49.

165. Lares MR, Rossi JJ, Ouellet DL. RNAi and small interfering RNAs in human disease therapeutic applications. Trends Biotechnol. 2010;28(11):570-9.

166. Judge AD, Bola G, Lee AC, MacLachlan I. Design of noninflammatory synthetic siRNA mediating potent gene silencing in vivo. Mol Ther. 2006;13(3):494-505.

167. Czauderna F, Fechtner M, Dames S, Aygun H, Klippel A, Pronk GJ, et al. Structural variations and stabilising modifications of synthetic siRNAs in mammalian cells. Nucleic Acids Res. 2003;31(11):2705-16.

168. Janssen HL, Reesink HW, Lawitz EJ, Zeuzem S, Rodriguez-Torres M, Patel K, et al. Treatment of HCV infection by targeting microRNA. N Engl J Med. 2013;368(18):1685-94.

169. van der Ree MH, van der Meer AJ, de Bruijne J, Maan R, van Vliet A, Welzel TM, et al. Long-term safety and efficacy of microRNA-targeted therapy in chronic hepatitis C patients. Antiviral Res. 2014;111:53-9.

170. Allerson CR, Sioufi N, Jarres R, Prakash TP, Naik N, Berdeja A, et al. Fully 2'-modified oligonucleotide duplexes with improved in vitro potency and stability compared to unmodified small interfering RNA. J Med Chem. 2005;48(4):901-4.

171. Hoerter JA, Walter NG. Chemical modification resolves the asymmetry of siRNA strand degradation in human blood serum. RNA. 2007;13(11):1887-93.

172. Soutschek J, Akinc A, Bramlage B, Charisse K, Constien R, Donoghue M, et al. Therapeutic silencing of an endogenous gene by systemic administration of modified siRNAs. Nature. 2004;432(7014):173-8.

173. Birmingham A, Anderson EM, Reynolds A, Ilsley-Tyree D, Leake D, Fedorov Y, et al. 3' UTR seed matches, but not overall identity, are associated with RNAi off-targets. Nat Methods. 2006;3(3):199-204.

174. Jackson AL, Burchard J, Schelter J, Chau BN, Cleary M, Lim L, et al. Widespread siRNA "off-target" transcript silencing mediated by seed region sequence complementarity. RNA. 2006;12(7):1179-87.

175. Lin X, Ruan X, Anderson MG, McDowell JA, Kroeger PE, Fesik SW, et al. siRNA-mediated off-target gene silencing triggered by a 7 nt complementation. Nucleic Acids Res. 2005;33(14):4527-35.

176. Bramsen JB, Laursen MB, Damgaard CK, Lena SW, Babu BR, Wengel J, et al. Improved silencing properties using small internally segmented interfering RNAs. Nucleic Acids Res. 2007;35(17):5886-97.

177. Alexopoulou L, Holt AC, Medzhitov R, Flavell RA. Recognition of double-stranded RNA and activation of NF-kappaB by Toll-like receptor 3. Nature. 2001;413(6857):732-8.

178. Judge AD, Sood V, Shaw JR, Fang D, McClintock K, MacLachlan I. Sequence-dependent stimulation of the mammalian innate immune response by synthetic siRNA. Nat Biotechnol. 2005;23(4):457-62.

179. Hornung V, Guenthner-Biller M, Bourquin C, Ablasser A, Schlee M, Uematsu S, et al. Sequence-specific potent induction of IFN-alpha by short interfering RNA in plasmacytoid dendritic cells through TLR7. Nat Med. 2005;11(3):263-70.

180. Morrissey DV, Lockridge JA, Shaw L, Blanchard K, Jensen K, Breen W, et al. Potent and persistent in vivo anti-HBV activity of chemically modified siRNAs. Nat Biotechnol. 2005;23(8):1002-7.

181. Sioud M, Furset G, Cekaite L. Suppression of immunostimulatory siRNA-driven innate immune activation by 2'-modified RNAs. Biochem Biophys Res Commun. 2007;361(1):122-6.

182. Marimani MD, Ely A, Buff MC, Bernhardt S, Engels JW, Arbuthnot P. Inhibition of hepatitis B virus replication in cultured cells and in vivo using 2'-O-guanidinopropyl modified siRNAs. Bioorg Med Chem. 2013;21(20):6145-55.

183. Fisher M, Abramov M, Van Aerschot A, Xu D, Juliano RL, Herdewijn P. Inhibition of MDR1 expression with altritol-modified siRNAs. Nucleic Acids Res. 2007;35(4):1064-74.

184. Hean J, Crowther C, Ely A, Ul Islam R, Barichievy S, Bloom K, et al. Inhibition of hepatitis B virus replication in vivo using lipoplexes containing altritol-modified antiviral siRNAs. Artif DNA PNA XNA. 2010;1(1):17-26.

185. Robbins M, Judge A, Ambegia E, Choi C, Yaworski E, Palmer L, et al. Misinterpreting the therapeutic effects of small interfering RNA caused by immune stimulation. Hum Gene Ther. 2008;19(10):991-9.

186. Arbuthnot P, Ely A, Weinberg MS. Hepatic delivery of RNA interference activators for therapeutic application. Curr Gene Ther. 2009;9(2):91-103.

187. Chen CC, Ko TM, Ma HI, Wu HL, Xiao X, Li J, et al. Long-term inhibition of hepatitis B virus in transgenic mice by double-stranded adeno-associated virus 8-delivered short hairpin RNA. Gene Ther. 2007;14(1):11-9.

188. Grimm D, Kay MA. Therapeutic short hairpin RNA expression in the liver: viral targets and vectors. Gene Ther. 2006;13(6):563-75.

189. Morris KV, Rossi JJ. Lentiviral-mediated delivery of siRNAs for antiviral therapy. Gene Ther. 2006;13(6):553-8.

190. Grimm D, Kleinschmidt JA. Progress in adeno-associated virus type 2 vector production: promises and prospects for clinical use. Hum Gene Ther. 1999;10(15):2445-50.

191. Crowther C, Mowa MB, Ely A, Arbuthnot P. Approaches to Delivering RNAi Therapeutics that Target Hepatitis B Virus. In: Cheng K, Mahato RI, editors. Advanced delivery and therapeutic applications of RNAi. First ed. Chichester, West Sussex England: John Wiley & Sons; 2013. p. 367-89.

192. Jacobs F, Wisse E, De Geest B. The role of liver sinusoidal cells in hepatocyte-directed gene transfer. Am J Pathol. 2010;176(1):14-21.

193. Khare R, Chen CY, Weaver EA, Barry MA. Advances and future challenges in adenoviral vector pharmacology and targeting. Curr Gene Ther. 2011;11(4):241-58.

194. Waddington SN, McVey JH, Bhella D, Parker AL, Barker K, Atoda H, et al. Adenovirus serotype 5 hexon mediates liver gene transfer. Cell. 2008;132(3):397-409.

195. Kotterman MA, Schaffer DV. Engineering adeno-associated viruses for clinical gene therapy. Nat Rev Genet. 2014;15(7):445-51.

196. George LA. Hemophilia gene therapy comes of age. Blood Adv. 2017;1(26):2591-9.

197. Buning H, Perabo L, Coutelle O, Quadt-Humme S, Hallek M. Recent developments in adeno-associated virus vector technology. J Gene Med. 2008;10(7):717-33.

198. McCaffrey AP, Fawcett P, Nakai H, McCaffrey RL, Ehrhardt A, Pham TT, et al. The host response to adenovirus, helper-dependent adenovirus, and adeno-associated virus in mouse liver. Mol Ther. 2008;16(5):931-41.

199. McCaffrey AP. RNA interference inhibitors of hepatitis B virus. Ann N Y Acad Sci. 2009;1175:15-23.

200. Chen CC, Sun CP, Ma HI, Fang CC, Wu PY, Xiao X, et al. Comparative study of anti-hepatitis B virus RNA interference by double-stranded adeno-associated virus serotypes 7, 8, and 9. Mol Ther. 2009;17(2):352-9.

201. Michler T, Grosse S, Mockenhaupt S, Roder N, Stuckler F, Knapp B, et al. Blocking sense-strand activity improves potency, safety and specificity of anti-hepatitis B virus short hairpin RNA. EMBO Mol Med. 2016;8(9):1082-98.

202. Yin H, Kanasty RL, Eltoukhy AA, Vegas AJ, Dorkin JR, Anderson DG. Non-viral vectors for gene-based therapy. Nat Rev Genet. 2014;15(8):541-55.

203. Tang MX, Szoka FC. The influence of polymer structure on the interactions of cationic polymers with DNA and morphology of the resulting complexes. Gene Ther. 1997;4(8):823-32.

204. Xia Y, Sun J, Liang D. Aggregation, fusion, and leakage of liposomes induced by peptides. Langmuir. 2014;30(25):7334-42.

205. Morille M, Passirani C, Vonarbourg A, Clavreul A, Benoit JP. Progress in developing cationic vectors for non-viral systemic gene therapy against cancer. Biomaterials. 2008;29(24-25):3477-96.

206. Kanasty RL, Whitehead KA, Vegas AJ, Anderson DG. Action and reaction: the biological response to siRNA and its delivery vehicles. Mol Ther. 2012;20(3):513-24.

207. Takeuchi O, Akira S. Pattern recognition receptors and inflammation. Cell. 2010;140(6):805-20.

208. Alexis F, Pridgen E, Molnar LK, Farokhzad OC. Factors affecting the clearance and biodistribution of polymeric nanoparticles. Mol Pharm. 2008;5(4):505-15.

209. Carugo D, Bottaro E, Owen J, Stride E, Nastruzzi C. Liposome production by microfluidics: potential and limiting factors. Scientific Reports. 2016;6:25876.

210. Bazile D, Prud'homme C, Bassoullet MT, Marlard M, Spenlehauer G, Veillard M. Stealth Me.PEG-PLA nanoparticles avoid uptake by the mononuclear phagocytes system. J Pharm Sci. 1995;84(4):493-8.

211. Kim HK, Davaa E, Myung CS, Park JS. Enhanced siRNA delivery using cationic liposomes with new polyarginine-conjugated PEG-lipid. Int J Pharm. 2010;392(1-2):141-7.

212. Carmona S, Jorgensen MR, Kolli S, Crowther C, Salazar FH, Marion PL, et al. Controlling HBV replication in vivo by intravenous administration of triggered PEGylated siRNA-nanoparticles. Mol Pharm. 2009;6(3):706-17.

213. Mintzer MA, Simanek EE. Nonviral vectors for gene delivery. Chem Rev. 2009;109(2):259-302.

214. Zimmermann TS, Lee AC, Akinc A, Bramlage B, Bumcrot D, Fedoruk MN, et al. RNAi-mediated gene silencing in non-human primates. Nature. 2006;441(7089):111-4.

215. Cullis PR, Hope MJ. Lipid Nanoparticle Systems for Enabling Gene Therapies. Mol Ther. 2017;25(7):1467-75.

216. Williams KJ, Chen K. Recent insights into factors affecting remnant lipoprotein uptake. Curr Opin Lipidol. 2010;21(3):218-28.

217. Yu B, Zhao X, Lee LJ, Lee RJ. Targeted delivery systems for oligonucleotide therapeutics. AAPS J. 2009;11(1):195-203.

218. Varshosaz J, Farzan M. Nanoparticles for targeted delivery of therapeutics and small interfering RNAs in hepatocellular carcinoma. World J Gastroenterol. 2015;21(42):12022-41.

219. Akinc A, Querbes W, De S, Qin J, Frank-Kamenetsky M, Jayaprakash KN, et al. Targeted delivery of RNAi therapeutics with endogenous and exogenous ligand-based mechanisms. Mol Ther. 2010;18(7):1357-64.

220. Biessen EA, Broxterman H, van Boom JH, van Berkel TJ. The cholesterol derivative of a triantennary galactoside with high affinity for hepatic asialoglycoprotein receptor: a potent cholesterol lowering agent. J Med Chem. 1995;38(11):1846-52.

221. Arbuthnot P, Carmona S, Ely A. Exploiting the RNA interference pathway to counter hepatitis B virus replication. Liver Int. 2005;25(1):9-15.

222. Uprichard SL, Boyd B, Althage A, Chisari FV. Clearance of hepatitis B virus from the liver of transgenic mice by short hairpin RNAs. Proc Natl Acad Sci U S A. 2005;102(3):773-8.

223. Shlomai A, Shaul Y. Inhibition of hepatitis B virus expression and replication by RNA interference. Hepatology. 2003;37(4):764-70.

224. Hamasaki K, Nakao K, Matsumoto K, Ichikawa T, Ishikawa H, Eguchi K. Short interfering RNA-directed inhibition of hepatitis B virus replication. FEBS Lett. 2003;543(1-3):51-4.

225. Giladi H, Ketzinel-Gilad M, Rivkin L, Felig Y, Nussbaum O, Galun E. Small interfering RNA inhibits hepatitis B virus replication in mice. Mol Ther. 2003;8(5):769-76.

226. Chen Y, Du D, Wu J, Chan CP, Tan Y, Kung HF, et al. Inhibition of hepatitis B virus replication by stably expressed shRNA. Biochem Biophys Res Commun. 2003;311(2):398-404.

227. McCaffrey AP, Nakai H, Pandey K, Huang Z, Salazar FH, Xu H, et al. Inhibition of hepatitis B virus in mice by RNA interference. Nat Biotechnol. 2003;21(6):639-44.

228. Fischer KP, Gutfreund KS, Tyrrell DL. Lamivudine resistance in hepatitis B: mechanisms and clinical implications. Drug Resist Updat. 2001;4(2):118-28.

229. Wilson JA, Richardson CD. Hepatitis C virus replicons escape RNA interference induced by a short interfering RNA directed against the NS5b coding region. J Virol. 2005;79(11):7050-8.

230. Weinberg MS, Ely A, Barichievy S, Crowther C, Mufamadi S, Carmona S, et al. Specific inhibition of HBV replication in vitro and in vivo with expressed long hairpin RNA. Mol Ther. 2007;15(3):534-41.

231. Mevel M, Kamaly N, Carmona S, Oliver MH, Jorgensen MR, Crowther C, et al. DODAG; a versatile new cationic lipid that mediates efficient delivery of pDNA and siRNA. J Control Release. 2010;143(2):222-32.

232. Boudreau RL, Martins I, Davidson BL. Artificial microRNAs as siRNA shuttles: improved safety as compared to shRNAs in vitro and in vivo. Mol Ther. 2009;17(1):169-75.

233. Ely A, Naidoo T, Mufamadi S, Crowther C, Arbuthnot P. Expressed anti-HBV primary microRNA shuttles inhibit viral replication efficiently in vitro and in vivo. Mol Ther. 2008;16(6):1105-12.

234. Fellmann C, Hoffmann T, Sridhar V, Hopfgartner B, Muhar M, Roth M, et al. An optimized microRNA backbone for effective single-copy RNAi. Cell Rep. 2013;5(6):1704-13.

235. Olejniczak M, Galka P, Krzyzosiak WJ. Sequence-non-specific effects of RNA interference triggers and microRNA regulators. Nucleic Acids Res. 2010;38(1):1-16.

236. Bauer M, Kinkl N, Meixner A, Kremmer E, Riemenschneider M, Forstl H, et al. Prevention of interferon-stimulated gene expression using microRNA-designed hairpins. Gene Ther. 2008.

237. Chang J, Nicolas E, Marks D, Sander C, Lerro A, Buendia MA, et al. miR-122, a mammalian liver-specific microRNA, is processed from hcr mRNA and may downregulate the high affinity cationic amino acid transporter CAT-1. RNA Biol. 2004;1(2):106-13.

238. Schwarz DS, Hutvagner G, Du T, Xu Z, Aronin N, Zamore PD. Asymmetry in the assembly of the RNAi enzyme complex. Cell. 2003;115(2):199-208.

239. Reynolds A, Leake D, Boese Q, Scaringe S, Marshall WS, Khvorova A. Rational siRNA design for RNA interference. Nat Biotechnol. 2004;22(3):326-30.

240. Lu S, Cullen BR. Adenovirus VA1 noncoding RNA can inhibit small interfering RNA and MicroRNA biogenesis. J Virol. 2004;78(23):12868-76.

241. Castanotto D, Sakurai K, Lingeman R, Li H, Shively L, Aagaard L, et al. Combinatorial delivery of small interfering RNAs reduces RNAi efficacy by selective incorporation into RISC. Nucleic Acids Res. 2007;35(15):5154-64.

242. Grimm D. The dose can make the poison: lessons learned from adverse in vivo toxicities caused by RNAi overexpression. Silence. 2011;2:8.

243. An DS, Qin FX, Auyeung VC, Mao SH, Kung SK, Baltimore D, et al. Optimization and functional effects of stable short hairpin RNA expression in primary human lymphocytes via lentiviral vectors. Mol Ther. 2006;14(4):494-504.

244. Zeng Y, Cai X, Cullen BR. Use of RNA polymerase II to transcribe artificial microRNAs. Methods Enzymol. 2005;392:371-80.

245. Zhou H, Xia XG, Xu Z. An RNA polymerase II construct synthesizes short-hairpin RNA with a quantitative indicator and mediates highly efficient RNAi. Nucleic Acids Res. 2005;33(6):e62.

246. Dickins RA, Hemann MT, Zilfou JT, Simpson DR, Ibarra I, Hannon GJ, et al. Probing tumor phenotypes using stable and regulated synthetic microRNA precursors. Nat Genet. 2005;37(11):1289-95.

247. SoRelle R. Human gene therapy: science under fire. Circulation. 2000;101(12):E9023-4.

248. Marshall E. Gene therapy death prompts review of adenovirus vector. Science. 1999;286(5448):2244-5.

249. Buchbinder SP, Mehrotra DV, Duerr A, Fitzgerald DW, Mogg R, Li D, et al. Efficacy assessment of a cell-mediated immunity HIV-1 vaccine (the Step Study): a double-blind, randomised, placebo-controlled, test-of-concept trial. Lancet. 2008.

250. McElrath MJ, De Rosa SC, Moodie Z, Dubey S, Kierstead L, Janes H, et al. HIV-1 vaccine-induced immunity in the test-of-concept Step Study: a case-cohort analysis. Lancet. 2008.

251. Brunetti-Pierri N, Ng P. Adenoviral Vectors for Hemophilia Gene Therapy. J Genet Syndr Gene Ther. 2013;2(Suppl 1):017.

252. Fumoto S, Kawakami S, Ito Y, Shigeta K, Yamashita F, Hashida M. Enhanced hepatocyte-selective in vivo gene expression by stabilized galactosylated liposome/plasmid DNA complex using sodium chloride for complex formation. Mol Ther. 2004;10(4):719-29.

253. Chu TC, Twu KY, Ellington AD, Levy M. Aptamer mediated siRNA delivery. Nucleic Acids Res. 2006;34(10):e73.

254. Lee SH, Kim SH, Park TG. Intracellular siRNA delivery system using polyelectrolyte complex micelles prepared from VEGF siRNA-PEG conjugate and cationic fusogenic peptide. Biochem Biophys Res Commun. 2007;357(2):511-6.

255. Wolfrum C, Shi S, Jayaprakash KN, Jayaraman M, Wang G, Pandey RK, et al. Mechanisms and optimization of in vivo delivery of lipophilic siRNAs. Nat Biotechnol. 2007;25(10):1149-57.

256. Wooddell CI, Rozema DB, Hossbach M, John M, Hamilton HL, Chu Q, et al. Hepatocyte-targeted RNAi therapeutics for the treatment of chronic hepatitis B virus infection. Mol Ther. 2013;21(5):973-85.

257. Wooddell CI, Yuen MF, Chan HL, Gish RG, Locarnini SA, Chavez D, et al. RNAi-based treatment of chronically infected patients and chimpanzees reveals that integrated hepatitis B virus DNA is a source of HBsAg. Sci Transl Med. 2017;9(409).

258. Li H, Haurigot V, Doyon Y, Li T, Wong SY, Bhagwat AS, et al. In vivo genome editing restores haemostasis in a mouse model of haemophilia. Nature. 2011;475(7355):217-21.

259. Hubbard N, Hagin D, Sommer K, Song Y, Khan I, Clough C, et al. Targeted gene editing restores regulated CD40L function in X-linked hyper-IgM syndrome. Blood. 2016;127(21):2513-22.

260. Holt N, Wang J, Kim K, Friedman G, Wang X, Taupin V, et al. Human hematopoietic stem/progenitor cells modified by zinc-finger nucleases targeted to CCR5 control HIV-1 in vivo. Nat Biotechnol. 2010;28(8):839-47.

261. Cornu TI, Mussolino C, Cathomen T. Refining strategies to translate genome editing to the clinic. Nat Med. 2017;23(4):415-23.

262. Dreyer T, Nicholson S, Ely A, Arbuthnot P, Bloom K. Improved antiviral efficacy using TALEN-mediated homology directed recombination to introduce artificial primary miRNAs into DNA of hepatitis B virus. Biochem Biophys Res Commun. 2016;478(4):1563-8.

263. Hong X, Kim ES, Guo H. Epigenetic regulation of hepatitis B virus covalently closed circular DNA: Implications for epigenetic therapy against chronic hepatitis B. Hepatology. 2017;66(6):2066-77.

264. Jackson AL, Bartz SR, Schelter J, Kobayashi SV, Burchard J, Mao M, et al. Expression profiling reveals off-target gene regulation by RNAi. Nat Biotechnol. 2003;21(6):635-7.

265. Schultz N, Marenstein DR, De Angelis DA, Wang WQ, Nelander S, Jacobsen A, et al. Off-target effects dominate a large-scale RNAi screen for modulators of the TGF-beta pathway and reveal microRNA regulation of TGFBR2. Silence. 2011;2:3.

266. Jackson AL, Linsley PS. Recognizing and avoiding siRNA off-target effects for target identification and therapeutic application. Nat Rev Drug Discov. 2010;9(1):57-67.

267. Kwak PB, Tomari Y. The N domain of Argonaute drives duplex unwinding during RISC assembly. Nat Struct Mol Biol. 2012;19(2):145-51.

268. Schurmann N, Trabuco LG, Bender C, Russell RB, Grimm D. Molecular dissection of human Argonaute proteins by DNA shuffling. Nat Struct Mol Biol. 2013;20(7):818-26.

269. Jackson AL, Burchard J, Leake D, Reynolds A, Schelter J, Guo J, et al. Position-specific chemical modification of siRNAs reduces "off-target" transcript silencing. RNA. 2006;12(7):1197-205.